

DISSERTATION

MEASURING AND PREDICTING EROSION AND SEDIMENT YIELDS
ON ST. JOHN, U.S. VIRGIN ISLANDS

Submitted by

Carlos E. Ramos-Scharrón

Department of Geosciences

In partial fulfillment of the requirements

for the degree of Doctor of Philosophy

Colorado State University

Fort Collins, Colorado

Spring 2004

UMI Number: 3131697

INFORMATION TO USERS

The quality of this reproduction is dependent upon the quality of the copy submitted. Broken or indistinct print, colored or poor quality illustrations and photographs, print bleed-through, substandard margins, and improper alignment can adversely affect reproduction.

In the unlikely event that the author did not send a complete manuscript and there are missing pages, these will be noted. Also, if unauthorized copyright material had to be removed, a note will indicate the deletion.

UMI[®]

UMI Microform 3131697

Copyright 2004 by ProQuest Information and Learning Company.

All rights reserved. This microform edition is protected against unauthorized copying under Title 17, United States Code.

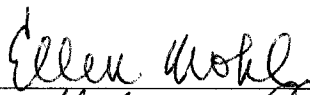
ProQuest Information and Learning Company
300 North Zeeb Road
P.O. Box 1346
Ann Arbor, MI 48106-1346

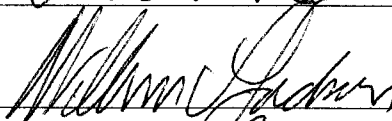
COLORADO STATE UNIVERSITY

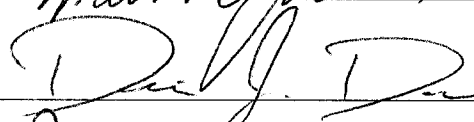
December 18, 2003


WE HEREBY RECOMMEND THAT THE DISSERTATION PREPARED UNDER OUR SUPERVISION BY CARLOS E. RAMOS-SCHARRÓN ENTITLED MEASURING AND PREDICTING EROSION AND SEDIMENT YIELDS ON ST. JOHN, U.S. VIRGIN ISLANDS BE ACCEPTED AS FULFILLING IN PART REQUIREMENTS FOR THE DEGREE OF DOCTOR OF PHILOSOPHY.

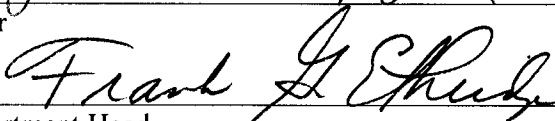
Committee on Graduate Work









Chair


Department Head

ABSTRACT OF DISSERTATION

MEASURING AND PREDICTING EROSION AND SEDIMENT YIELDS ON ST. JOHN, U.S. VIRGIN ISLANDS

Increased sediment delivery rates are believed to be causing adverse effects on the nearshore coral reef communities of St. John, U.S. Virgin Islands. The objectives of this study were to: (1) measure runoff and sediment yields from undisturbed hillslopes and a road segment; (2) measure and predict sediment production rates from natural sources and unpaved roads; and (3) develop and apply a GIS-based sediment yield model.

Runoff on undisturbed hillslopes only occurred when storm precipitation exceeded 2-3 cm, while only 0.3 cm was needed to generate runoff from unpaved roads. Runoff coefficients for the undisturbed hillslopes averaged 3% and had a maximum of 8%, while the road segment had a mean runoff coefficient of 6% and a maximum of 70%. The road segment data were used to develop runoff models that combined the Green-Ampt infiltration with either an empirical unit hydrograph or a kinematic wave routing component. Both models underestimated runoff for storms with less than 1 cm of rainfall, but predictions improved when rainfall exceeded 1 cm.

Streambanks produced sediment at a rate of $10 \text{ kg m}^{-2} \text{ yr}^{-1}$, and treethrow produced 0.17 tons per kilometer of stream per year. Annual sediment production rates from undisturbed hillslope plots ranged from $1\text{-}27 \text{ g m}^{-2}$, while mean rates from undisturbed zero- and first-order catchments were 1 and 8 g m^{-2} , respectively. Sediment production rates from unpaved road segments averaged $7.4 \text{ kg m}^{-2} \text{ yr}^{-1}$ and were significantly related to total precipitation and slope. After normalizing by precipitation and slope, the mean annual sediment production rate for roads graded within the last two years was $0.96 \text{ kg m}^{-2} \text{ cm}^{-1} \text{ m m}^{-1}$, while rates for ungraded and abandoned roads were 0.56 and $0.071 \text{ kg m}^{-2} \text{ cm}^{-1} \text{ m m}^{-1}$, respectively. Cutslopes were responsible for only 9% of road-segment scale sediment yields.

STJ-EROS is a GIS-based system that uses empirical sediment production functions and delivery ratios to estimate watershed-scale sediment yields. STJ-EROS indicated that unpaved

roads are increasing sediment yields by 5-40 times above undisturbed conditions. Predicted values were within the range of estimated sediment yields and bay sedimentation rates. The results indicate that road improvements are needed to protect the marine resources of St. John.

Carlos E Ramos-Scharrón
Department of Geosciences
Colorado State University
Fort Collins, CO 80523
Spring 2004

DEDICATION

This work is an offering to Olofi, God the Creator.
She/He who knows the true value
of all the processes that I have
measured, modeled, and described in this dissertation.
Processes that are naturally divine, as they are as much
an expression of Him/Her as my breath and my heartbeat.
To You I dedicate this work.

Any mountain stream is dangerous to ford,
even the shallowest of them,
chiefly because of the way the bed shifts.
It's like a kaleidoscope, changing every day
with the force of the current,
and where there is a rock one day,
there will be a hole the next.

Mikhail Lermontov
A Hero of Our Time

¡Río Grande de Loíza!... Azul. Moreno. Rojo.
Espejo azul, caído pedazo azul de cielo;
desnuda carne blanca que se te vuelve negra
cada vez que la noche se te mete en el lecho;
roja franja de sangre, cuando bajo la lluvia
a torrentes su barro te vomitan los cerros.

Julia de Burgos
Río Grande de Loiza

How he loved this river...
Yes, he wanted to learn from it, he wanted to listen to it.
It seemed to him that whoever understood this river
and its secrets,
would understand much more, many secrets, all secrets.

Hermann Hesse
Siddhartha

ACKNOWLEDGEMENTS

Completion of this project required financial, professional, logistical, and emotional support from many organizations and individuals. Funds for this study were provided by the Water Resources Division of the National Park Service, the Water Resources Research Institute at the University of the Virgin Islands, the Virgin Islands Department of Planning and Natural Resources, and the Friends of the Virgin Islands National Park.

Thanks to Don Anderson and Rob Sampson, fellow graduate students at Colorado State University for setting the tone for the work presented here. Thanks to my committee members Prof. Ellen Wohl, Prof. Denis Dean, and Dr. Bill Jackson for useful feedback on my dissertation. Special thanks to my adviser Prof. Lee MacDonald for allowing this project to evolve according to our instincts and for always respecting the fact that this was MY dissertation project. Lee's many (and much needed) comments on earlier versions of my dissertation made this document what it is today.

My gratitude goes to: Rick Inglis from the National Park Service Water Resources Division, who devoted many hours and days providing technical and field support for this project; James St. Hillaire and Tom Atkinson for sharing the load of 600,000 lbs of sediment, many miles of road mapping and sometimes treacherous stream surveys, and countless mosquito bites; and Laurie Requa for her impeccable work in the lab.

Thanks to VI National Park personnel for providing lodging in beautiful Maho Bay. Thanks to Rafe Boulon (VINP) for providing a space in the lab where I could do my "dirty" work. Thanks to Dr. Caroline Rogers (USGS-Biological Resources Division) for her generosity in allowing me to tap into some of her project funds and for constantly reminding me that "it is all worth it at the end". Thanks to members of the Fish Bay Homeowners Association for looking after my equipment and for always stopping by to see how things were going. Thanks to the anonymous donor of cold drinks that I sometimes found in my Jeep after a long day in the field. Special thanks to the makers of "Caribe" for a truly refreshing, not-filling, and full-tasting beer.

In every acknowledgement section there is always a phrase stating something to the fact that "this project could not have been completed without the support..." In this case, this is absolutely true for the support that I got from Dr. Ed Towle, Mrs. Judith Towle, and Mr. Bruce Potter from the Island Resources Foundation. The Foundation not only provided a "classy Jeep" as my means of transportation, but also the means to extend my funding for an additional two years, a stage to disseminate the study findings in the VI and in the rest of the Eastern Caribbean,

and more importantly, an example of what true environmental work should be. I look forward to maintaining a close professional and personal relationship with you in the future.

Thanks to all of those who have supported me throughout the years... Gracias!

Thanks to my friends and family in Puerto Rico... Mami, Papi, Frankie, Jonnie, Ricky...

For love that follows me wherever I go.

Thanks to friends I met in California... Elim, Harold, Ray...

For much needed support several thousand miles away from home.

Thanks to friends in Colorado... the Báez and Martínez families, Juan Benavides...

For allowing me to feel at home 4,984 ft above sea level.

Thanks to friends in St. John... Jim, Trudy, Ginger, the Sunday volleyball crew ...

For not allowing me to go insane at sea level.

Thanks to my dear friends in Santiago de Cuba... Emma, Leo, Patri, Villa y los nenes...

For providing me with a second family.

Thanks to my wife Jossianna...

For being beautiful and for helping me find peace within myself.

Thanks to my Leilah...

For also being beautiful and for arriving just in time to share this achievement with me.

TABLE OF CONTENTS

<u>Chapter</u>	<u>Page</u>
1. INTRODUCTION	1
1.1 Project Background	1
1.2 Study Objectives	2
1.3 Physiography of St. John	3
1.3.1 Topography	3
1.3.2 Geology	3
1.3.3 Soils	4
1.3.4 Climate	4
1.3.5 Surface Hydrology	5
1.3.6 Vegetation	5
1.3.7 Land Use	6
1.4 Literature Review	6
1.4.1 Erosion Studies in St. John	6
1.4.2 Road Erosion	8
1.4.3 Sediment Budgets	10
1.5 Organization of Dissertation.	11
1.6 References Cited	12
2. MEASUREMENT AND PREDICTION OF ROAD SEGMENT SCALE SEDIMENT PRODUCTION	17
Abstract	17
2.1 Introduction	19
2.1.1 Problem Statement and Objectives	19
2.1.2 Modeling Road Sediment Production	20
2.2 Study Area	23
2.3 Methods	25
2.4 Results	28
2.4.1 Precipitation	28
2.4.2 Road Segment Sediment Production	29
2.4.3 General Linear Models for Graded and Ungraded Road Segments	32
2.4.4 Particle-Size Distribution	33
2.5 Discussion	34
2.5.1 Effects of Precipitation, Slope, and Grading in Road Sediment Production	34
2.5.2 Abandoned Roads and Undisturbed Hillslopes	36
2.5.3 Comparisons with Previous Studies	38
2.5.4 Recommendations for Road Erosion Control.	39
2.6 Conclusions.	40
2.7 References Cited	42
3. RUNOFF AND SEDIMENT YIELDS FROM AN UNPAVED ROAD SEGMENT	62
Abstract	62
3.1 Introduction	64
3.1.1 Problem Statement	64

3.1.2	Previous Road-Runoff Studies and Models	65
3.2	Study Area	67
3.3	Methods	68
3.3.1	Field Methods	68
3.3.2	Modeling Infiltration Capacity	69
3.3.3	Unit Hydrograph Runoff Modeling	72
3.3.4	Kinematic Wave Runoff Modeling	73
3.3.5	Model Calibration	75
3.3.6	Suspended Sediment Analysis and Modeling.	75
3.3.7	Model Application	76
3.4	Results	76
3.4.1	General Results	76
3.4.2	Infiltration Curve	77
3.4.3	GA-UH Model Calibration	78
3.4.4	GA-KW Model Calibration	79
3.4.5	Model Validation	80
3.4.6	Suspended Sediment Concentration and Yields	83
3.4.7	Model Application	84
3.5	Discussion	86
3.5.1	Predicted Runoff	86
3.5.2	Estimated Suspended Sediment Yields	87
3.6	Conclusions	90
3.7	References Cited	92
4.	MEASUREMENT AND PREDICTION OF NATURAL AND ANTHROPOGENIC SEDIMENT SOURCES	110
	Abstract	110
4.1	Introduction	112
4.2	Study Area	113
4.3	Methods	115
4.3.1	Streambank Erosion.	115
4.3.2	Treethrow	116
4.3.3	Plot-scale Runoff and Sediment Production	117
4.3.4	Runoff and Sediment Production from Zero- and First-order Catchments	118
4.3.5	Surface Erosion from Unpaved Road Segments	119
4.3.6	Sediment Production from Road Cutslopes	120
4.4	Results and Discussion	121
4.4.1	Streambank Erosion.	121
4.4.2	Sediment Delivery by Treethrow	123
4.4.3	Plot-scale Runoff and Sediment Production from Undisturbed Hillslopes	125
4.4.4	Runoff and Sediment Production from Zero- and First-order Catchments	126
4.4.5	Surface Erosion from Unpaved Roads	129
4.4.6	Sediment Production from Road Cutslopes	130
4.3	Conclusions	131
4.4	References Cited	134

5. DEVELOPMENT AND APPLICATION OF A GIS-BASED SEDIMENT BUDGET MODEL	153
Abstract	153
5.1 Introduction	155
5.2 Study Area	158
5.3 Field Methods and Results	159
5.4 St. John Sediment Budget model (STJ-EROS).	161
5.4.1 Overview	161
5.4.2 Input Routines	161
5.4.3 Sediment Yield Calculation Routines	164
5.5 Model Application	169
5.5.1 Basin Description	169
5.5.2 Predicted Sediment Yields	170
5.5.3 Effects of Varying Sediment Delivery Ratios on Basin-scale Sediment Yields	173
5.5.4 Comparison of Model Results to Other Sources of Data	175
5.6 Conclusions	178
5.7 References Cited	180
6. CONCLUSIONS, FUTURE RESEARCH, AND MANAGEMENT RECOMMENDATIONS	201
6.1 Runoff Generation from Hillslope Plots and Roads	201
6.2 Measuring and Predicting Sediment Production and Delivery	202
6.3 Recommendations for Future Research	204
6.5 Management Recommendations.	205
Appendix I-A Monthly Precipitation Totals Recorded During Study Period	209
Appendix I-B Relationship Between Road Sediment Production and Precipitation	215
Appendix I-C Summary of Road Erosion Model Regression Analysis	219
Appendix I-D Particle-size Distributions of Material Eroded from Unpaved Roads	224
Appendix II-A Hydrographs Used for Calibration of GA-UH and GA-KW Models	229
Appendix II-B Runoff Data and Model Results from Maho-Road	232
Appendix II-C Observed and predicted hydrographs: GA-UH Model	234
Appendix II-D Observed and predicted hydrographs: GA-KW Model	237
Appendix II-E Maho-Road Sediment Concentration.	240
Appendix III Particle-size Distributions of Material Eroded from Zero and First-Order Catchments	242
Appendix IV-A Characterization of the Stream Network in St. John	246
Appendix IV-B Spatial Database Requirements for STJ-EROS	259
Appendix IV-C STJ-EROS Routine Flowcharts	277
Appendix IV-D STJ-EROS Arc Macro Language Code	285
Appendix IV-E Suspended Sediment Yield from Main Fish Bay Gut Watershed	304

LIST OF FIGURES

	<u>Page</u>
 Chapter 1	
Figure 1. Map of St. John showing the VINP boundary.	16
 Chapter 2	
Figure 1. Map of St. John showing the locations of the rain gauges and road sediment traps.	48
Figure 2. Example of steep road segment in the Bordeaux Mountain area.	49
Figure 3. Sketches of the three types of road drainage patterns found on St. John.	49
Figure 4. Monthly precipitation over the study period at Maho Bay.	50
Figure 5. Frequency distribution of storm precipitation for Maho Bay during the study period and long-term rainfall at Caneel Bay.	50
Figure 6. Relationship between 15-minute erosivities and total storm precipitation at Maho Bay.	51
Figure 7. Relationship between sediment production and slope for seven recently-graded, light-usage road segments.	51
Figure 8. Example of a grading operation along road segment FB-Coco.	52
Figure 9. Relationship between sediment production and time since grading.	52
Figure 10. Relationship between mean sediment production and average slope for graded and ungraded road segments.	53
Figure 11. Predicted versus observed sediment production rates for graded and ungraded roads.	53
Figure 12. Relationship between sediment production and cumulative precipitation after grading.	54
Figure 13. Mass-weighted average particle size distributions for graded, ungraded, and abandoned roads.	54
Figure 14. Relationship between measured annual sediment production rates using sediment traps and rates predicted by the ROADMOD model.	55
Figure 15. Range of sediment production rates for roads in St. John compared to values from other studies.	55
 Chapter 3	
Figure 1. Map of the Maho Bay area.	97
Figure 2a. Photo of the lower sections of Maho Road.	98
Figure 2b. Photo of a portable cutthroat flume.	98
Figure 3. Relationship between precipitation and observed discharge for Maho Road.	99
Figure 4. Relationship between duration of discharge and infiltration rate for Maho Road.	99
Figure 5. Inferred infiltration curve for Maho Road.	100
Figure 6. Mean 2.5-minute unit hydrograph for Maho Road.	100
Figure 7. Total observed discharge against net predicted error for the GA-UH and GA-KW runoff models.	101

Figure 8.	Relationship between the coefficient of determination of predicted hydrographs against total discharge.	101
Figure 9.	Measured versus predicted peak flow rates.	102
Figure 10a.	Hyetograph, measured, and predicted hydrographs for the 5 January 2000 event.	103
Figure 10b.	Hyetograph, measured, and predicted hydrographs for the 27 September 1999-c event.	103
Figure 11.	Sediment rating curve for the Maho Road.	104
Figure 12.	Frequency distribution for the number of storm events, total rainfall, predicted discharge, and estimated sediment yields for 5 storm-size classes.	104
Figure 13.	Relationship between total rainfall and sediment production as estimated by the GA-KW sediment rating curve model.	105
Figure 14.	Particle-size distribution for sediment trap data and suspended sediment samples.	105

Chapter 4

Figure 1.	Map of St. John showing the location of measurement sites for natural sediment sources.	139
Figure 2a.	Photo of undisturbed plots in Haulover Bay.	140
Figure 2b.	Photo of undisturbed plot in Fish Bay.	140
Figure 3a.	Photo of graded road segment JH-A1.	141
Figure 3b.	Photo of ungraded road segment FB-Coco.	141
Figure 3c.	Photo of abandoned road segment LE-Top.	142
Figure 4.	Location of road travelway and cutslope sediment traps.	143
Figure 5.	Average bank retreat rates by study site.	144
Figure 6.	Annual sediment production rates from natural and road-related sediment sources.	144
Figure 7.	Runoff versus the sum of the antecedent precipitation index and storm rainfall for the three undisturbed hillslope plots.	145
Figure 8.	Depth of saturated zone against total storm precipitation.	145
Figure 9.	Particle-size distribution of sediment from zero- and first-order catchments.	146
Figure 10.	Relationship between sediment production and drainage area for hillslope plots, zero- and first-order catchments, and unpaved roads.	146
Figure 11.	Particle-size distribution of sediment from unpaved roads and cutslopes.	147

Chapter 5

Figure 1.	Map showing the three study basins.	184
Figure 2.	Measured sediment production rates from natural and anthropogenic sediment sources.	185
Figure 3.	Flow chart of the STJ-EROS model.	186
Figure 4.	Calculated sediment yields for the Lameshur Bay, Fish Bay, and Cinnamon Bay basins.	187
Figure 5a.	Map of sediment yields for unpaved roads and sediment delivery areas for the Lameshur Bay basin.	188
Figure 5b.	Map of sediment yields for unpaved roads and sediment delivery areas for the Fish Bay basin.	189
Figure 5c.	Map of sediment yields for unpaved roads and sediment delivery areas for	

	the Cinnamon Bay basin.	190
Figure 6a.	Relative contribution of natural and road-related sediment sources to Lameshur Bay.	191
Figure 6b.	Relative contribution of natural and road-related sediment sources to Fish Bay.	191
Figure 6c.	Relative contribution of natural and road-related sediment sources to Cinnamon Bay.	192
Figure 7a.	Relationship between sediment yields and sediment delivery ratios for Lameshur Bay.	192
Figure 7b.	Relationship between sediment yields and sediment delivery ratios for Fish Bay.	193
Figure 7c.	Relationship between sediment yields and sediment delivery ratios for Cinnamon Bay.	193

Chapter 6

Figure 1.	Relationship between runoff and storm precipitation for natural and road surfaces.	208
Figure 2.	Relationship between sediment yield and source area.	208

LIST OF TABLES

		<u>Page</u>
 Chapter 2		
Table 1.	Type, resolution, and period of record for raingauges used in this study.	56
Table 2.	Characteristics of the 21 monitored road segments.	57
Table 3.	R ² , p values, and slope coefficients for the relationship between sediment production and precipitation for 14 road segments.	58
Table 4.	Sediment production by road segment.	59
Table 5.	General linear regression model for predicting road sediment production.	60
Table 6.	Mean particle-size by road slope and grading road class.	61
 Chapter 3		
Table 1.	Summary of hydrologic and suspended sediment data from unpaved roads.	106
Table 2.	Characteristics of Maho Road.	107
Table 3.	List of storm events used for model calibration and testing.	107
Table 4.	Parameter values used for runoff model calibration.	108
Table 5.	Summary of model validation results.	109
 Chapter 4		
Table 1.	Summary of published bank retreat rates.	148
Table 2.	Summary of treethrow surveys along several streams in St. John.	148
Table 3.	Runoff and sediment production data from three undisturbed hillslope plots.	149
Table 4.	Sediment production rates from zero- and first-order catchments.	150
Table 5.	Cutslope characteristics and sediment production rates.	150
Table 6.	Summary of published cutslope sediment production rates.	151
Table 7.	Estimated contribution of cutslopes to road-segment scale sediment yields.	152
 Chapter 5		
Table 1.	Sediment production functions used by STJ-EROS.	194
Table 2a.	Variables and GIS data layers used by input routines in STJ-EROS.	195
Table 2b.	Variables and GIS data layers used by routines that calculate sediment yields in STJ-EROS.	196
Table 3.	Description of input data layers used by STJ-EROS.	197
Table 4.	Proportion of sediment by particle-size class for six sediment sources.	198
Table 5.	Characteristics of three basins where STJ-EROS was applied.	199
Table 6.	Comparison of sediment yields estimated by STJ-EROS to other data.	200

CHAPTER 1.

INTRODUCTION

1.1 Project Background

St. John is the third largest island composing the United States Virgin Islands and it is located approximately 80 km east of Puerto Rico (Figure 1). This 50 km² island is well known because of its pristine beaches and the richness of its marine environment. Approximately 56% of the total land area and 23 km² of its offshore waters are located within the boundaries of the Virgin Islands National Park. An additional 47 km² of its offshore waters were designated as the V.I. Coral Reef National Monument in 2001. The National Park Service, local authorities and residents have been concerned with the potential environmental impact induced by the rapid development that has occurred on privately-owned lands over the past 30 years. Increases in erosion and sediment delivery rates to the marine environment are perceived to be one of the most important environmental issues on St. John (Rogers, 1998).

Several studies have used the sediments deposited in bays and salt ponds to assess the impacts of land use on long-term erosion rates on St. John (Hubbard et al., 1987; Nichols and Brush, 1988). Hubbard et al. (1987) concluded that extensive agriculture during the plantation era on the island had “exceedingly long-term repercussions” on the rate of sediment delivery to the marine environment, and that these effects still dominated the effects of more recent development. On the other hand, Nichols and Brush (1988) found that land use during the plantation era had no massive effect on sedimentation in the Reef Bay swamp.

More recent attempts have complemented sedimentation data with direct estimates of sediment production rates from different sources (Anderson, 1994; Sampson, 2000). These studies determined that the unpaved road network is probably the major source of sediment on the island (MacDonald et al., 1997, 2001). While these earlier studies provided a basic understanding of erosion processes on St. John, a more intense and longer-term study was needed to better understand runoff and erosion rates, and the delivery of sediment to the marine environment.

1.2 Study Objectives

The main tasks of this study were to:

- Measure sediment production rates from road travelways, identify the factors controlling erosion rates, and develop an empirical model for road sediment production;
- Measure runoff from a road segment and develop two event-based runoff models;
- Couple the road segment runoff model to a sediment-rating curve to compare suspended sediment yields to those measured by a sediment trap;
- Measure sediment production from streambanks, treethrow, undisturbed hillslopes, and road cutslopes.
- Develop a GIS-based sediment budget model (STJ_EROS) using empirical sediment production and delivery functions;
- Apply STJ-EROS to three basins on St. John and estimate the contribution of unpaved roads to watershed-scale sediment yields.

The results of this study are expected to become a useful addition to the literature on erosion in the Virgin Islands and the Caribbean. The results also can improve the assessment of erosion problems in several ways. First, sediment yield rates for small islands in the Caribbean are not well documented (UNEP, 1994). This study will provide one of the few estimates of undisturbed sediment yield rates for dry tropical islands in the Caribbean. Knowledge of these background rates is required in any attempt to quantify the effects of land development. Second, even though unpaved road networks have been recognized as an important sediment source in other regions,

erosion from unpaved roads has been generally overlooked in the Caribbean. Third, the GIS-based STJ-EROS model will provide a means to quantify the relative contribution of different sediment sources, identify appropriate erosion control strategies, and aid in guiding future development.

1.3 Physiography of St. John

1.3.1 Topography

The topography of St. John is very rugged, as more than 80% of the island has slopes greater than 30%, and only about 9% of the island has slopes of 10% or less (CH2M Hill, 1979; Anderson, 1994). The island has a central ridge that runs east-west across the length of the island, and the highest point is Bordeaux Mountain at 387 m (Figure 1). Since the central ridge is closer to the northern coast of the island, watersheds draining to the south tend to be larger than their counterparts to the north. The shoreline is made up of sheltered coves or rocky promontories containing sand and cobble beach deposits.

This topography plays an important role in erosion and sediment transport processes. First, slope is a very important factor controlling surface erosion rates (Kirkby, 1980). Second, the steep topography affects the morphology of the stream network and its capacity to transport sediment.

1.3.2 Geology

The lithology of St. John is dominated by two distinct formations of volcanic origins (Meyerhoff, 1926; Donnelly, 1966; Rankin, 2002). The oldest rocks on the island are the basalt and volcanic wacke of the Water Island formation, and these were formed as volcanic flows on the ocean floor during the Early Cretaceous period. These volcanic rocks were eventually uplifted by regional tectonic stresses. The second period of rock development in St. John occurred as explosive shallow water and subaerial volcanism during the Late Cretaceous age.

These rocks form the Louisenhoj formation. These formations have eventually undergone periods of deformation and magmatic intrusions that hydrothermally altered some of these rocks. A limestone formation was deposited after the second volcanic period, but these rocks only have limited exposure on the island.

1.3.3 Soils

Soils are dominated by the Cramer clay loam series, which is characterized by a fine clayey matrix with abundant coarse fragments (Soil Conservation Service, 1970). These soils tend to be shallow (< 30 cm), moderately permeable, well-drained, and underlain by nearly impervious bedrock. The moderate permeability and high infiltration rates of these soils largely preclude the development of Hortonian (precipitation-excess) overland flow. Shallow soils underlain by a nearly impermeable layer favor the development of saturation overland flow. When overland flow does occur, the dense vegetation and high proportion of coarse fragments in the soil result in a high surface roughness that reduces runoff velocities and the potential for erosion.

1.3.4 Climate

The climate of St. John is described as dry tropical. Rainfall on the island falls frequently in the form of brief showers caused by the orographic lifting of the predominant easterly winds (Calversbert, 1970). The island has been divided into five zones based on annual average precipitation. Values range from 89-102 cm on the East End to 127-140 cm close to Bordeaux Mountain (Bowden et al., 1970). There are no sharply defined wet and dry seasons, but there is a relatively dry season from about February to July and a relatively wet season from August until January.

Easterly waves moving through the Caribbean are important sources of rainfall from May through November, while cold fronts affect the rainfall regime the rest of the year (Calversbert,

1970). Easterly waves sometime develop into tropical storms and hurricanes, which may result in large amounts of rain, strong winds, and high seas.

1.3.5 Surface Hydrology

Potential evapotranspiration (PET) is very high throughout the entire year. Bowden et al. (1970) estimated PET for two climatic stations in St. John using the Thornwaite method, and determined that the average monthly PET is generally greater than average monthly precipitation. The deficit of rainfall relative to PET means that the island has no perennial streams (MacDonald et al., 1997). The combination of steep slopes, small drainage areas, shallow soils with low water holding capacities, and occasional intense storm events results in “flashy” runoff hydrographs with steep rising and recession limbs. According to MacDonald et al. (1997), there is little evidence for widespread Horton overland flow, so peak runoff is controlled primarily by saturation overland flow and subsurface stormflow.

Runoff processes have never been formally studied in St. John. The nature of runoff development has important implications in how sediment is produced, stored, and transported through the landscape. While short-lived storms during dry periods are not likely to trigger runoff in the streams (known as guts in the Virgin Islands), these events produce runoff and sediment from road surfaces. This sediment is deposited on the hillslopes or in the guts until a larger storm triggers sufficient runoff to transport it through the stream network.

1.3.6 Vegetation

The original forests of St. John were eliminated or degraded and are now in various stages of recovery. Dry evergreen forests and shrubs cover approximately 63% of the total land area, moist forest and secondary vegetation cover about 30%, while urban, wetland, and pasture each cover about 2% of the island (Woodbury and Weaver, 1987).

1.3.7 Land Use

The history of land use in St. John is very similar to that of most of the islands in the eastern Caribbean. Originally St. John was completely forested and experienced only minor changes during the settling of Amerindian groups. During the 1700's and 1800's, approximately 90% of the forests were removed to be replaced by sugarcane fields (Tyson, 1987). The decline of the sugarcane industry in the late 19th century forced the abandonment of agricultural fields and the beginning of the forest recovery period. The United States purchased the Virgin Islands from Denmark in 1917, and in 1956 Virgin Islands National Park was established. The park was designated an International Biosphere Reserve in 1976, and it is one of the few reserves that has both marine and terrestrial resources (Rogers, 1992). In 2001 an additional 47 km² of offshore waters were designated as the V.I. Coral Reef National Monument.

The island currently is believed to be experiencing the highest sediment production and yield rates in historical times (MacDonald et al., 1997). Development on privately-owned lands outside the park boundaries has increased drastically over the past 30 years. Homesite development may affect erosion processes by: (1) clearing of forest vegetation; (2) displacing soil and rock into unstable areas; and (3) increasing the density of unpaved roads. For example, a 1971 aerial photograph indicated 8.3 km of roads in the 6.0 km² Fish Bay basin. By 2000 the road network had increased to 23.2 km with 13.1 km or 56% still unpaved. The unpaved road density of 2.2 km km⁻² in the Fish Bay basin contrasts to the unpaved road density of 0.8 km km⁻² in the 4.3 km² Greater Lameshur Bay basin (Nemeth et al., 2001). The Greater Lameshur Bay basin has remained mostly undeveloped, as most of it is within VINP.

1.4 Literature Review

1.4.1 Erosion Studies in St. John

One of the first publications dealing with erosion issues in the Virgin Islands was by Hubbard (1987). This report did not include any data, but it provided a good summary of the status of

sediment-related management strategies, and drew attention to the potential effects of sedimentation on coral reefs. It identified siltation and light attenuation as the most important adverse effects of increased sedimentation rates. Upland development and marine dredging were highlighted as the two main causes of these increased rates.

A contemporaneous study assessing the long-term impacts of historical development in St. John concluded that “[land] development impacts appear to still be exerting a secondary control behind the factors of watershed size and [bay] geometry” (Hubbard et al., 1987). The observed long-term decline in coral growth rates was attributed to the long-term delivery of sediments eroded during the plantation era.

Long-term sedimentation rates were estimated from core samples taken from the Reef Bay swamp and Mandal Pond on the southern part of St John (Nichols and Brush, 1988) (Figure 1). These deposits consisted of 8% sand, 23% silt, and 69% clay, and the estimated sediment yield rates were on the order of 40 tons per year over the past 3,000 years. The authors concluded that the effects of humans on sedimentation rates over several thousand years were minor compared to the natural variations.

The ANSWERS model was applied to the Great Cruz Bay basin and the estimated suspended sediment loads for individual storms with recurrence intervals of less than two years ranged from 15 to 4,100 tons km⁻² (Ramsarran, 1992). These sediment yield rates are up to two orders of magnitude higher than the annual sediment yields estimated by other studies.

Watershed-scale sediment yield rates for St. John were estimated to range from 7 to 40 tons km⁻² yr⁻¹ as part of a sediment budget study (Anderson, 1994). These long-term estimates are at the low end of rates for tropical forests, but are justified by the occurrence of low erodibility of the soils, the relatively dry climatic regime, and the rare occurrence of mass wasting processes (De Graff et al., 1989; MacDonald et al., 1997). Anderson (1994) concluded that current sediment yield rates are higher than during any other historical period. Application of a simple GIS-based road erosion model (ROADMOD) identified the unpaved road network as an

important source of sediment. The unpaved road network was estimated to be quadrupling natural sediment yields in the Fish Bay basin, while in Lameshur Bay roads were estimated to be increasing sediment yields by only 40% above background levels (Anderson and MacDonald, 1998).

Anderson and MacDonald (1998) made the following recommendations for future research: (1) estimate erosion from road cuts, fill slopes, and drainage ditches; (2) develop a time-dependent variable for estimating road erosion rates; (3) calibrate the road erosion model to individual runoff events so that varying weather conditions can be simulated; and (4) integrate the road sediment production model with hillslope and stream channel sediment production and delivery models. This study addresses most of these recommendations.

In another study, runoff and sediment production rates were measured from undisturbed hillslopes and road surfaces (Sampson, 2000; MacDonald et al., 1997). Plots on undisturbed hillslopes produced runoff only during large rainfall events related to hurricanes and no measurable sediment. Plots on unpaved roads produced measurable amounts of runoff for all storms exceeding 6 mm of rainfall. Sediment production rates from unpaved roads were strongly correlated with storm energy. Road-segment scale sediment production measured by sediment fences ranged from 0.1 to 7 kg m⁻² yr⁻¹. Erosion rates at the road-segment scale were only 20-30% of the values measured at the plot-scale (0.9 to 15 kg m⁻² yr⁻¹).

1.4.2 Road Erosion

Erosion of road surfaces has been identified as an important erosion problem in a wide variety of forested areas. Roads have proven to be an important source of sediment in forested areas of the Pacific Northwest of the United States (e.g., Reid et al., 1981), New Zealand (Fahey and Coker, 1989), Australia (Grayson et al., 1993), Kenya (Dunne, 1979), Ecuador (Harden, 1992), and on St. John in the U.S. Virgin Islands (MacDonald et al., 1997). The seriousness of the problem in the United States may be appreciated by the following statement: "... sediment

production from forest roads is the greatest problem in the mountains of the Pacific coast from Alaska to California, the northern and central Rocky Mountains, and the mountainous East” (Burroughs et al., 1991). Surface erosion from roads can be an important source of fine sediment, even in areas with a high frequency of mass wasting (e.g., Reid et al., 1981).

In sloping terrain the road prism typically consists of three main surfaces: the travelway, cutslope, and fillslope. Since erosion processes act at different rates on each of these surfaces, sediment production rates were measured from both road travelways and cutslopes.

Travelways have been the subject of numerous studies, and they can be the main source of fine sediment being delivered to streams (e.g., Reid, 1981). The road tread poses a challenge to researchers because these surfaces are affected by unique processes, such as traffic and regrading, that can affect erosion rates. Ramos (1997) suggested that the factors affecting sediment production from roads can be grouped into two categories: (1) those that significantly change over time; and (2) those that are more stable with time. Variable factors include road age, road use, road maintenance, the particle-size distribution of the road surface material, road drainage patterns, and climate. Constant factors are primarily road surfacing, and road gradient.

Sediment production from cutslopes may be induced by mass wasting, rockfall, dry ravel, rainsplash, and rilling (Ramos, 1997). Studies have shown that sediment production rates from cutslopes may be controlled by cutslope age, climatic regime, aspect, cutslope gradient, strength of parent material, vegetation density, and hillslope drainage area. Sediment produced from cutslopes is never delivered directly to the fluvial system, as it is first routed to an inside ditch, where it is either transported by runoff or removed during maintenance operations. This study estimates the rate at which cutslopes contribute to road-segment scale sediment production.

A large number of methods have been used to quantify road sediment production and the contribution of roads to sediment yields (Ramos, 1997). One general approach has been to measure watershed-scale sediment yields from areas before and after road construction (e.g., Beschta, 1978; Rice et al., 1979; Anderson and Potts, 1987; Grayson et al., 1993). Other studies

have quantified small-scale sediment production rates from centimeter-scale rainfall simulators (Harden, 1992), bounded field plots with rainfall simulators (e.g., Johnston et al., 1980; Burroughs and King, 1989; Burroughs et al., 1991), small bounded plots under natural precipitation events (e.g., Vincent, 1979; Sampson, 2000), and flume experiments (Zhang and Cundy, 1987). Other studies have measured sediment production rates at the road segment scale by measuring runoff rates and collecting suspended sediment samples manually (e.g., Reid, 1981) or with automatic samplers (Kahklen, 1993), flow splitters (e.g., Swift, 1984), or sediment-runoff collection troughs (e.g., Luce and Black, 2001). Others have estimated road erosion rates from volumetric analysis of rilled surfaces (Froehlich, 1991; Anderson and MacDonald, 1998). The sediment fence method (Robichaud and Brown, 2002) was used to measure sediment production rates from unpaved roads as part of this study. This method was also used to measure road erosion rates in a smaller, shorter-term study on St. John (MacDonald et al., 2001).

1.4.3 Sediment Budgets

According to Reid and Dunne (1996) a sediment budget is "... an accounting of the sources and disposition of sediment as it travels from its point of origin to its eventual exit from a drainage basin." The method for developing a sediment budget was first outlined by Gilbert (1917) and first implemented in a field-based measuring strategy by Leopold et al. (1966). The methodology gained popularity in the early 1980's when it was recognized as an useful tool to assess the effects of forestry and other land disturbances on sediment production and sediment yields. Swanson et al. (1982) define a sediment budget as "a quantitative description of the movement of sediment through a single landscape unit". This definition implies the estimation of sediment production rates from areas with relatively homogeneous physical characteristics. In this study landscape units were defined and used to stratify measurements of sediment production measurements from natural and anthropogenic sources. These data were used to develop empirical sediment production models within a GIS-based sediment budget model (STJ_EROS).

The development of a sediment budget also requires a routing component. STJ_EROS uses sediment delivery ratios to estimate watershed-scale sediment delivery rates. The sediment delivery ratio (SDR) has been defined as the ratio of sediment delivered to the catchment outlet to the gross erosion occurring within the basin (Walling, 1983). SDR's have been used in previous GIS models, as they provide simple sediment routing procedures when the data required for more physically-based models are not available. The sediment delivery ratios used in STJ_EROS calculate the long-term ratio of sediment delivered to the marine environment (i.e., not retained within the fluvial network, salt ponds, or coastal wetlands).

1.5 Organization of Dissertation

This dissertation is organized into six chapters. Chapter 2 discusses the measurement and modeling of sediment production from 21 unpaved road segments with varying slopes, drainage areas, and frequency of grading. Chapter 3 presents detailed runoff and suspended sediment measurements from an unpaved road segment in the Maho Bay area, and the use of these data to develop and test two runoff models. Sediment production rates from streambank erosion, treethrow, undisturbed areas, and road cutslopes are presented in Chapter 4. Chapter 5 describes the development of the STJ-EROS sediment budget model and its application to three different basins on St. John. Chapter 6 presents the overall conclusions of the study, identifies additional research needs, and presents recommendations for resource managers and regulatory agencies.

1.6 References Cited

- Anderson B, Potts DF. 1987. Suspended sediment and turbidity following road construction and logging in western Montana. *Water Resources Bulletin* 23: 681-690.
- Anderson DM. 1994. Analysis and modeling of erosion hazards and sediment delivery on St. John, US Virgin Islands. Tech. Rep. NPS/NRWRD/NRTR/34, US National Park Service, Fort Collins, CO, 153 p.
- Anderson DM, MacDonald LH. 1998. Modelling road surface sediment production using a vector geographic information system. *Earth Surface Processes and Landforms* 23: 95-107.
- Beschta RL. 1978. Long-term patterns of sediment production following road construction and logging in the Oregon Coast Range. *Water Resources Research* 14(6): 1011-1016.
- Bowden MJ, Fischman N, Cook P, Wood J, and Omasta E. 1970. Climate, water balance, and climatic change in the north-west Virgin Islands. Caribbean Research Institute, College of the Virgin Islands, 127 p.
- Burroughs ER, King JG. 1989. Reduction of soil erosion on forest roads. US Forest Service, General Technical Report INT-264, Ogden, UT, 21 p.
- Burroughs ER, Foltz RB, Robichaud PR. 1991. United States Forest Service research on sediment production from forest roads and timber harvest areas. Proceedings of the 10th World Forestry Congress; 187-193.
- Calversbert RJ. 1970. Climate of Puerto Rico and the U.S. Virgin Islands. Climatography of the United States No. 60-52, US Dept. of Commerce, 29 p.
- CH2M Hill. 1979. A sediment reduction program: Report to the Department of Conservation and Cultural Affairs, Government of the U.S. Virgin Islands, St. Thomas, U.S.V.I.
- DeGraff JV, Bryce R, Jibson RW, Mora S, Rogers CT. 1989. Landslides: Their extent and significance in the Caribbean. In Landslides: Extent and Economic Significance, Proceedings of the 28th International Geological Congress: Symposium on Landslides, Brabb EE, Harrod BL (eds.), Washington D.C., 17 July 1989, pp. 51-80.
- Donnelly TW. 1966. Geology of St. Thomas and St. John. *Geological Society of America Memoir* 98: 85-176.
- Dunne T. 1979. Sediment yield and land use in tropical catchments. *Journal of Hydrology* 42: 281-300.
- Fahey BD, Coker RJ. 1989. Forest road erosion in the granite terrain of southwest Nelson, New Zealand. *Journal of Hydrology (NZ)* 28(2): 123-141.
- Froehlich W. 1991. Sediment production from unmetalled road surfaces. In *Sediment and stream water quality in a changing environment: Trends and explanation*, IAHS Publication 203: 21-29.

- Gilbert GK. 1917. Hydraulic-mining debris in the Sierra Nevada, US Geological Survey Professional Paper 105, 154 p.
- Grayson RB, Haydon SR, Jayasuriya MDA, Finlayson BL. 1993. Water quality in mountain ash forests- separating the impacts of roads from those of logging operations. *Journal of Hydrology* 150: 459-480.
- Harden CP. 1992. Incorporating roads and footpaths in watershed-scale hydrologic and soil erosion models. *Physical Geography* 13(4): 368-385.
- Hubbard DK. 1987. A general review of sedimentation as it relates to environmental stress in the Virgin Islands Biosphere Reserve and the eastern Caribbean in general. Biosphere Reserve Report no. 20, Virgin Islands Resource Management Cooperative, St. Thomas, USVI, 42 p.
- Hubbard DK., Stump JD, Carter B. 1987. Sedimentation and reef development in Hawknest, Fish and Reef Bays, St. John. US Virgin Islands. Biosphere Reserve Research Rep. No. 21, Virgin Islands Resource Management Cooperative, St. Thomas, 99 p.
- Johnston RS, Sundberg ES, Burroughs ER, Armijo JD. 1980. Simulated rainfall to generate runoff and sediment from surface mine haul roads. In Proceedings of the Symposium on Surface Mining Hydrology, Sedimentology, and Reclamation, University of Kentucky, Lexington, KY; 75-82.
- Kahklen KF. 1994. Surface erosion from a forest road, Polk Inlet, Prince of Wales Island, Alaska. M.S. thesis, Oregon State University, Corvallis, OR, 95 p.
- Kirkby MJ. 1980. Modelling water erosion processes. In *Soil Erosion*, Kirkby MJ, Morgan RPC (eds.). John Wiley, New York; 425-442.
- Leopold LB, Emmet WW, Myrick RM. 1966. Channel and hillslope processes in a semiarid area, New Mexico, US Geological Survey Professional Paper 352G: 193-253.
- Luce CH, Black TA. 2001. Spatial and temporal patterns in erosion from forest roads. In: Influence of Urban and Forest Land Uses on the Hydrologic-Geomorphic Responses of Watersheds. Wigmosta MS, Burges SJ (eds.). Water Resources Monographs, American Geophysical Union, Washington, DC; 165-178.
- Meyerhoff HA. 1926. Geology of the Virgin Islands, Culebra, and Vieques: Physiography. N.Y. Academy of Sciences Scientific Survey of Porto Rico and the Virgin Islands 4(1): 71-141.
- MacDonald LH, Anderson DM, Dietrich WE. 1997. Paradise threatened: Land use and erosion on St. John, U.S. Virgin Islands. *Environmental Management* 21(6): 851-863.
- MacDonald LH, Sampson RW, Anderson DM. 2001. Runoff and road erosion at the plot and road segment scales, St. John, US Virgin Islands. *Earth Surface Processes and Landforms* 26: 251-272.
- Nemeth RS, MacDonald LH, Ramos-Scharrón CE. 2001. Delivery, deposition, and effects of land-based sediments on corals in St. John, U.S. Virgin Islands. *Water Resources*

- Research Institute-University of the Virgin Islands, St. Thomas, USVI, Report on project no. VI99-2, 24 p.
- Nichols MN, Brush GS. 1988. Man's long-term impact on sedimentation: Evidence from salt pond deposits. Biosphere Reserve Research Rep. No. 23, Virgin Islands Resource Management Cooperative, St. Thomas, 26 p.
- Ramos CE. 1997. Surface Erosion from Roads: A Literature Review and General Recommendations for the Development of a Sediment Monitoring Strategy. Unpublished report to the Northwest Indian Fisheries Commission, Olympia, Washington, 66 p.
- Ramsarran C. 1992. Simulation of the effects of urbanization on soil loss and runoff from a small tropical watershed using the ANSWERS model. MS thesis, Colorado State University, Fort Collins, Colorado, 119 p.
- Rankin DW. 2002. Geology of St. John, U.S. Virgin Islands. U.S. Geological Survey professional paper 1631, 36 p.
- Reid LM. 1981. Sediment production from gravel-surfaced roads, Clearwater Basin, Washington. University of Washington Fisheries Research Institute, FRI-UW-8108, Seattle, WA, 301 p.
- Reid LM, Dunne T, Cederholm CJ. 1981. Application of sediment budget studies to the evaluation of logging road impact. *Journal of Hydrology (N.Z.)* 20(1): 49-62.
- Reid LM, Dunne T. 1996. Rapid evaluation of sediment budgets. Reiskirchen, Germany: Catena Verlag, 164 p.
- Rice RM, Tilley FB, Datzman PA. 1979. A watershed's response to logging and roads: South Fork of Caspar Creek, California, 1967-1976. US Forest Service, Research Paper PSW-146, Berkeley, CA, 12 p.
- Robichaud PR, Brown RE. 2002. Silt fences: An economical technique for measuring hillslope soil erosion. General Technical Report RMRS-GTR-94, US Forest Service, Rocky Mountain Research Station, Fort Collins, CO; 24 p.
- Rogers CS. 1998. Coral reefs of the U.S. Virgin Islands. In: Status and Trends of the Nation's Biological Resources, Vol. I. P. Haeker & P.D. Doran (eds.). U.S. Department of the Interior, U.S. Geological Survey, Reston, VA; 322-324.
- Rogers CS. 1992. An integrated approach to marine and terrestrial research in Virgin Islands National Park and Biosphere Reserve. *Park Science* 12(2): 1,27.
- Sampson RW. 2000. Road runoff and erosion at the plot and road segment scales on St John US Virgin Islands. MS thesis, Department of Earth Resources, Colorado State University, Fort Collins, 189 p.
- Soil Conservation Service. 1970. Soil Survey, Virgin Islands of the United States. 78 p.
- Swanson FJ, Janda RJ, Dunne T, Swanston DN. 1982. Introduction: Workshop on sediment budgets and routing in forested drainage basins. In, F.J. Swanson et al. (eds.) *Sediment*

- Budgets and Routing in Forested Drainage Basins. US Forest Service General Technical Report PNW-141, Corvallis, OR; 1-4.
- Swift LW. 1984. Soil losses from roadbeds and cut and fillslopes in the Southern Appalachian Mountains. *Southern Journal of Applied Forestry* 8:209-216.
- Tyson GF. 1987. Historic land use in the Reef Bay, Fish Bay and Hawknest Bay watersheds, St. John, US Virgin Islands, 1718-1950. Virgin Islands Resource Management Cooperative, Biosphere Reserve Report No. 19, 54 p.
- UNEP. 1994. Regional overview of land-based sources of pollution in the Wider Caribbean Region. CEP-Technical Report No. 33, 56 p.
- Vincent KR. 1979. Runoff and erosion from a logging road in response to snowmelt and rainfall. M.S. thesis, University of California-Berkeley, 60 p.
- Walling DE. 1983. The sediment delivery problem. *Journal of Hydrology* 65: 209-237.
- Woodbury RO, Weaver PL 1987. The vegetation of St. John and Hassel Island, U.S. Virgin Islands. National Park Service, Southeast Region, Research/Resources Management Report SER-83, Atlanta, GA; 26 p.
- Zhang W, Cundy T. 1987. Test of a surface runoff and soil erosion model for forest road surfaces. In *Erosion and Sedimentation in the Pacific Rim*, Proceedings of the Corvallis Symposium, August 1987, IAHS Publication 165: 263-264.

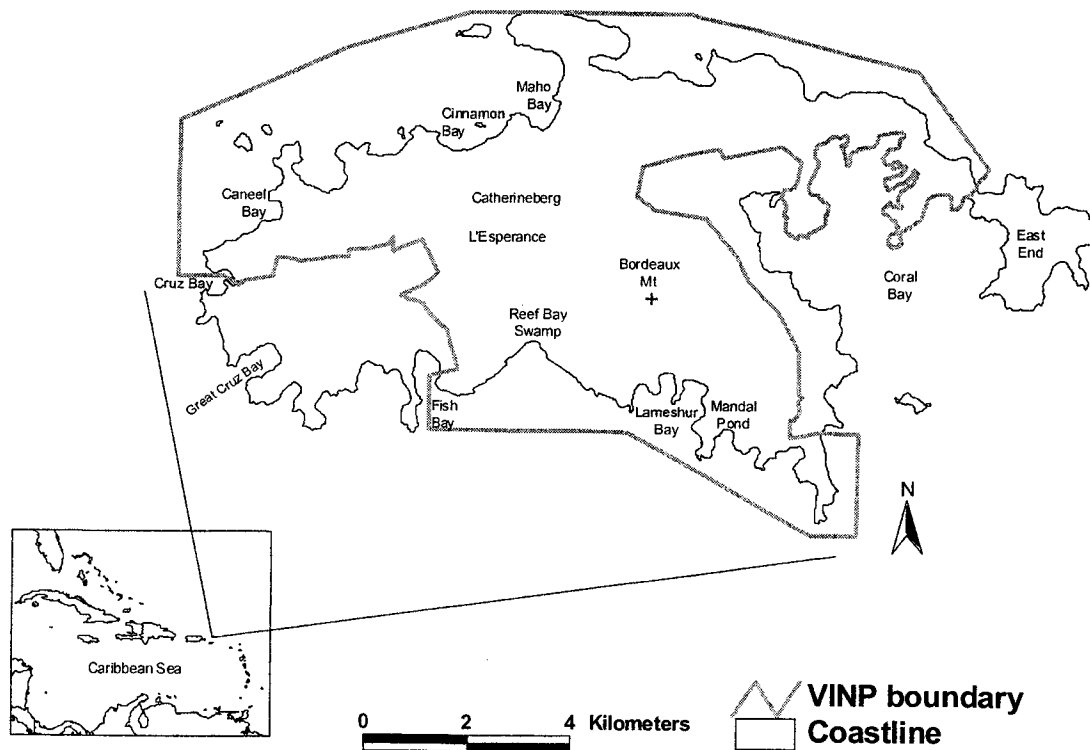


Figure 1. Map of St. John showing the boundaries of Virgin Islands National Park.

CHAPTER 2.
MEASUREMENT AND PREDICTION OF SEDIMENT PRODUCTION FROM
UNPAVED ROADS, ST. JOHN, U.S. VIRGIN ISLANDS

ABSTRACT

Excess delivery of land-based sediments is an important control on the overall condition of nearshore coral reef ecosystems. Unpaved roads have been identified as the primary sediment source on St. John in the U.S. Virgin Islands. An improved understanding of road sediment production rates is needed to guide future development and erosion control efforts. The main objectives of this study were to: (1) measure sediment production rates at the road segment scale; (2) evaluate the importance of precipitation, site factors, traffic, and grading on road sediment production; (3) develop an empirical road erosion predictive model; and (4) compare our measured erosion rates to other published data. Sediment production from 21 road segments was monitored with sediment traps from July 1998 to November 2001. The selected road segments had varying contributing areas, slopes, and traffic loads. Precipitation was measured by four recording rain gauges.

Sediment production was related to total precipitation and to road segment slope. After normalizing by precipitation and slope, the mean sediment production rate for roads that had been graded within the last two years was $0.96 \text{ kg m}^{-2} \text{ cm}^{-1} \text{ m m}^{-1}$ or approximately $11 \text{ kg m}^{-2} \text{ yr}^{-1}$ for a typical road with a 10% slope and an annual rainfall of 115 cm yr^{-1} . The mean erosion rate for ungraded roads was 41% lower, or $0.56 \text{ kg m}^{-2} \text{ cm}^{-1} \text{ m m}^{-1}$. The normalized mean sediment

production rate for road segments that had been abandoned for over fifteen years was only about 10% of the mean value for ungraded roads. Traffic loads were not related to sediment production. Multiple regression analysis led to the development of an empirical model based on precipitation, slope to the 1.5 power, and a categorical grading variable.

The measured and predicted erosion rates indicate that roads are capable of increasing hillslope-scale sediment production rates by up to four orders of magnitude relative to undisturbed conditions. The values from St. John are at the high end of reported road erosion rates, a finding that is consistent with the high rainfall erosivities on the island. Other than paving, the most practical methods to reduce current erosion rates is to minimize the frequency of grading and to improve road drainage design.

2.1 Introduction

2.1.1 Problem Statement and Objectives

Unpaved roads have been shown to be a primary sediment source and cause of increased sediment yields in a wide range of forested areas (e.g., Luce and Wemple, 2001; Megahan, 1987). The disruption of geomorphologic and hydrologic processes by roads increases both surface erosion and the frequency of mass wasting (e.g., Larsen and Parks, 1997; Sidle et al., 1985; Gresswell et al., 1979). These increases are of particular concern in forested areas because the natural erosion rates are very low. Surface erosion from unpaved road surfaces has been shown to be an important sediment source in Australia (Grayson et al., 1993), New Zealand (Fransen et al., 2001; Fahey and Coker, 1989), Malaysia (Douglas et al., 1993), the United States (e.g., Reid and Dunne, 1984; Burroughs et al., 1991), Poland (Froehlich and Walling, 1997; Froehlich, 1991), Ghana (Kumapley, 1987), and Kenya (Dunne, 1979).

Collaborative work among geomorphologists, hydrologists, and stream ecologists has helped document the adverse impacts of excessive sediment inputs on freshwater fluvial systems (e.g., Everest et al., 1987; National Research Council, 1992; Waters, 1995). Marine ecosystems, such as nearshore coral reef communities, also can be adversely affected by excessive inputs of fine sediment following land disturbance (Hubbard, 1987; Hodgson, 1989, 1997; Rogers, 1990). The effects of increased erosion on reef communities is of particular concern in the Caribbean because of the high potential erosion rates following disturbance and the importance of coral reefs to the tourism-based economy. In recent years marine ecologists have documented the effects of high sediment inputs on coral reefs in the Dominican Republic (Torres et al., 2001), Puerto Rico (Acevedo et al., 1989; Torres, 2001) and the nearby island of Culebra (Hernández-Delgado, 2001), Virgin Gorda in the British Virgin Islands (C. Rogers, USGS, pers. comm., 2001), as well as in St. Croix (Hubbard, 1986), St. Thomas (Nemeth and Nowlis, 2001) and St. John (Rogers, 1998; Nemeth et al., 2001) in the U.S. Virgin Islands.

Within the U.S. Virgin Islands, the coral reefs near St. John have received special attention because 56 percent of the island's 50 km² of land area and 23 km² of its offshore waters comprise Virgin Islands National Park (Figure 1) and have been designated as a Biosphere Reserve. In 2001 an additional 47 km² of offshore waters were designated as the Virgin Islands Coral Reef National Monument. Previous research showed that sediment production rates from unpaved roads are several orders of magnitude higher than sediment production rates from undisturbed hillslopes, and that unpaved roads were probably the primary source of the fine sediment being delivered to the marine environment (MacDonald et al., 2001). The cross-sectional area of rills on the road surface was used to develop an empirical road erosion model based on road segment area times slope (Anderson and MacDonald, 1998). The application of this model suggested that road erosion is increasing watershed-scale sediment yields by up to four times above background levels (MacDonald et al., 1997), but their work did not directly measure road erosion or several key factors shown to affect road erosion in other areas.

The development of improved predictive equations is needed to better estimate sediment production and delivery from different road segments, identify erosion control strategies, and guide future development. Hence the specific objectives of this study were to: (1) measure sediment production rates from unpaved road surfaces; (2) evaluate the effect of precipitation, slope, contributing area, traffic, and grading on sediment production rates; (3) develop a model to predict road sediment production rates; and (4) compare the measured road sediment production rates to published data from St. John and elsewhere.

2.1.2 Modeling Road Sediment Production

An exposed soil surface is subject to two primary surface erosion processes—raindrop impact and the shear stress of overland flow. Rainsplash energy is a function of precipitation intensity as well as the size and terminal velocity of the raindrops (Carter et al., 1974; Wischmeier and Smith, 1958). Flow hydraulics determine the shear stress of surface runoff, while the resistance to

erosion is controlled by the size and cohesion of the underlying material. If one assumes that rainsplash erosion is rapidly eliminated after surface runoff has begun (Moss and Green, 1983), the surface erosion rate (E_t) is proportional to the difference between the shear stress applied by overland flow (τ) and the resistance of the material to erosion (τ_c) (equation 1):

$$E_t \propto k_1 (\tau - \tau_c)^n \quad (\text{eq. 1})$$

where k_1 is an index of the erodibility of the sediment and n is an exponent between 1 and 2 (Kirkby, 1980). The shear stress applied by overland flow is equal to:

$$\tau = \rho_w g h s \quad (\text{eq. 2})$$

where ρ_w is the density of water, g is the acceleration due to gravity, h is the depth of flow, and s is the water surface slope (Julien, 1995). τ_c is generally a function of the particle-size distribution, as this controls the exposure of particles to hydraulic forces, the cohesive forces between particles, and the tractive force needed to detach individual particles (Knighton, 1998).

Infiltration rates on unpaved roads are typically very low (Ziegler and Giambelluca, 1997; Harden, 1992; Bren and Leitch, 1985). Hence, the frequency and magnitude of infiltration-excess (Horton) overland flow is much greater from unpaved roads than undisturbed areas. On St. John only 3-6 mm of precipitation are needed to initiate overland flow on unpaved road surfaces (MacDonald et al., 2001; Ramos-Scharrón and MacDonald, 2001; Chapter 3). Equations 1 and 2 indicate that the surface erosion rate is directly proportional to flow depth. The continuity equation for a road segment requires that the inflow rate [$Q_i(t)$] must equal the outflow rate [$Q_o(t)$] plus temporary water storage [$S(t)$] as shown in equation 3:

$$Q_i(t) = Q_o(t) + S(t) \quad (\text{eq. 3})$$

For an isolated road segment, the inflow rate is determined by precipitation excess, which is the difference between precipitation intensity $[P(t)]$ and infiltration rate $[I(t)]$ times the surface area of the road segment (A) (equation 4):

$$Q_i(t) = [P(t) - I(t)] \cdot A \quad (\text{eq. 4})$$

Since storage and outflow rates are each a function of water depth, increasing inflow (precipitation excess) increases flow depth and thus the potential for surface erosion (equation 2).

Parent material exerts a major control on the resistance to erosion of unpaved roads by controlling the surface particle-size distribution (Luce and Black, 1999). The particle-size distribution of the road surface is affected by the amount and type of traffic (e.g., Wald, 1975; Reid, 1981; Grayson et al., 1993; MacDonald et al., 2001), the preferential erosion of particles in a given size class, and time since construction or grading.

The amount and type of traffic affects road surface erodibility by increasing the availability of fine particles by particle attrition between storms (Bilby et al., 1989; Kahklen, 1993; Foltz, 1996; Ziegler et al., 2001a) and the pumping of fine particles onto the surface as the road tread is compacted, especially during wet conditions (Ziegler et al., 2001b; Bilby et al., 1989; Reid, 1981). Gravel roads subjected to more than four heavy truck passes per day have been found to have higher erosion rates than roads with less traffic (Reid and Dunne, 1984).

Newly-constructed and freshly-resurfaced roads typically have very high sediment production rates due to the abundance of easily-erodible fine particles (Megahan and Kidd, 1972; Megahan et al., 1986). The rapid erosion of fine sediment immediately after construction or regrading leads to a coarsening of the road surface, which increases its resistance to erosion. Only a few studies have directly measured time trends in sediment production after regrading. In the Oregon Coast Range blading of the ditch along gravel-surfaced roads increased sediment production rates more than road surface grading alone (Black and Luce, 1999; Luce and Black 1999, 2001a, b). On St. John the absence of road ditches and vehicle rutting keeps much of the runoff on the road

surface and allows it to readily access and transport the loose, fine sediment applied during grading.

The decline in road erosion rates after construction or grading has been modeled using equation 5:

$$E_t = E_n + k_2 S_0 e^{-k_2 t} \quad (\text{eq. 5})$$

where E_t is the erosion rate in $\text{tons km}^{-2} \text{ day}^{-1}$, E_n is the erosion rate approached after a long period without any disturbance ($\text{tons km}^{-2} \text{ day}^{-1}$), S_0 is the total amount of material available for erosion immediately after construction or grading (tons km^{-2}), k_2 (in days^{-1}) is an index of the rate of decline in erosion following the disturbance, and t is the time after disturbance in days (Megahan, 1974).

The dependence of erosion rates on the interplay between the available energy and the erodibility of loose material has led to the development of a dynamic erodibility model for unpaved road surfaces (Ziegler et al., 2000, 2001a, b). These studies modeled the changes in surface erodibility over time as a function of traffic and the degree to which the road surface has been depleted of highly erodible material.

Given this theoretical background, our study design, field measurements, and model development efforts focused on precipitation characteristics, road slope, active road area, traffic, and time since grading, as these factors control the amount of runoff, the tractive forces applied by overland flow, and the resistance of the road surface to erosion.

2.2 Study Area

St. John is the third largest island of the U.S. Virgin Islands, and it lies in the eastern Caribbean approximately 80 km east of Puerto Rico (Figure 1). The topography is very rugged, as more than 80% of the slopes are greater than 30% (CH2M Hill, 1979; Anderson, 1994). Bordeaux Mountain is the highest point of the island at an elevation of 387 m.

The lithology of St. John is dominated by rocks originating from volcanic flows (Donnelly, 1966; Rankin, 2002) that have undergone periods of deformation, magmatic intrusions, and hydrothermal alterations. Soils are dominated by gravelly loams and clay loams (USDA, 1995). They have a fine clayey to loamy matrix with abundant coarse fragments (Soil Conservation Service, 1970). The soils tend to be shallow, moderately permeable, well drained, and underlain by nearly impervious bedrock (USDA, 1995).

The climate of St. John is characterized as dry tropical. Bowden et al. (1970) identified five precipitation zones ranging from a low of 89-102 cm yr⁻¹ on the eastern end of the island to a high of 127-140 cm yr⁻¹ near Bordeaux Mountain. Easterly waves, which can develop into tropical storms and hurricanes, generate most of the rainfall from May through November, while cold fronts are important sources of rainfall from December through April (Calversbert, 1970). There are no sharply defined wet and dry seasons in the Virgin Islands, but a relatively dry season extends from about February to July, and a relatively wet season lasts from August until January (Bowden et al., 1970). Mean monthly potential evapotranspiration (PET) exceeds mean monthly precipitation for most of the year (Bowden et al., 1970; Sampson, 2000), so there are no perennial streams on St. John (MacDonald et al., 1997).

Precipitation in St. John is highly erosive. The average annual erosivity at Caneel Bay was estimated to be 13,500 MJ mm ha⁻¹ hr⁻¹ (Sampson, 2000). The 15-minute precipitation intensity at Caneel Bay exceeded 100 mm hr⁻¹ sixteen times from 1979 to 1995.

Dry evergreen forests and shrubs cover approximately 63% of the total land area, moist forest and secondary vegetation about 30%, while urban, wetland, and pasture each cover about 2% of the island (Woodbury and Weaver, 1987). Rapid development on privately-owned lands over the past 30 years has resulted in a dense road network on St. John.

Construction and maintenance standards of the unpaved roads on St. John are generally very poor. The spacing of road drainage structures (i.e., ditches, culverts, or cross-drains) is very sparse, even on extremely steep road segments. As a result of the high rainfall erosivity and poor

drainage design, deep rills commonly develop on the road surface, especially on the steeper road segments (Figure 2). On these segments regrading is done every year or so to facilitate the passage of standard passenger cars.

2.3 Methods

Precipitation was measured with four recording rain gauges (Figure 1). Table 1 lists the type, resolution, and period of record for each rain gauge. The precipitation recorded at each station was compared to monthly and annual means (Bowden et al., 1970) and to the mean values measured at Caneel Bay from 1979 to 1995 (EarthInfo, 1996). The precipitation data were used to determine total storm precipitation and 15-minute erosivities following Wischmeier and Smith (1958). An individual storm was defined as a precipitation event isolated from other events by at least one hour with no precipitation. This definition was used because runoff from unpaved road surfaces continues for only 30-60 minutes after precipitation has ceased (Chapter 3). Fifteen-minute erosivities were calculated for individual storm events for the three gauges with sufficient temporal resolution.

Sediment production rates were periodically measured from 21 unpaved road segments (Figure 1; Table 2) from July 1998 to April 2000 (n=105). A few segments were less-intensively monitored from April 2000 through November 2001 (n=5). To the extent possible, the segments were selected to represent a wide range of surface areas and slopes. The mean width was 4.7 m and the mean road surface area—including both the active travelway and inside-ditch—was 850 m². The 21 road segments showed three distinct drainage patterns (Figure 3): (1) insloped travelways directing the runoff into inside ditches; (2) insloped sections with blocked ditches that forced the runoff back onto the road surface; and (3) sub-segments that lacked any effective cross-slope drainage due to deep ruts or the lack of an inside ditch.

Each of the 21 segments was broken into sub-segments as defined by changes in gradient or drainage pattern. The length and mean width of each segment and sub-segment was measured

with measuring tapes and hip-chains; slopes were measured with a clinometer, and flow paths were drawn in sketch maps. The drainage pattern of each sub-segment was considered when calculating the product of road surface area times road slope, as segments with similar total lengths and slopes can have very different area-slope factors (Figure 3). Hence, the area-slope and slope of each segment was calculated as the areally-weighted values for each sub-segment. The mean area times slope for the 21 road segments was 31 m^2 , while the range was from 2.0 to 93 m^2 . The mean slope was 10% with values ranging from 1% to 21% (Table 2). Road slope and width were correlated ($r^2 = 0.51$; $p < 0.001$), as the road segments tended to be either steep and narrow or flat and wide.

Road use was stratified into three classes, and these were: abandoned roads, roads exclusively used by light vehicles, and roads receiving over four heavy truck passes per day in addition to light vehicle traffic. The *a priori* classification of segments into one of these three classes provided a secondary criterion for site selection. An equal block design based on three area-slope classes and the three traffic classes was not possible because only two segments were in the heavy use category and only one abandoned road had suitable sites for measuring sediment production rates. This meant that it was not possible to measure sediment production from abandoned roads with low area-slope values or roads with heavy truck usage and high area-slope values. Time since construction or grading was not a primary site selection criterion because all of the recently-constructed road segments were privately owned, the grading history was not always known when the road segments were being selected, and we had no control on when regrading occurred.

Sediment production rates were measured by weighing the mass of material trapped in sediment fences (Robichaud and Brown, 2002) placed immediately below a point of concentrated road drainage such as a cemented swale, unprotected cross-dip, or culvert. Drainage from the two abandoned road segments (LE-Bottom and LE-Top) and one segment in Fish Bay (FB-E) was forced off the road surface by installing a 30 cm wide rubber strip at a 30° angle to the general

direction of the road. The rubber strip was set into a trench 15 cm deep that was backfilled and sealed with concrete.

The sediment fences consisted of filter fabric attached to approximately 1 m long pieces of rebar hammered vertically into the ground. This created a sediment trap about 50 cm high, and the remaining 50 cm of fabric was placed flat on the ground to serve as an apron and a base for removing the accumulated sediment. The leading edge was secured to the ground surface with rocks or u-shaped pieces of rebar to prevent underflow. The tight weave of the filter fabric did not readily allow water to flow through it, so the sediment fences acted more like a dam than a filter.

The fences were regularly checked after storm events, and once a substantial amount of sediment had accumulated, the material was shoveled into buckets and weighed with a radial scale to the nearest 0.2 kg. One or two well-mixed samples of 1-4 kg were collected and placed in watertight bags. Percent moisture content was measured in the lab (Gardner, 1986) and used to correct the field-measured wet weights to a dry mass.

The particle-size distributions of 40 samples from different fences were determined by dry sieving (Bowles, 1992) for particles coarser than 0.075 mm, and the hydrometer method (Gee and Bauder, 1986) for particles smaller than 0.075 mm. The 40 samples were selected to represent road segments with varying slopes, amounts of traffic, and times since grading. The mean mass-weighted particle-size distribution of the eroded sediment was determined for 20 of the 21 road segments. Multiple-comparison statistical procedures (F-protected LSD and Tukey's HSD) were used to determine if road grading and slope had any effect on the particle-size distribution of the material captured in the sediment fences.

Thirty of the 110 measurements from sediment fences had to be discarded because precipitation data were not available or because the sediment production data were affected by overtopping of the sediment fences, clogged culverts, or vandalism of the sediment fences.

For each road segment the effect of precipitation was evaluated by plotting sediment production against total precipitation and the sum of 15-minute rainfall erosivity values over the period of a given measurement. After normalizing by precipitation, the effect of road gradient was evaluated by plotting sediment production against slope for roads with similar amounts of traffic and time since grading. The effect of traffic was determined by comparing mean sediment production rates—normalized by road segment slope and total precipitation—for two different traffic levels. Heavy-traffic road segments were used by about four to six heavy trucks and 110-280 light vehicles per day (Table 2), while those with light traffic were used by 2-160 vehicles per day and only rarely traversed by heavy trucks. Grading effects were identified by plotting sediment production—normalized by precipitation and gradient—against time since grading. The results of this initial data analysis led to the formulation of several multiple regression models with the following general form:

$$E_r = A * (\text{precipitation or erosivity}) + B * (\text{slope}^i \text{ or area-slope}) + C * (\text{grading}) + D_i * (\text{two and three-way interaction terms}) + \text{Intercept} \quad (\text{eq. 6})$$

where E_r is sediment production (kg m^{-2}), capital letters are empirical parameters, precipitation denotes total rainfall (cm), slope is the areally-weighted road segment slope (m m^{-1}), i is an exponent with tested values ranging from 1.0 to 2.0 in 0.1 increments, area-slope is the areally-weighted road segment area times slope (m^2), and grading is a binary variable equal to one for graded roads and zero for ungraded roads.

2.4 Results

2.4.1 Precipitation

The presentation of precipitation data will focus on the Maho Bay rain gauge, as this site had the longest continuous record (Table 1). Precipitation data from the other three gauges generally follow the same trends as the Maho Bay station (Appendix I-A). The total rainfall at Maho Bay

from 13 July 1998 to 13 April 2000 was 206 cm. An additional 5-10 cm of rainfall fell during the 8-day gap in September 1998 when Hurricane Georges passed through. This total is only 6% more than the corresponding long-term mean for Caneel Bay, which lies within the same precipitation zone as Maho Bay (Bowden et al., 1970). Monthly precipitation generally followed the normal seasonal trends (Figure 4), but there was lower than normal rainfall during most of the drier months (February to July) and higher than normal rainfall during most of the wetter months (approximately October to January). The below normal rainfall in September 1998 is misleading because it does not include the rainfall from Hurricane Georges. The exceptionally high amount of precipitation in November 1999 was due largely to Hurricane Lenny, which dropped 14 cm of rainfall over a two-day period.

The frequency distribution of storm precipitation shows that the study period had a larger proportion of small storms (< 0.5 cm) relative to the long-term record at Caneel Bay (Figure 5). Part of this discrepancy may be due to the higher resolution of the rain gauge used at Maho Bay (0.025 cm) compared to the Caneel Bay rain gauge (0.25 cm). The relative frequency of storms larger than 2.0 cm was very similar for both stations.

The maximum one-hour precipitation recorded at Maho Bay was 3.6 cm, and the sum of 15-minute erosivity values calculated at Maho Bay was $2,670 \text{ MJ mm ha}^{-1} \text{ hr}^{-1}$ for a single storm event. Storm precipitation was non-linearly related to the erosivity of individual storm events ($p < 0.0001$) (Figure 6). Similar regressions were developed for the Fish Bay, Bordeaux Mountain, and Caneel Bay precipitation data, and they were used to estimate the total erosivity for storms when 15-minute data were not available (Table 1).

2.4.2 Road Segment Sediment Production

Sediment production rates for most road segments showed a linear relationship to total precipitation, but the significance of these relationships for the 16 segments with three or more observations varied widely (Table 3; Appendix I-B). Sediment production from the two

abandoned road segments was poorly correlated with total precipitation. For the remaining 14 segments the median R^2 between precipitation and sediment production was 0.71, but the range was from 0.13 to 0.99. Only five segments had a statistically significant relationship ($p \leq 0.05$) between sediment production and precipitation, three showed borderline significance ($p = 0.05$ - 0.10), and six had p-values greater than 0.10. In some cases the low significance of these regressions is due to the small variation in total precipitation. Road segments with a statistically significant relationship had an average precipitation range of approximately 37 cm as compared to a range of 15 cm for the segments with a non-significant relationship. Another important cause of the poor relationship between precipitation and sediment production is the fact that the fences were more likely to be cleaned out shortly after the largest storm events. In such cases the amount of sediment was large relative to the cumulative precipitation. Longer time periods with fewer large storms often had more cumulative precipitation but smaller amounts of trapped sediment. Unfortunately, the nature and resolution of the sediment fence measurements do not allow an explicit analysis of the relationship between storm precipitation and sediment production.

The overall sediment production rate for the 21 road segments was 0.064 kg m^{-2} per centimeter of precipitation. The median slope of the relationship between sediment production and precipitation was $0.09 \text{ kg m}^{-2} \text{ cm}^{-1}$, and the range was from 0.018 to $0.39 \text{ kg m}^{-2} \text{ cm}^{-1}$ (Table 3). This indicates that different road segments can yield widely varying amounts of sediment for a given amount of precipitation. The highest slope coefficients were associated with steep roads that had been graded at least once within the last two years.

Since sediment production from at least some segments was significantly related to storm precipitation, the data were normalized by precipitation to assess the relative effect of slope, road surface area, traffic, and grading. Figure 7 shows sediment production normalized by precipitation versus average slope for recently-graded, lightly-used road segments. This indicates that for these road segments sediment production rates per centimeter of precipitation tend to

exponentially increase with increasing road slope ($R^2 = 0.55$; $p < 0.001$). A similar but slightly stronger trend was observed for road surface area times slope ($R^2 = 0.62$; $p < 0.001$).

A similar analysis indicated that use class was not a significant control on sediment production rates. The five segments in the heavy-use class consisted of three segments in the Fish Bay basin (FB-A, C, and D segments) and two segments leading to the Maho Bay Eco-Resort (MB-A, and C). After normalizing by precipitation and slope, the 14 measurements from the five road segments in the heavy use category had an average sediment production rate of $1.28 \text{ kg m}^{-2} \text{ cm}^{-1} \text{ m m}^{-1}$ (s.d. = 1.24) (Table 4). The 59 measurements from the 14 road segments in the light use category averaged $0.81 \text{ kg m}^{-2} \text{ cm}^{-1} \text{ m m}^{-1}$ (s.d. = 0.62). The high variability within each category meant that there was no significant difference between these sediment production rates ($p = 0.19$).

Regrading did significantly affect sediment production rates. In nearly all cases the material used to resurface a road is simply scraped from the cutslopes or taken from an inside ditch. This material is spread by a bulldozer over the road segment but is not systematically compacted (Figure 8). Figure 9 shows that sediment production rates—again normalized by precipitation and slope—declined significantly with time since grading ($p < 0.001$). Sediment production rates were highest in the first year after grading, and there was a notable reduction in both the magnitude and variability of sediment production rates between one and two years after grading. This suggests that the unpaved roads on St. John can be grouped into two grading categories: (1) roads graded at least once every two years; and (2) roads that have not been graded for over two years (“ungraded”). The mean normalized sediment production rates for graded and ungraded roads were $0.96 \text{ kg m}^{-2} \text{ cm}^{-1} \text{ m m}^{-1}$ (s.d. = 0.63) and $0.56 \text{ kg m}^{-2} \text{ cm}^{-1} \text{ m m}^{-1}$ (s.d. = 0.12), respectively (Table 4), and these values are significantly different ($p < 0.0001$). Annual sediment production rates for typical graded and ungraded roads with a 10% slope and an annual rainfall of 115 cm yr^{-1} are $11 \text{ kg m}^{-2} \text{ yr}^{-1}$ and $6.4 \text{ kg m}^{-2} \text{ yr}^{-1}$, respectively.

Figure 10 shows how sediment production—normalized by precipitation—varies with road segment slope for graded and ungraded roads. This indicates that sediment production rates for the graded roads exponentially increase with increasing slope. In contrast, the sediment production rates for ungraded roads with similar slopes are much lower, and the data suggest a linear relationship with increasing slope (Figure 10).

Sediment production rates from the two abandoned road segments were much lower than the other 19 segments. The mean sediment production rate from these two segments over most of the study period was $0.071 \text{ kg m}^{-2} \text{ cm}^{-1} \text{ m m}^{-1}$ ($n=5$), or 13% of the mean value for ungraded roads. However, the mean normalized sediment production rate in November 1999 was $0.27 \text{ kg m}^{-2} \text{ cm}^{-1} \text{ m m}^{-1}$ ($n=2$), or four times the value over the rest of the study period and nearly 50% of the value for actively-used, ungraded roads. November 1999 included the intense rainfall associated with Hurricane Lenny, and this apparently induced sufficient overland flow to rapidly erode the surface of the two abandoned road segments.

2.4.3 General Linear Models for Graded and Ungraded Road Segments

Multiple regression showed that interaction terms including slope were always statistically significant. Models based on slope had higher R^2 values than models using area times slope. Models using erosivity and total erosive energy had slightly lower R^2 values than models using total precipitation. The best models were based on a two-way interaction of total precipitation and slope, and a three-way interaction of total precipitation, slope, and grading. Exponent values between 1.0 and 2.0 were sequentially tested for the slope parameter at 0.1 increments. All of the resulting models had statistically-significant terms and R^2 values ranging from 0.61 to 0.76 (Appendix I-C). The similarity of R^2 values meant that a graphical analysis of model residuals was used to select the best model. The model based on slope^{1.5} was chosen because the residuals were normally distributed and this model minimized the error in sediment production, especially for the steepest road segments (Table 5; Appendix I-C). Since the grading parameter is best

treated as a binary variable with values of 1 for graded roads and 0 for ungraded roads, the road erosion model can be simplified into equations for graded roads (equation 7a) and ungraded roads (equation 7b), as follows:

$$E_r = -0.432 + 4.73 \cdot (S^{1.5} \cdot P) \quad (\text{eq. 7a})$$

$$E_r = -0.432 + 1.88 \cdot (S^{1.5} \cdot P) \quad (\text{eq. 7b})$$

where E_r is sediment production in kg m^{-2} , S is slope in m m^{-1} , and P is total precipitation in cm.

A plot of the measured data against predicted values shows that the predicted values generally follow the 1:1 line (Figure 11). The mean absolute errors for graded and ungraded roads were 1.15 and 0.69 kg m^{-2} , respectively.

Figure 12 shows that sediment production—when normalized by precipitation and slope—declines with cumulative precipitation after grading. An extrapolation of the non-linear regression suggests that slightly more than two years of precipitation (> 230 cm) are needed before the sediment production rate from graded roads approximates the mean value for ungraded roads ($0.56 \text{ kg m}^{-2} \text{ cm}^{-2} \text{ m m}^{-1}$). The observed decline in the magnitude and variability in erosion rates after 90-100 cm of precipitation is consistent with the decline over time shown in Figure 9.

2.4.4 Particle-Size Distribution

The mass-weighted average particle-size distribution showed that the material eroded from the unpaved road surfaces was 40% gravel, 54% sand, and 6% silt and clay (Table 6; Appendix I-D). The median particle-size (D_{50}) for all road segments was 0.12 mm, and the 16th (D_{16}) and 84th (D_{84}) percentiles were 0.72 and 4.1 mm, respectively. On average, graded roads produced 36% gravel, 58% sand, and 6% silt and clay, while ungraded roads produced 41% gravel, 53% sand, and 6% silt and clay (Figure 13). Abandoned roads produced 73% gravel, 27% sand, and 0.1% silt and clay. There were no significant differences in the particle-size distributions of the

sediment collected from graded and ungraded roads (Table 6). The statistical analyses did not include samples from abandoned roads as this class was represented by only two samples.

When sorted by slope class, the sediment eroded from the steepest road segments was significantly coarser than the sediment produced from the low-gradient roads (Table 6). There were no significant differences between the steep- and moderately-sloped roads for any of the particle-size categories as well as the D_{16} , D_{50} , and D_{84} .

2.5 Discussion

2.5.1 Effects of Precipitation, Slope, and Grading in Road Sediment Production

Total precipitation, slope, and grading all affect road sediment production rates on St. John. The use of total precipitation is a simplification of the erosion processes described by equations 1-4, as this presumes that—after controlling for slope and grading—all rainfall events have the same erosive potential per unit depth of rainfall. The model presumes a linear relationship between total precipitation and sediment production and this implies that total runoff from an unpaved road segment is linearly related to total precipitation. For a given storm magnitude, equations 1-4 suggest that sediment production should be controlled by the intensity of rainfall, as this controls the depth of overland flow and thus the magnitude of the shear stresses applied to the road surface. The problem is that the sediment trap data aggregate sediment production from numerous rainfall events over time periods extending from several weeks to several months. The effects of varying rainfall intensities are largely lost, and total precipitation emerges as the best predictor of road segment sediment production. If sediment production were measured over shorter time periods, erosivity might emerge as a better predictor of road sediment production.

Road segment slope was an important control on road sediment production. The models show that sediment production per unit rainfall is best predicted by slope elevated to the 1.5 power. The presence of slope as a two- and three-way interaction term in the model (Table 5)

indicates that its effect on road erosion rates varies with grading category. Slope differences will have a larger effect on sediment production rates for graded roads than ungraded roads.

Road segment slope was a better predictor of sediment production rates than road surface area times slope. The three-way interaction term of precipitation, area times slope, and grading was only marginally significant ($p = 0.06$) and produced a model with an overall R^2 of 0.68 (Appendix I-C). The lower significance for the model using area times slope may be due to the difficulty in accurately measuring the contributing areas of individual road segments.

Montgomery (1994) noted that road drainage areas measured when there was no surface runoff may have errors of up to $\pm 30\%$. Another complication is that the area times slope factor depends on the route followed by runoff over the road surface. Field observations showed that surface microtopography and runoff paths changed over time due to rilling, traffic, grading, and clogging of ditches. Area times slope values for the monitored road segments could not account for these changes as they were only measured once during the study period.

Time since grading also had an important effect on sediment production. Sediment production rates—normalized by rainfall and slope—exponentially declined with time since grading (Figure 9) and with cumulative precipitation after grading. The large variability in sediment production rates and the limited time-resolution of the sediment data preclude a calibration of the parameters in equation 5 (Megahan, 1974) or the development of a new exponential decay model. Roads that were graded at least once every two years had significantly higher sediment production rates than ungraded roads (Table 4). Although the data suggest that sediment production rates decline after about 80 cm of total precipitation, the regression equations suggests that approximately 230 cm of cumulative rainfall are required before a graded road erodes at nearly the same rate as an ungraded road (Figure 12). The road erosion model was simplified to a step function, in that equation 7a applies to the first 230 cm of cumulative precipitation after regrading, and 7b to all subsequent rainfall.

The predicted declines in sediment production through time are similar to or slightly less than previous studies. Using equation 7a, the predicted annual sediment production rates for graded roads are 0.11 and 52 kg m⁻² yr⁻¹ assuming an annual rainfall rate of 115 cm and road slopes of 1% and 21%, respectively. Using equation 7b, the corresponding values are 0.0 and 12 kg m⁻² yr⁻¹. These values suggest that sediment production rates should decline by 61-84% within two years after grading. In Idaho sediment production rates declined by 40-80% within one year after construction (Vincent, 1979). A field-based calibration of equation 5 in Idaho indicates that sediment production should decline by 95% within one year after road construction (Megahan, 1974). In the Oregon Coast range, sediment production rates decreased by 70% one year after disturbing both the travelway and the ditch, and by 90% after two years (Luce and Black, 2001b).

2.5.2 Abandoned Roads and Undisturbed Hillslopes

The mean rate of sediment production for abandoned roads with a mean slope of 15% was 0.010 kg m⁻² per cm of precipitation, or approximately an order of magnitude lower than comparable ungraded roads. This indicates that sediment production rates after grading continue to decline for the ungraded road segments beyond the 3-year period documented in this study (Figure 9). The low erosion rates for the abandoned road segments may be attributed to a well-armored road surface and lower runoff rates for all but the most extreme storm events. A storm in February 2000, for example, produced 9.5 cm of rainfall in 2.5 hours following a 24-hour period with no precipitation. Field observations showed that this generated precipitation-excess overland flow on the road surface but there was no interception of subsurface storm flow and almost no sediment captured in the sediment traps.

Efforts to model sediment production rates from abandoned roads are hindered by the almost 400% increase in sediment production observed during Hurricane Lenny. The pattern of rainfall generated by Hurricane Lenny was unique, as the maximum 1-hr intensity of 4.7 cm hr⁻¹ occurred after 4.9 cm of rain had fallen in the previous 24 hours. This high-intensity burst of rain

at the end of the storm presumably triggered both Horton overland flow and the interception of subsurface flow on the abandoned road segments. The resulting surface runoff caused a marked increase in sediment production per unit rainfall. Although detailed hydrometric data are not available, the difference in antecedent precipitation and subsurface flow interception is believed to explain why Hurricane Lenny produced much more sediment than the 9.5-cm storm in February 1999.

Annual sediment production estimates from abandoned roads are necessarily based on the total sediment produced from the two abandoned road segments over the two-year study period. As noted earlier, rainfall over the study period was very similar to the long-term pattern of precipitation recorded at Caneel Bay (Figure 5). Hence the long-term frequency of events like Hurricane Lenny may be similar to their frequency during the study period. If the normalized average sediment production for abandoned roads is 0.071 kg m^{-2} per unit precipitation per unit percent slope, then the annual erosion rates for abandoned roads with slopes of 1% and 21% are estimated to be 0.08 and $1.7 \text{ kg m}^{-2} \text{ yr}^{-1}$, respectively. The values for roads with 1% slope show relatively little change with grading class. For roads with a slope of 21% the effect of grading is much greater, as recently-graded roads produce 30 times as much sediment as abandoned roads. Steep ungraded segments produce about 7 times as much sediment as comparable abandoned roads.

Measured surface erosion rates from undisturbed zero-order basins are on the order of $0.001 \text{ kg m}^{-2} \text{ yr}^{-1}$ (Chapter 4). This indicates that actively used roads can increase sediment production rates by more than four orders of magnitude relative to undisturbed conditions. The sediment production rate from the two abandoned road segments monitored in this study were still about three orders of magnitude higher than the rates measured from undisturbed hillslopes.

2.5.3 Comparisons with Previous Studies

A previous study developed an empirical road erosion model for St. John (ROADMOD). This model was based on a linear relationship between annual sediment production rate and the product of road surface drainage area (A) times road slope (S) (Anderson, 1994):

$$E = 0.00057A \cdot S + 0.034 \quad (\text{eq. 8})$$

where E is the average annual road surface cross-sectional erosion ($\text{m}^2 \text{yr}^{-1}$), A is in m^2 , and S is in m m^{-1} . Annual sediment production rates at the road segment scale are predicted using the road drainage area at the midpoint of the segment and the average road segment slope (Anderson and MacDonald, 1998).

The application of ROADMOD to the 21 monitored road segments yields a mean annual sediment production rate of $22 \text{ kg m}^{-2} \text{yr}^{-1}$, or 18 times higher than the measured mean of $1.8 \text{ kg m}^{-2} \text{yr}^{-1}$. Only road segments FB-E and MB-A had measured values higher than those predicted by ROADMOD. Erosion rates predicted by ROADMOD were poorly correlated to those measured by the sediment traps ($R^2 = 0.04$; $p > 0.25$). Erosion rates based on sediment trap measurements were poorly correlated with the area-slope product as defined by Anderson (1994) ($R^2 = 0.006$; $p > 0.25$).

The lack of a stronger correlation may be due to the fact that equation 8 was developed on severely-rilled road segments with no effective cross-slope drainage (Type 3 in Figure 3). The correlation between sediment production rates estimated by ROADMOD and those measured with sediment traps improves when the area times slope product is based on a method that accounts for varying road drainage patterns. Using the area times slope product shown in Table 2, the mean sediment production rate estimated by ROADMOD for the 21 road segments drops by nearly one-third to $15 \text{ kg m}^{-2} \text{yr}^{-1}$. Although this value is still an order of magnitude higher than the mean value from the sediment traps, the correlation between the predicted and measured

values is stronger ($R^2 = 0.19$; $p < 0.001$) than those using the total surface area times slope product.

Figure 15 compares estimated annual sediment production rates for unpaved roads in St. John to other published values. Annual erosion rates measured by this current study suggest that road segment scale sediment production rates are of similar magnitude as the 0.9 to 15 kg m⁻² yr⁻¹ previously estimated from 40 m² road surface plots with slopes ranging from 7 to 18 percent (MacDonald et al., 2001).

Sediment production rates from unpaved roads on St. John are higher than the values reported for the Southern Appalachian Mountains (Swift, 1984) and central Idaho (Vincent, 1979) in the U.S., New Zealand (Fahey and Coker, 1989), and Australia (Grayson et al., 1993) (Figure 15). The higher erosion rates for St. John are consistent with the steep road segment slopes and the high rainfall erosivities on the island. The only published study with higher erosion rates was a high rainfall area in the northwestern U.S. (Reid and Dunne, 1984). Their maximum rate assumed a mean traffic of at least four loaded logging trucks per day, while none of the road segments in this study was subjected to more than 4-6 delivery trucks per day.

2.5.4 Recommendations for Road Erosion Control

The improved understanding of road surface erosion developed here can be translated into specific recommendations for reducing road surface sediment production. First, given the important role of grading and slope in sediment production (Figure 10), frequently-graded steep road segments should be the first targets for implementing erosion control practices. If possible, roads and driveways with steep slopes should be paved immediately after construction as the highest sediment production rates can be expected immediately after grading and road construction. Second, given that grading plays such an important role in road erosion, the frequency and area of road grading should be kept to a minimum. Third, the borderline-significance ($p = 0.06$) of the area times slope factor term in multiple regression highlights the

importance of proper road drainage in minimizing sediment production rates. Proper design may include insloping, outsloping, constructing and maintaining well-protected ditches along roads, and increasing the density of road drains.

2.6 Conclusions

Sediment production from 21 road segments with varying contributing areas, slopes, and traffic loads was monitored with sediment traps from July 1998 to November 2001. Precipitation was measured by four recording rain gauges. Total precipitation over the study period was 206 cm. Total rainfall and the frequency distribution of storm magnitudes were very similar to long-term averages, although the total erosive energy was approximately 12% larger than the long-term average.

Sediment production rates were linearly related to total precipitation for most of the 21 road segments monitored in this study. The average road erosion rate for all segments was 0.064 kg m^{-2} per centimeter of precipitation. Steeper roads had higher sediment production rates, and the recently-graded roads showed a significant, non-linear increase in sediment production with increasing road slope. Regrading significantly increased sediment production rates. Roads graded at least once during the two-year study period had a mean sediment production rate of 0.96 kg m^{-2} per centimeter of rainfall and unit slope, or approximately $11 \text{ kg m}^{-2} \text{ yr}^{-1}$ for a typical road with a 10% slope and an annual rainfall of 115 cm yr^{-1} . The mean erosion rate for ungraded roads was 41% lower, or $6.4 \text{ kg m}^{-2} \text{ yr}^{-1}$ for a road segment with a 10% slope. Roads with 15% slopes that had been abandoned for about 15 years showed an average erosion rate of $1.1 \text{ kg m}^{-2} \text{ yr}^{-1}$. Differences in traffic loads did not significantly affect sediment production.

Models using total precipitation and slope yielded higher R^2 values than models using rainfall erosivity, total erosive energy, and area times slope. The best predictive model used total precipitation, slope to the 1.5 power, and a binary variable for grading, and had a R^2 value of 0.75.

The measured erosion rates indicate that unpaved roads on St. John can increase hillslope-scale sediment production rates by more than four orders of magnitude relative to undisturbed conditions. These rates place roads in St. John at the high end of reported road erosion rates, a finding that is consistent with the high rainfall erosivities on the island. The improved understanding of road surface erosion can be translated into specific recommendations for reducing road surface sediment production.

2.7 References Cited

- Acevedo R, Morelock J, Olivieri RA. 1989. Modification of coral reef zonation by terrigenous sediment stress. *Palaios* 4: 92-100.
- Anderson DM. 1994. Analysis and modeling of erosion hazards and sediment delivery on St. John, U.S. Virgin Islands, US National Park Service Water Resources Division, Technical Report NPS/NRWRD/NRTR-94-34, Fort Collins, Colorado; 153 p.
- Anderson DM, MacDonald LH. 1998. Modelling road surface sediment production using a vector geographic information system. *Earth Surface Processes and Landforms* 23: 95-107.
- Bilby RE, Sullivan K, Duncan SH. 1989. The generation and fate of road-surface sediment in forested watersheds in southwestern Washington. *Forest Science* 35(2): 453-468.
- Black TA, CH Luce. 1999. Changes in erosion from gravel surfaced forest roads through time. Proceedings of the International mountain logging and 10th Pacific Northwest skyline symposium; pp. 204-218.
- Bowden MJ, Fischman N, Cook P, Wood J, and Omasta E. 1970. Climate, water balance, and climatic change in the north-west Virgin Islands. Caribbean Research Institute, College of the Virgin Islands; 127 p.
- Bowles JE. 1992. Engineering Properties of Soils and their Measurement. McGraw-Hill Inc., New York; 218 p.
- Bren LJ, Leitch CJ. 1985. Hydrologic effects of a stretch of forest road. *Australian Forest Research* 15(2): 183-194.
- Burroughs ER, Foltz RB, Robichaud PR. 1991. United States Forest Service research on sediment production from forest roads and timber harvest areas. Proceedings of the 10th World Forestry Congress; 187-193.
- Calvesbert RJ. 1970. Climate of Puerto Rico and the U.S. Virgin Islands. Climatography of the United States No. 60-52, US Dept. of Commerce; 29 p.
- Carter CE, Greer JD, Braud HJ, Floyd JM. 1974. Raindrop characteristics in southcentral United States. *Transactions of the ASAE* 17(6): 1033-1037.
- CH2M Hill. 1979. A sediment reduction program: Report to the Department of Conservation and Cultural Affairs, Government of the U.S. Virgin Islands, St. Thomas, USVI.
- Donnelly TW. 1966. Geology of St. Thomas and St. John. *Geological Society of America, Memoir* 98: 85-176.
- Douglas I, Greer T, Bidin K, Sinun W. 1993. Impact of roads and compacted ground on post-logging sediment yield in a small drainage basin, Sabah, Malaysia. In Hydrology of Warm Humid Regions, Gladwell JS (ed.), IAHS Publication 216: 213-218.
- Dunne T. 1979. Sediment yield and land use in tropical catchments. *Journal of Hydrology* 42: 281-300.

EarthInfo, Inc. 1996. NCDC 15-minute precipitation values. CD-ROM disk. Earth Info, Inc.: Boulder, CO.

Everest FH, Beschta RL, Scrivener JC, Koski KV, Sedell JR, Cederholm CJ. 1987. Fine sediment and salmonid production: a paradox. In Streamside Management: Forestry and Fishery Interactions, Salo EO and Cundy TW (eds.), College of Forest Resources, University of Washington, Seattle, WA; 98-142.

Fahey BD, Coker RJ. 1989. Forest road erosion in the granite terrain of southwest Nelson, New Zealand. *Journal of Hydrology (NZ)* 28(2): 123-141.

Foltz RB. 1996. Traffic and no-traffic on an aggregate surfaced road: Sediment production differences. Paper presented in "Environmentally sound forest road and wood transport Conference"; June 1996; Rome, Italy: FAO; 13 p.

Fransen PJB, Phillips CJ, Fahey BD. 2001. Forest road erosion in New Zealand: Overview. *Earth Surface Processes and Landforms* 26: 165-174.

Froelich W, Walling DE. 1997. The role of unmetalled roads as a sediment source in the fluvial systems of the Polish Flysch Carpathians. In Human Impact on Erosion and Sedimentation, IAHS Publication 245: 159-168.

Froehlich W. 1991. Sediment production from unmetalled road surfaces. In Sediment and stream water quality in a changing environment: Trends and explanation, IAHS Publication 203: 21-29.

Gardner WH. 1986. Chapter 21: Water Content. In Methods of Soil Analysis Part I: Physical and Mineralogical Methods. 2nd edition Number 9 (Part 1) Agronomy Series, Klute A (ed.). American Society of Agronomy, Madison, WI; 493-544.

Gee GW, Bauder JW 1986. Particle-size analysis. In Methods of Soil Analysis Part 1: Physical and Mineralogical Methods. 2nd edition Number 9 (Part 1), Agronomy Series, Klute A (ed.) American Society of Agronomy, Madison, WI; 383-411.

Grayson RB, Haydon SR, Jayasuriya MDA, Finlayson BL. 1993. Water quality in mountain ash forests-separating the impacts of roads from those of logging operations. *Journal of Hydrology* 150: 459-480.

Gresswell S, Heller D, Swanston DN. 1979. Mass movement response to forest management in the central Oregon Coast Ranges. USDA Forest Service Resource Bulletin PNW-84, Portland, OR, 26 p.

Harden CP. 1992. Incorporating roads and footpaths in watershed-scale hydrologic and soil erosion models. *Physical Geography* 13(4): 368-385.

Hernández-Delgado EA. 2001. Enfermedades, competencia por sobrecrecimiento y otras causas de mortalidad en el coral (*Monastrea annularis*). Paper presented at the XXIV Symposium of Natural Resources, Univ. Politécnica, San Juan-Puerto Rico, 16 November 2001.

Hodgson G. 1989. The effects of sedimentation on Indo-Pacific Reef Corals. Ph.D. Dissertation, University of Hawaii, Honolulu, HI; 338 p.

- Hodgson G. 1997. Resource use: Conflicts and management solutions. In Life and Death of Coral Reefs. Birkeland C (ed.), Chapman and Hill, New York, NY; 386-411.
- Hubbard DK. 1986. Sedimentation as a control of reef development: St. Croix, USVI. *Coral Reefs* 5: 117-125.
- Hubbard DK. 1987. A general review of sedimentation as it relates to environmental stress in the Virgin Islands Biosphere Reserve and the eastern Caribbean in general. Biosphere Reserve Report no. 20, Virgin Islands Resource Management Cooperative, St. Thomas, VI; 42 p.
- Julien PY. 1995. Erosion and Sedimentation. Cambridge University Press; 280 p.
- Kirkby MJ. 1980. Modelling water erosion processes. In Soil Erosion, Kirkby MJ, Morgan RPC (eds.). John Wiley, New York; 425-442.
- Knighton D. 1998. Fluvial forms and processes. E Arnold Publishers; 383 p.
- Kumapley NK. 1987. Erosion of unsurfaced earth and gravel roads. In Proceedings of 9th Regional Conference for Africa on Soil Mechanics and Foundation Engineering. Lagos, Nigeria; 397-404.
- Larsen MC, Parks JE. 1997. How wide is a road? The association of roads and mass-wasting in a forested montane environment. *Earth Surface Processes and Landforms* 22: 835-848.
- Luce CH, Black TA. 1999. Sediment production from forest roads in western Washington. *Water Resources Research* 35(8): 2561-2570.
- Luce CH, Black TA. 2001a. Effects of traffic and ditch maintenance on forest road sediment production. In Proceedings of the Seventh Federal Interagency Sedimentation Conference, Reno, Nevada.
- Luce CH, Black TA. 2001b. Spatial and temporal patterns in erosion from forest roads. In Influence of Urban and Forest Land Uses on the Hydrologic-Geomorphic Responses of Watersheds. Wigmosta MS, Burges SJ (eds.). Water Resources Monographs, American Geophysical Union, Washington, DC; 165-178.
- Luce CH, Wemple BC. 2001. Introduction to special issue on hydrologic and geomorphic effects of forest roads. *Earth Surface Processes and Landforms* 26:111-113.
- MacDonald LH, Sampson RW, Anderson DM. 2001. Runoff and road erosion at the plot and road segment scales, St. John, US Virgin Islands. *Earth Surface Processes and Landforms* 26: 251-272.
- MacDonald LH, Anderson DM, Dietrich WE. 1997. Paradise threatened: Land use and erosion on St. John, U.S. Virgin Islands. *Environmental Management* 21(6): 851-863.
- Megahan WF. 1987. Effects of forest roads on watershed function in mountainous areas. In Environmental geotechnics and problematic soils and rocks. Balasubramiam et al. (eds.); 335-347.

- Megahan WF. 1974. Erosion over time on severely disturbed granitic soils: A model. USDA Forest Service Research Paper INT-156, Ogden, UT; 14 p.
- Megahan WF, Kidd WJ. 1972. Effects of logging roads on sediment production rates in the Idaho batholith. USDA Forest Service Research Paper INT-123, Ogden, UT; 14 p.
- Megahan WF, Seyedbagheri KA, Mosko, TL. 1986. Construction phase sediment budget for forest roads in granitic slopes in Idaho. In Drainage basin sediment delivery. Hadley RF (ed.), IAHS Publication 159: 31-39.
- Montgomery DR. 1994. Road surface drainage, channel initiation, and slope instability. *Water Resources Research* 30(6): 1925-1932.
- Moss AJ, Green P. 1983. Movement of solids in air and water by raindrop impact, effects of drop-size and water-depth variations. *Australian Journal of Soil Research* 21: 257-269.
- National Research Council. 1992. Restoration of Aquatic Ecosystems., National Academy Press, Washington, DC; 552 p.
- Nemeth RS, Nowlis JS. 2001. Monitoring the effects of land development on the near-shore marine environment of St. Thomas, USVI. *Bulletin of Marine Science* 69(2):759-775.
- Nemeth RS, MacDonald LH, Ramos-Scharrón CE. 2001. Delivery, deposition, and effects of land-based sediments on corals in St. John, U.S. Virgin Islands. Report on Project No. VI99-2, Water Resources Research Institute, University of the Virgin Islands, St. Thomas, USVI; 24 p.
- Ramos-Scharrón CE, MacDonald LH. 2001. Measuring and Modeling Sediment Production from Unpaved Roads, St. John, U.S. Virgin Islands. *Eos, Transactions AGU*, 82(47): F-510.
- Rankin DW. 2002. Geology of St. John, U.S. Virgin Islands. U.S. Geological Survey professional paper 1631; 36 p.
- Reid LM, Dunne T. 1984. Sediment production from forest road surfaces. *Water Resources Research* 10(11): 1753-1761.
- Reid LM. 1981. Sediment production from gravel-surfaced roads, Clearwater basin, Washington, Publication FRI-UW-8108, University of Washington Fisheries Research Institute, Seattle, WA; 247 p.
- Robichaud PR, Brown RE. 2002. Silt fences: an economical technique for measuring hillslope soil erosion. General Technical Report RMRS-GTR-94, Fort Collins, CO; 24 p.
- Rogers CS. 1998. Coral reefs of the U.S. Virgin Islands. In: Status and Trends of the Nation's Biological Resources, Vol. I. Haeker P and Doran PD (eds.). U.S. Department of the Interior, U.S. Geological Survey, Reston, VA; 322-324.
- Rogers CS 1990. Responses of coral reefs and reef organisms to sedimentation. *Marine Ecology Progress Series* 62: 185-202.

- Sampson RW. 2000. Road runoff and erosion at the plot and road segment scales on St John US Virgin Islands. MS thesis, Department of Earth Resources, Colorado State University, Fort Collins, CO; 189 p.
- Sidle RC, Pearce AJ, O'Loughlin CL. 1985. Hillslope stability and land use. American Geophysical Union, Water Resources Monograph Series No. 11; 140 p.
- Soil Conservation Service. 1970. Soil Survey, Virgin Islands of the United States. 78 p.
- Swift LW. 1984. Soil losses from roadbeds and cut and fillslopes in the Southern Appalachian Mountains. *Southern Journal of Applied Forestry* 8: 209-216.
- Torres J. 2001. Impacts of sedimentation on the growth rates of *Montastraea annularis* in Southwest Puerto Rico. *Bulletin of Marine Science* 69(2): 631-637.
- Torres R, Chiappone M, Geraldles F, Rodríguez Y, Vega M. 2001. Sedimentation as an important environmental influence on Dominican Republic reefs. *Bulletin of Marine Science* 69(2): 805-818.
- USDA. 1995. Classification and Correlation of the Soils of the Virgin Islands of the United States. US Department of Agriculture: Hato Rey, Puerto Rico.
- Vincent KR. 1979. Runoff and erosion from a logging road in response to snowmelt and rainfall. M.S. thesis, University of California, Berkeley, CA; 60 p.
- Wald AR. 1975. The impact of truck traffic and road maintenance on suspended-sediment yield from a 14' standard forest road. MS thesis, University of Washington, Seattle.
- Waters TF. 1995. Sediment in Streams: Sources, Biological Effects and Control. American Fisheries Society Monograph 7; 251 p.
- Wischmeier WH, Smith DD. 1958. Rainfall energy and its relationship to soil loss. *Transactions of the American Geophysical Union* 39(3): 285-291.
- Woodbury RO, Weaver PL. 1987. The vegetation of St. John and Hassel Island, U.S. Virgin Islands. National Park Service, Southeast Region, Research/Resources Management Report SER-83, Atlanta, GA; 26 p.
- Ziegler AD, Sutherland RA, Giambelluca TW. 2001a. Interstorm surface preparation and sediment detachment by vehicle traffic on unpaved mountain roads. *Earth Surface Processes and Landforms* 26: 235-250.
- Ziegler AD, Giambelluca TW, Sutherland RA. 2001b. Erosion prediction on unpaved mountain roads in northern Thailand: validation of dynamic erodibility modelling using KINEROS2. *Hydrological Processes* 15: 337-358.
- Ziegler AD, Sutherland RA, Giambelluca TW. 2000. Partitioning total erosion on unpaved roads into splash and hydraulic components: The roles of interstorm surface preparation and dynamic erodibility. *Water Resources Research* 36(9): 2787-2791.

Ziegler AD, Giambelluca TW. 1997. Importance of rural roads as source areas for runoff in mountainous areas of northern Thailand. *Journal of Hydrology* 196: 204-229.

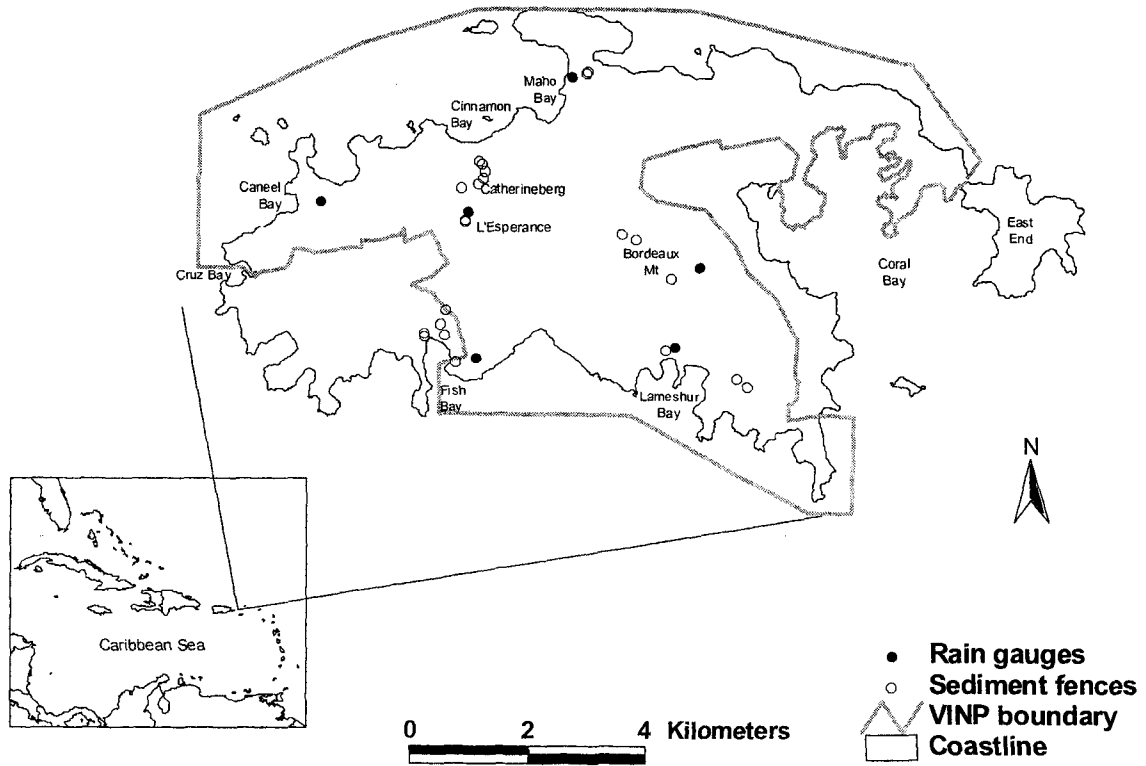


Figure 1. Map of St. John showing the locations of the rain gauges and road segment sediment traps.



Figure 2. Example of a steep road segment near Bordeaux Mountain with a deeply-rilled travelway.

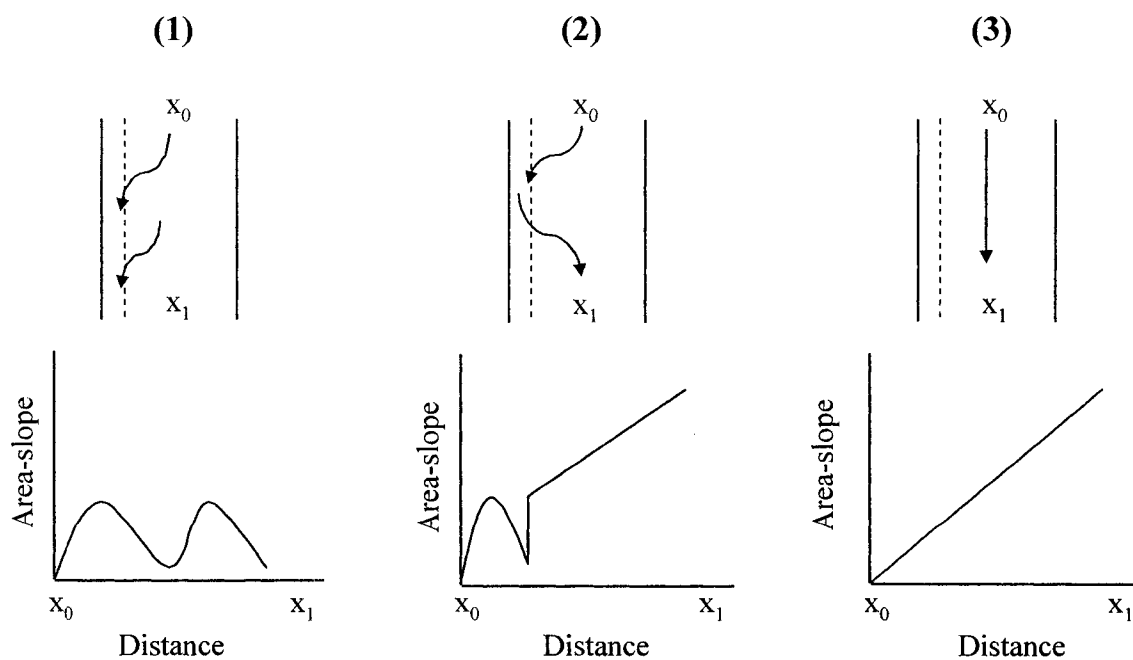


Figure 3. Sketches showing the three main types of drainage patterns exhibited by roads on St. John and their effects on the area times slope factor: (1) insloped; (2) insloped with blocked ditch; and (3) no effective cross-slope drainage. Dashed lines indicates the inside edge of the ditch.

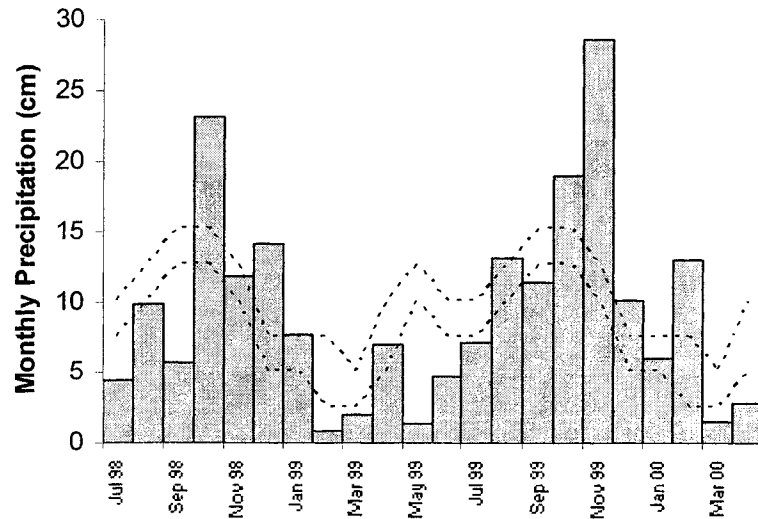


Figure 4. Monthly precipitation over the study period at Maho Bay. Dashed lines show the average monthly range of precipitation as defined by the mean and plus or minus one standard deviation (Bowden et al., 1970).

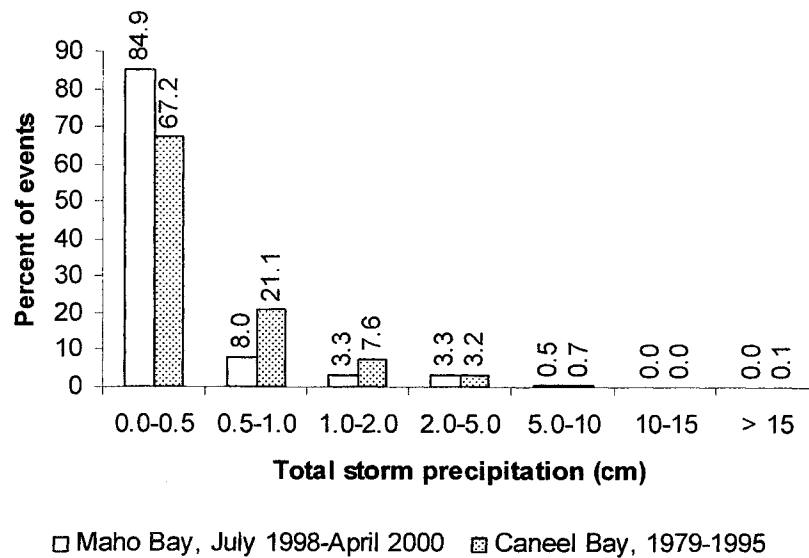


Figure 5. Frequency distribution of storm precipitation from Maho Bay for the period of study (n=614) versus the long-term average for Caneel Bay (n=2,921).

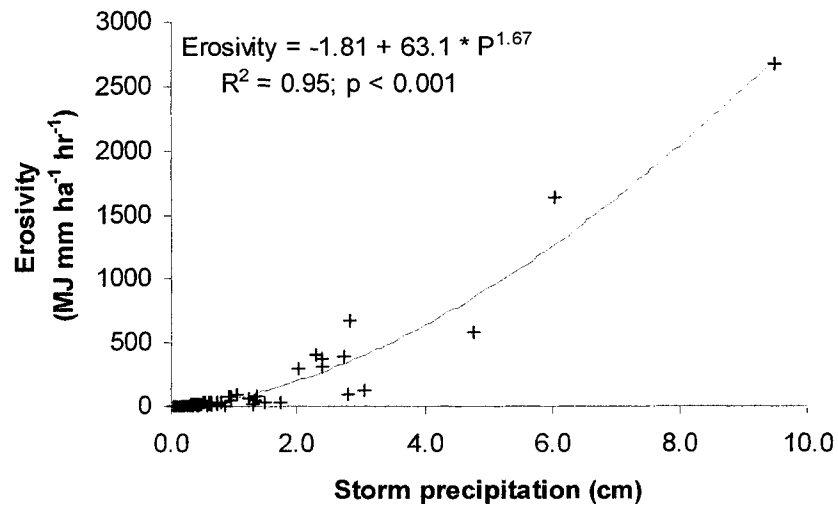


Figure 6. Relationship between 15-min erosivities and total storm precipitation (P) for 309 storm events at Maho Bay for which 15-min rainfall data was available (September 1999 to May 2000).

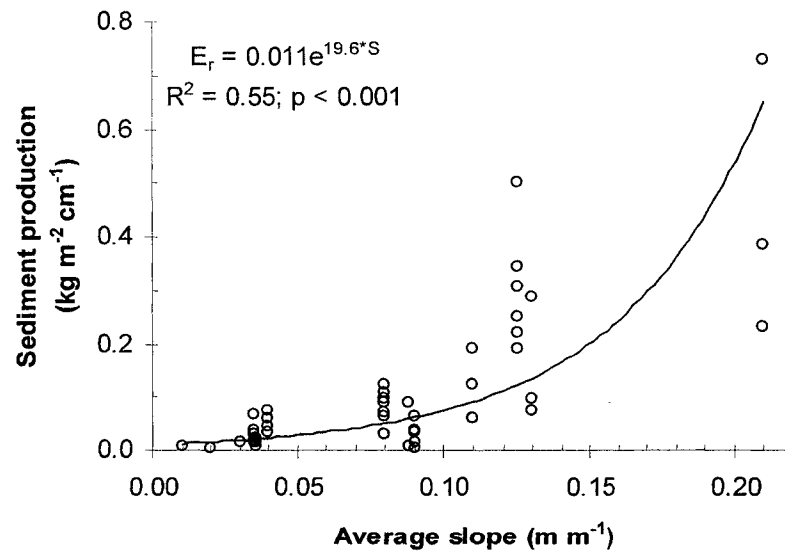


Figure 7. Relationship between sediment production (E_r) normalized by precipitation and slope (S) for seven recently-graded, lightly-used road segments.

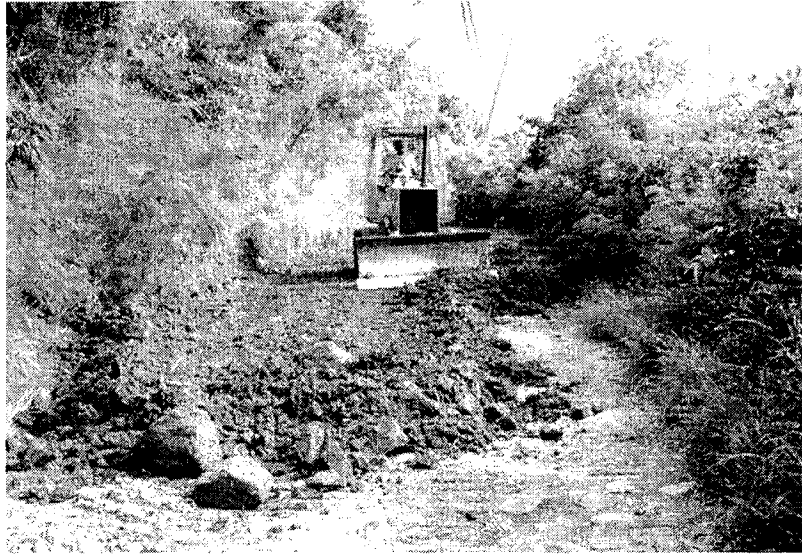


Figure 8. Example of a grading operation along road segment FB-Coco on 11 December 1998.

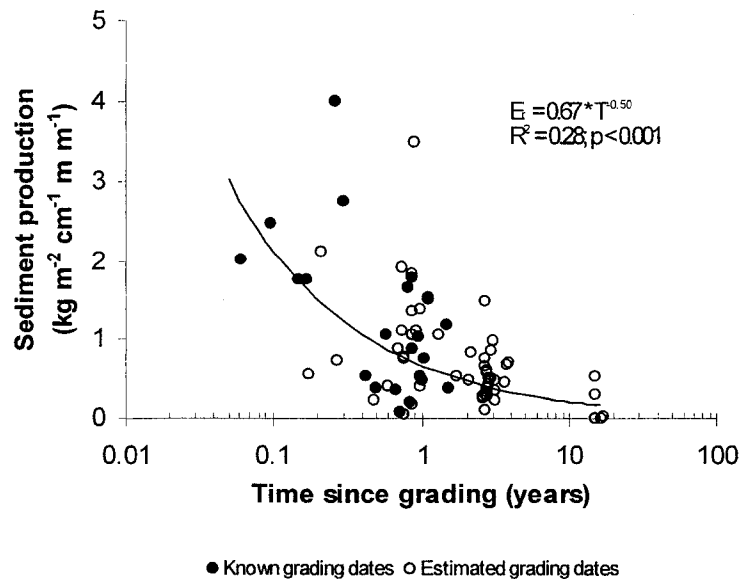


Figure 9. Relationship between sediment production rates (E_r)—normalized by precipitation and slope—versus time since grading (T). Solid circles represent known dates of grading and open circles represent data points for which the date of grading was estimated.

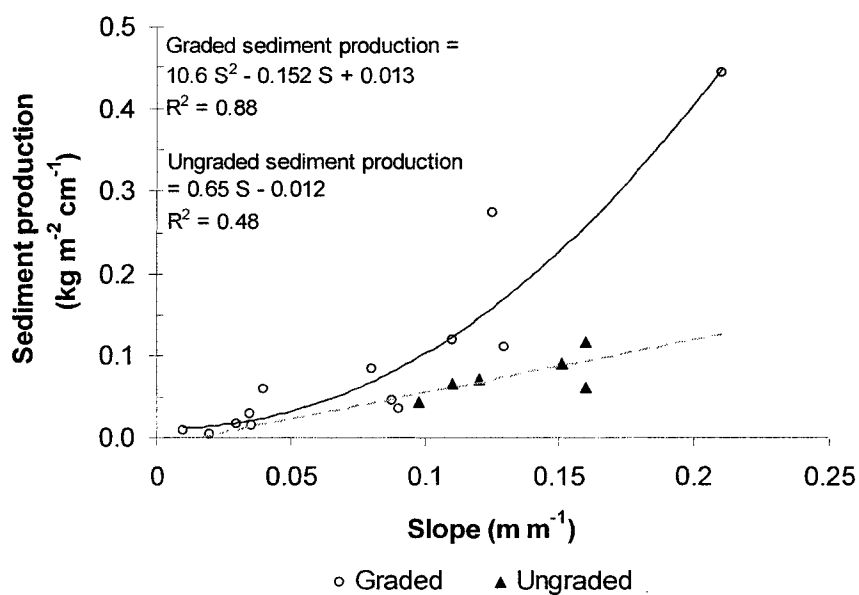


Figure 10. Relationship between mean sediment production—normalized by precipitation—and average segment slope (S) for graded and ungraded road segments. Solid black line is for graded road segments and dashed gray line is for ungraded road segments.

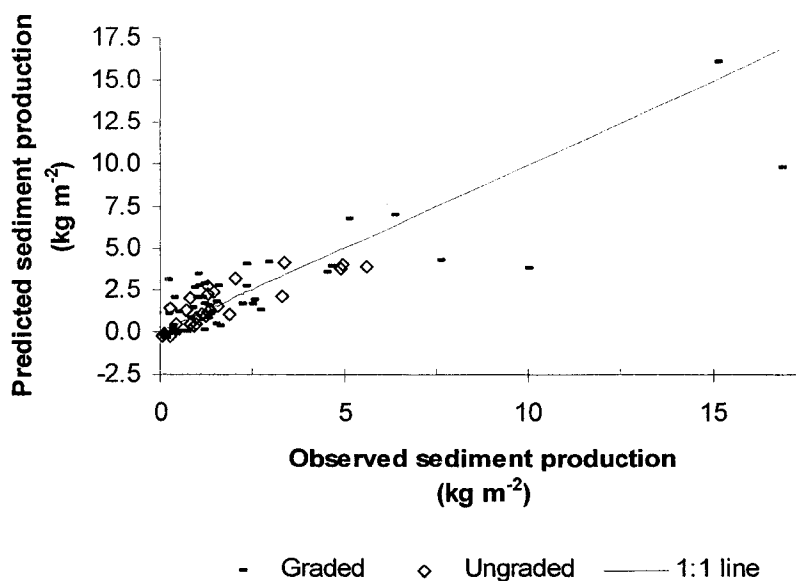


Figure 11. Predicted versus observed sediment production rates for graded and ungraded roads.

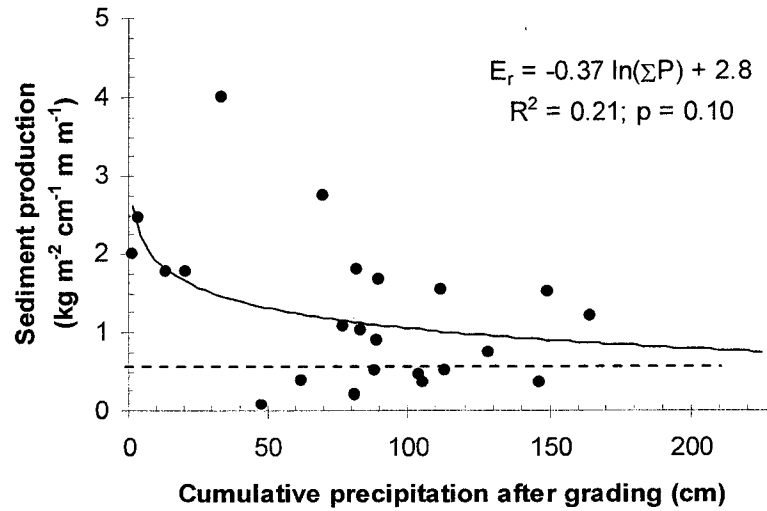


Figure 12. Relationship between sediment production (E_r)—normalized by precipitation and average gradient—and cumulative precipitation after grading (ΣP). Data are for 8 road segments where the date of grading was known ($n=24$). Dashed line represents the mean erosion rate for ungraded roads.

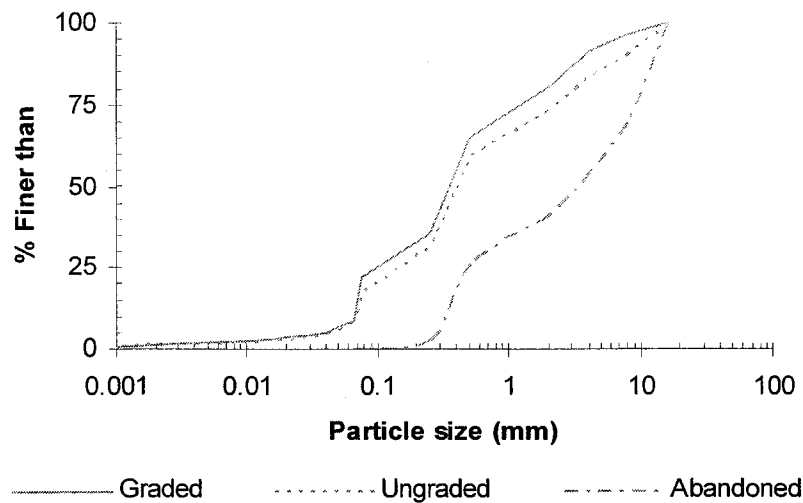


Figure 13. Mass-weighted particle-size distribution for sediment from graded, ungraded, and abandoned roads.

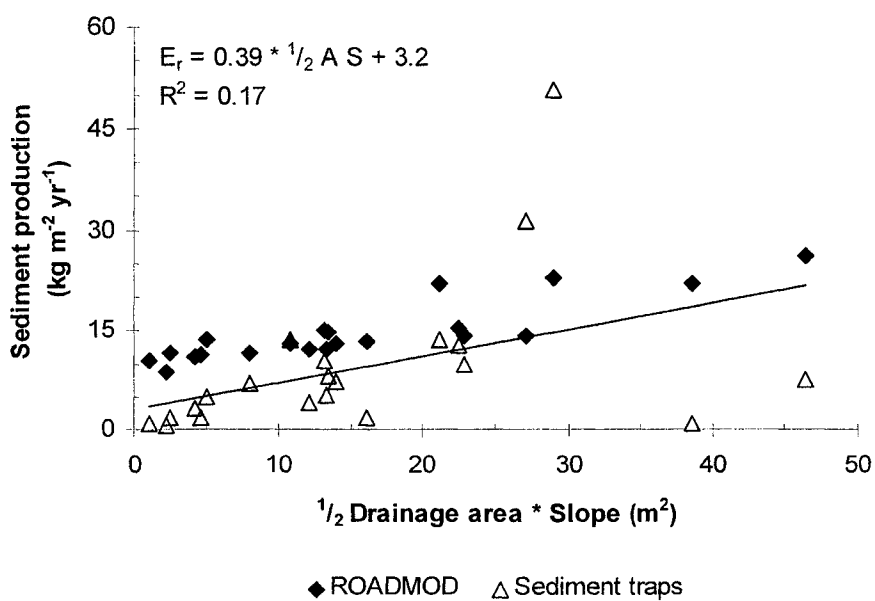


Figure 14. Relationship between measured annual sediment production rates (E_r) using sediment traps and predicted sediment production using ROADMOD versus one-half of the drainage area (A) times slope (S) product. Regression line is for the sediment trap data.

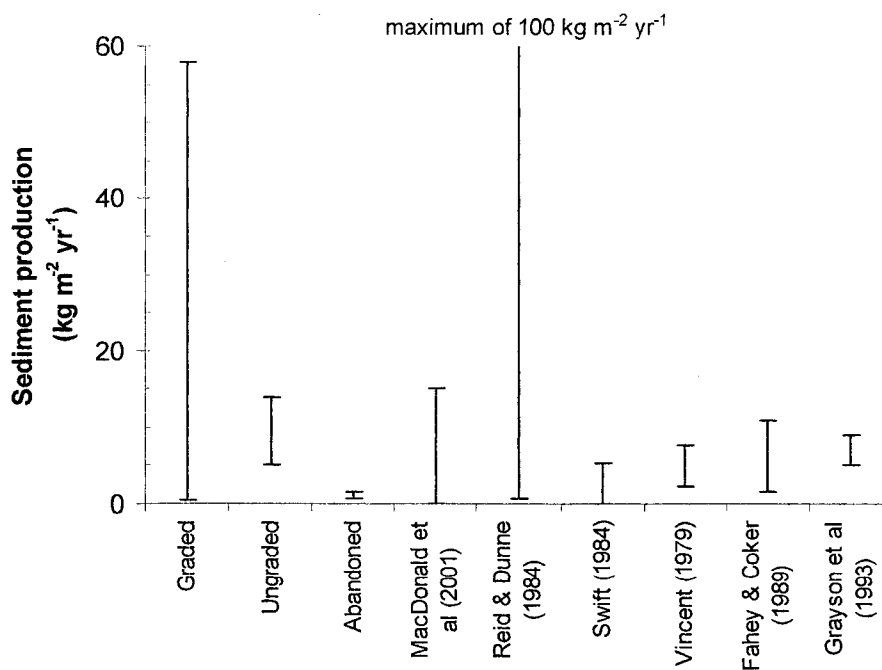


Figure 15. Range of annual sediment production rates for graded, ungraded, and abandoned roads in St. John as compared to values reported from other studies.

Table 1. Type, resolution, and period of record for the rain gauges used in this study.

Station	Type of gage	Time and depth resolution	Period of record [Gaps in data]
Bordeaux Mountain	Tipping bucket	15 min; 0.025 cm	14 Sep 98 to 2 Sep 99 [28 Feb 99 to 28 Jun 99]
	Weighing-bucket	60 min; 0.25 cm	2 Sep 99 to 3 May 00 [None]
Fish Bay	Tipping bucket	15 min; 0.025 cm	20 Jul 98 to 3 May 00 [8 Feb 99 to 8 Jul 99; 20 Oct 99 to 7 Nov 99]
Lameshur Bay	Tipping-bucket	15 min; 0.25 cm	19 Aug 98 to 3 May 00 [8 Feb 99 to 12 Jul 99; 19 Oct 99 to 3 May 00]
Maho Bay	Weighing-bucket	60 min; 0.025 cm	13 Jul 98 to 2 Sep 99 [20 Sep 98 to 28 Sep 98]
	Tipping-bucket	15 min; 0.025 cm	2 Sep 99 to 13 Apr 00 [None]

Table 2. Characteristics of the 21 road segments used in this study.

Road Segment ¹	Area (m ²)	Average slope (m m ⁻¹)	Area times slope (m ² m m ⁻¹)	Average width (m)	Traffic rate (vehicles day ⁻¹)	Heavy traffic (trucks day ⁻¹)	Date(s) of regrading	Measurement period (dd/mm/yr)	Number of observations
BM-A	2113	0.08	25.7	5.1	9	0	Nov 1998	28/07/98 to 18/11/99	6
BM-B	469	0.04	16.1	5.0	156	0	Oct 98, Mar 00	28/07/98 to 12/11/99	4
BM-C	1343	0.08	45.8	5.0	156	0	Oct 98, Mar 00	28/07/98 to 26/04/00	7
FB-A	560	0.02	4.48	6.1	282	4-6*	Early 99, Feb 00	10/07/98 to 19/01/00	1
FB-C	536	0.03	9.26	4.9	220	4-6*	Early 99, Feb 00	16/07/98 to 20/01/00	1
FB-D	314	0.01	2.01	4.9	220	4-6*	Early 99, Feb 00	10/07/98 to 21/01/00	1
FB-E	277	0.21	58.1	3.3	4*	0	Late 1997	18/08/98 to 17/11/99**	3
FB-Coco	1110	0.11	92.8	3.5	54	0	Prior to 1996	27/07/98 to 10/09/98	2
JH-A	1098	0.13	45.0	4.6	10	0	Sep 1998	03/07/98 to 28/10/98	4
JH-A-1	266	0.11	21.7	4.7	10	0	Sep 1998	28/10/98 to 02/11/99	3
JH-A-2	324	0.16	42.3	3.6	10	0	Prior to 1996	19/10/98 to 15/11/99	3
JH-B	1669	0.12	26.9	4.3	106	0	Prior to 1996	08/07/98 to 10/12/99	6
JH-C	1189	0.04	8.45	5.0	71	0	Late 1999	08/07/98 to 26/01/00	6
JH-D	721	0.16	28.0	4.9	106	0	Prior to 1996	15/07/99 to 28/02/00	4
JH-E	1053	0.10	10.2	4.6	106	0	Prior to 1996	16/07/98 to 28/02/00	3
LB-A	1056	0.15	26.4	4.3	2*	0	Prior to 1998	31/07/98 to 15/01/00**	3
LB-C	1285	0.09	26.5	5.2	23	0	Feb 99	16/07/99 to 19/11/99	2
LE-Bottom	381	0.14	32.1	4.9	Abandoned	0	Prior to 1985	08/10/99 to 8/03/01**	3
LE-Top	845	0.16	77.0	3.9	Abandoned	0	Prior to 1985	09/11/99 to 06/11/01	4
MB-A	941	0.09	54.3	5.3	108 to 268	4-6*	Jun 98, Aug 99	06/07/98 to 17/11/99	7
MB-C	341	0.04	5.05	5.0	108 to 268	4-6*	Jun 98, Aug 99	08/10/99 to 07/11/01	4
Mean	852	0.10	31.3	4.7					

¹BM= Bordeaux Mountain, FB=Fish Bay, JH=John Head road, LB=Lameshur Bay, LE=L'Esperance, and MB=Maho Bay.

* Estimated values.

** Occasional gaps in the data.

Table 3. R^2 , p values, and slope coefficients for the relationship between precipitation and sediment production (kg m^{-2}) for each segment with at least three observations. Significant relationships are in bold.

Road segment	Number of observations	R^2	p value	Slope coefficient ($\text{kg m}^{-2} \text{cm}^{-1}$)
BM-A	6	0.67	0.045	0.048
BM-B	4	0.97	0.016	0.061
BM-C	7	0.61	0.037	0.094
FB-E	3	0.13	0.77	0.28
JH-A	4	0.82	0.12	0.076
JH-A1	3	0.73	0.34	0.11
JH-A2	3	0.99	0.066	0.27
JH-B	9	0.55	0.056	0.064
JH-C	6	0.58	0.076	0.023
JH-D	4	0.97	0.012	0.12
JH-E	4	0.68	0.17	0.048
LB-A	3	0.93	0.17	0.39
LE-Bottom	3	0.007	> 0.25	-0.0028
LE-Top	4	0.11	> 0.25	-0.0047
MB-A	7	0.79	0.011	0.21
MB-C	4	0.63	0.20	0.018

Table 4. Sediment production by road segment normalized by precipitation and slope. The means and standard deviations are shown for the different traffic and grading categories.

Road segment	Traffic category	Grading category	Normalized sediment production (kg m ⁻² cm ⁻¹ m m ⁻¹)
BM-A	Light	Graded	0.39
BM-B	Light	Graded	1.50
BM-C	Light	Graded	1.06
FB-Coco	Light	Ungraded	0.60
FB-A	Heavy	Graded	0.25
FB-C	Heavy	Graded	0.52
FB-D	Heavy	Graded	0.78
FB-E	Light	Graded	2.11
JH-A	Light	Graded	0.85
JH-A1	Light	Graded	1.08
JH-A2	Light	Ungraded	0.74
JH-B	Light	Ungraded	0.60
JH-C	Light	Graded	0.82
JH-D	Light	Ungraded	0.39
JH-E	Light	Ungraded	0.45
LB-A	Light	Ungraded	0.59
LB-C	Light	Graded	0.53
LE-Bottom	Abandoned	Abandoned	0.10
LE-Top	Abandoned	Abandoned	0.04
MB-A	Heavy	Graded	2.18
MB-C	Heavy	Graded	0.42
		Mean heavy traffic (n=14)	1.28 (s.d.=1.24)
		Mean light traffic (n=59)	0.81 (s.d.=0.62)
		Mean graded (n=48)	1.12 (s.d.=0.87)
		Mean ungraded (n=25)	0.56 (s.d.=0.30)

Table 5. General linear regression model for predicting sediment production rates for unpaved road segments on St. John.

ROAD EROSION MODEL

($R^2 = 0.75$; $p < 0.0001$)

<u>Parameter</u>	<u>Regression coefficient</u>	<u>Standard error</u>	<u>p-value</u>	<u>Partial R^2</u>
Intercept	-0.432	0.26	0.1047	--
Precipitation*Slope ^{1.5} (cm m m ⁻¹)	1.88	0.29	< 0.0001	0.15
Precipitation*Slope ^{1.5} *Grading (cm m m ⁻¹)	2.85	0.34	< 0.0001	0.60

Table 6. Weighted mean particle sizes by grading, and average slope. Values with different letters indicate that the means are statistically different.

Grading and slope class	Number of road plots per class	Percent gravel	Percent sand	Percent silt and clay	Mean D ₁₆ (mm)	Mean D ₅₀ (mm)	Mean D ₈₄ (mm)
All samples	20	40	54	6	0.12	0.72	4.1
<u>Grading class</u>							
Abandoned	2	73	27	0.1	0.35	3.1	11
Graded	12	36 ^a	58 ^b	6 ^c	0.08 ^A	0.36 ^B	2.5 ^C
Ungraded	6	41 ^a	53 ^b	6 ^c	0.11 ^A	0.64 ^B	4.8 ^C
<u>Slope class</u>							
Low (<10%)	9	32 ^d	60 ^f	8 ^h	0.08 ^D	0.33 ^E	2.5 ^F
Moderate (10-15%)	7	43 ^{d e}	51 ^{f g}	5 ^{h i}	0.11 ^D	0.79 ^E	4.3 ^{F G}
High (>15%)	4	51 ^e	46 ^g	3 ^{h i}	0.20 ^D	1.5 ^E	7.2 ^G

CHAPTER 3.
RUNOFF AND SEDIMENT YIELDS FROM AN UNPAVED ROAD SEGMENT,
ST. JOHN, U.S. VIRGIN ISLANDS

ABSTRACT

Unpaved roads have been identified as the primary source of terrigenous sediments being delivered to marine ecosystems around the island of St. John. These sediments pose a threat to the growth and overall condition of nearshore coral reef communities. The goal of this project was to calibrate and test event-based runoff and sediment yield models for an unpaved road segment, as these could provide a better understanding of processes and help in the design of erosion control strategies. The specific objectives were to: (1) measure runoff and suspended sediment yields from a road segment; (2) develop, calibrate, and test the performance of two event-based runoff models; and (3) compare predicted suspended sediment yields to sediment yields measured by a sediment trap. The first runoff model (GA-UH) combines the Green-Ampt infiltration equation with an empirically-derived unit hydrograph. The second model (GA-KW) uses the same infiltration equation, but routes the excess precipitation using a physically-based kinematic wave approach.

Precipitation and runoff data were collected from a 230-m long, mostly-unpaved road segment in the Maho Bay area of St. John over an 8-month period. Over the study period there were 135 storm events with a total rainfall of 42.3 cm. Total runoff was of 9.8 cm from 26 events. From 0.3 to 0.5 cm of precipitation was needed to initiate runoff and discharge was non-linearly correlated with precipitation.

The two models were calibrated based on a set of eight storms. Both models performed very similarly when tested using a different set of 18 storm events. Model performance was poor for rainfall events smaller than 1 cm, but improved for larger events. These problems appear to be due to the difficulty of accurately characterizing infiltration rates during the initial portion of storm events. Overall, the GA-KW performed slightly better as it resulted in hydrographs with higher correlation values than those from GA-UH.

Suspended sediment concentration showed a significant non-linear correlation with runoff rates. Coupling the GA-KW model with an empirical sediment-rating curve estimated sediment yields that were linearly correlated with total precipitation ($r^2 = 0.93$). The estimated sediment yield rate of 0.29 kg m^{-2} per centimeter of precipitation was very similar to that measured by a sediment trap. However, yield rates by particle size categories showed that close agreement only occurred for sand-size particles, while large discrepancies existed for all other size categories. An erosion rate of $0.42 \text{ kg m}^{-2} \text{ cm}^{-1}$ ($48 \text{ kg m}^{-2} \text{ yr}^{-1}$) appears to be a more accurate sediment yield rate estimate for this road segment with eroded material consisting of 29% gravel, 31% sand, 38% silt, and 2% clay. The estimated annual sediment yield rate represents a four-order increase over rates measured from undisturbed hillslopes. The models developed by this study could be used as a tool to develop and implement better road drainage design aimed at reducing road erosion and sediment yields into the nearshore marine ecosystem of St. John.

3.1 Introduction

3.1.1 Problem Statement

Roads alter a series of processes that control the storage and distribution of water on the landscape. The most obvious effect of roads is to increase the frequency and magnitude of surface runoff by creating a compacted, low-permeability surface (Bren and Leitch, 1985; Harden, 1992; Ziegler and Giambelluca, 1997). Roads can intercept subsurface flows (e.g., Megahan, 1972) and disrupt natural drainage patterns (Montgomery, 1994). It is less clear whether these total changes can induce significant changes in runoff at the basin scale (Jones and Grant, 1996; Thomas and Megahan, 1998; La Marche and Lettenmaier, 2001).

Roads also alter the rate at which sediment is produced, routed, and eventually exported from a catchment. Surface erosion rates are typically much higher on cutslopes, fillslopes, and unpaved travelways than on undisturbed hillslopes (e.g., Megahan, 1978; Reid, 1981; Megahan et al., 2001). Hillslope gullies formed by the concentration of road drainage are an additional source of sediment and an important conduit for delivering runoff and sediment to the fluvial network (Wemple et al., 1996; Croke and Mockler, 2001). Unpaved roads have been shown to increase the frequency of mass-wasting events (e.g., Gresswell et al., 1979; Wemple et al., 2001) and watershed-scale sediment yields (e.g., Rice et al., 1979; Anderson and Potts, 1987).

The generation and delivery of terrestrial sediments is a particular concern in the eastern Caribbean because this can adversely affect nearshore coral reef communities (Hubbard, 1987). This issue has received special attention on the island of St. John because of the importance of the surrounding coral reefs to tourism and the local economy. Over 70 km² of St. John's offshore waters have been designated as an International Biosphere Reserve and are either part of the Virgin Islands National Park (VINP) or the V.I. Coral Reef National Monument.

Earlier studies showed that unpaved roads on St. John can increase sediment production rates at the plot and hillslope scale by several orders of magnitude relative to undisturbed areas (MacDonald et al., 2001). Unpaved roads are believed to be the primary source of fine sediment

being delivered to the marine environment (MacDonald et al., 1997; Anderson and MacDonald, 1998; Ramos-Scharrón and MacDonald, 2003). An empirical model developed from sediment trap data concluded that road erosion is a function of total precipitation, road gradient, drainage pattern, and the frequency of grading (Chapter 2). MacDonald et al. (2001) captured the runoff from several road segments and showed that only 6 mm of precipitation was needed to initiate overland flow but just 2 to 13% of the rainfall from small-to-moderate storms was transformed into runoff.

The primary limitation of earlier work was that it aggregated runoff and sediment yields from one or more storms. A more process-based understanding of the relationships between rainfall intensity, runoff rates, and suspended sediment concentrations is needed to better predict runoff and sediment yield at the road-segment scale. More process-based models could compensate for the likely underestimate of silt and clays from the sediment traps that have been used to assess sediment production rates on St. John (Sampson, 1999; Chapter 2; Chapter 4). More explicit models could also provide better predictions of runoff and erosion rates from more extreme events and make predictions for a wider range of road conditions.

The main objectives of this study were to: (1) assess the relationship between precipitation, runoff, and suspended sediment yields for a single road segment at a high temporal resolution; (2) develop, calibrate, and test the performance of two runoff models; (3) couple a runoff model with a sediment-rating curve; and (4) compare predicted sediment yields to values measured with a sediment trap and values estimated with an empirical road segment erosion model.

3.1.2 Previous Road-Runoff Studies and Models

Event-based models for predicting road runoff and suspended sediment yields generally share a three-step structure. First, models quantify rainfall excess by determining the difference between rainfall intensity and infiltration rates. Empirical models generally have either applied an average infiltration rate to all events (e.g., Reid, 1981) or constructed a time-dependent

infiltration capacity curve (e.g., Ziegler and Giambelluca, 1997). Runoff data from road plots also have been used to calibrate physically-based infiltration models (e.g., Luce, 1990; Ziegler et al. 2001a). Reported infiltration rates for unpaved roads range from 0.02 to 3.7 cm hr⁻¹, while calibrated or measured saturated hydraulic conductivity values have varied from 0.02 to 0.60 cm hr⁻¹ (Table 1).

The second step in event-based modeling is to transform excess precipitation into an outflow hydrograph. Unit hydrographs have been a common method to transform excess precipitation into outflow (e.g., Kahklen, 1994; Reid and Dunne, 1984). More physically-based models for routing excess precipitation generally use a kinematic wave approach, where overland flow rates are approximated either by the Darcy-Weisbach (e.g., Luce and Cundy, 1992; Simons et al., 1977, 1978) or Manning's equations (e.g., Ziegler et al., 2001a).

The third component uses the predicted runoff to calculate sediment production rates. Some studies have used a sediment-rating curve, which is an empirical relationship between discharge and suspended sediment concentrations (e.g., Reid and Dunne, 1984). Alternatively, sediment production rates can be estimated by physically-based models. These compare the erosive forces applied by rainfall and overland flow to the erodibility of the road surface material (e.g., Simons et al., 1977, 1978). While erodibility is typically treated as a constant for a given road segment, the erodibility of a road surface can vary with maintenance practices, traffic, and the amount of material already eroded (Ziegler et al., 2000). At least one recent study has attempted to incorporate these effects into a more physically-based road erosion model (Ziegler et al., 2001a).

This study developed, calibrated, and tested the performance of two runoff models. The first model calculated infiltration rates using the Green-Ampt equation (GA). The precipitation excess estimated by this model (GA-UH) was transformed into outflow based on an empirically-derived unit hydrograph. The second model (GA-KW) also used the GA equation and combined

it with a kinematic wave routing approach. The GA-KW model was coupled with an empirical sediment rating curve to estimate sediment yields.

3.2 Study Area

St. John lies approximately 80 km east of Puerto Rico and is the third largest island of the U.S. Virgin Islands. The topography of St. John is very rugged, as more than 80% of the island has slopes greater than 30% (CH2M Hill, 1979; Anderson, 1994). Vegetation is dominated by dry evergreen formations and moist tropical forests (Woodburry and Weaver, 1987).

The climate of St. John is characterized as dry tropical. Easterly waves moving through the Caribbean are important contributors to rainfall from May through November, while cold fronts control the rainfall regime the rest of the year (Calversbert, 1970). Bowden et al. (1970) identified five different precipitation zones with values ranging from 89-102 cm yr⁻¹ to 127-140 cm yr⁻¹. Precipitation in St. John can be highly erosive. Maximum 15-min intensities at Caneel Bay exceeded 10 cm hr⁻¹ sixteen times between 1979 and 1995, and these were generally associated with the largest storm events. Sampson (1999) estimated that annual precipitation energy at Caneel Bay averages 13,500 MJ mm ha⁻¹ hr⁻¹.

Rapid development on privately-owned lands has led to a dense network of unpaved roads. Construction and maintenance standards of public roads and private driveways are generally very poor. The spacing of effective road drainage structures (i.e., ditches, culverts, or cross-drains) is very sparse, even on extremely steep road segments. The steep gradients, poor drainage design, and high rainfall erosivity result in the development of deep rills on the road surfaces. Roads with considerable light vehicle traffic have to be regraded approximately every year.

Rainfall, runoff, and suspended sediment yields were collected from a 230-m long road segment in the Maho Bay area on the north-central portion of St. John (Figures 1 and 2a). The study segment (hereafter referred as Maho-Road) was divided into four sub-segments according to differences in road surface material and slope (Table 2). Maho-Road has a total road tread area

of 1,240 m², an average slope of 12.5%, and a partially-paved section that is 48 m long and has an area of 190 m². The partially-paved section has a thin layer of non-reinforced concrete on a poorly-prepared native surface. The concrete is breaking apart and exposes some of the underlying material. The unpaved portions of Maho-Road are regraded about twice a year, as deep rills on the road surface hinders the daily traffic load of 100-270 light vehicles and 4-6 heavy trucks.

Rocks in the Maho Bay area are part of the Picara Member of the Tutu Formation, which consist of metamorphosed volcanic wacke, conglomerate, siltstone, limestone, with some basalt (Rankin, 2002). Soils in the area are part of the Maho Bay loamy soil series (NRCS, 1995). These soils are typically shallow, moderately permeable, well drained, and underlain by nearly impervious material. These characteristics are largely responsible for the high infiltration rates on undisturbed areas and a lack of Hortonian overland flow. The average annual rainfall in the Maho Bay area is between 114 and 127 cm (Bowden et al., 1970).

3.3 Methods

3.3.1 Field Methods

Precipitation intensities were measured by rain gauges located about 25 m from the top or western end of Maho-Road (Figure 1). A weighing-bucket rain gauge provided one-hour precipitation intensity data with a resolution of 2.5 mm from 22 August 1999 to 2 September 1999, while a tipping-bucket rain gauge with a resolution of 0.25 mm was used from 2 September 1999 to 16 May 2000. The data collected by the tipping-bucket gauge were aggregated to 5-minute intervals. Individual storms were defined as a precipitation event separated from other events by at least one hour with no precipitation.

A 20.3-cm portable cutthroat flume was used to measure runoff (Figure 2b). The flume was installed in a natural swale about 8 m downslope from a broad dip that diverted all of the runoff from the road surface (Figure 1). The flume had a maximum capacity of 65 L s⁻¹, which

equates to a runoff rate of 19.0 cm hr^{-1} for the surface area of Maho-Road. Stage was measured at 5-minute intervals by a pressure transducer inserted into a stilling well attached to the flume, and recorded by a data logger. An equation provided by the flume manufacturer (Baski, Inc.) was used to convert the stage data to discharge. During some runoff events manual staff gage readings were taken at 2.5 to 5 minute intervals.

Data collection was interrupted several times during the study period. From 13 to 23 October 1999 the orifice leading to the stilling well was clogged with sediment, and this led to erroneous stage values. On 25 October 1999 the flume was dislodged by high flows and it was not reset until 30 October 1999. The flume was also dislodged on 17 November 1999 by runoff from Hurricane Lenny, and measurements were not resumed until 17 December 1999.

Since the road segment was unbounded and the flume was in a natural drainage, visual observations were used to identify when there was additional runoff from upslope areas. Observations during most of the storm events indicated that upslope areas produced runoff only during intense rainfall events with wet antecedent conditions. Subsurface flow interception at the road cutslopes was short-lived and very rare. Flow from upslope areas or the cutslope were observed on 12 November 1999, 17 November 1999, and 23 February 2000, and these events have been excluded from the data set.

During some flow events 1-6 grab samples were collected at the outlet of the flume in 250-ml plastic bottles. The samples were collected by submerging a bottle with a loosely-fitted cap into the flow, briefly removing the cap until the bottle was filled, and then replacing the cap before removing the bottle.

3.3.2 Modeling Infiltration Capacity

Direct calculation of an infiltration curve over time was not possible for time periods shorter than the duration of events because the infiltration losses could not be separated from the effects of flow routing along the road segment. The average infiltration rate for the road segment

was calculated for each event by subtracting the depth of runoff from precipitation, and dividing this value by the duration of runoff. By fitting a non-linear regression equation to the relationship between average infiltration rate and flow duration, infiltration rates could be estimated for 1-minute intervals (equation 1):

$$i(t_i) = [n \cdot \{\bar{I}(t_i)\}] - \sum_1^{i-1} i(t_i) \quad (\text{eq. 1})$$

where $i(t_i)$ is the infiltration i minutes after the beginning of the event, n is the rank of one-minute intervals with $n=1$ at five minutes after the onset of precipitation, $\bar{I}(t_i)$ is the average infiltration rate calculated from the regression equation on the relationship between average infiltration and duration, and $\sum_1^{i-1} i(t_i)$ is the summed infiltration from all previous time periods. The resulting infiltration rates were used to help select the initial values and limits for parameters in the Green-Ampt infiltration equation.

The Green-Ampt (GA) infiltration model is based on a one-dimensional approximation of Darcy's Law. It effectively assumes that piston flow creates a distinct wetting front, and that the suction head and hydraulic conductivity values are constant for a site (Scott, 2000). The GA model is:

$$i(t) = K_s \left[\frac{h_o + h_f + z_f(t)}{z_f(t)} \right] \quad (\text{eq. 2})$$

where $i(t)$ is infiltration capacity in cm hr^{-1} , K_s is the saturated hydraulic conductivity in cm hr^{-1} , h_o is the depth of water ponded on the soil surface in centimeters, h_f is the suction head in centimeters, and $z_f(t)$ is the time-dependent depth of the wetting front in centimeters. As in previous studies, h_o was assumed to be zero to simplify calculations (e.g., Simons et al., 1977;

Flerchinger and Watts, 1987). By assuming that infiltrated water moves downwards as piston flow, the time-dependent depth of the wetting front can be estimated by:

$$z_f(t) = \frac{I(t)}{\Delta\theta_v} \quad (\text{eq. 3})$$

where $I(t)$ is the cumulative depth of infiltration in centimeters and $\Delta\theta_v$ is the volumetric water content deficit of the soil in $\text{cm}^3 \text{cm}^{-3}$. The latter term is defined as the difference between the effective porosity of the soil, which is approximated by its water content at saturation (θ_{sat}), and the water content at the beginning of an individual storm event (θ_i). Combining equations 3 and 4, the infiltration rate can be expressed as:

$$i(t) = K_s \left[\frac{h_f \cdot \Delta\theta_v}{I(t)} + 1 \right] \quad (\text{eq. 4})$$

In the absence of data on changes in θ_v during and after storm events, it was not possible to directly model the increase in infiltration in periods without ponded water due to drying between storms. The initial values for K_s , h_f , and θ_{sat} were calibrated using only those storms with no 6-hr antecedent precipitation and an assumed value of zero for θ_i . θ_i was then used as the only calibration parameter for those events that had a 6-hr antecedent precipitation greater than zero.

Precipitation excess was calculated as the difference between precipitation intensities and the infiltration rates from equation 4. Precipitation excess was calculated using 2.5-minute time steps by assuming that the precipitation intensity for each 2.5-minute step was equal to those measured at a 5-minute resolution.

Three main differences exist in the use of the Green-Ampt infiltration equation by the GA-UH and the GA-KW models. First, the decline in infiltration over time was calculated in the GA-UH model every 5-minutes, while 2.5-minute time steps were used to calculate infiltration in

the GA-KW model. Second, water is available for infiltration in the GA-UH model only during the time step when it is being received as precipitation. All of the excess precipitation calculated by the GA-UH model is routed as overland flow to the outlet of Maho-Road by the unit hydrograph transform function. On the other hand, the GA-KW model continues to calculate infiltration losses even after precipitation has ceased. Total infiltration losses at times with no precipitation are further reduced by a scaling parameter. This parameter reduces the proportion of the Maho-Road with ponded water as the runoff successively drains from each of the four sub-segments. The value of this parameter is derived from an estimated average flow velocity and the length of each sub-segment.

The third difference between the two models with respect to the GA equation is that at each time step the GA-UH model calculates precipitation excess for the entire Maho-Road, while the GA-KW model calculates precipitation excess in each of the four sub-segments. In the GA-KW model the suction head, initial water content, and saturated water content are treated as lumped parameters, but the hydraulic conductivity has different values in the partially-paved and the unpaved sections. The lumped hydraulic conductivity value for Maho-Road ($K_{s \text{ road}}$) used by the GA-UH model is defined in terms of the saturated hydraulic conductivity of both the partially-paved (K_p) and unpaved (K_u) road sections (Equation 5):

$$K_{s \text{ road}} = \left[\frac{A_1 \cdot K_u}{A_t} \right] + \left[\frac{A_2 \cdot K_p}{A_t} \right] + \left[\frac{A_3 \cdot K_u}{A_t} \right] + \left[\frac{A_4 \cdot K_u}{A_t} \right] \quad (\text{eq. 5})$$

where $K_{s \text{ road}}$ is in cm hr^{-1} , A_i is the area in m^2 for each of the four road sub-segments, A_t is the total road segment area in m^2 , and K_u and K_p are in cm hr^{-1} .

3.3.3 Unit Hydrograph Runoff Modeling

The unit hydrograph (UH) is an empirically-defined function that transforms precipitation excess into an outflow hydrograph (McCuen, 1998). The UH approach assumes that the runoff

hydrograph is linearly proportional to excess precipitation, and that the duration of the runoff hydrograph is constant for storms with the same duration (Gray, 1960). Hydrographs from eight storms were used to develop a 2.5-minute unit hydrograph following the rainfall-excess reciprocal method (Dunne and Leopold, 1978). These events were selected because the method requires hydrographs that are single-peaked and generated by storms with similar durations. These criteria meant that the eight storms used were all short-duration and had generally low runoff rates (Appendix II-A).

Runoff data with a 2.5-min resolution were available for all eight of these storms except for the 27 September-c 1999 and 4 January 2000 events, which had data at a 5-minute resolution. The S-Hydrograph method was used to transform the 5-minute unit hydrographs derived from these two storms into 2.5-minute unit hydrographs (McCuen, 1998). The eight 2.5-minute unit hydrographs were shifted in time so that their origin was set at the same time relative to the beginning of excess rainfall (Appendix II-A). The final unit hydrograph was constructed by calculating the mean flow value for each 2.5-minute interval. No additional normalization was required as the resulting unit hydrograph represented one centimeter of precipitation excess.

3.3.4 Kinematic Wave Runoff Modeling

Kinematic waves are a simplified version of the one-dimensional, distributed routing models described by the St. Venant equations (Chow, 1998). These equations include the effect of momentum while neglecting the dynamic effects of pressure and acceleration. Hence the movement of water over a plane can be defined by any equation that conserves momentum, such as Manning's equation (equation 6). The transfer of water from one plane to another can be described by mass conservation (equation 7).

$$Q = \left[\frac{S_o^{1/2}}{n \cdot P^{2/3}} \right] \cdot A \quad (\text{eq. 6})$$

$$q = \frac{\delta Q}{\delta x} + \frac{\delta A}{\delta t} \quad (\text{eq. 7})$$

In these equations Q is discharge in $\text{m}^3 \text{s}^{-1}$, S_o represents the downstream water surface slope in percent, n is Manning's roughness coefficient in seconds $\text{m}^{-1/3}$, P is the wetted perimeter of the flow in meters, A is the flow area in m^2 , x is downslope distance in meters, t is time in seconds, and q refers to inflows or outflows in $\text{m}^3 \text{s}^{-1}$ in the form of precipitation or infiltration. A can be expressed as a power function of Q (equation 8):

$$A = \alpha Q^\beta \quad (\text{eq. 8})$$

where α and β are empirical coefficients. Equations 6 and 8 can be combined to calculate α , while β is usually set to 0.60 (Chow, 1998). After differentiating by time, equation 8 can be combined with equation 7 to produce the kinematic flow equation (equation 9):

$$q = \frac{\delta Q}{\delta x} + \left[\alpha \beta Q^{\beta-1} \left(\frac{\delta Q}{\delta t} \right) \right] \quad (\text{eq. 9})$$

Since discharge (Q) is the only dependent variable, all of other parameters can be measured or estimated from the physical characteristics of the overland flow plane.

Equation 9 was solved for the Maho-Road by following a backward linear difference method to approximate the time and space derivative of discharge (Chow, 1998). The solution to equation 9 was used to calculate the discharge from each of the four sub-segments.

One difficulty of the kinematic wave approach is that discharge on the recession limb asymptotically approaches zero (Henderson and Wooding, 1964). This results in infinitely long recession limbs, which do not match field observations. This problem was noted in the GA-KW simulations and stems from the lack of infiltration during the latter stages of the runoff hydrograph when the scaling parameter had reduced the proportion of the road still experiencing

infiltration to zero. This problem was solved by forcing all flows less than 0.03 cm hr^{-1} to zero, as this discharge is lower than the minimum flow that could be measured with the flume.

3.3.5 Model Calibration

Model calibration required the simultaneous consideration of different parameters. The GA equation has four input parameters that require calibration (K_s , h_f , θ_i , and θ_{sat}). The GA-UH model did not require calibration of parameters in addition to those needed by the GA equation, but additional calibration parameters in the GA-KW model were the hydraulic conductivity (K_s) and surface roughness (n) values for each of the sub-segments.

The calibration of both routing methods was done manually using a multi-objective calibration procedure. The three objectives used for calibration and assessing model error were the percent error in total discharge, the coefficient of determination (R^2) for the overall shapes of the simulated hydrographs as defined by Nash and Sutcliffe (1970), and the percent error in peak discharge. The coefficient of determination is defined as:

$$R^2 = \frac{\sum (q_i - \bar{q}_i)^2 - \sum (\hat{q}_i - q_i)^2}{\sum (q_i - \bar{q}_i)^2} \quad (\text{eq. 10})$$

where q_i is the measured discharge at time i , \bar{q}_i is the mean of all measured runoff rates, and \hat{q}_i is the predicted runoff at time i . An R^2 value of 1.0 indicates perfect agreement, while a negative value indicates that the error in the predicted hydrograph is greater than the variability of the observed hydrograph around the mean discharge. Both routing models were calibrated using the same eight storms used to develop the unit hydrograph.

3.3.6 Suspended Sediment Analysis and Modeling

A total of 70 suspended sediment samples were collected during 21 storm events over the 8-month study period. Suspended sediment concentrations were determined by measuring the

volume of the sample, filtering it using a pre-weighed 24-cm diameter ashless filter with a pore size of 3 μm , drying the filter at 100-110° C for about 24 hours, and weighing it to the nearest 0.01 g. Forty-six samples were also analyzed for their particle-size distribution by use of the hydrometer method (Gee and Bauder, 1986). Regression analyses were used to determine whether discharge affected either the suspended sediment concentration or the particle-size distribution.

3.3.7 Model Application

The GA-UH and GA-KW models were used to estimate total runoff for the 160 storms larger than 0.07 cm that occurred between 2 September 1999 and 19 May 2000. Total discharge predicted for these 160 events was used to estimate runoff responses for storms with precipitation exceeding 2.8 cm, which was the size of the largest storm used for calibration and validation. The performances of the two models were compared on the basis of their percent error in total discharge, the coefficient of determination, and percent error in peak discharge.

Predicted hydrographs from the model with the best overall performance were combined with the empirical sediment-rating curve to estimate suspended sediment yields for all 160 storm events. The mean sediment yield per cm of rainfall value resulting from the runoff-sediment rating curve model was compared to that measured by a sediment trap and that estimated by a general road erosion model (Chapter 2).

3.4 Results

3.4.1 General Results

Reliable precipitation and runoff data were obtained for 135 events with a total rainfall of 41.3 cm between 2 September 1999 and 16 May 2000. These storms lasted for only 10-30 minutes. The largest storm had 2.8 cm of precipitation, a maximum 5-minute intensity of 12.8 cm hr^{-1} , and a total erosivity of 38.6 $\text{MJ cm ha}^{-1} \text{hr}^{-1}$.

Twenty-six of these 135 events produced runoff, and the total discharge was 9.8 cm or 24% of the total rainfall (Table 3). The mean rainfall of the 26 runoff-producing storms was 0.95 cm as opposed to 0.15 cm for the 109 events that did not generate runoff. Total discharge showed a non-linear increase with total rainfall (Figure 3). At least 0.3 to 0.5 cm of rainfall and a 5-minute intensity of 1.8 cm hr^{-1} were required to initiate runoff. Runoff coefficients for storms with less than 1.3 cm of precipitation ranged up to 0.61, while the runoff coefficients for storms larger than 2.2 cm ranged from 0.39 to 0.76 (Table 3; Appendix II-B). The highest peak discharge rate was 12.0 cm hr^{-1} from a storm with a maximum 5-minute rainfall intensity of 7.6 cm hr^{-1} . Peak flow rates were strongly correlated with total precipitation ($r^2=0.81$), and this is because the larger events tended to have higher precipitation intensities (Appendix II-B).

3.4.2 Infiltration Curve

The mean infiltration rate was 1.2 cm hr^{-1} for the 26 events that generated runoff, and the range was from 0.25 to 3.8 cm hr^{-1} . Average infiltration rates were initially highly variable but tended to approximate an asymptotic rate of 0.4 cm hr^{-1} after 40 minutes (Figure 4). The regression equation from Figure 4 was combined with equation 1 to calculate the infiltration curve for Maho-Road (Figure 5). The infiltration rate was limited to 4.0 cm hr^{-1} for the first 10 minutes of an event in order to eliminate the problem of infinitely high infiltration rates at very short time periods. This value is slightly higher than the maximum average infiltration rate in Figure 4. The resulting infiltration curve approaches an asymptotic value of 0.17 cm hr^{-1} by 30 minutes after the onset of infiltration (Figure 5). The estimated asymptotic value of 0.17 cm hr^{-1} was used as the initial estimate of the saturated hydraulic conductivity of the road surface in the GA model.

3.4.3 GA-UH Model Calibration

The mean 2.5-minute unit hydrograph for 1.0 cm of runoff is shown in Figure 6. This has a time to peak of 2.5 minutes, a peak runoff rate of 10.0 cm hr^{-1} , and a total duration of 37.5 minutes. Table 4 shows the range of values considered in calibrating the four parameters needed for the GA-UH model (Equation 4). The mean K_s for Maho-Road ranged only from 0.12 to 0.22 cm hr^{-1} , as this should remain close to the value of 0.17 cm hr^{-1} estimated from the infiltration curve (Figure 5). A value of 0.20 cm hr^{-1} yielded the best match to the observed hydrographs. This value is similar to the other values in the literature (Table 1).

Suction head was allowed to vary between 2.0 and 8.0 cm, as this was the range of values found by Flerchinger and Watts (1987) for unpaved roads in the western United States. A suction head of 5.4 cm was used for the GA-UH model.

The saturated water content (θ_{sat}) was allowed to vary between $0.25 \text{ cm}^3 \text{ cm}^{-3}$ and $0.60 \text{ cm}^3 \text{ cm}^{-3}$. The low-end was similar to the minimum values found by Flerchinger and Watts (1987) for unpaved roads and the high-end was comparable to the value determined for sandy-loam soils (Rawls et al., 1983). This range also falls within the porosity values of 0.25 to $0.40 \text{ cm}^3 \text{ cm}^{-3}$ back-calculated from the surface bulk-density of unpaved roads (Helvey and Kochenderfer, 1990). A θ_{sat} of $0.40 \text{ cm}^3 \text{ cm}^{-3}$ provided the best calibration for the GA-UH model.

During the calibration procedure it was noted that storms with precipitation in the previous six hours necessitated lower infiltration rates than storms without antecedent rainfall. The effect of antecedent precipitation on infiltration was addressed by varying θ_i . A θ_i value of zero was assigned to storms with no 6-hr antecedent precipitation, while θ_i was set to $0.18 \text{ cm}^3 \text{ cm}^{-3}$ for storms with 6-hr antecedent precipitation.

3.4.4 GA-KW Model Calibration

The saturated hydraulic conductivity values for the unpaved (K_u) and paved sections (K_p) of Maho-Road were calculated by applying equation 5 to the different sub-segments listed in Table 2. $K_{s \text{ road}}$ was set to 0.20 cm hr^{-1} in accordance with the results of the GA-UH model calibration, and this resulted in equation 11.

$$K_p = 1.10 - 5.49 * K_u \quad (\text{eq. 11})$$

K_u values ranged from 0.17 to 0.20 cm hr^{-1} in order to keep K_p greater than zero, but lower than K_u . The final hydraulic conductivity values for the GA-KW model were 0.23 and 0.04 cm hr^{-1} for the unpaved and partially-paved sub-segments, respectively. The chosen K_u value falls within the range of values used in previous studies (Table 1).

The calibrated value of θ_{sat} in the GA-KW model was the same as for the GA-UH model ($0.40 \text{ cm}^3 \text{ cm}^{-3}$) and the suction head was 6.4 cm , or only slightly higher than the 5.4 cm used in the GA-UH model. θ_i for storm events with no 6-hr antecedent precipitation was assumed to be zero, while a θ_i of $0.11 \text{ cm}^3 \text{ cm}^{-3}$ was used for events that had antecedent precipitation.

The typical duration of the recession limbs was about 22.5 minutes after the end of precipitation. This suggested that 22.5 minutes was needed for runoff to travel from the top of the road segment to its outlet. Given the total length of 230 m, this yields an average velocity of 0.17 m s^{-1} (10.3 m min^{-1}). Hence, the empirical scaling factor (S_c) to attenuate infiltration after the end of precipitation was defined as:

$$S_c = 1 - \left(t_0 \cdot \frac{10.3}{l_i} \right) \quad (\text{eq. 12})$$

where t_0 is the time in minutes after the precipitation or inflow from upslope sections has ceased, and l_i is the length of road section i in meters (Table 2).

Manning's n for the unpaved sections was allowed to vary from 0.01 to 0.03 $\text{s m}^{-1/3}$ (Table 4). This range was based on values for bare sand and graveled surfaces (Woolhiser, 1975). Manning's n for the concrete paved section was varied from 0.010 to 0.013 $\text{s m}^{-1/3}$ (Woolhiser, 1975). A common value of 0.010 $\text{s m}^{-1/3}$ was finally chosen for both surfaces. Given the advanced state of decay of the concrete in the partially-paved sub-segment it seems reasonable to accept a common surface roughness value for the unpaved and partially-paved sub-segments.

3.4.5 Model Validation

3.4.5.1 GA-UH Model

The GA-UH model was used to compute hydrographs for the 18 events in Table 3 that were not used for calibration (Table 5; Appendix II-C). The mean observed runoff was 0.51 cm, the mean absolute error in the predicted runoff was 0.15 cm or 29%. Absolute errors for individual storms ranged up to 0.63 cm or 43%. Runoff coefficients ranged from 0.00 to 0.72 cm cm^{-1} . The mean runoff coefficient of the predictions was 0.32 cm cm^{-1} or only 10% lower than the observed value of 0.36 cm cm^{-1} .

The accuracy of the GA-UH model in predicting discharge increases with increasing discharge totals. The model predicted runoff for only two of the seven events with less than 0.7 cm of precipitation and exhibited no trends in the absolute error in discharge with increasing runoff (Figure 7). The mean absolute error for the fourteen events with less than 0.5 cm of runoff was 0.13 cm or 69%. The mean absolute error for the four storms exceeding 0.5 cm of discharge was 0.21 cm or 32%.

The overall agreement between observed and simulated hydrographs as expressed by the R^2 parameter was highly variable. The mean R^2 value for the GA-UH model was -0.06 ($n=13$ storms), with values ranging from -2.21 to 0.67 . The events with the largest rainfall totals generally had the lowest variability and the highest R^2 values (Figure 8). R^2 values for the seven

storms with less than 1 cm of precipitation for which runoff was predicted was -0.59 (s.d. = 1.23), while storms larger than 1 cm had an average value of 0.57 (s.d. = 0.19).

The predicted peak flow timings were much closer to the observed values than the magnitude of peak flows. The mean error in the timing of the predicted peak flows was 1.7 minutes. The GA-UH model did tend to predict longer and less steep recession limbs than the observed hydrographs. The mean difference between the observed and predicted peak flows was 1.3 cm hr^{-1} or 61%, with individual values ranging from 0.05 to 5.8 cm hr^{-1} (Figure 8). The model tended to underestimate the largest peak flows and the predicted peak flows were within 25% of the observed value for only three of the 18 storms used for validation (Figure 9).

The rainfall, observed runoff, and predicted runoff for the 5 January 2000 and the 27 September-c 1999 events are shown in Figures 10a and 10b, respectively. Total precipitation in the first of these two storms was 2.36 cm, and the total runoff was within 9% of the measured value (Figure 10a). In Figure 10b the GA-UH model predicted 3.3 times more discharge than the observed and the R^2 value was -1.83. The GA-UH simulations presented in Figures 10a and 10b show two typical errors in predicted hydrographs. First, predicted hydrographs were more responsive to changes in precipitation than observed hydrographs. Second, simulated hydrographs had a tendency to have longer and less steep recession limbs than the observed.

3.4.5.2 GA-KW Model

The GA-KW model was used to predict runoff for the same 18 events that were used to evaluate the GA-UH model (Table 5; Appendix II-D). Mean observed runoff was 0.47 cm and the mean absolute error in the predicted runoff was 0.15 cm or 32%. Absolute errors for individual storms ranged from 0.01 to 0.52 cm. Runoff coefficients ranged from 0.00 to 0.68 cm cm^{-1} . The mean runoff coefficient was 0.26 cm cm^{-1} or 28% lower than the observed value of 0.36 cm cm^{-1} .

The GA-KW model was unable to accurately estimate runoff for the smallest storms, as it predicted no runoff for six of the seven events with less than 0.7 cm of precipitation. The ability of the model to match observed discharges increases with increasing storm size. There were no trends in the absolute error in predicted runoff with an increase in the observed discharge (Figure 7). The mean absolute error for events with less than 0.5 cm of runoff was 0.13 cm or 76%, while the mean error for those storms exceeding 0.5 cm of runoff was 0.23 cm or 31%. Overall, the GA-KW model estimated discharges that were slightly lower than those resulting from the GA-UH model.

The mean R^2 for the predicted hydrographs using the GA-KW model was 0.29 ($n=12$ storms). The largest events generally had the lowest variability in R^2 and the highest and most consistent R^2 values (Figure 8). The R^2 values for the six smallest storms with predicted runoff was -0.08 (s.d. = 0.75), while the mean R^2 for storms with more than 1.0 cm of precipitation was 0.67 (s.d. = 0.22). While the GA-UH and GA-KW models generally produced hydrographs with similar R^2 values, the GA-KW model resulted in hydrographs with higher correlation values than those resulting from GA-UH.

As in the case of the GA-UH model, the predicted peak flows generally were within 2.5 minutes of the observed peaks (Appendix II-D). The GA-KW model also tended to predict longer and less steep recession limbs than the observed hydrographs. The predicted peak flows were generally lower than the observed, especially for the events with the largest peak flows (Figure 9). The mean absolute difference between the observed and the predicted peak flows was 1.3 cm hr^{-1} or 61%, with individual values ranging from 0.05 to 5.3 cm hr^{-1} . Out of the eighteen storms used for model validation, the predicted peak flows were within 25% of the observed values for only two events. The GA-KW model predicted slightly higher peak runoff rates than the GA-UH model, especially for events with observed peak rates exceeding 3.7 cm hr^{-1} .

The GA-KW model produced a hydrograph that was very similar to the observed for the 5 January 2000 event (Figure 10a). The predicted hydrograph for this storm had a R^2 of 0.74 and

a total predicted discharge that was within 1% of the measured runoff. Figure 10b shows an event for which the model produced a hydrograph that did not agree as well with the observed, as evidenced by a R^2 value of -1.53 and a predicted total discharge that was 3.1 times higher than the observed. As in the case with the GA-UH model, these two examples demonstrate that hydrographs predicted by the GA-KW model also predicted hydrographs that were more responsive to changes in precipitation than the observed and recession limbs that were longer and less steep than those from measured hydrographs.

3.4.6 Suspended Sediment Concentration and Yields

The mean suspended sediment concentration for all 70 samples was $20,800 \text{ mg L}^{-1}$ (s.d. $17,800 \text{ mg L}^{-1}$), and the range was from $1,270$ to $84,400 \text{ mg L}^{-1}$. This range is consistent with values from other studies (Table 1).

Suspended sediment concentrations rapidly increased with discharge, but beyond approximately 0.5 cm hr^{-1} there was no clear relationship between discharge and suspended sediment concentrations (Figure 11). The highest concentrations were for 27 samples collected over eight storms between 12 September and 25 October 1999. The mean concentration during these storms was nearly $30,000 \text{ mg L}^{-1}$ compared to $15,300 \text{ mg L}^{-1}$ for the remaining 43 samples. These higher suspended sediment concentrations are presumed to be associated with an increase in erodibility caused by grading of the road surface on 10 September 1999.

Non-linear regression analysis of concentration as a function of discharge for samples that were presumably affected by grading resulted in an exponent equal to 0.25, and the exponent for samples not affected by grading was 0.20. The differences in the exponents for graded and ungraded samples were not significant. As a result the entire 70 samples were used to develop the following sediment-rating curve:

$$C_o = 26,500 \cdot Q^{0.233} \quad (\text{eq. 13})$$

where C_o is total suspended sediment concentration in mg L^{-1} and Q is the instantaneous runoff rate in cm hr^{-1} . The use of a single sediment rating curve assumes a constant relationship between discharge and suspended sediment concentration, and thereby implicitly assumes constant erodibility of the road surface.

The particle-size distribution was determined for 46 samples from 18 different storm events with discharge ranging from 0.03 to 14 cm hr^{-1} . The relative percentage of sand, silt, and clay was highly variable, and there was no correlation between discharge and the particle-size distribution. On average, the samples consisted of 40% sand, 56% silt, and 3% clay with standard deviations of 34%, 34%, and 11%, respectively.

An analysis of the particle-size distributions over time showed that the amount of sand tended to be highest in the six weeks immediately after grading (Appendix II-E). During this period the mean percent sand was 65% and the mean percent silt was 34%. Nine samples had sand contents exceeding 75%. For the other 27 samples the mean sand content was 22% and the mean silt content was 70%. Since this increase in sand content coincides with the increase in sediment concentrations, no changes in the concentration of silt or clay appear to have occurred as a response to the regrading operation (Appendix II-E).

3.4.7 Model Application

3.4.7.1 Runoff

Both models were used to estimate the runoff from all of the 160 storms between 2 September 1999 and 19 May 2000 with at least 0.07 cm of precipitation. Ninety percent of these events had less than 1.0 cm of rainfall, but these events represented only 49% of the total rainfall over this period (Figure 12). Only 10% of the storms had more than 1.0 cm of rainfall, but these accounted for 51% of the total rainfall. The largest event during this period had 9.4 cm of rainfall and a maximum 5-minute precipitation intensity of 11.3 cm hr^{-1} . Long-term precipitation data

from Caneel Bay confirm that storms with less than 1.0 cm of precipitation represent nearly 90% of all storms, but account for only 49% of the total rainfall.

The total runoff estimated by the GA-UH model was 6% higher than the GA-KW model. Both models show a transition from a non-linear relationship between discharge and precipitation to a more linear trend for events with higher precipitation totals than those used for calibration or validation (Appendix II-B). For the 144 events with less than 1.0 cm of precipitation, the predicted runoff from the GA-UH model was 3.6 cm or 67% larger than the comparable value using the GA-KW model. For the larger events the difference in total runoff was only 2.8 cm or 6%. Although both models produced similar results, the GA-KW model was used to estimate runoff and sediment yields because it yielded a better overall match to observed hydrographs.

The predicted runoff for five different storm size classes using the GA-KW model are shown in Figure 12. The storm events larger than 1.0 cm produce 92% of the estimated runoff. The two storms with more than 5 cm of rainfall produced 17% of the total rainfall and 40% of the total runoff.

3.4.7.2 Sediment Yield

The limited number of suspended sediment samples meant that the accuracy of predicted sediment yields could not be tested against measured data. Nevertheless, by coupling the GA-KW model with the sediment rating curve (equation 13), it is possible to estimate sediment yields for the same group of 160 storm events for which total runoff was calculated.

The predicted sediment yields for five different storm size classes are shown in Figure 12. This shows that the storm events larger than 1.0 cm produced 95% of the total sediment yield. The maximum sediment yield for a single storm was 3,900 kg for a 9.4-cm storm on 23 February 2000. The two storms with more than 5 cm of rainfall produced 17% of the total rainfall but 45% of the total sediment yield.

3.5 Discussion

3.5.1 Predicted Runoff

Comparisons of the observed and predicted hydrographs showed similar errors for both models. Both models underestimated the amount of runoff for storms with less than 1 cm of rainfall, underestimated peak flows, and overestimated flow duration. These errors appear to be related to the calculation of precipitation excess rather than to the routing of runoff. The fact that both models are experiencing the same problems, and that their routing algorithms seem to represent different flow velocities, was interpreted as an indication that the routing of runoff was playing a secondary role to the development of precipitation excess. The mean unit hydrograph was derived from relatively small events with low runoff rates, and thus relatively slow flow velocities (Julien, 1995). In contrast, calibrated Manning's n values for both the unpaved and paved sub-segments in the GA-KW model was only $0.010 \text{ s m}^{-1/3}$, which was the lowest calibration value allowed for these parameters (Table 4). This low Manning's n value allows relatively high flow velocities given the inverse relationship between flow velocity and Manning's n (Equation 6).

The measured hydrographs showed considerable variability in total discharge for the storms with less than 1 cm of precipitation (Figure 3). The 0.00 to 0.48 cm total discharges shown for these small storms are comparable to the 0.00 to 0.38 cm discharge range previously reported for storms smaller than 1 cm for other roads on St. John (Sampson, 1999; MacDonald et al., 2001). The observed variability in total discharge and the errors in estimating runoff hydrographs appear to result from large fluctuations in infiltration rates occurring at the beginning of different storm events.

At the beginning of a storm infiltration rates were estimated from the steep portion of the infiltration curve defined by the GA equation. Large errors in the estimation of precipitation excess were likely, given the large changes in infiltration rates during the initial 20 to 25 minutes of an event (Figure 5). Both models were generally unable to predict any discharge for storms

smaller than 0.7 cm and they produced hydrographs with attenuated peak flows relative to the observed. This suggests that the GA model consistently erred in its predictions of initial infiltration by estimating rates that were too high relative to infiltration rates in the field. The calibration procedure resulted in hydraulic conductivity values that appear to compensate for too little runoff during the beginning of an event by considerably decreasing infiltration rates during latter periods. The resulting hydrographs are more responsive to precipitation and longer than the observed.

Previous efforts to physically model road surface runoff at the plot scale also have had problems in accurately predicting discharge during the initial stages of storms. These problems have been attributed to difficulties in quantifying depression storage, as well as antecedent soil moisture content and infiltration rates during the initial stages of storm events (Simons et al., 1978; Luce, 1990; Luce and Cundy, 1994).

3.5.2 Estimated Sediment Yields

The suspended sediment yields estimated by coupling the GA-KW model with the sediment rating curve (equation 13) were compared to sediment trap data for Maho-Road and an empirical sediment production model at the road segment scale (Chapter 2) hereafter referred as the R&M model. The R&M model uses total precipitation, average road slope, and frequency of road grading to predict the mass of sediment collected in traps. Sediment production for a given road segment was found to be linearly related to total precipitation. This has been interpreted as an indication that runoff, precipitation, and suspended sediment yields are linearly correlated. Therefore, the interpretation implies that, in the absence of grading, the concentration of suspended sediment in road runoff must remain rather constant over a time period not exceeding two years. Roads that were graded within the last two years produced more sediment than road segments that had not been graded over two years, but the sediment trap data did not show a short-term increase in sediment production immediately after grading.

In contrast, the suspended sediment data from Maho-Road showed higher sediment concentrations for the first six weeks after grading. During this period there were 22 cm of rainfall and an estimated 6.6 cm of runoff, and this may have been enough runoff to remove much of the easily erodible material. It appears that peaks in sediment production immediately after grading are too short-lived to alter the longer-term sediment yields that were measured with the sediment traps.

Sediment yield rates were estimated by coupling the GA-KW model with the empirical sediment-rating curve (equation 13) for 160 storms between 2 September 1999 and 19 May 2000. The estimated sediment yield was linearly related to precipitation ($R^2 = 0.93$) (Figure 13). The predicted sediment yields from the GA-KW-sediment rating curve model closely match the sediment trap data while the estimated sediment yields using the GA-KW-sediment rating curve are 50% higher than the values predicted by the R&M model.

The apparent similarity in sediment yield rates between the GA-KW-sediment rating curve model, the sediment trap data, and the R&M model does not verify these models, as the three values represent very different particle-size distributions. The mean particle-size distribution for the suspended sediment samples was much finer than the mass-weighted size distribution of the material collected from the sediment trap (Figure 14). The median particle size (D_{50}) for the suspended sediment samples was 0.02 mm versus 0.5 mm for the sediment trap data. The suspended sediment samples did not contain any material larger than coarse sand, while the material captured in the sediment trap consisted of 42% gravel, 51% sand, 5% silt, and 2% clay. The estimated production rates for silt from the GA-KW-sediment rating curve model were 9 times higher than the sediment trap.

The discrepancy in sediment production rates by particle-size class can be attributed to the differences in how sediment production was measured. Grab samples are unlikely to collect gravel-sized fragments for two reasons. First, the transport of coarse fragments is intermittent and spatially-variable across the bottom of the flume. Given the small volume of the sample

bottles, the collection of these particles is unlikely. Second, the coarser particles were probably produced during the most intense storm events when samples were not collected. In contrast, sediment traps are most effective in trapping larger particles but they are less effective in trapping particles finer than 0.025 mm (Ice, 1986).

The actual sediment production rate from Maho-Road is probably closer to 0.42 kg m^2 per centimeter of precipitation than the 0.29 or $0.27 \text{ kg m}^{-2} \text{ cm}^{-1}$ estimated by the GA-KW-sediment rating curve model and sediment trap, respectively. This estimate is obtained by summing the estimated silt and clay fractions from the suspended sediment data to the sand and gravel fraction from the sediment trap. This yields an average of 27% gravel, 33% sand, 38% silt, and 2% clay.

The particle-size distribution of material produced from unpaved road surfaces may vary widely among different sites. The variability is a result of differences in rainfall erosivities, overland flow erosive forces, and road surface particle-size distributions. Only a few studies have measured the entire size distribution of sediment eroded from road segments—including both its suspended and bed load components (Table 1). In New Zealand the sediment from unpaved roads in areas dominated by silty clays and silty-clay loams was 85% silt and clay and only 15% sand or coarser material (Fahey and Coker, 1992). In Australia about two-thirds of the annual sediment production from roads was transported as suspended sediment (Grayson et al., 1993). These contrast with the 40% of silt and clay-sized material being produced from the Maho-Road in St. John.

Results presented here show that unpaved roads in St. John can produce sediment at a very high rate. Assuming an annual rainfall rate of 115 cm, the Maho-Road is estimated to erode at a rate of nearly $50 \text{ kg m}^{-2} \text{ yr}^{-1}$. This rate is four orders of magnitude higher than for undisturbed zero-order hillslopes (Chapter 4). This confirms the important role of unpaved roads in producing sediment on St. John. The event-based models developed by this study may improve runoff and sediment yield predictions for unpaved roads on St. John. Better predictions may

result in the improvement of road drainage design, and a reduction on the quantity of sediment reaching the marine environment of St. John.

3.6 Conclusions

Precipitation and runoff data were collected from 135 storms on a 230-m long road segment on the island of St. John. These storms produced 41.3 cm of rainfall, and the precipitation for individual storms ranged up to 2.84 cm. Five-minute rainfall intensities ranged up to 12 cm hr⁻¹. Only 9.8 cm or 24% of this precipitation was converted into runoff. Between 0.3 and 0.5 cm of precipitation were needed to initiate runoff and only 26 of the 135 storms generated runoff. Runoff increased non-linearly with storm rainfall ($p < 0.0001$). The calculated mean infiltration rate for the 26 events that produced runoff was 1.2 cm hr⁻¹, and the range was from 0.25 to 3.8 cm hr⁻¹. Average infiltration rates were initially highly variable but tended to approximate an asymptotic rate of 0.4 cm hr⁻¹ after 40 minutes.

Precipitation and runoff data from eight events were used to develop and calibrate two runoff models. The first model (GA-UH) predicted runoff using the Green-Ampt infiltration equation and an empirically-derived unit hydrograph. The second model (GA-KW) used the Green-Ampt infiltration equation to calculate precipitation excess and a kinematic wave approach to route this runoff. Model calibration yielded parameter sets with physically realistic values.

The two models were evaluated by comparing predicted against measured hydrographs for the other 18 storms. The GA-UH model had a mean error in discharge prediction of 29%, a mean absolute difference between predicted and observed peak flows of 1.3 cm hr⁻¹, and a mean R² of -0.06. The GA-KW model had a mean error in discharge prediction of 32%, a mean absolute difference between predicted and observed peak flows of 1.3 cm hr⁻¹, and a mean R² value of 0.29. The predicted hydrographs from the two models were very similar, as both models predicted no runoff for most events with less than 0.7 cm of rainfall. Errors in predicting discharge did not increase with increasing storm size. Both models tended to underestimate peak

flows. Much of the error in predicting storm runoff was attributed to the difficulty of predicting the initial infiltration rate. Overall, the GA-KW model performed slightly better than the GA-UH model.

The mean suspended sediment concentration from 70 grab samples was 20,800 mg L⁻¹, and the maximum values were around 84,400 mg L⁻¹. Suspended sediment concentrations increased non-linearly with discharge ($p < 0.0001$). Grading appeared to increase sediment concentrations for approximately six weeks. By combining the GA-KW model with the sediment rating curve, the sediment yield for 160 storm events was 0.29 kg m⁻² per centimeter of rainfall. This value was very similar to the value of 0.27 kg m⁻² cm⁻¹ determined from sediment trap data for the same road segment.

The similarity between these erosion rates does not verify either value as the modeled sediment yield was dominated by fine particles and the sediment trap captured mostly sand and gravel. There was close agreement only for the sand-sized particles. Given the sampling bias of each method, the true sediment yield can be more accurately estimated by summing the rates for silt and clay from the models developed here to the sand and gravel material measured from the sediment fence. On this basis the total sediment yield for the road segment is estimated to be 0.42 kg m⁻² cm⁻¹ or 40-50% more than the value predicted from either one of the two methods individually. The estimated particle-size distribution of the material being eroded consists of 27% gravel, 33% sand, 38% silt, and only 2% clay.

On an annual basis, road surface erosion from Maho-Road is estimated to be close to 50 kg m⁻², or four orders of magnitude more than the erosion for undisturbed zero-order hillslopes. This confirms that unpaved roads are a dominant source of sediment on St. John. The event-based models developed in this study can improve the quality of road runoff and sediment yield predictions on St. John. Better predictions may result in the improvement of road drainage design and a reduction on the quantity of sediment reaching the marine environment of St. John.

3.7 References Cited

- Anderson B, Potts DF. 1987. Suspended sediment and turbidity following road construction and logging in western Montana. *Water Resources Bulletin* 23: 681-690.
- Anderson DM. 1994. Analysis and modeling of erosion hazards and sediment delivery on St. John, U.S. Virgin Islands. US National Park Service Water Resources Division, Technical Report NPS/NRWRD/NRTR-94-34, Fort Collins, Colorado, 153 p.
- Anderson DM, MacDonald LH. 1998. Modelling road surface sediment production using a vector geographic information system. *Earth Surface Processes and Landforms* 23: 95-107.
- Bilby RE, Sullivan K, Duncan SH. 1989. The generation and fate of road-surface sediment in forested watersheds in southwestern Washington. *Forest Science* 35(2): 453-468.
- Bowden MJ, Fischman N, Cook P, Wood J, and Omasta E. 1970. Climate, water balance, and climatic change in the northwest Virgin Islands. Caribbean Research Institute, College of the Virgin Islands, 127 p.
- Bren LJ, Leitch CJ. 1985. Hydrologic effects of a stretch of forest road. *Australian Forest Research* 15(2): 183-194.
- Calversbert RJ. 1970. Climate of Puerto Rico and the U.S. Virgin Islands. Climatography of the United States No. 60-52, US Dept. of Commerce, 29 p.
- CH2M Hill. 1979. A sediment reduction program: Report to the Department of Conservation and Cultural Affairs, Government of the U.S. Virgin Islands, St. Thomas, USVI.
- Chow, VT. 1998. Handbook of Applied Hydrology. McGraw-Hill, New York, NY.
- Coker RJ, Fahey BD, Payne JJ. 1993. Fine sediment production from truck traffic, Queen Charlotte Forest, Marlborough Sounds, New Zealand. *Journal of Hydrology (N.Z.)* 31(1): 56-64.
- Croke J, Mockler S. 2001. Gully initiation and road-to-stream linkage in a forested catchment, southeastern Australia. *Earth Surface Processes and Landforms* 26(2): 205-218.
- Dunne T, Leopold L. 1978. Water in Environmental Planning. W.H. Freeman and Company, New York, NY, 818 p.
- Fahey BD, Coker RJ. 1992. Sediment production from forest roads in Queen Charlotte Forest and potential impact on marine water quality, Marlborough Sounds, New Zealand. *New Zealand Journal of Marine and Freshwater Research* 26: 187-195.
- Flerchinger GN, Watts FJ. 1987. Predicting infiltration parameters for a road sediment model. *Transactions of the ASAE* 30(6): 1700-1705.
- Gee GW, Bauder JW. 1986. Particle-size analysis. In: A. Klute (ed.) *Methods of Soil Analysis Part 1: Physical and Mineralogical Methods*. American Society of Agronomy: 383-411.

- Gray DM. 1960. Derivation of hydrographs for small watersheds from measurable physical characteristics. Ph.D. dissertation, Iowa State University of Science and Technology, 208 p.
- Grayson RB, Haydon SR, Jayasuriya MDA, Finlayson BL. 1993. Water quality in mountain ash forests- separating the impacts of roads from those of logging operation. *Journal of Hydrology* 150: 459-480.
- Gresswell S, Heller D, Swanston DN. 1979. Mass movement response to forest management in the central Oregon Coast Ranges. USDA Forest Service Resource Bulletin PNW-84, Portland, OR, 26 p.
- Harden CP. 1992. Incorporating roads and footpaths in watershed-scale hydrologic and soil erosion models. *Physical Geography* 13(4): 368-385.
- Helvey JD, Kochenderfer JN. 1990. Soil density and moisture content on two unused forest roads during first 30 months after construction. USDA Forest Service Research Paper NE-629, 6 p.
- Henderson FM, Wooding RA. 1964. Overland flow and groundwater flow from a steady rainfall of finite duration. *Journal of Geophysical Research* 69(8): 1531-1540.
- Hubbard DK. 1987. A general review of sedimentation as it relates to environmental stress in the Virgin Islands Biosphere Reserve and the eastern Caribbean in general. Biosphere Reserve Report no. 20, Virgin Islands Resource Management Cooperative, St. Thomas, 42 p.
- Ice G. 1986. A study of the effectiveness of sediment traps for the collection of sediment from small plot studies. NCASI Technical Bulletin 483, New York, NY, 27 p.
- Jones JA, Grant GE. 1996. Peak flow responses to clear-cutting and roads in small and large basins, western Cascades, Oregon. *Water Resources Research* 32(4): 959-974.
- Julien PY. 1995. Erosion and Sedimentation. Cambridge University Press, 280 p.
- Kahklen KF. 1994. Surface erosion from a forest road, Polk Inlet, Prince of Wales Island, Alaska. M.S. thesis, Oregon State University, Corvallis, OR, 95 p.
- La Marche JL, Lettenmaier DP. 2001. Effects of forest roads on flood flows in the Deschutes River, Washington. *Earth Surface Processes and Landforms* 26(2): 115-134.
- Luce C. 1990. Analysis of infiltration and overland flow from small plots on forest roads. M.S. thesis, University of Washington, Seattle, WA, 64 p.
- Luce CH, Cundy TW. 1992. Modification of the kinematic wave-Phillip infiltration overland flow model. *Water Resources Research* 28(4): 1179-1186.
- Luce CH, Cundy TW. 1994. Parameter identification for a runoff model for forest roads. *Water Resources Research* 30(4): 1057-1069.

- MacDonald LH, Anderson DM, Dietrich WE. 1997. Paradise threatened: Land use and erosion on St. John, US Virgin Islands. *Environmental Management* 21(6): 851-863.
- MacDonald LH, Sampson RW, Anderson DM. 2001. Runoff and road erosion at the plot and road segment scales, St. John, US Virgin Islands. *Earth Surface Processes and Landforms* 26: 251-272.
- McCuen RH. 1998. Hydrologic Analysis and Design. Prentice Hall, New Jersey, 814 p.
- Megahan WF. 1972. Subsurface flow interception by a logging road in mountains of central Idaho. National Symposium on Watersheds in Transition. American Water Resources Association and Colorado State University, 350-356.
- Megahan WF. 1978. Erosion processes on steep granitic road fills in central Idaho. *Soil Science Society of America Journal* 42(2): 350-357.
- Megahan WF, Wilson M, Monsen SB. 2001. Sediment production from granitic cutslopes on forest roads in Idaho, USA. *Earth Surface Processes and Landforms* 26(2): 153-164.
- Montgomery DR. 1994. Road surface drainage, channel initiation, and slope instability. *Water Resources Research* 30(6): 1925-1932.
- Nash JE, Sutcliffe JV. 1970. River flow forecasting through conceptual models, Part 1- A discussion of principles. *Journal of Hydrology* 10: 282-290.
- Natural Resources Conservation Service. 1995. Classification and correlation of the soils of the Virgin Islands of the United States-Update. U.S. Department of Agriculture, Hato Rey, Puerto Rico, 18 p.
- Ramos-Scharrón, MacDonald LH. 2003. Measuring and modeling the effects of development on sediment production and delivery, St. John, U.S. Virgin Islands. *EOS, Transactions AGU Fall Meeting Supplement* 84(46), Abstract H51F-07: F755-F756.
- Rankin DW. 2002. Geology of St. John, U.S. Virgin Islands. U.S. Geological Survey Professional Paper 1631, 36 p.
- Rawls WJ, Brakensiek DL, Miller N. 1983. Green-Ampt infiltration parameters from soils data. *Journal of Hydraulic Engineering* 109(1): 62-70.
- Reid LM. 1981. Sediment production from gravel-surfaced roads, Clearwater basin, Washington, Publication FRI-UW-8108, University of Washington Fisheries Research Institute, Seattle, WA, 247 p.
- Reid LM, Dunne T. 1984. Sediment production from forest road surfaces. *Water Resources Research* 20(11): 1753-1761.
- Rice RM, Tilley FB, Datzman PA. 1979. A watershed's response to logging and roads: South Fork of Caspar Creek, California, 1967-1976. U.S. Dept. of Agriculture, Forest Service, Research Paper PSW-146, Berkeley, CA, 12 p.

- Sampson RW. 1999. Road runoff and erosion at the plot and road segment scales on St. John, US Virgin Islands. M.S. thesis, Department of Earth Resources, Colorado State University, Fort Collins, CO, 189 p.
- Scott HD. 2000. Soil Physics- Agricultural and Environmental Applications. Iowa State University Press, Iowa, 421 p.
- Simons DB, Li RM, Shiao LY. 1977. Formation of a road sediment model. Civil Engineering Dept., Engineering Research Center. Colorado State University, Fort Collins, CO, Report CER76-77DBS-RML-LYS50, 107 p.
- Simons DB, Li RM, Ward TJ, Shiao LY. 1978. Simple road sediment yield model. USDA Forest Service Report, Fort Collins, CO, Report CER77-78-DBS-RML-TJW-LYS41, 70 p.
- Thomas RB, Megahan WF. 1998. Peak flow responses to clear-cutting and roads in small and large basins, western Cascades, Oregon: A second opinion. *Water Resources Research* 34(12): 3393-3403.
- Vincent KR. 1979. Runoff and erosion from a logging road in response to snowmelt and rainfall. M.S. thesis, University of California, Berkeley, CA; 60 p.
- Wald AR. 1975. The impact of truck traffic and road maintenance on suspended-sediment yield from a 14' standard forest road. MS thesis, University of Washington, Seattle.
- Wemple BC, Jones JA, Grant GE. 1996. Channel network extension by logging roads in two basins, western Cascades, Oregon. *Water Resources Bulletin* 32(6): 1195-1207.
- Wemple BC, Swanson FJ, Jones JA. 2001. Forest roads and geomorphic process interactions, Cascade Range, Oregon. *Earth Surface Processes and Landforms* 26(2): 191-204.
- Woodbury RO, Weaver PL. 1987. The vegetation of St. John and Hassel Island, USVI. National Park Service, Southeast Region, Research/Resources Management Report SER-83, Atlanta, GA, 26 p.
- Woolhiser DA. 1975. Simulation of unsteady overland flow. In: Unsteady Flow in Open Channels (K Mahmood and V. Yevjevich, Eds), Water Resources Publications, Fort Collins, CO, Vol. 2: 485-508.
- Ziegler AD, Giambelluca TW. 1997. Importance of rural roads as source areas for runoff in mountainous areas of northern Thailand. *Journal of Hydrology* 196: 204-229.
- Ziegler AD, Sutherland RA, Giambelluca TW. 2000. Partitioning total erosion on unpaved roads into splash and hydraulic components: The roles of interstorm surface preparation and dynamic erodibility. *Water Resources Research* 36(9): 2787-2791.
- Ziegler AD, Giambelluca TW, Sutherland RA. 2001a. Erosion prediction on unpaved mountain roads in northern Thailand: validation of dynamic erodibility modelling using KINEROS2. *Hydrological Processes* 15: 337-358.

Ziegler AD, Sutherland RA, Giambelluca TW. 2001b. Interstorm surface preparation and sediment detachment by vehicle traffic on unpaved mountain roads. *Earth Surface Processes and Landforms* 26: 235-250.

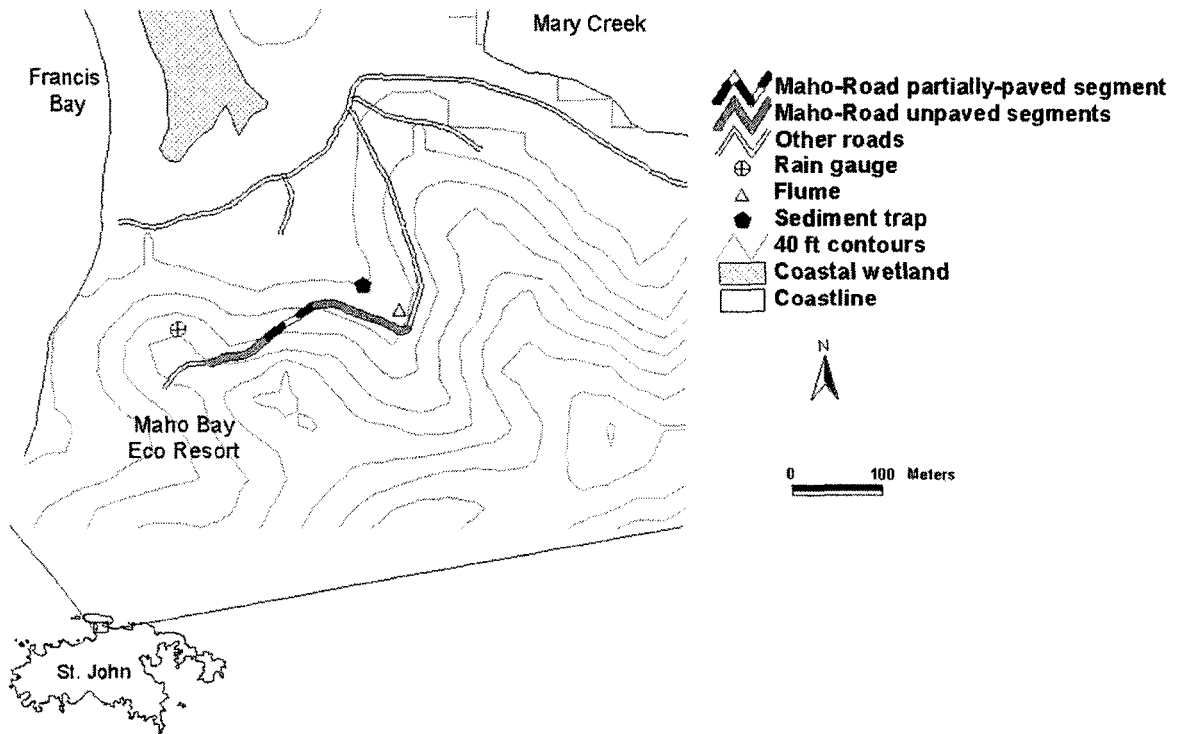


Figure 1. Map of the Maho Bay area showing the road segment that was studied and the location of the rain gauge, cutthroat flume, and sediment trap.



Figure 2a. Picture of the lower sections of Maho-Road.

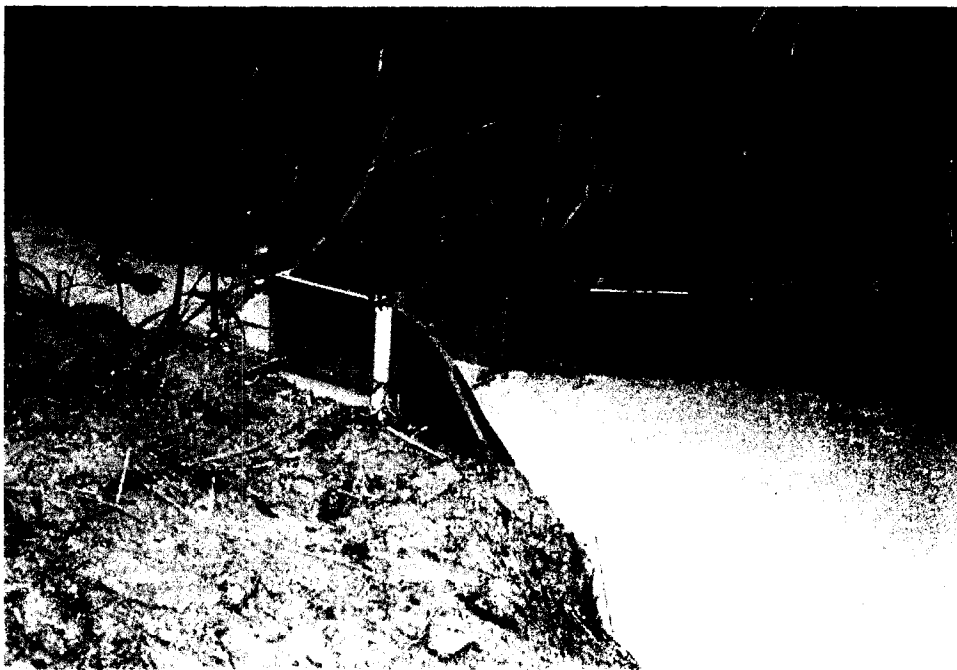


Figure 2b. Picture of a portable cutthroat flume similar to the one used to measure runoff from Maho-Road.

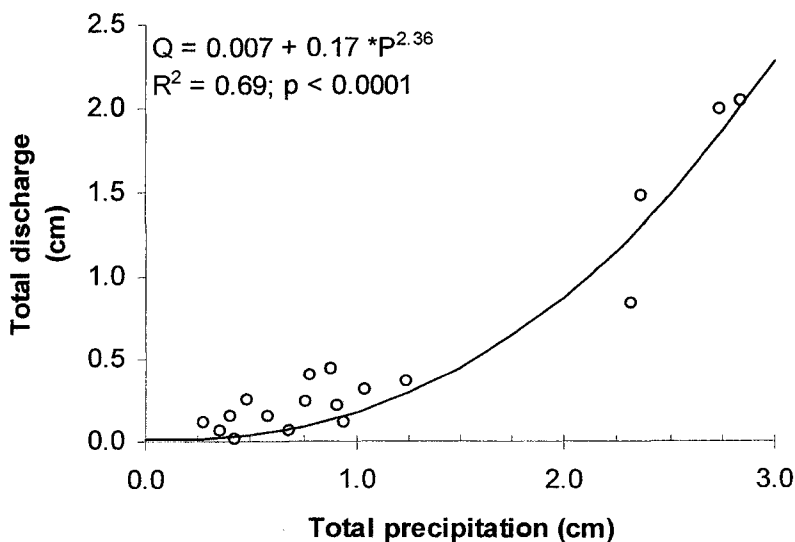


Figure 3. Relationship between precipitation (P) and observed discharge (Q) for the 26 events that produced runoff.

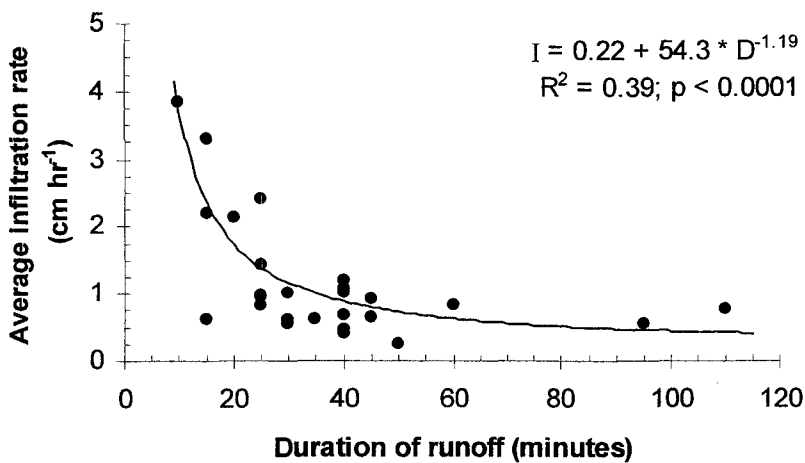


Figure 4. Relationship between duration of runoff (D) and average infiltration rate (I) for the 26 events that produced runoff.

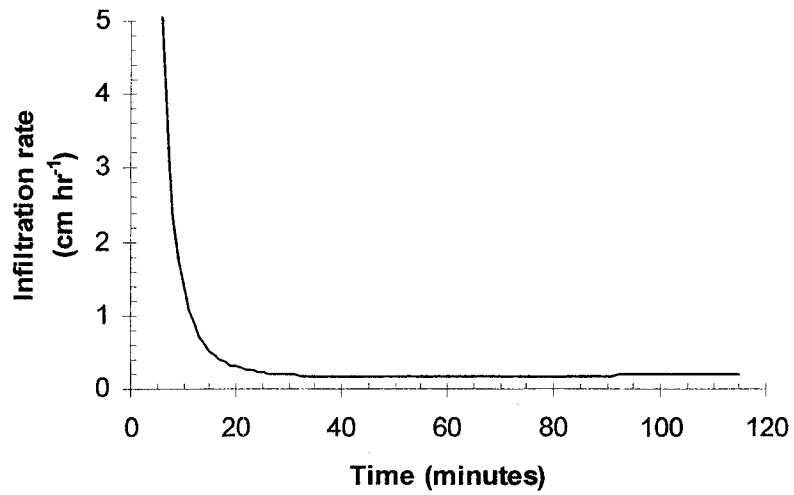


Figure 5. Inferred infiltration curve for Maho-Road.

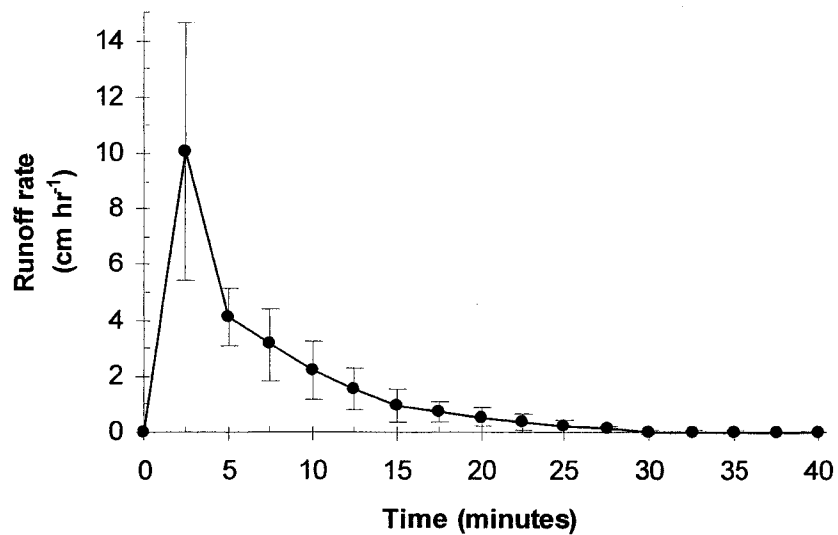


Figure 6. Mean 2.5-minute unit hydrograph from 1.0 cm of excess precipitation for Maho-Road. Bars indicate one standard deviation.

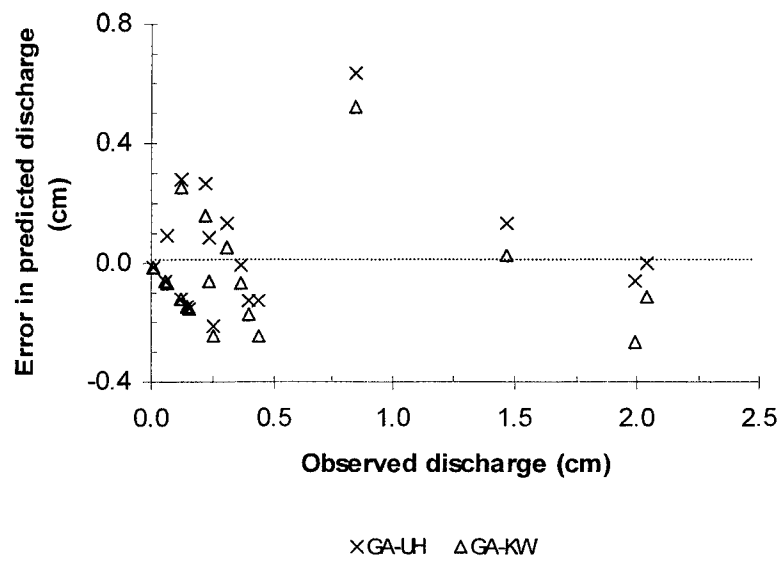


Figure 7. Relationship between total observed discharge and the net error in discharge prediction for 18 event used for model validation.

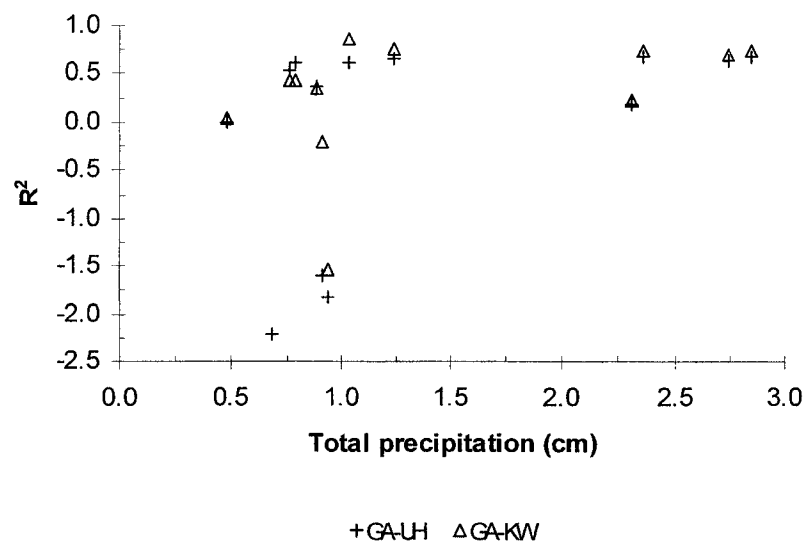


Figure 8. Plot of the coefficient of determination (R^2) between the predicted and observed hydrographs as a function of storm size.

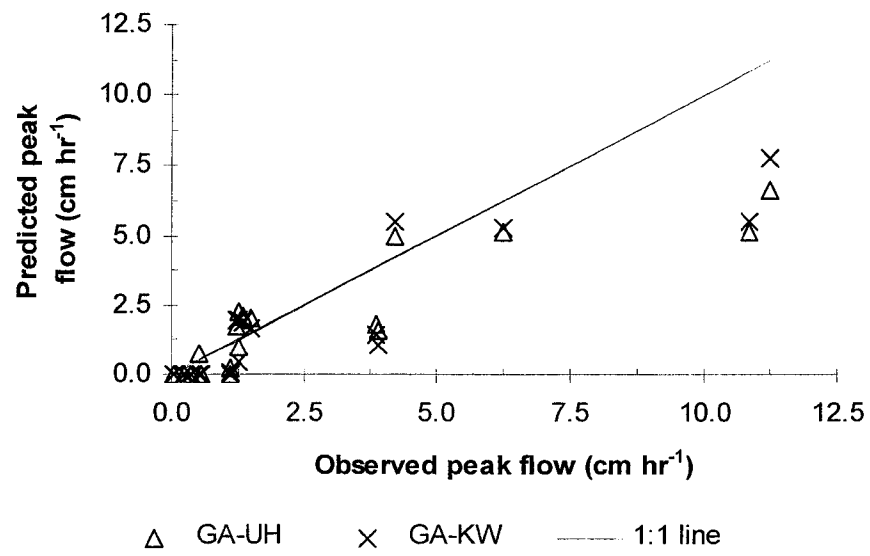


Figure 9. Relationship between measured and predicted peak runoff rates for the 18 storms used for model validation.

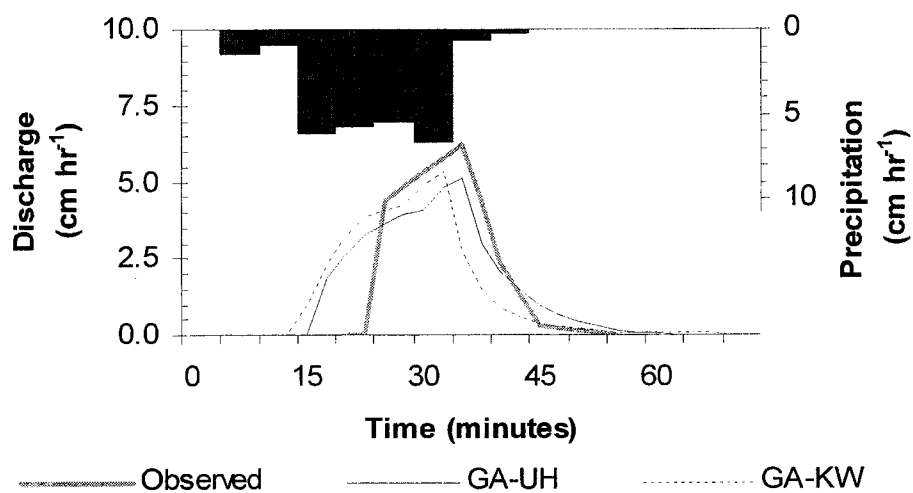


Figure 10a. Hyetograph, observed hydrograph, and simulated hydrograph for the storm on 5 January 2000.

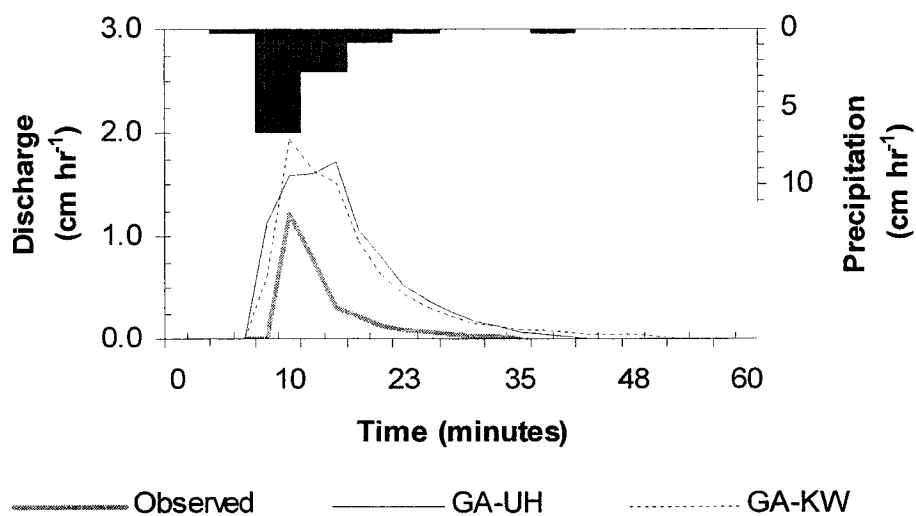


Figure 10b. Hyetograph, observed hydrograph, and simulated hydrograph for the 27 September 1999_c storm.

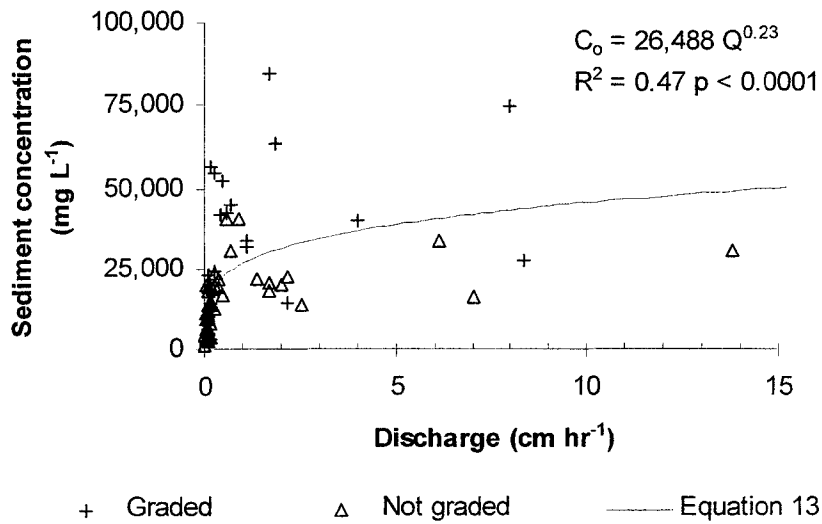


Figure 11. Relationship between suspended sediment concentrations (C_0) and discharge (Q). Maho-Road was graded on 10 September 1999, and the data from 12 September to 25 October 1999 are plotted using a plus sign.

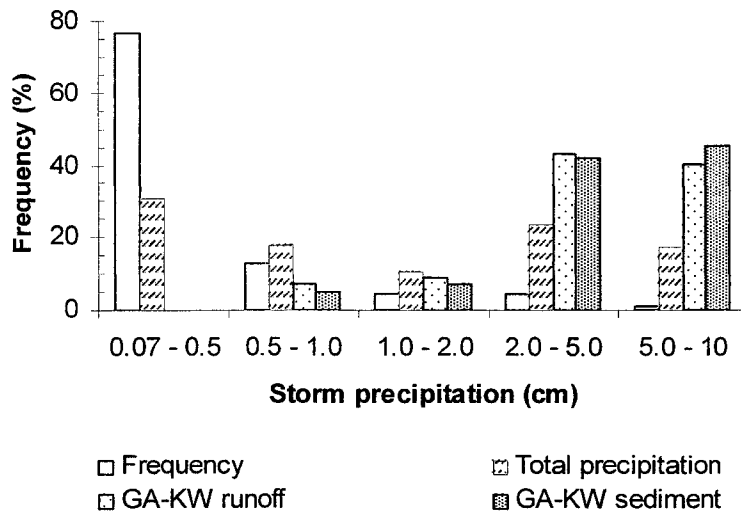


Figure 12. Relative frequency by storm size for 160 storms between 2 September 1999 and 16 May 2000. Percent of the total runoff and sediment yields were calculated with the GA-KW model and equation 13, respectively.

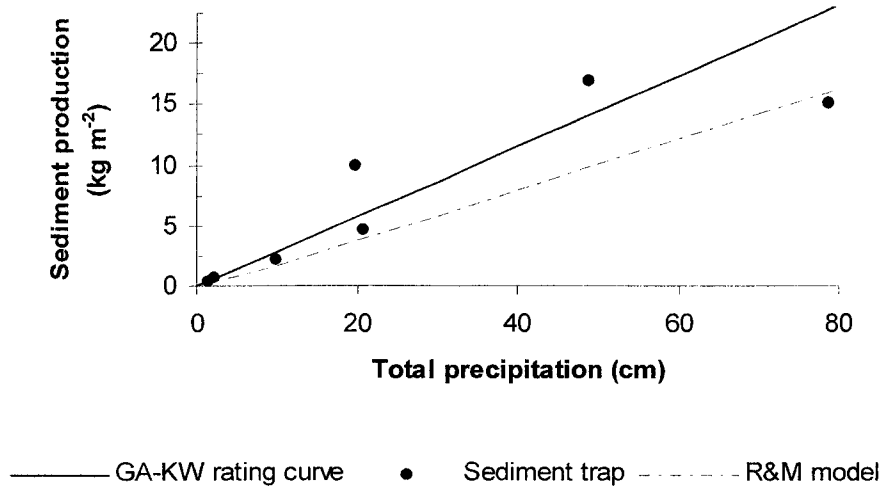


Figure 13. Relationship between total precipitation and sediment production for the GA-KW-sediment rating curve model, the sediment trap from Maho-Road, and the R&M empirical sediment production model.

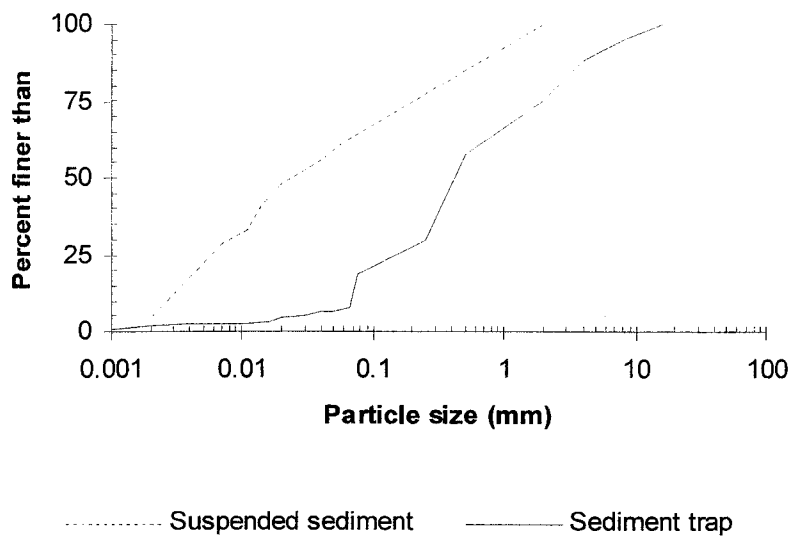


Figure 14. Average particle-size distribution for the suspended sediment samples and the sediment trap data.

Table 1. Summary of previous hydrologic and suspended sediment data for unpaved roads.

Reference	Scale and type of measurements	Runoff coefficient (cm cm ⁻¹)	Average infiltration (cm hr ⁻¹)	Hydraulic conductivity (cm hr ⁻¹)	Sediment concentration (mg L ⁻¹)	Percentage of sediment by size categories
Bilby et al., 1989	Segment scale (700-3,600 m ²) runoff/sed. yield measurements	--	--	--	70 to 10,000 all traffic intensities	80% clays 20% silt and coarser
Bren & Leitch, 1985	Segment scale (2,100 m ²) runoff measurements	0.04 to 0.80	--	--	--	--
Coker et al., 1993	Sub-segment scale (35-60 m ²) runoff/sed. yield measurements	0.42 to 0.66	--	--	3,000 to 15,000 no truck traffic 130,000 during truck passes	--
Fahey & Coker, 1992	Sub-segment scale (100 m ²) runoff/sed. yield measurements	--	0.3	--	3,000	85% silts & clays 15% sand & coarser
Grayson et al., 1993	Segment scale (~1,100 m ²) sediment yield measurements	--	--	--	23,000 low use/maint. 35,000-40,000 high use/maint.	66% fines 33% coarse
Harden, 1992	Sub-plot scale (0.02 m ²) infiltration/rainsplash measurements	0.00 to 1.0	0.4 to 3.6	--	520 to 227,000	--
Kahklien, 1994	Road-segment scale (100-250 m ²) runoff/sed. yield measurements	--	0.09	--	0.2 to 118	--
Luce, 1990 Luce & Cundy, 1992	Plot scale (1 m ²) runoff measurements	--	--	0.17 to 0.60	--	--
Luce & Cundy, 1994	Plot scale (1-5 m ²) runoff measurements	--	--	0.21 to 0.50	--	--
Reid, 1981 Reid and Dunne, 1984	Road-segment scale (250-920 m ²) runoff/sed. yield measurements	0.44 to 0.58	0.05	--	400 to 30,000 heavy use 70 to 1,000 temporary use	--
Sampson, 1999 MacDonald et al., 2001	Sub-segment scale (35-60 m ²) runoff/sed. yield measurements	0.04 to 0.13	--	--	5,000 to 50,000	4-40% silts & clays 60-96% sand & coarser
Vincent, 1979	Road-segment scale (110-160 m ²) runoff/sed. yield measurements	0.37 to 0.80	0.02 to 0.05	--	--	--
Wald, 1975	Road-segment scale (400-800 m ²) sediment yield measurements	1.0 (assumed)	--	--	100 low use/maintenance 1,300- high use/maintenance	--
Ziegler & Giambelluca, 1997	Sub-plot scale (< 1 m ²) infiltration measurements	0.02 to 0.88 (from simulations)	--	0.02 to 0.5	--	--
Ziegler et al., 2000	Plot scale (~3 m ²) runoff/sed. yield measurements	0.62 to 0.84	0.62 to 3.7	--	--	--
Ziegler et al., 2001b	Plot scale (~3-5 m ²) runoff/sed. yield measurements	0.60 to 0.86	0.62 to 1.6	--	~25,000- mean for control roads 68,000- mean during truck passes 44,000- mean immediately after grading	--

Table 2. Characteristics of the four sub-segments comprising Maho-Road.

Section Number	Total length (m)	Average width (m)	Average slope (m m ⁻¹)	Comments
1	49	4.4	0.10	Top section, unpaved surface
2	48	4.0	0.26	Partially-paved
3	40	6.0	0.13	Unpaved
4	95	6.3	0.09	Lowermost section, unpaved

Table 3. List of storms with reliable rainfall and runoff data. An asterisk indicates those events used in the development of the unit hydrograph and for model calibration.

Event date	Total precipitation (cm)	Erosivity (MJ cm ha ⁻¹ hr ⁻¹)	Max 5-min precipitation intensity (cm hr ⁻¹)	Total discharge (cm)	Peak discharge (cm hr ⁻¹)	Runoff coefficient
6-Sep-99	1.04	5.32	4.27	0.312	1.34	0.30
8-Sep-99	0.91	4.27	4.88	0.200	1.23	0.22
12-Sep-99	0.89	2.29	3.35	0.439	3.91	0.49
27-Sep-99_a	0.94	4.34	6.71	0.119	1.22	0.13
27-Sep-99_b*	0.36	0.65	3.35	0.022	0.16	0.06
27-Sep-99_c*	0.61	1.68	3.36	0.060	0.64	0.10
5-Oct-99*	0.94	4.97	7.92	0.144	1.77	0.15
12-Oct-99	0.58	1.10	2.44	0.140	0.24	0.24
13-Oct-99*	0.48	1.16	3.96	0.072	0.40	0.15
20-Oct-99	0.79	2.84	3.96	0.480	3.86	0.61
23-Oct-99	2.84	38.6	12.80	2.16	11.2	0.76
25-Oct-99	0.48	0.91	2.74	0.240	1.08	0.50
30-Oct-99	2.31	23.3	7.92	0.910	4.22	0.39
6-Nov-99	0.41	0.60	1.83	0.148	0.56	0.36
10-Nov-99	1.24	3.55	4.57	0.360	1.50	0.29
11-Nov-99	2.74	22.5	7.62	1.93	12.0	0.70
13-Nov-99	0.28	0.35	2.44	0.130	1.09	0.46
14-Nov-99	0.69	1.29	2.13	0.050	0.56	0.07
16-Nov-99	0.76	1.95	2.44	0.260	1.34	0.34
4-Jan-99*	0.41	0.77	2.40	0.013	0.05	0.03
5-Jan-00	2.36	21.6	6.71	1.36	6.25	0.58
29-Jan-00*	0.61	1.20	3.36	0.016	0.10	0.03
20-Apr-00	0.43	0.50	2.44	0.078	0.05	0.18
22-Apr-00*	0.71	1.82	3.66	0.027	0.16	0.04
29-Apr-00*	0.53	1.49	4.88	0.045	0.50	0.08
2-May-00	0.36	0.25	2.74	0.060	0.33	0.17

Table 4. Range of parameter values considered in model calibration and the final calibrated values selected for the GA-UH and GA-KW models, respectively. Wet conditions refer to events with 6-hr antecedent precipitation greater than zero. NA indicates not applicable.

Parameter	Range of possible values	Unit hydrograph model	Kinematic wave model
Mean K_s (cm hr ⁻¹)	0.12 - 0.22	0.20	NA
K_s unpaved sections (cm hr ⁻¹)	0.15 - 0.23	NA	0.23
K_s partially-paved section (cm hr ⁻¹)	0.00 - 0.22	NA	0.04
Max infiltration rate (cm hr ⁻¹)	0 - ∞	4.0	4.0
h_f (cm)	2.0 - 8.0	5.4	6.4
$\theta_{\text{saturated}}$ (cm ³ cm ⁻³)	0.25 - 0.60	0.4	0.4
$\theta_{\text{initial-dry conditions}}$ (cm ³ cm ⁻³)	0.00 - θ_{sat}	0.00	0.00
$\theta_{\text{initial-wet conditions}}$ (cm ³ cm ⁻³)	0.00 - θ_{sat}	0.18	0.11
Manning's n, unpaved sections (s m ^{-1/3})	0.010 - 0.030	NA	0.010
Manning's n, paved section (s m ^{-1/3})	0.010 - 0.013	NA	0.010
β	0 - 1	NA	0.6

Table 5. Summary of model validation results. NA indicates not applicable.

Event	OBSERVED			GA-UH MODEL						GA-KW MODEL					
	Runoff (cm)	Runoff coefficient (cm cm ⁻¹)	Peak flow (cm hr ⁻¹)	Predicted runoff (cm)	Error in runoff (cm)	Runoff coefficient (cm cm ⁻¹)	Peak flow (cm hr ⁻¹)	Error in peak flow (cm hr ⁻¹)	R ²	Predicted runoff (cm)	Error in runoff (cm)	Runoff coefficient (cm cm ⁻¹)	Peak flow (cm hr ⁻¹)	Error in peak flow (cm hr ⁻¹)	R ²
6-Sep-99	0.31	0.30	1.34	0.45	0.13	0.43	2.11	0.77	0.61	0.37	0.05	0.35	1.89	0.55	0.86
8-Sep-99	0.22	0.24	1.23	0.48	0.27	0.53	2.26	1.03	-1.60	0.38	0.16	0.41	1.97	0.74	-0.21
12-Sep_b-99	0.44	0.49	3.91	0.31	0.13	0.35	1.57	2.34	0.36	0.20	0.24	0.24	1.09	2.82	0.35
27-Sep_c-99	0.12	0.13	1.22	0.40	0.28	0.42	1.71	0.49	-1.83	0.37	0.25	0.40	1.94	0.72	-1.53
12-Oct-99	0.15	0.26	0.24	0.00	0.15	0.00	0.00	0.24	n/a	0.00	0.15	0.00	0.00	0.24	n/a
20-Oct-99	0.40	0.51	3.86	0.27	0.13	0.35	1.83	2.03	0.61	0.23	0.17	0.29	1.44	2.42	0.42
23-Oct-99	2.04	0.72	11.24	2.04	0.00	0.72	6.66	4.58	0.67	1.92	0.11	0.68	7.76	3.48	0.73
25-Oct-99	0.25	0.52	1.08	0.03	0.22	0.07	0.25	0.83	0.01	0.00	0.25	0.01	0.07	1.01	0.03
30-Oct-99	0.84	0.36	4.22	1.47	0.63	0.64	4.98	0.76	0.18	1.36	0.52	0.59	5.48	1.26	0.23
6-Nov-99	0.15	0.36	0.56	0.00	0.15	0.00	0.00	0.56	n/a	0.00	0.15	0.00	0.00	0.56	n/a
10-Nov-99	0.36	0.29	1.50	0.36	0.01	0.29	2.02	0.52	0.65	0.30	0.06	0.26	1.63	0.13	0.75
11-Nov-99	1.99	0.72	10.86	1.93	0.06	0.70	5.08	5.78	0.62	1.72	0.27	0.63	5.51	5.35	0.70
13-Nov-99	0.12	0.42	1.09	0.00	0.12	0.00	0.00	1.09	n/a	0.00	0.12	0.00	0.00	1.09	n/a
14-Nov-99	0.07	0.10	0.52	0.16	0.10	0.24	0.72	0.20	-2.21	0.00	0.07	0.00	0.00	0.52	n/a
16-Nov-99	0.24	0.24	1.25	0.32	0.08	0.35	0.98	0.27	0.53	0.17	0.06	0.18	0.43	0.82	0.43
5-Jan-00	1.47	0.62	6.25	1.60	0.13	0.68	5.11	1.14	0.67	1.49	0.02	0.63	5.30	0.95	0.74
20-Apr-00	0.01	0.03	0.05	0.00	0.01	0.00	0.00	0.05	n/a	0.00	0.01	0.00	0.00	0.05	n/a
2-May-00	0.06	0.17	0.33	0.00	0.06	0.00	0.00	0.33	n/a	0.00	0.06	0.00	0.00	0.33	n/a
Sum	9.23			9.82	2.65					8.51	2.74				
Mean	0.51	0.36		0.55	0.15	0.32		1.28	-0.06	0.47	0.15	0.26		1.28	0.29
Std. Dev.	0.64	0.21		0.70	0.14	0.26		1.55	1.1	0.66	0.12	0.25		1.38	0.66

CHAPTER 4.
MEASUREMENT AND PREDICTION OF NATURAL AND ANTHROPOGENIC SEDIMENT SOURCES ON
ST. JOHN, U.S. VIRGIN ISLANDS

ABSTRACT

An increase in the amount of sediment delivered to the marine environment can adversely affect nearshore coral reef communities. The development of scientifically-sound erosion control strategies requires an understanding of natural and anthropogenic sediment sources. The objectives of this study were to measure and develop predictive models for both natural and anthropogenic sediment sources on St. John in the U.S. Virgin Islands. Erosion rates from streambanks, treethrow, hillslopes, zero- and first-order basins, road surfaces, and cutslopes were measured by different methods between 1998 and 2001.

Streambank erosion had the highest natural erosion rate, with an average value of 10 kg m⁻² yr⁻¹. Uprooting of trees along stream margins is estimated to deliver sediment at a rate of 0.17 tonnes km⁻¹ yr⁻¹, or 11 g m⁻² yr⁻¹ for a 15 meter wide stream corridor. Sediment production rates from undisturbed 40 m² hillslope plots ranged from 1 to 27 g m⁻² yr⁻¹. Mean rates from zero- and first-order catchments were 1 and 8 g m⁻² yr⁻¹, respectively.

Roads that are graded once every two years had sediment production rates of 0.57 and 58 kg m⁻² yr⁻¹ for roads with average slopes of 1 and 21%, respectively. Ungraded roads had sediment production rates ranging from 5.1 to 14 kg m⁻² yr⁻¹ for roads with slopes of 10 and 16%, respectively. Abandoned roads with a 15% slope had an average erosion rate of 1.1 kg m⁻² yr⁻¹. Although cutslopes eroded at rates ranging from 2 to 17 kg m⁻² yr⁻¹, their contribution to sediment

yields at the road-segment scale was estimated to be only about $0.9 \text{ kg m}^{-2} \text{ yr}^{-1}$. Actively-used roads on St. John produce sediment at a rate that is up to four orders of magnitude higher than from undisturbed plots and zero-order catchments. First-order catchments receiving sediment from unpaved roads showed a mean yield rate of $38 \text{ g m}^{-2} \text{ yr}^{-1}$, or about five times the rate of comparable undisturbed catchments.

The relative importance of each of these sediment sources in watershed-scale sediment production and yield rates is likely to change from catchment to catchment as a result of the abundance and spatial distribution of each landscape type. The data presented here are needed to develop a GIS-based model that predicts sediment production and yields at the catchment scale.

4.1 Introduction

Land disturbance generally increases sediment production rates and sediment yields above natural conditions (Walling, 1997). The effects of land disturbance in forested areas are of particular concern because natural erosion rates are so low (Dunne, 2001). Marine ecosystems—particularly nearshore coral reef communities—are sensitive to increased sediment inputs resulting from land disturbance (Hubbard, 1987; Hodgson, 1989, 1997; Rogers, 1990). An increase in sediment inputs is of particular concern in many parts of the Caribbean because of the importance of coral reefs to the local economies.

In the Caribbean region very little information is available on the amount of sediment being delivered to the marine environment (UNEP, 1994). Mass wasting processes have received significant attention from researchers because of their widespread occurrence throughout the region, and their potential for destruction and loss of life (e.g., De Graff et al., 1989; Jibson, 1989; Scatena and Larsen, 1991; Larsen and Parks, 1997; Larsen and Torres-Sánchez, 1998). Studies of surface erosion have concentrated on agricultural fields in Puerto Rico (Smith and Abruña, 1955), Tobago (Ahmad and Breckner, 1974), and Jamaica (McGregor, 1988). Other studies have used uncalibrated empirical models to predict sediment yields from areas with different land uses (e.g., Del Mar-López et al., 1998).

Increased sediment yields from land development are believed to be adversely affecting the nearshore coral reef communities of St. John in the U.S. Virgin Islands (Rogers, 1998). The unpaved road network has been identified as the primary source of the fine sediment being delivered to the marine environment (Anderson, 1994). The development and application of an empirical road erosion model (Anderson and MacDonald, 1998) suggested that road erosion is increasing watershed-scale sediment yields by up to four times above background levels (MacDonald et al., 1997). This model was based on very limited data and did not include some of the key factors controlling road erosion rates, such as precipitation, traffic, or the frequency of grading. The road erosion model also could not quantify erosion

rates from natural sediment sources, and this meant that the effects of roads could not be quantified relative to natural conditions.

Improved equations to predict both natural and road-related sediment production are needed for the development of a GIS-based sediment budget model (Chapter 5). The sediment budget model is needed to quantify the sediment being delivered from different sources, identify appropriate erosion control strategies, and guide future development. Hence the main objectives of this study were to: (1) measure sediment production rates from natural and anthropogenic sources; (2) compare sediment production estimates to published data from other areas; and (3) develop empirical sediment production models for each of these sources.

A sediment budget approach provides a useful framework for evaluating the absolute and relative contribution of different sediment sources (Reid and Dunne, 1996). For a single landscape unit, a sediment budget quantitatively describes the production, movement, and storage of sediment (Dietrich et al., 1982). In this paper a landscape unit is defined as the portion of a drainage basin with similar erosion processes acting at a relatively uniform rate.

Previous work and initial field observations led to the identification of the following six landscape units on St. John: (1) streambanks, (2) stream margins subjected to soil disturbance by uprooted trees, (3) undisturbed hillslopes, (4) zero-order (unchannelled) and first-order catchments, (5) road travelways, and (6) road cutslopes. The predictive equations developed for each of these landscape units are being used in the GIS-based sediment budget model (Chapter 5).

4.2 Study Area

The island of St. John is located about 80 km east of Puerto Rico and is the third largest island within the U.S. Virgin Islands (Figure 1). Fifty-six percent of the total 50 km² of land area and 23 km² of offshore waters have been designated as a Biosphere Reserve and

comprise the Virgin Islands National Park (VINP). In 2001 an additional 47 km² of offshore waters were incorporated into the Virgin Islands Coral Reef National Monument.

The lithology of St. John is dominated by rocks originating from volcanic flows (Donnelly, 1966; Rankin, 2002) that have undergone periods of deformation, magmatic intrusions, and hydrothermal alterations. Soils are dominated by gravelly loams and clay loams (USDA, 1995), and are characterized by abundant coarse fragments (Soil Conservation Service, 1970). Soils tend to be shallow, moderately permeable, well-drained, and underlain by nearly impervious rocks. The topography of St. John is very rugged, as more than 80% of the slopes are greater than 30% (CH2M Hill, 1979; Anderson, 1994). Bordeaux Mountain is the highest point of the island at an elevation of 387 m.

The climate of St. John is characterized as dry tropical. Bowden et al. (1970) identified five precipitation zones ranging from a low of 89-102 cm yr⁻¹ on the easternmost end of the island to a high of 127-140 cm yr⁻¹ near Bordeaux Mountain. Easterly waves, which can develop into tropical storms and hurricanes, generate most of the rainfall from May through November, while cold fronts are important sources of rainfall from December through April (Calversbert, 1970). There are no sharply defined wet and dry seasons in the Virgin Islands, but a relatively dry season extends from about February to July, and a relatively wet season lasts from August until January (Bowden et al., 1970). Mean monthly potential evapotranspiration (PET) exceeds mean monthly precipitation for most of the year (Sampson, 2000), and there are no perennial streams on St. John.

Precipitation in St. John can be highly erosive. The average erosivity at Caneel Bay was estimated to be 13,500 MJ mm ha⁻¹ hr⁻¹ (Sampson, 2000). On average, the 15-minute precipitation intensity at Caneel Bay exceeds 10 cm hr⁻¹ about once a year.

Erodible banks on St. John are generally restricted to areas where streams intersect alluvial or colluvial deposits. These deposits are found primarily along the larger channels that drain to the southern coast of St. John, as the lower portions of these basins are not nearly

as steep as the smaller basins draining to the north. The alluvial deposits are composed of loose, angular, gravel-sized fragments supported by a fine sand-silt matrix. The deposits show little layering or weathering and are poorly sorted. Streambanks in these areas are very steep, mostly unvegetated, and range from 0.6 to 2.5 m in height.

Dry evergreen forests and shrubs cover approximately 63% of St. John, moist forest and secondary vegetation cover another 30%, while urban, wetland, and pasture each cover about 2% of the island (Woodbury and Weaver, 1987). The shallow soils and high winds during tropical weather systems make trees very susceptible to uprooting. The taller trees along stream corridors are especially susceptible to uprooting as they are more exposed to the winds (Reilly, 1991) and their larger boles may make them less susceptible to breaking.

Over the past 30 years rapid development has resulted in the growth of the road network on St. John, particularly on private lands outside of the VINP. For example, there are 8.3 km of roads in a 1971 aerial photograph of the Fish Bay basin. By 2000 the road network has nearly tripled to 23.2 km. Fifty-six percent or 13.1 km of these roads are unpaved. The unpaved road density of the Fish Bay basin is 2.2 km km^{-2} as compared to 0.8 km km^{-2} for the Greater Lameshur Bay basin (Nemeth et al., 2001). The latter is mostly undeveloped because most of the basin is located within the VINP. This difference in density of unpaved roads should result in a marked difference in watershed-scale sediment yields.

4.3 Methods

4.3.1 Streambank Erosion

Sediment production from erodible streambanks was measured by erosion pins (Hill, 1973; Lawler, 1993; Couper et al., 2002). Four representative reaches were chosen for measurement (Figure 1). The Lameshur Bay Gut, Main Fish Bay Gut, and Little Fish Bay Gut sites (*gut* is the local term for streams) were chosen to represent second- and third-order step-pool streams with gradients ranging from 3 to 5 percent, channel widths of roughly 9

meters, and drainage areas from 0.9 to 3.8 km². The average streambank height was 1.8 m. The Reef Bay site was chosen to represent first-order, cascade-type streams, as it had a drainage area of 0.1 km², a channel gradient of 22 percent, a channel width of 6.5 m, and an average bank height of 2.3 m. All sites were located on straight reaches.

At each site 2 to 4 vertical columns of five to nine 15-cm long erosion pins were installed. Columns were spaced about 3 m apart and pins within individual columns were roughly 15 to 30 cm apart. A total of 82 pins were installed, with 2-3 cm of each pin protruding from the bank. The length protruding from the bank was measured to the nearest millimeter at the time of installation and 1-3 more times at frequencies ranging from approximately six months to just over two years. A total of 160 erosion pin measurements were collected from 1998 to 2001. The erosion/aggradation rate was the difference between consecutive pin measurements divided by the time between measurements. ANOVA tests were used to determine whether erosion rates depended on stream order, drainage area, or vertical location on the bank profile.

4.3.2 Treethrow

The number and volume of rootwads within approximately 3 m of the guts was assessed in early 2000 along 6.7 km of streams in three different south-draining basins. The second- and third-order main Fish Bay and Greater Lameshur gut reaches were chosen because these two basins were the focus of our sediment modeling (Chapter 5). Three reaches in the Reef Bay basin were chosen to represent the first-order guts draining to the south.

The volume of rootwads within 3 m of the guts was determined by measuring the diameter and thickness and assuming that the shape of the rootwad could be approximated by a cylinder. The condition of each rootwad was qualitatively described in terms of wood strength, bark condition, and the presence or absence of soil and small roots within the

rootwad (Dynesius and Jonsson, 1991). The mass of sediment delivered to the stream from each rootwad was estimated as the product of its volume, percent soil, and an estimated bulk density for dry soil. The percent soil per volume was determined for those uprooted trees that had a significant amount of soil in the rootwads. The average percent soil from these rootwads was extrapolated to the more decayed rootwads for which there was no sufficient soil to make an estimate. The rate of sediment delivery to the stream network in tonnes of soil per kilometer of stream per year was calculated from the sum of the soil in the rootwads divided by the total length of the reach surveyed and the time represented by our field observations. The last component was the most difficult, as this necessitated the age of the oldest rootwads and whether the frequency of rootwads observed in 2000 was representative of long-term conditions.

4.3.3 Plot-scale Runoff and Sediment Production

Runoff and sediment production were measured from three 40 m² plots on undisturbed planar hillslopes. Two of the plots were in the Haulover Bay area on the eastern end of the island and one in the Fish Bay basin (Figure 1). The two Haulover plots were on 30% slopes dominated by dry evergreen thorn and cactus vegetation (Figure 2a). The Fish Bay plot was located on a 23% slope covered by dry evergreen thicket and scrub (Figure 2b). The plots were installed in 1996 (Sampson, 2000; MacDonald et al., 2001) and intermittently monitored from the latter part of 1998 through December 1999. The plots were approximately 10 m long and 4 m wide, and were bounded by 15-cm wide aluminum flashing inserted into a 5-cm trench dug along the boundaries of the plot. Runoff was routed into 100-L plastic reservoirs. An equivalent runoff total of 0.25 cm was the maximum runoff depth that could be measured from the plots. Two 0.5-L water samples were collected immediately after vigorously mixing the water in the containers. The total concentration of solids in each

of the samples was determined in the lab following standard filtering and drying techniques (ASTM, 1997).

Rainfall data for all Fish Bay plot measurements and the 21 September 1998 Haulover-B plot measurement were obtained from a raingauge in the lower Fish Bay basin (Figure 1) located about 1.2 and 8 km from the Fish Bay and Haulover plots, respectively. Rainfall data for the remaining measurements at the Haulover plots were obtained from a raingauge in Maho Bay (Figure 1). The rainfall data were used to calculate storm event precipitation, maximum 60-minute intensities, storm erosivities, and an antecedent precipitation index (API) (Dunne and Leopold, 1978). The API for any given day was calculated as

$$I_n = I_{n-1}k^t \quad (\text{eq. 1})$$

where I_n is the antecedent precipitation index value in centimeters, n is the day number starting from 1 at the beginning of the calculation period, k is a constant with a value of 0.9, and t is the time in days since the last rainfall. The index for any day is obtained by keeping a running calculation in which the previous day's value is multiplied by k^t . If rain occurs, the amount of rain is added to the index, t is set to zero, and the procedure is continued.

4.3.4 Runoff and Sediment Production from Zero- and First-order Catchments

Sediment production rates from forested sub-catchments were measured by sediment fences (Robichaud and Brown, 2002). Fences on undisturbed areas were installed in three zero-order catchments near Bordeaux Mountain, one zero-order and one first-order catchment in Maho Bay, and one first-order basin in the Reef Bay catchment (Figure 1). Sediment fences were also installed on two first-order catchments in the Reef Bay basin that are receiving sediment from unpaved roads (Figure 1). The drainage areas of these catchments

ranged from 0.9 to 15 ha and the average hillslope gradients ranged from 15% to 37% (Table 4). All of these catchments were covered by moist forest vegetation. The sediment trapped in the fences was collected and weighed about once a year, as only the most intense precipitation events produced measurable amounts of sediment. Samples were collected to determine percent moisture (Gardner, 1986), and the data were used to convert the field-measured wet weights to a dry mass. The particle-size distribution was analyzed by dry sieving (Bowles, 1992) for one sample from each basin except for the Zero-BM-C and 1st-RB-A sites. No particle-size distribution was determined for the Zero-BM-C catchment, while the particle-size distribution for the sediment collected from the 1st-RB-A catchment was a mass-weighted average of three samples.

Three crest gages were used to monitor peak water levels on the west-facing sideslope of the 2.3 ha zero-order catchment at Maho Bay (Zero-MB-A). Crest gage MB-R1 was about 6 m from the axis of the catchment, while MB-R2 and MB-R3 were 10 and 36 m from the axis, respectively. During or immediately after rainfall events field observations were made at the intersection of the Zero-MB-A catchment with the Maho Bay road to determine if the catchment had generated surface runoff. More intensive observations were made from August 1999 to May 2000 because the runoff was affecting an unpaved road segment that was being intensively studied (Chapter 3). Rainfall intensities and totals were recorded by a tipping-bucket rain gauge located approximately 200 m from the lower end of the catchment (Figure 1). The maximum water heights were related to storm rainfall, antecedent precipitation index, and distance from the axis.

4.3.5 Surface Erosion from Unpaved Road Segments

As described in Chapter 2, sediment production from 21 road segments was monitored from July 1998 to November 2001 with sediment fences (Robichaud and Brown, 2002) (Figures 3a-3c). The road segments were in different precipitation zones and selected

to represent a range of road surface areas, slopes, and traffic rates (Figure 4). The mean slope of these segments was 10% and the range was from 1% to 21%. Precipitation was measured by five recording raingauges (Figure 1).

Eighty sediment production measurements were obtained during the study period. For each road segment the effect of precipitation was evaluated by plotting sediment production against total precipitation. After normalizing by precipitation the effect of road gradient was evaluated by plotting sediment production against slope for roads with similar amounts of traffic and time since grading. The effect of traffic was determined by comparing mean sediment production rates—normalized by gradient and total precipitation—for two different traffic levels. Grading effects were identified by plotting sediment production—normalized by precipitation and gradient—against time since grading. Multiple regression analyses led to the development of an empirical road erosion model based on precipitation, slope^{1.5}, and a categorical variable representing time since grading.

The particle-size distribution of 40 samples from the sediment fences was determined by dry sieving (Bowles, 1992) for particles coarser than 0.075 mm, and the hydrometer method (Gee and Bauder, 1986) for particles smaller than 0.075 mm. The 40 samples were selected to represent road segments with varying slopes, amounts of traffic, and the three classes of graded, ungraded, and abandoned roads. A mass-weighted average particle-size distribution was calculated for each of the 21 road segments.

4.3.6 Sediment Production from Road Cutslopes

The sediment fences on road segments incorporated sediment from both the road tread and the cutslopes. To separate these two components, 10 sediment fences were installed at the base of cutslopes. Two fences were quickly vandalized, and the remaining eight plots were in the Maho Bay area and along John Head Road in Catherineberg Estate (Figure 4).

The eight cutslopes were nearly vertical with less than 10% vegetation cover. Cutslope heights ranged from 1.2 to 4.2 m. The average contributing area was 16 m², and values ranged from 5.2 to 34 m². Two of the cutslopes were exclusively composed of residual soil, two others were made mostly of slightly weathered bedrock, and the remaining four cutslopes were dominated by moderately weathered bedrock. Eighteen measurements were taken between 1998 and 2000 at frequencies ranging from a few months to just over a year, and two measurements were taken from the JH-A and JH-B plots in 2001. Multiple regression analysis was used to determine whether total precipitation, cutslope height, or the weathering degree had any effects on sediment production rates. The particle-size distribution was determined for eight sediment samples by the dry-sieving method (Bowles, 1992). These samples represented all of the cutslope plots except for the MB-A and MB-B.

The proportion of the cutslope sediment that might be delivered to the outlet of a road segment was estimated by a visual classification system. A delivery potential of 75% was assumed for cutslopes with ditches or concentrated flowpath at their toe, as the presence of depositional aprons indicated that sediment delivery was less than 100%. Cutslopes within 3 m from the road tread but not delivering sediment directly to a ditch or concentrated flowpath were assumed to have a delivery ratio of 10%. Zero delivery was assumed for cutslopes located more than 3 m from a ditch or flowpath. The measured cutslope sediment production rates and estimated delivery rates were used to estimate the relative contribution of cutslopes to the measured sediment production rates at the road segment scale.

4.4 Results and Discussion

4.4.1 Streambank Erosion

The mean bank erosion for all 160 measurements was 0.4 cm yr⁻¹, but the data were highly variable as the standard deviation was 2.8 cm yr⁻¹. Values for individual pin measurements varied from -13 cm yr⁻¹ to 18 cm yr⁻¹. The data showed a complex temporal

and spatial pattern of deposition (negative values), inactivity (zero values), and erosion (positive values). In order to minimize the temporal variability in the data, a net erosion/aggradation rate for each pin was calculated as the difference between the initial and the last measurement divided by the total study period. The resulting 79 measurements represented time periods of 0.7 to 3 years, and the mean erosion rate was 0.7 cm yr^{-1} (s.d. 1.5 cm yr^{-1}). The highest average erosion rate was the Main Fish Bay Gut at 1.5 cm yr^{-1} , while the lowest rate was 0.1 cm yr^{-1} at Lameshur Gut (Figure 5).

Stream order did not appear to affect bank erosion rates. Erosion rates from the first-order Reef Bay site averaged 0.6 cm yr^{-1} , and the mean erosion rate on the second- and third-order streams was only slightly higher at 0.8 cm yr^{-1} . This difference was not statistically significant ($p = 0.65$). Similarly, bank erosion rates were not related to drainage area ($p = 0.08$, $R^2 = 0.21$). The lack of relationship between bank erosion rates and drainage area is presumed to be due to the limited number of study sites and the limited range in drainage area.

Vertical location along the bank profile did appear to be an important control on bank erosion rates. Pins in the upper one-third of the streambank had a mean erosion rate of 1.2 cm yr^{-1} (s.d. 1.9 cm yr^{-1}), while the average erosion rate for pins in the middle third of the streambank was only 0.3 cm yr^{-1} (s.d. 0.7 cm yr^{-1}). Pins in the lower third of the streambank had a mean erosion rate of 1.2 cm yr^{-1} (s.d. 2.3 cm yr^{-1}). The differences in erosion rates between the upper and mid sections, and between the lower and mid sections were both statistically significant ($p = 0.01$ and 0.03 , respectively). The high rates of erosion in the upper portion of the streambank imply continuing erosion and an unstable bank shape. The slower erosion rate in the middle section is probably due to temporary storage of some of the material produced from the upper portions of the banks. Material stored on the lowermost portions of streambanks was probably removed by streamflow, and this is also expected to occur on the middle sections over a longer time period.

The overall mean erosion rate of 0.7 cm yr^{-1} provides an initial estimate of long-term bank erosion rates on St. John. Assuming a dry bulk density of $1.4 \text{ tonnes m}^{-3}$, the average sediment production rate is nearly $10 \text{ kg m}^{-2} \text{ yr}^{-1}$ (Figure 6). Published data indicate that bank erosion rates increase with increasing drainage area (e.g., Hooke, 1980; Lawler, 1993). Studies from other areas have reported streambank erosion rates of 0.6 to 8.0 cm yr^{-1} for streams with drainage areas ranging from 0.13 to 9.6 km^2 (Table 1). The values for St. John fall at the low end of this range.

4.4.2 Sediment Delivery by Treethrow

The mean number of uprooted trees along the five surveyed stream reaches was 11 trees km^{-1} , and the range was from 7 to nearly 20 trees km^{-1} (Table 2). On average each rootwad contained 1.1 m^3 of sediment, yielding a mean value of 12 m^3 of treethrow sediment per kilometer of stream. Assuming a dry bulk density of $1.4 \text{ tonnes m}^{-3}$, approximately 17 tonnes of sediment are delivered to the stream network per kilometer of stream channel.

The conversion of these values into a sediment delivery rate per unit time proved to be difficult. The oldest uprooted trees had softened wood, smooth trunk surfaces that had lost over half of their bark, and had lost most of their soil and small roots. The use of published techniques to determine the time since uprooting (Dynesius and Jonsson, 1991) was questionable because there are no published data on log decay rates in a dry tropical environment such as St. John. The literature suggests that log decay in a dry tropical environment will be faster than the 100 years estimated for boreal forests (Dynesius and Jonsson, 1991), but slower than the 10 years documented for wet tropical environments in Panamá (Lang and Knight, 1979) and Puerto Rico (Odum, 1970). Hurricane Hugo in 1989 was the first major hurricane to affect St. John in 73 years (Potter et al., 1995), so the treethrow surveys effectively represent treethrow over the past eleven years (G. Ray, University of the Virgin Islands, pers. comm.; P. Weaver, U.S. Forest Service, pers. comm.).

Dividing the 17 tonnes per kilometer of stream by 11 years yields a rate of 1.5 tonnes $\text{km}^{-1} \text{yr}^{-1}$. This value is probably an overestimate because St. John has experienced a marked increase in the frequency of severe hurricanes in the last 11 years. Sustained winds on the nearby island of St. Thomas reached 192 km hr^{-1} during Hurricane Hugo in 1989 (Case and Mayfield, 1990), 165 km hr^{-1} during Hurricane Marilyn in 1995 (Lawrence et al., 1998), 237 km hr^{-1} during Hurricane Georges in 1998 (Pasch et al., 2001), and 165 km hr^{-1} during Hurricane Lenny in 1999 (Lawrence et al., 2001).

The average interval between major treethrow events on St. John is difficult to determine. The entire territory of the U.S. Virgin Islands—including the islands of St. Croix, St. Thomas, and St. John—is affected by major hurricanes about once every 12 to 15 years (Potter et al., 1995). The return period of hurricanes in Jamaica is in the order of once every 15 years, but the return period of storms that induce significant treethrow and forest damage is much longer (Bellingham, 1991). The mean time period for a major hurricane to pass over a given island in the Caribbean is 70 years (Neumman et al., 1978), which is close to the 50-60 year interval calculated for the Luquillo Experimental Forest in eastern Puerto Rico (Scatena and Larsen, 1991).

If the hurricanes that cause substantial amounts of treethrow occur about once every 50 years on St. John, and two such events occurred in 1989 and 2000 (hurricanes Hugo and Georges, respectively), then the measured treethrow actually represents the mass of sediment that would normally occur over 100 years. On this basis, the long-term sediment production rate by treethrow is $0.17 \text{ tonnes km}^{-1} \text{yr}^{-1}$. For a 15 meter wide stream corridor—consisting of 9 m of channel and a 3 m wide buffer zone—the treethrow sediment production rate by unit area is estimated as $11 \text{ g m}^{-2} \text{yr}^{-1}$.

The only other estimate of sediment delivery rates from uprooted trees along stream margins is $1 \text{ m}^3 \text{ km}^{-1} \text{yr}^{-1}$ for the Olympic Mountains in the northwestern U.S. (Reid, 1981). This converts to $1.3 \text{ tonnes km}^{-1} \text{yr}^{-1}$ if a dry bulk density of $1.4 \text{ tonnes m}^{-3}$ is assumed. This

rate is almost an order of magnitude higher than the $0.17 \text{ tonnes km}^{-1} \text{ yr}^{-1}$ estimated for St. John, and the difference is due to a much larger volume of soil in each rootwad as well as the larger number of overturned trees per kilometer of stream channel.

4.4.3 Plot-scale Runoff and Sediment Production from Undisturbed Hillslopes

Runoff volumes and sediment concentrations were obtained for five events between August 1998 and December 1999. Runoff and sediment might have been produced at other times, but problems with the operation of the plots did not permit the collection of measurements during those events. The measurements taken between 1998 and 1999 and the data collected in 1996 (Sampson, 2000) are shown in Table 3. Storm precipitation ranged from 2.1 to 13.1 cm. Mean runoff values for the Haulover-A, Haulover-B, and Fish Bay plots were 0.07, 0.11, and 0.11 cm, respectively. Runoff was produced only by storms with at least two centimeters of rainfall, while storms larger than 6.4 cm sometimes exceeded the capacity of the runoff storage containers. For example, runoff volumes for the 10 September 1996 storm on the Fish Bay plot and the 16 November 1999 event for all three plots are minimum values as the storage capacity of 0.25 cm of runoff was exceeded. Excluding these four measurements the mean runoff coefficient was 0.02 cm cm^{-1} and the range was from 0.00 to 0.07 cm cm^{-1} . This indicates that for storms with less than 6.4 cm of rainfall, runoff from undisturbed hillslopes was only a very small fraction of the total rainfall.

Runoff totals were poorly correlated with storm precipitation, maximum 60-minute rainfall intensities, and storm erosivities ($R^2 = 0.34, 0.02, 0.23$, respectively). Storm runoff was more closely related to the sum of storm rainfall (P) and antecedent precipitation index (API), but the data still show considerable variability in runoff response (Figure 7).

Sediment concentrations ranged from 0.00 to 2.56 g L^{-1} . The mean sediment concentrations from the plots at Haulover Bay were about an order of magnitude higher than

the Fish Bay plot (Table 3). The higher concentrations at Haulover are probably due to the slightly higher slopes and less ground cover relative to Fish Bay.

Sediment concentrations were not correlated with storm rainfall, maximum 60-minute precipitation, or rainfall erosivity (R^2 values < 0.002). This justifies the use of average concentrations for estimating longer-term erosion rates. Using the mean sediment concentrations and the mean runoff totals, the mean sediment production rate per centimeter of rainfall is 0.2, 0.8, and 0.03 $\text{g m}^{-2} \text{cm}^{-1}$ for the Haulover-A, Haulover-B, and Fish Bay plots, respectively. Annual erosion rates are estimated based on the assumption that all storms larger than 2 cm will produce runoff and sediment, regardless of their API value. Long-term rainfall data from Caneel Bay shows that storms with at least 2.0 cm of rainfall account for 34 cm or 32% of the mean annual rainfall. The long-term estimated erosion rates for the Haulover-A and Haulover-B plots are 10 and 27 $\text{g m}^{-2} \text{yr}^{-1}$, while the Fish Bay plot is estimated to erode at a rate of 1 $\text{g m}^{-2} \text{yr}^{-1}$.

4.4.4 Runoff and Sediment Production from Zero- and First-order Catchments

The crest gage data suggest that saturated conditions begin to develop within the soil profile when storm rainfall exceeds about 2 cm. As storm precipitation increases the height of saturation appears to asymptotically approach the soil surface (Figure 8). For a given storm, events with higher API values tended to have higher crest gage readings. Distance from the catchment axis was not a major control on the depth to saturation, although the crest gage closest to the axis (MB-R1) did tend to have slightly lower water levels for intermediate-sized storms (Figure 8).

Qualitative runoff observations were made at the bottom of the Zero-MB-A catchment for many of the 602 storm events from July 1998 to May 2000. Storm rainfall over this period ranged from 0.03 to 9.5 cm with a maximum 60-minute intensity of 7.9 cm hr^{-1} . Surface runoff was observed for only seven storms and it generally lasted less than one

hour after the end of precipitation. All seven of those storms had API values greater than 5 cm, and all but one had at least 3.5 cm of rainfall. Only three events resulted in measurable sediment accumulations in the sediment trap, and these were the only events with at least 6 cm of precipitation.

Sediment yields from the four zero-order basins ranged from 9-41 kg, while the two undisturbed first-order basins yielded 310 and 2100 kg, respectively (Table 4). The two disturbed first-order basins yielded 12,500 and 5,850 kg of sediment. When divided by the amount of precipitation that fell in storms of at least 6 cm, the average sediment yield rate from the four zero-order basins was 0.064 g m^{-2} per centimeter of precipitation versus $0.5 \text{ g m}^{-2} \text{ cm}^{-1}$ for the two undisturbed first-order basins. The two disturbed first-order basins yielded sediment at a rate of $2.4 \text{ g m}^{-2} \text{ cm}^{-1}$, or almost five times higher than the value from the comparable undisturbed basins. It must be noted that the values from the two undisturbed catchments are minimum rates, as the traps were overtopped by sediment during Hurricane Georges in 1998 and Hurricane Lenny in 1999. The approximately 0.3 km of unpaved roads in each of these two catchments are assumed to be responsible for these higher rates.

The long-term rainfall data from Caneel Bay shows that events larger than 6 cm account for 16 cm or 14% of the mean annual rainfall. If the normalized rates in Table 4 are multiplied by 16 cm yr^{-1} , the resulting sediment yield rates from zero-order basins are approximately $1 \text{ g m}^{-2} \text{ yr}^{-1}$, while the undisturbed first-order basins yield approximately $8 \text{ g m}^{-2} \text{ yr}^{-1}$ (Figure 6). The two first-order catchments receiving sediment from unpaved roads yield sediment at a rate of $38 \text{ g m}^{-2} \text{ yr}^{-1}$.

On average, the sediment from the zero-order catchments had more sand and less gravel than the sediment from the undisturbed first-order catchments. The mass-weighted average of the sediment from the zero-order catchments was 42% gravel, 57% sand, and 0.4% silt and clay (Figure 9; Appendix III). The mean particle-size distribution of the sediment from the two undisturbed first-order catchments was 71% gravel, 28% sand, and 1%

silt and clay. The sediment from the two disturbed first-order catchments had much more sand than the sediment from the undisturbed first-order basins, as the mass-weighted average from the disturbed basin was 43% gravel, 55% sand, and 2% silt and clay.

Plot-scale sediment production rates were generally higher and more variable than the rates obtained from zero-order basins (Figure 6). The differences might be due to lower slopes and higher sediment storage capacities of zero-order catchments relative to hillslope plots (Tables 3 and 4). Sediment production rates from undisturbed first-order catchments were one or two orders of magnitude higher than the rates from zero-order catchments. The addition of streambank and treethrow erosion could account for the higher rates measured from first-order catchments.

In the Maho Bay first-order catchment the entire 50 m of channel had erodible streambanks 0.75 m in height. If the treethrow rate is $1.3 \text{ tonnes km}^{-1} \text{ yr}^{-1}$, the bank erosion rate is $10 \text{ kg m}^{-2} \text{ yr}^{-1}$, and the surface erosion rate is $1 \text{ g m}^{-2} \text{ yr}^{-1}$, the total sediment yield over the 5.4 ha area is $16 \text{ g m}^{-2} \text{ yr}^{-1}$. This value is 3.7 times higher than the measured rate of $4.3 \text{ g m}^{-2} \text{ yr}^{-1}$ over the study period. The four-fold difference is probably due to sediment storage within the basin and spatial variability in the estimated erosion rates.

The same calculation was performed for the undisturbed first-order catchment in Reef Bay. In this case there were no erodible streambanks along the 660 m of channel upstream of the sediment trap, so the estimated sediment production rate from treethrow and surface erosion was $6.8 \text{ g m}^{-2} \text{ yr}^{-1}$. This value is 43% lower than the measured value of $12 \text{ g m}^{-2} \text{ yr}^{-1}$. Although there are discrepancies between the calculated and measured sediment yields for these two undisturbed first-order catchments, the similar order of magnitude is encouraging and supports the validity of the underlying estimates.

4.4.5 Surface Erosion from Unpaved Roads

The average road erosion rate for the 21 road segments was 0.064 kg m^{-2} per centimeter of precipitation. Sediment production from unpaved roads was related to total precipitation and road segment slope. After normalizing by precipitation and slope, roads that had been graded within the last two years had a mean sediment production rate of $0.96 \text{ kg m}^{-2} \text{ cm}^{-1}$, while the mean erosion rate for ungraded roads was 41% lower, or $0.56 \text{ kg m}^{-2} \text{ cm}^{-1}$. Road segments that had been abandoned for over fifteen years had an average normalized sediment production rate of $0.071 \text{ kg m}^{-2} \text{ cm}^{-1}$, or only about 10% of the average for ungraded roads. Traffic levels were not related to sediment production.

Multiple regression led to the development of empirical road erosion models for graded (eq. 2a) and ungraded (eq. 2b) roads.

$$E_r = -0.432 + 4.73 \cdot \text{slope}^{1.5} \cdot \text{precipitation} \quad (\text{eq. 2a})$$

$$E_r = -0.432 + 1.88 \cdot \text{slope}^{1.5} \cdot \text{precipitation} \quad (\text{eq. 2b})$$

where E_r is sediment production in kg m^{-2} , slope is in m m^{-1} , and precipitation refers to total rainfall in cm.

Estimated annual erosion rates for graded road segments averaged $11 \text{ kg m}^{-2} \text{ yr}^{-1}$ (Figure 6). Measured sediment production rates for graded roads with slopes of 2 and 21 percent were 0.57 and $58 \text{ kg m}^{-2} \text{ yr}^{-1}$, respectively. Ungraded roads had an average measured sediment production rate of $8.6 \text{ kg m}^{-2} \text{ yr}^{-1}$, with values ranging from 5.1 to $14 \text{ kg m}^{-2} \text{ yr}^{-1}$ for roads with slopes of 10% and 16%, respectively. The average erosion rate for abandoned roads with a 15% slope was $1.1 \text{ kg m}^{-2} \text{ yr}^{-1}$. These rates indicate that actively used roads are capable of increasing road-segment and hillslope-scale sediment production by up to four orders of magnitude relative to undisturbed plots and zero-order catchments (Figures 6 and 10).

The particle-size distribution of the sediment produced from roads is much finer than the sediment produced from undisturbed first-order catchments, but similar to the sediment from undisturbed zero-order catchments (Figures 9 and 11). For the 20 actively-used road segments, 40% of the eroded material was gravel, 54% was sand, and 6% was silt and clay. For the undisturbed first-order basins, gravel comprised 71% of the eroded sediment, and sand was only 28%.

4.4.6 Sediment Production from Road Cutslopes

The mean sediment production rate from cutslopes was $10 \text{ kg m}^{-2} \text{ yr}^{-1}$ ($n=20$), and the range was from 2.0 to $17 \text{ kg m}^{-2} \text{ yr}^{-1}$ (Table 5). The range of values over the time period represented by individual measurements was from 0.3 to $35 \text{ kg m}^{-2} \text{ yr}^{-1}$.

The mean sediment production rate from slightly-weathered cutslopes was $3.9 \text{ kg m}^{-2} \text{ yr}^{-1}$, while cutslopes composed of moderately-weathered bedrock and residual soil had mean sediment production rates of 9.3 and $14 \text{ kg m}^{-2} \text{ yr}^{-1}$, respectively. The small sample sizes relative to the variability meant that the differences in mean erosion rates among the three weathering classes were not statistically significant. Cutslope erosion rates were not related to precipitation or cutslope height.

The reported range of sediment production rates for cutslopes is from 0.01 to $37 \text{ kg m}^{-2} \text{ yr}^{-1}$, and this easily encompasses the measured values from St. John (Table 6). At $10 \text{ kg m}^{-2} \text{ yr}^{-1}$, the mean sediment production rate from cutslopes is only 10% lower than the mean production rate from graded roads, and 1.1 times higher than the value from ungraded roads (Figure 6).

The particle-size analyses showed that the sediment from cutslopes was coarser than the sediment collected at the road-segment scale. On average, the sediment produced from cutslopes was 61% gravel, 38% sand, and only 1% silt and clay (Figure 11; Appendix III).

A visual classification system determined that cutslopes contributed from 0 to 62% of the sediment collected at the road segment scale (Table 7). The total amount of sediment from the 20 road segments was about 1500 kg per centimeter of rainfall, and the total sediment from cutslopes for these road segments was 160 kg cm⁻¹. The data indicate that, on average, only 11% of the sediment produced at the road segment scale is derived from cutslopes. The average sediment production rate for cutslopes at the road segment scale is estimated to be 0.04 kg m⁻¹ cm⁻¹. Assuming an annual rainfall of 115 cm and a 5 m wide road, cutslopes are estimated to contribute a total of 0.9 kg m⁻² yr⁻¹ to sediment yields at the road segment scale. This estimate suggests that on average only 9% of the mean cutslope sediment production rate (10 kg m⁻² yr⁻¹) contributes to road segment scale sediment production.

The relative contribution of cutslopes to sediment yields from road segments has been rarely reported. In the Olympic Peninsula of Washington cutslopes were estimated to contribute 0.8 kg of sediment per meter of road per year, or less than 2% of the sediment produced from the travelways of actively-used logging roads (Reid, 1981). In the Oregon Coast Range the lack of a significant relationship between cutslope height and road segment sediment yields suggested that cutslope contributions play a secondary role relative to factors controlling the rate of sediment production from the travelway and ditch (Luce and Black, 2001).

4.5 Conclusions

Sediment production rates were measured from both natural and road-related sources on the island of St. John. The resulting values ranged over five orders of magnitude. Streambanks eroded at an average rate of 10 kg m⁻² yr⁻¹, which was the highest sediment production rate among natural sources of sediment. The uprooting of trees along stream

margins was estimated to deliver 0.17 tonnes of sediment per kilometer of stream per year, or $11 \text{ g m}^{-2} \text{ yr}^{-1}$ for a 15-m wide stream corridor.

Sediment production from undisturbed areas ranged from 0.5 to $27 \text{ g m}^{-2} \text{ yr}^{-1}$ at the zero-order and plot scales, respectively. These differences in sediment production rates might be due to lower average slopes and higher sediment storage capacities of the zero-order catchments relative to the hillslope plots. Undisturbed first-order catchments yielded sediment at a mean rate of $8 \text{ g m}^{-2} \text{ yr}^{-1}$. The addition of streambank and treethrow erosion appears to account for the higher rates measured from first-order catchments relative to zero-order catchments. Contributions from unpaved roads to two first-order catchments are responsible for a mean sediment production rate of $38 \text{ g m}^{-2} \text{ yr}^{-1}$, which is five times higher than sediment production rates from undisturbed first-order catchments.

Rainfall, road slope, and frequency of grading significantly affected sediment production rates from road segments. Sediment production rates from road segments that are regraded once every two years ranged from 0.57 to $58 \text{ kg m}^{-2} \text{ yr}^{-1}$ for roads with average slopes of 1 to 21%, respectively. Ungraded roads had sediment production rates ranging from 5.1 to $14 \text{ kg m}^{-2} \text{ yr}^{-1}$ for roads with slopes of 10 and 16%, respectively. Abandoned road segments with a slope of 15% had a mean erosion rate of $1.1 \text{ kg m}^{-2} \text{ yr}^{-1}$. Sediment production rates from cutslopes ranged from 2 to $17 \text{ kg m}^{-2} \text{ yr}^{-1}$, but their estimated contribution to sediment yields at the road segment scale is only $0.9 \text{ kg m}^{-2} \text{ yr}^{-1}$. The latter value is an order of magnitude less than their production rates.

These values indicate that actively-used roads can increase road segment and hillslope scale sediment production rates by up to four orders of magnitude relative to values from undisturbed plots and zero-order catchments. The relative importance of each of these sediment sources in watershed-scale sediment production and yield rates is likely to change from catchment to catchment as a result of the abundance and spatial distribution of the

different landscape units. The development and application of a GIS-based sediment model is presented in Chapter 5.

4.6 References Cited

- Ahmad N, Breckner E. 1974. Soil erosion on three Tobago soils. *Tropical Agriculture (Trinidad)* 51(2): 313-324.
- Anderson DM. 1994. Analysis and modeling of erosion hazards and sediment delivery on St. John, US Virgin Islands. Tech. Rep. NPS/NRWRD/NRTR/34, US National Park Service, Fort Collins, CO, 153 p.
- Anderson DM, MacDonald LH. 1998. Modelling road surface sediment production using a vector geographic information system. *Earth Surface Processes and Landforms* 23: 95-107.
- ASTM-D 3977-97. 1997. Standard test methods for determining sediment concentration in water samples. Annual Book of ASTM Standards. 11.01.
- Bellingham PJ. 1991. Landforms influence patterns of hurricane damage: Evidence from Jamaican montane forests. *Biotropica* 23(4a): 427-433.
- Blong RJ, Humphreys GS. 1982. Erosion of road batters in Chim Shale, Papua New Guinea. *Civil Engineering Transactions, Institution Engineers Australia* CE24(1): 62-68.
- Bowden MJ, Fischman N, Cook P, Wood J, and Omasta E. 1970. Climate, water balance, and climatic change in the north-west Virgin Islands. Caribbean Research Institute, College of the Virgin Islands, 127 p.
- Bowles JE. 1992. Engineering Properties of Soils and their Measurement. McGraw-Hill Inc., New York.
- Calversbert RJ. 1970. Climate of Puerto Rico and the U.S. Virgin Islands. Climatography of the United States No. 60-52, US Dept. of Commerce, 29 p.
- Case B, Mayfield M. 1990. Annual summaries: Atlantic hurricane season of 1989. *Monthly Weather Review* 118: 1165-1177.
- CH2M Hill. 1979. A sediment reduction program: Report to the Department of Conservation and Cultural Affairs, Government of the U.S. Virgin Islands, St. Thomas, U.S.V.I.
- Couper P, Stott T, Maddock I. 2002. Insights into river bank erosion processes derived from analysis of negative erosion-pin recordings: observations from three recent UK studies. *Earth Surface Processes and Landforms* 27: 59-79.
- DeGraff JV, Bryce R, Jibson RW, Mora S, Rogers CT. 1989. Landslides: Their extent and significance in the Caribbean. In Landslides: Extent and economic significance. Brabb EE, Harrod BL (eds.): 51-80.
- Del Mar-López T, Mitchell T, Scatena FN. 1998. The effect of land use on soil erosion in the Guadiana Watershed in Puerto Rico. *Caribbean Journal of Science* 34(3-4): 298-307.

- Dietrich WE, Dunne T, Humphrey N, Reid L. 1982. Construction of sediment budgets for drainage basins. In *Sediment Budgets and Routing in Forested Drainage Basins*, Swanson FJ et al., (eds.), US Forest Service General Technical Report PNW-141, Corvallis, OR; 5-23.
- Diseker EG, Richardson EC. 1962. Erosion rates and control methods on highway cuts. *Transactions of the American Society Agricultural Engineers* 5: 153-155.
- Donnelly TW. 1966. Geology of St. Thomas and St. John. *Geological Society of America, Memoir* 98: 85-176.
- Dunne T. 2001. Problems in measuring and modeling the influence of forest management on hydrologic and geomorphic processes. In: Land Use and Watersheds: Human Influence on Hydrology and Geomorphology in Urban and Forest Areas. American Geophysical Union; 77-83.
- Dunne T, Leopold LB. 1978. *Water in Environmental Planning*, W.H. Freeman and Co., San Francisco, 818 p.
- Dynesius M, BG Jonsson. 1991. Dating uprooted trees: comparison and application of eight methods in a boreal forest. *Canadian Journal of Forest Research* 21: 655-665.
- Dyrness CT. 1975. Grass-legume mixtures for erosion control along forest roads in western Oregon. *Journal of Soil and Water Conservation* 30: 169-173.
- Dyrness CT. 1970. Stabilization of newly constructed road back-slopes by mulch and grass-legume treatments. USDA Forest Service Research Note, PNW-123.
- Fahey BD, Coker RJ. 1992. Sediment production from forest roads in Queen Charlotte Forest and potential impact on marine water quality, Marlborough Sounds. *New Zealand Journal of Marine and Freshwater Research* 26: 187-195.
- Fahey BD, Coker RJ. 1989. Forest road erosion in the granite terrain of southwest Nelson, New Zealand. *Journal of Hydrology (N.Z.)* 28(2): 123-141.
- Gardner WH. 1986. Chapter 21: Water content. In Methods of Soil Analysis Part I: Physical and Mineralogical Methods. 2nd edition Number 9, Agronomy Series, Klute A (ed.). American Society of Agronomy, Madison, WI; 338-411.
- Gee GW, Bauder JW 1986. Particle-size analysis. In Methods of Soil Analysis Part 1: Physical and Mineralogical Methods. 2nd edition Number 9 (Part 1), Agronomy Series, Klute A (ed.) American Society of Agronomy, Madison, WI; 383-411.
- Hill AR. 1973. Erosion of river banks composed of glacial till near Belfast, Northern Ireland. *Zeitschrift fur Geomorphologie* 17: 428-442.
- Hodgson G. 1989. The effects of sedimentation on Indo-Pacific Reef Corals. Ph.D. dissertation, University of Hawaii, 338 p.
- Hodgson G. 1997. Resource use: Conflicts and management solutions. In Life and Death of Coral Reefs. Birkeland C. (ed.); pp. 386-411.

- Hooke JM. 1980. Magnitude and distribution of rates of river bank erosion. *Earth Surface Processes* 5: 143-157.
- Hubbard DK. 1987. A general review of sedimentation as it relates to environmental stress in the Virgin Islands Biosphere Reserve and the eastern Caribbean in general. Biosphere Reserve Report no. 20, Virgin Islands Resource Management Cooperative, St. Thomas, 42 p.
- Imeson AC, Jungerius PD. 1974. Landscape stability in the Luxembourg Ardennes as exemplified by hydrological and (micro) pedological investigations of a catena in a experimental watershed. *Catena* 1: 273-295.
- Jibson, R.W. (1989). Debris flows in southern Puerto Rico. Geological Society of America, Special Paper 236: 29-55.
- Lang GE, Knight DH. 1979. Decay rates for boles of tropical trees in Panama. *Biotropica* 11: 316-317.
- Larsen MC, Parks J. 1997. How wide is a road? The association of roads and mass-wasting in a forested montane environment. *Earth Surface Processes and Landforms* 22: 835-848.
- Larsen MC, Torres-Sánchez AJ. 1998. The frequency and distribution of recent landslides in three montane tropical regions of Puerto Rico. *Geomorphology* 24: 309-331.
- Lawler DM. 1993. The measurement of river bank erosion and lateral channel change: A review. *Earth Surface Processes and Landforms* 18: 777-821.
- Lawrence MB, Ávila LA, Beven JL, Franklin JL, Guineay JL, Pasch RJ. 2001. Atlantic Hurricane Season of 1999. *Monthly Weather Review* 129: 3057-3184.
- Lawrence MB, Mayfield BM, Ávila LA, Pasch RJ, Rappaport EN. 1998. Atlantic hurricane season of 1995. *Monthly Weather Review* 126: 1124-1151.
- Leopold LB, Emmett WW, Myrick RH. 1966. Channel and hillslope processes in a semi-arid area, New Mexico. U.S. Geological Survey Professional Paper, 352-G.
- Lewin J, Cryer R, Harrison DI. 1974. Sources for sediments and solutes in Mid-Wales. *Institute of British Geographers Special Publication* 6: 73-85.
- Luce CH, Black TA. 2001. Spatial and temporal patterns in erosion from forest roads. In: Land Use and Watersheds: Human Influence on Hydrology and Geomorphology in Urban Forest Areas. Water Science and Application, Vol. 2: 165-178.
- MacDonald LH, Anderson DM, Dietrich WE. 1997. Paradise threatened: Land use and erosion on St. John, U.S. Virgin Islands. *Environmental Management* 21(6): 851-863.
- MacDonald LH, Sampson RW, Anderson DM. 2001. Runoff and road erosion at the plot and road segment scales, St. John, US Virgin Islands. *Earth Surface Processes and Landforms* 26: 251-272.
- McGregor DF. 1988. An investigation of soil status and landuse on a steeply sloping hillside, Blue Mountains, Jamaica. Singapore. *Journal of Tropical Geography* 9(1): 60-71.

- Megahan WF. 1980. Erosion from roadcuts in granitic slopes of the Idaho batholith. Abstract. Cordilleran section of the Geological Society of America, 76th Annual Meeting, Oregon State Univ., Corvallis.
- Megahan WF, Wilson M, Monsen SB. 2001. Sediment production from granitic cutslopes on forest roads in Idaho, USA. *Earth Surface Processes and Landforms* 26: 153-163.
- Megahan WF, Seyedbagheri KA, Dodson PC. 1983. Long term erosion on granitic roadcuts based on exposed tree roots. *Earth Surface Processes and Landforms* 8: 19-28.
- Murgatroyd AL, Ternan JL. 1983. The impact of afforestation on stream bank erosion and channel form. *Earth Surface Processes and Landforms* 8: 357-369.
- Nemeth RS, MacDonald LH, Ramos-Scharrón CE. 2001. Delivery, deposition, and effects of land-based sediments on corals in St. John, U.S. Virgin Islands. Water Resources Research Institute-University of the Virgin Islands, St. Thomas, Report on project no. VI99-2; 24 p.
- Neumann CJ, Cry GW, Caso EL, Jarvinen BR. 1978. Tropical cyclones of the North Atlantic Ocean, 1871-1977. National Climatic Center, NOAA, Asheville, North Carolina.
- Odum HT. 1970. Summary: an emerging view of the ecological system at El Verde. In A Tropical Rainforest. Odum HT and Piegen RF (eds.), USAEC. Tech. Info. Ctr. Oak Ridge, Tennessee; I-191-I-281.
- Pasch RJ, Ávila LA, Guiney JL. 2001. Atlantic hurricane season of 1998. *Monthly Weather Review* 129: 3085-3123.
- Potter B, Brower DJ, Turnbull B. 1995. Mitigating the impacts of natural hazards in the U.S. Virgin Islands. Prepared for the Virgin Islands Territorial Emergency Management Service, St. Thomas, VI, 75 p.
- Rankin DW. 2002. Geology of St. John, U.S. Virgin Islands. U.S. Geological Survey professional paper 1631, 36 p.
- Reid LM. 1981. Sediment production from gravel-surfaced roads, Clearwater Basin, Washington. University of Washington Fisheries Research Institute, Seattle. Publ. FRI-UW-8108. 301 p.
- Reid LM, Dunne T. 1996. Rapid evaluation of sediment budgets. Reiskirchen, Germany: Catena Verlag, 164 p.
- Reilly AE. 1991. The effects of Hurricane Hugo in three tropical forests in the U.S. Virgin Islands. *Biotropica* 23(4a): 414-419.
- Riley SJ. 1988. Soil loss from road batters in the Karuah State Forest, eastern Australia. *Soil Technology* 1: 313-332.
- Robichaud PR, Brown RE. 2002. Silt fences: An economical technique for measuring hillslope soil erosion. General Technical Report RMRS-GTR-94, US Forest Service, Rocky Mountain Research Station, Fort Collin, CO; 24 p.

- Rogers CS 1990. Responses of coral reefs and reef organisms to sedimentation. *Marine Ecology Progress Series* 62: 185-202.
- Rogers CS. 1998. Coral reefs of the U.S. Virgin Islands. In Status and Trends of the Nation's Biological Resources, Vol I. Haeker P, Doran PD (eds.). U.S. Geological Survey, Reston, VA: 322-324.
- Sampson RW. 2000. Road runoff and erosion at the plot and road segment scales on St John US Virgin Islands. M.S. thesis, Department of Earth Resources, Colorado State University, Fort Collins, 189 p.
- Scatena FN, Larsen MC. 1991. Physical aspects of Hurricane Hugo in Puerto Rico. *Biotropica* 23(4a): 317-323.
- Smith RM, Abruña F. 1955. Soil and water conservation research in Puerto Rico, 1938 to 1947. Bulletin no. 124, Univ. of Puerto Rico Agricultural Experiment Station, Rio Piedras, Puerto Rico; 51 p.
- Smith M, Fenton T. 1993. Sediment yields from logging tracks in Kaingaroa Forest. New Zealand Logging Industry Research Organisation Report, vol. 18, no. 18, 10 p.
- Soil Conservation Service. 1970. Soil Survey, Virgin Islands of the United States. 78 p.
- UNEP. 1994. Regional overview of land-based sources of pollution in the Wider Caribbean Region. CEP-Technical Report No. 33; 56 p.
- USDA. 1995. Classification and Correlation of the Soils of the Virgin Islands of the United States. US Department of Agriculture: Hato Rey, Puerto Rico.
- Walling DE. 1997. The response of sediment yields to environmental change. In: Human Impact on Erosion and Sedimentation. IAHS Publication 245: 77-89.
- Wilson RL. 1963. Source of erosion on newly constructed logging roads in the H. J. Andrews experimental forest. Unpublished Report, Bureau of Land Management, University of Washington, Seattle, WA; 21 p.
- Woodbury RO, Weaver PL 1987. The vegetation of St. John and Hassel Island, U.S. Virgin Islands. National Park Service, Southeast Region, Research/Resources Management Report SER-83, Atlanta, GA; 26 p.

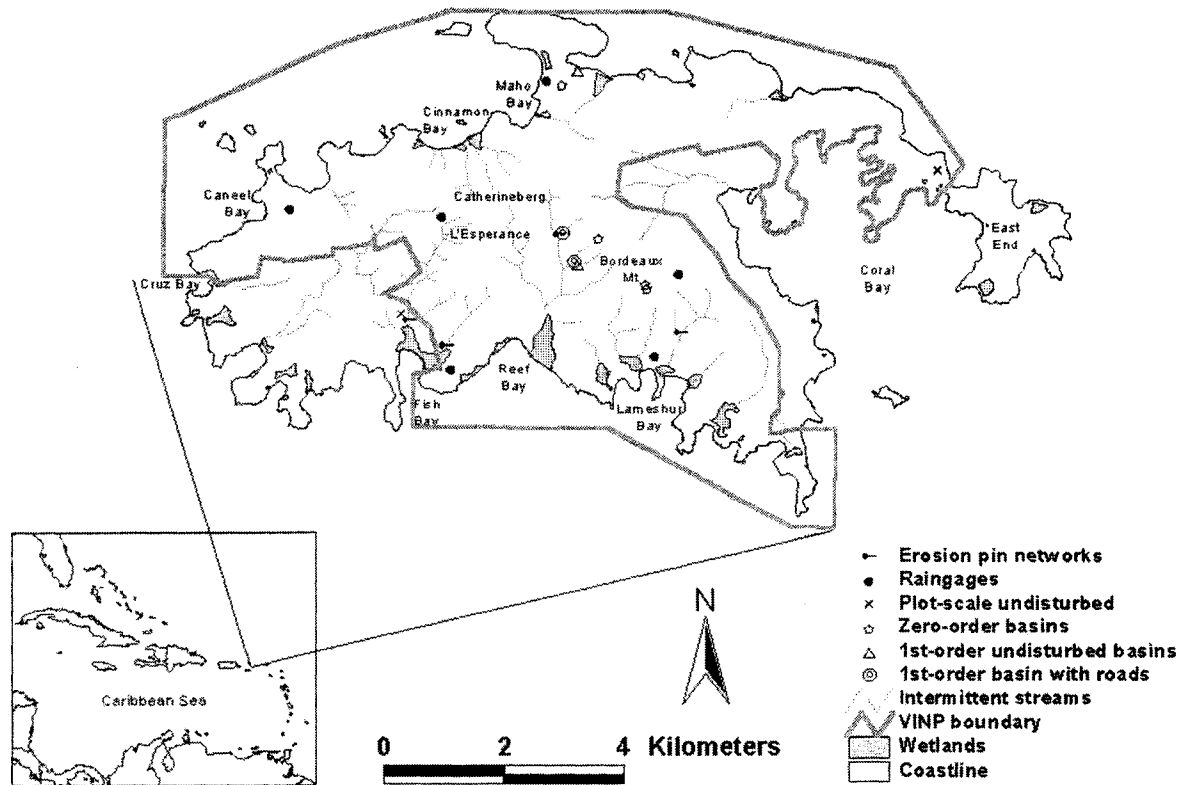


Figure 1. Map of St. John showing the Virgin Islands National Park boundary and the location of measurement sites for natural sediment sources.

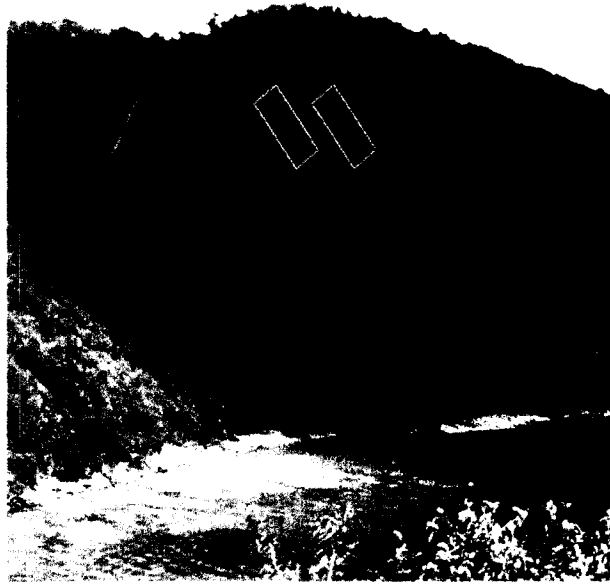


Figure 2a. Undisturbed plots at Haulover Bay.

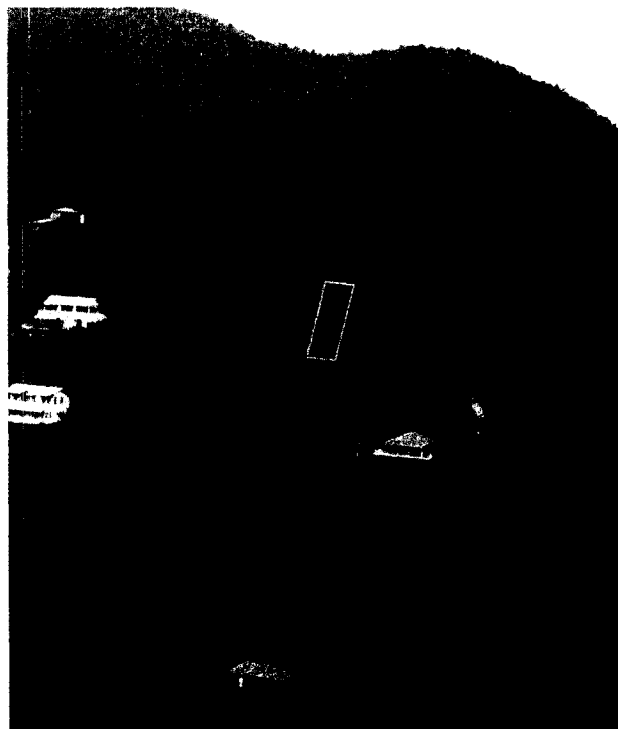


Figure 2b. Undisturbed plot at Fish Bay.



Figure 3a. Graded road segment JH-A1.



Figure 3b. Ungraded road segment FB-Coco.



Figure 3c. Abandoned road segment LE-Top.

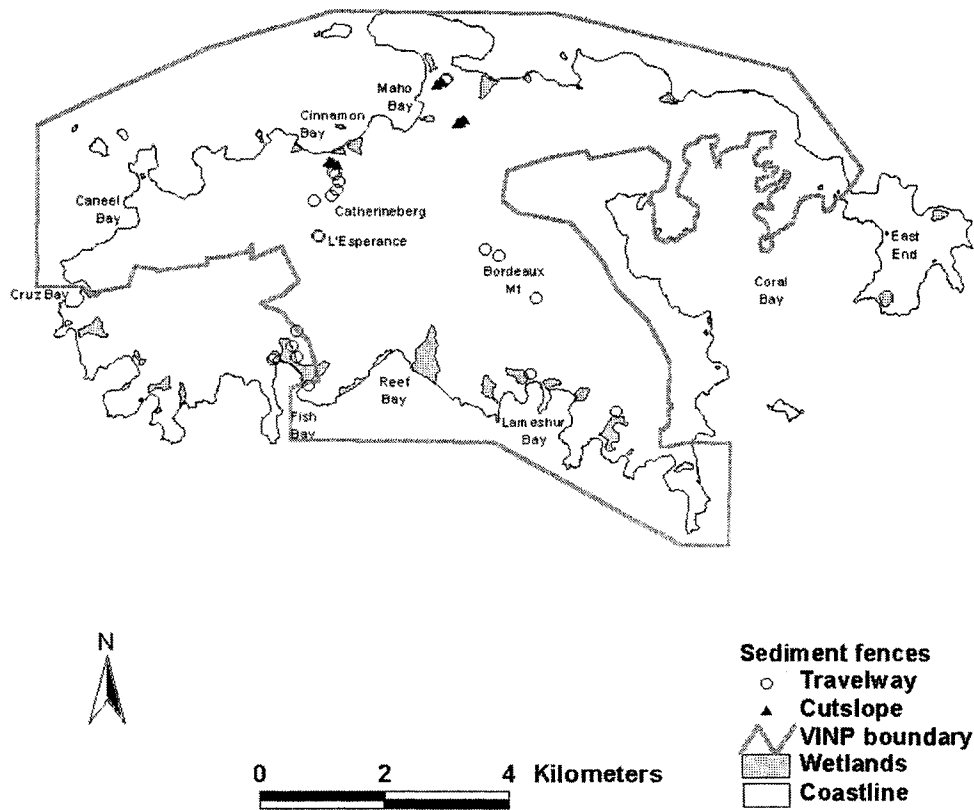


Figure 4. Map of St. John showing the location of the sediment fences used to measure erosion from road segments and road cutslopes.

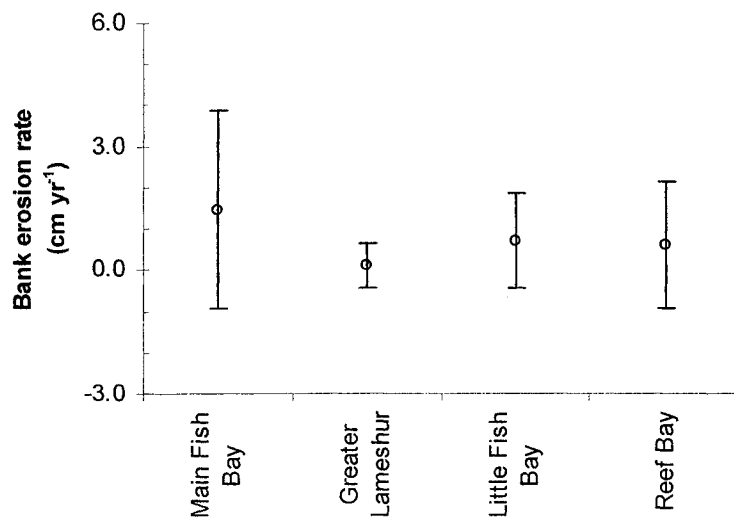


Figure 5. Average bank retreat rates by study site. Error bars indicate one standard deviation, and negative values indicate net deposition.

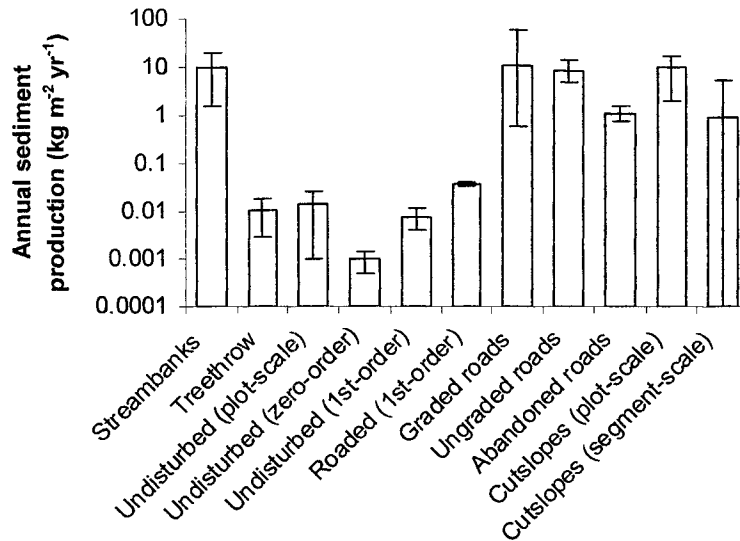


Figure 6. Annual sediment production rates from natural and anthropogenic sediment sources on St. John. Columns show average values, and bars indicate the range of values.

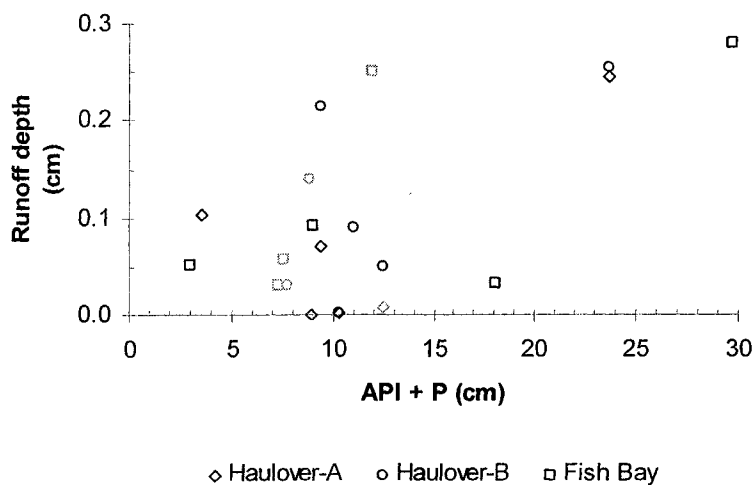


Figure 7. Runoff depth from the three undisturbed plots versus the sum of the antecedent precipitation index (API) plus storm precipitation (P). The points plotted in gray are the data collected by Sampson (2000).

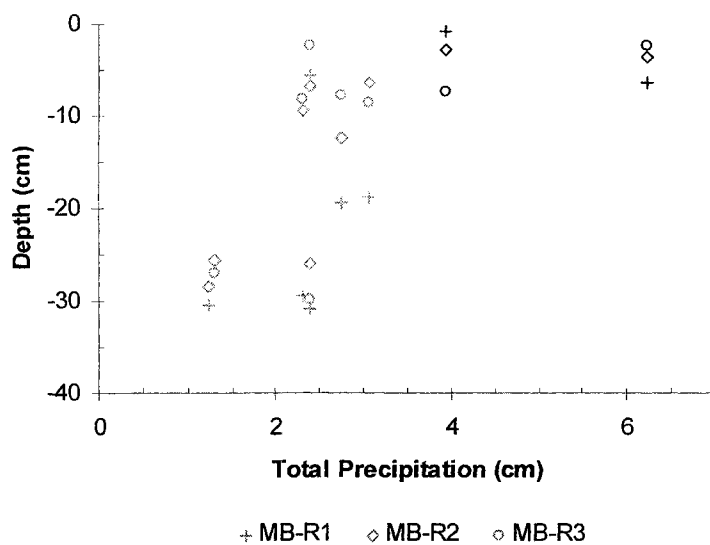


Figure 8. Depth to the saturated zone for each of the three crest gages versus storm precipitation. Points in bold are the storms that generated runoff from the zero-order catchment where the crest gages were located.

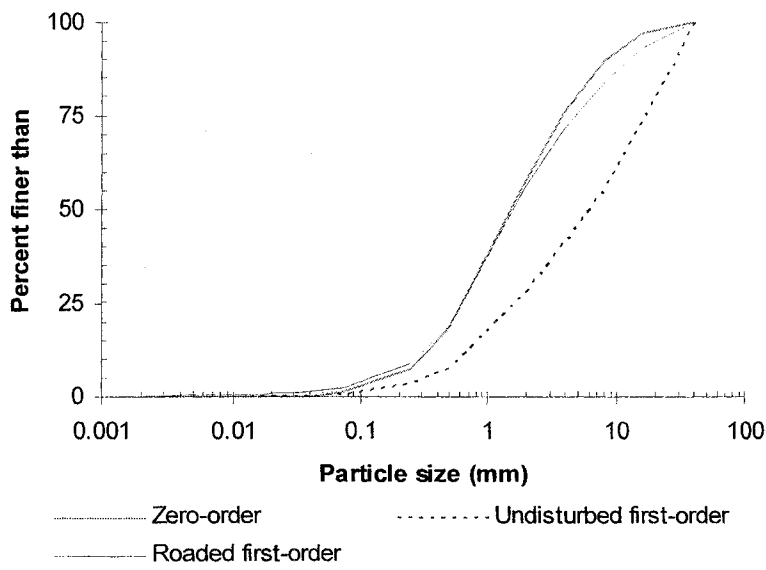


Figure 9. Mass-weighted particle-size distribution for the sediment from undisturbed zero-order catchments, undisturbed first-order catchments and roaded first-order catchments.

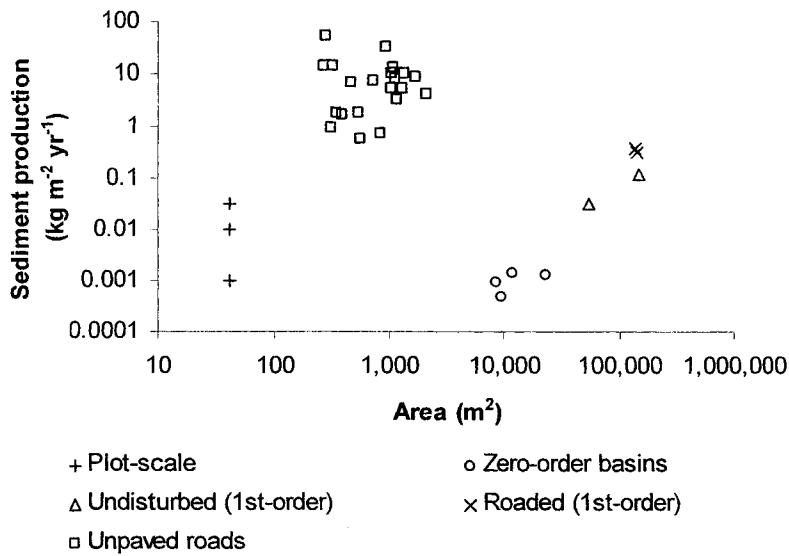


Figure 10. Sediment production rates per unit area per centimeter of rainfall versus contributing area.

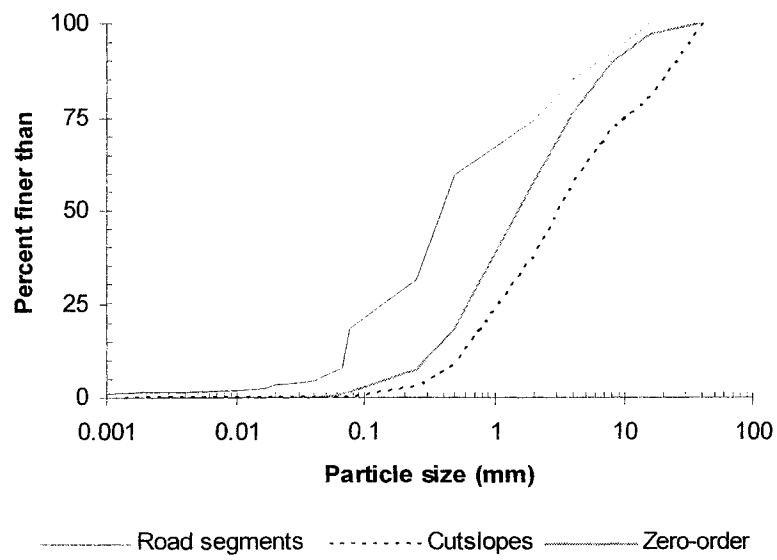


Figure 11. Mass-weighted particle-size distribution for the unpaved roads, the cutslopes, and the zero-order catchments.

Table 1. Summary of bank retreat rates measured from streams with drainage areas smaller than 10 km² (data from Lawler, 1993).

Location	Drainage area (km ²)	Bank retreat rates (cm yr ⁻¹)	Reference
Maryland, USA	0.13	0.6	Leopold et al. (1966)
Northern Ireland	3.4	0.03 -0.05	Hill (1973)
Luxemburg	1.6	0.8	Imeson and Jungerius (1974)
Wales	0.5	~3.0	Lewin et al. (1974)
England	10	8.0	Hooke (1979)
England	4.7	< 3.0	Murgatroyd and Ternan (1983)
St. John	0.14 – 3.8	0.1 – 1.5	This study

Table 2. Summary of treethrow surveys along five stream reaches on St. John.

Reach	Length of reach (km)	Number of uprooted trees	Uprooted trees per km of stream	Total sediment in rootwads (m ³)	Mean volume of sediment per rootwad (m ³)	Volume of sediment per km of stream (m ³ km ⁻¹)	Mass of sediment per km of stream (tons km ⁻¹)
Reef Bay-A	0.61	12	19.6	3.0	0.3	4.9	6.9
Reef Bay-B	0.96	14	14.6	19	1.4	20	28
Reef Bay-C	0.95	9	9.5	3.2	0.4	3.4	4.7
Lameshur	0.80	6	7.5	2.6	0.4	3.2	4.5
Fish Bay	3.35	33	9.8	52	1.6	16	22
Mean	1.1	12	11.1		1.1	12	17

Table 3. Runoff and sediment production from the three undisturbed plots. Sediment production per unit rainfall was calculated by multiplying the plot average sediment concentration by the total runoff per event. An asterisk indicates those events for which runoff is underestimated. NA indicates not available.

Plot	Date of storm	Total Rainfall (cm)	Maximum 1-hr rainfall intensity (cm hr ⁻¹)	Antecedent precipitation index (cm)	Runoff (cm)	Runoff coefficient (cm cm ⁻¹)	Sediment concentration (g L ⁻¹)	Sediment production per unit rainfall (g m ² cm ⁻¹)
Haulover-A	10 Sep 96	5.6	1.6	3.4	0.000	0.000	NA	0.00
	4 Dec 98	2.1	1.1	8.3	0.002	0.001	NA	0.02
	8 Apr 99	3.6	1.7	0.0	0.103	0.029	0.18	0.42
	10 Nov 99	3.1	2.8	6.2	0.070	0.022	0.75	0.33
	16 Nov 99	7.2	1.4	16.6	0.244*	0.034	0.33	0.50
	5 Dec 99	4.9	1.1	7.6	0.007	0.002	0.20	0.02
					Mean		0.015	0.37
Haulover-B	6 Jul 96	6.4	3.6	1.3	0.030	0.005	NA	0.16
	10 Sep 96	5.5	1.6	3.4	0.140	0.025	NA	0.86
	21 Sep 98	5.6	1.6	5.5	0.089	0.016	2.56	0.54
	4 Dec 98	2.1	1.1	8.3	0.002	0.001	NA	0.04
	10 Nov 99	3.1	2.8	6.2	0.214	0.068	0.42	2.29
	16 Nov 99	7.2	1.4	16.6	0.254*	0.035	0.32	1.19
	5 Dec 99	4.9	1.1	7.6	0.050	0.010	0.06	0.34
				Mean		0.023	0.84	0.77
Fish Bay	6 Jul 96	6.4	3.6	0.9	0.030	0.005	NA	0.01
	10 Sep 96	5.5	1.6	6.4	0.250*	0.045	NA	0.06
	4 Dec 98	2.2	2.1	15.8	0.033	0.015	NA	0.02
	8 Apr 99	3.0	1.7	0.0	0.051	0.017	0.10	0.02
	10 Nov 99	2.6	2.4	6.4	0.091	0.035	0.01	0.04
	16 Nov 99	13.1	3.4	16.7	0.280*	0.021	0.00	0.03
	5 Dec 99	4.5	1.2	3.1	0.058	0.013	0.01	0.02
				Mean		0.022	0.03	0.03

Table 4. Sediment production rates from zero- and first-order catchments. Undisturbed first-order catchments are identified with an asterisk, and the first-order basins with unpaved roads are identified by a double asterisk.

Site	Drainage area (ha)	Mean slope (%)	Start Date	End Date	Total sediment production (kg)	Total precipitation events > 6 cm (cm)	Sediment production per unit rainfall ($\text{g m}^{-1} \text{cm}^{-1}$)
Zero-BM-A	1.2	20	28 Jul 98	3 Nov 01	30	30.2	0.085
Zero-BM-B	1.0	15	29 Jul 98	3 Nov 01	8.8	30.2	0.031
Zero-BM-C	0.9	15	28 Jul 98	3 Nov 01	15	30.2	0.058
Zero-MB-A	2.3	20	14 Jul 99	7 Nov 01	41	21.7	0.081
1st-MB-A*	5.4	27	14 Jul 99	7 Nov 01	311	21.7	0.27
1st-RB-C*	15	37	29 Aug 99	6 Nov 01	2,115	19.2	0.74
1st-RB-A**	14	32	30 Jul 98	6 Nov 01	12,475	34.5	2.6
1st-RB-B**	14	25	27 Aug 99	6 Nov 01	5,848	19.2	2.1

Table 5. Cutslope characteristics and sediment production rates.

Plot	Cutslope height (m)	Cutslope area (m^2)	Degree of weathering	Period of measurement (years)	Annual sediment production ($\text{kg m}^{-2} \text{yr}^{-1}$)
MB-A	4.0	34	moderate	2.0	8.9
MB-B	4.2	26	moderate	1.0	12
MB-C	4.2	29	slightly	2.1	3.9
MB-L	1.3	5.2	residual soil	2.0	7.2
MB-U	1.2	6.8	moderate	2.0	3.4
JH-A	1.7	8.4	slightly	1.7	2.0
JH-B	1.4	7.9	moderate	3.2	7.7
JH-C	1.4	7.8	residual soil	3.2	17
Mean	2.4	16		2.1	7.8

Table 6. Cutslope sediment production rates reported in the literature. NA indicates not available or not applicable.

Reference	Location	Cutslope description	Sediment production rate reported	Sediment production (kg m ² yr ⁻¹)
Diseker and Richardson (1962)	Georgia, US	Unvegetated	102-230 t ha ⁻¹ yr ⁻¹	5.1-11
Wilson (1963)	Oregon, US	6-7 yr old cutslopes	153 t ha ⁻¹ yr ⁻¹	15
		new cutslopes	370 t ha ⁻¹ yr ⁻¹	37
Dyrness (1970, 1975)	Oregon, US	5 yr old cutslopes	0.5 cm yr ⁻¹	7.5
		1 yr old cutslopes	0.7 cm yr ⁻¹	10
Megahan (1980)	Idaho, US	45 yr old cutslopes, soil	0.01 m ³ m ⁻² yr ⁻¹	15
		45 yr old cutslopes, granite	0.011 m ³ m ⁻² yr ⁻¹	16
Reid (1981)	Washington, US	55-70 degrees	16.5 mm yr ⁻¹	25
Blong and Humphreys (1982)	Papua, New Guinea	NA	70 mm yr ⁻¹	105
Megahan et al. (1983)	Idaho, US	NA	11 mm yr ⁻¹	16
Riley (1988)	New South Wales, Australia	NA	2.4-3.9 mm yr ⁻¹	3.6-5.8
Fahey and Coker (1989, 1992) Smith and Fenton (1993)	New Zealand	Unvegetated, granite	NA	5.2-15
Megahan (2001)	Idaho, U.S.	Cover density 0.1-89% 55-104% gradient	0.1-248 t ha ⁻¹ yr ⁻¹	0.01-25
This study	St. John, USVI	Unvegetated, 2-5 m high	NA	2 - 17

Table 7. Estimated contribution of cutslopes to sediment yields at the road segment scale. The asterisk indicates that the values were estimated based on a visual classification system.

Road plot	Length of road segment (m)	Measured sediment production rate ($\text{kg m}^{-1} \text{cm}^{-1}$)	Road-segment sediment production (kg cm^{-1})	Percent of segment-scale sediment production contributed by cutslopes*	Estimated cutslope contribution (kg cm^{-1})
BM-A	420	0.18	78	46	36
BM-B	93	0.30	28	2.4	0.7
BM-C	270	0.43	115	9.0	10
FB-A	93	0.03	2.8	51.5	1.4
FB-C	109	0.08	8.5	30.9	2.6
FB-D	64	0.38	24	62.3	15
FB-E	83	2.21	183	0	0
JH-A	240	0.91	219	0.8	1.7
JH-A1	58	0.52	30	3.5	1.0
JH-A2	103	0.46	47	1.3	0.6
JH-B	394	0.40	158	14.5	23
JH-C	237	0.15	35	6.1	2.1
JH-D	148	0.28	41	15	6.2
JH-E	257	0.32	82	8.6	7.1
LB-A	256	0.39	100	1.3	1.3
LB-C	254	0.24	60	47.9	29
LE-Bottom	78	0.11	8.8	0.9	0.1
LE-Top	222	0.03	7.2	10.5	0.8
MB-A	179	1.48	264	7.0	18
MB-C	74	0.08	5.6	23.3	1.3
Sum			1497		158

CHAPTER 5.

DEVELOPMENT AND APPLICATION OF A GIS-BASED SEDIMENT BUDGET MODEL FOR ST. JOHN, U.S. VIRGIN ISLANDS

ABSTRACT

Increases in the delivery of sediment to the marine environment pose a serious threat to the coral reef communities of the Caribbean. Resource managers and decision-makers need to evaluate the changes in erosion rates and sediment delivery due to unpaved roads or other types of land disturbance. This is a particularly critical issue on St. John in the U.S. Virgin Islands because of the rapid development and exceptional resources at risk. The specific objectives of this study were to: (1) develop a GIS-based sediment budget model for St. John; (2) use the model to evaluate the effects of unpaved roads on sediment delivery rates in three watersheds; and (3) compare model predictions to measured data.

The St. John Erosion Model (STJ-EROS) is an Arc/Info-based system that quantifies watershed-scale sediment yields based on empirically-derived sediment production functions and delivery ratios. The STJ-EROS Arc Macro Language program code consists of six input routines and five routines to calculate sediment production and delivery. The six input routines have interfaces that allow the user to adjust the key variables that control sediment production and delivery, such as rainfall rates and sediment delivery ratios. The remaining five routines use pre-set erosion rate constants, user-defined variables, and values from nine input data layers to calculate watershed-scale sediment yields from unpaved road travelways, road cutslopes, streambanks, treethrow, and undisturbed hillslopes.

STJ-EROS was applied to three basins on St. John with varying levels of development. Predicted sediment yields ranged from 12 to 65 tons km⁻² yr⁻¹. Sediment from unpaved roads is believed to be increasing sediment delivery rates by 5-6 times for Lameshur Bay, 7-8 times for Fish Bay, and 24-40 times for Cinnamon Bay. The differences in estimated sediment yields and the relative impact of unpaved roads are largely due to differences in the amount of development in the three basins. The basin-scale sediment yields estimated by the model for both undisturbed and current conditions are within the range of sediment yield and bay sedimentation rates measured by previous studies on St. John. The structure and user interfaces in STJ-EROS mean that the model can be readily adapted to other areas and used to assess the impact of existing and proposed unpaved roads on sediment production and delivery.

5.1 Introduction

Accelerated erosion and increased watershed-scale sediment yields resulting from vegetation removal and land use are critical environmental problems (Walling, 1997). The rapid pace of land development in the Insular Caribbean, when combined with steep slopes and high precipitation intensities, make this region very susceptible to accelerated erosion (Lal, 1990). Sedimentation is one of the most important stressors of coral reef communities in the Caribbean (Hubbard, 1987; Gardner et al., 2003), but very little information is available on past and current sediment delivery rates to the marine environment (UNEP, 1994). High sediment loads are placing increasing stress on coral reef systems in the Dominican Republic (Torres et al., 2001), Puerto Rico (Torres, 2001; Acevedo et al., 1989) and the nearby island of Culebra (Hernández-Delgado, 2001), Virgin Gorda in the British Virgin Islands (C. Rogers, USGS, pers. comm.), as well as St. Croix (Hubbard, 1986), St. Thomas (Nemeth and Nowlis, 2001), and St. John (Rogers, 1990, 1998; Nemeth et al., 2001) in the U.S. Virgin Islands.

The processes and issues related to erosion in the Caribbean are as varied as the physiographic characteristics and land use practices. Although land disturbance has been widely recognized as the main cause of high erosion rates, historically there have been few efforts to remedy this problem (Lugo et al., 1981). The widespread lack of attention to erosion issues can be attributed in part to the lack of models to assess the different sediment sources and determine priorities for remediation. In general, studies have concentrated on mass wasting (e.g., De Graff et al., 1989; Jibson, 1989; Larsen and Parks, 1997; Larsen and Torres-Sánchez, 1998), surface erosion in agricultural fields (e.g., Smith and Abruña, 1955; Ahmad and Breckner, 1974; McGregor, 1988), or the application of uncalibrated erosion models to watersheds under variable land uses (e.g., Ramsarran, 1992; Radke, 1997; Del Mar-López et al., 1998). None of these efforts has addressed the combination of natural and anthropogenic sediment sources that are operating on St. John. Hence these studies cannot provide accurate estimates of sediment yields

in St. John, or provide guidance on how land managers might minimize erosion rates and the delivery of sediment to the marine environment.

Erosion issues have received special attention on St. John because land development is believed to be increasing sediment yields and adversely affecting the nearshore coral reef communities in the Virgin Islands National Park (Rogers, 1998). Previous studies on St. John concluded that sediment production rates from unpaved roads are several orders of magnitude higher than surface erosion rates from undisturbed hillslopes, and that unpaved roads are the primary source of the fine sediment being delivered to the marine environment (MacDonald et al., 2001). An empirical road erosion model (ROADMOD) developed by Anderson and MacDonald (1998) suggested that road erosion is increasing watershed-scale sediment yields by up to four times above background levels (MacDonald et al., 1997).

The present study emerged from the need to more accurately model watershed-scale erosion and sediment yields on St. John. The objectives were to: (1) develop a GIS-based model for calculating sediment budgets (STJ-EROS); (2) apply the model to several basins on St. John and quantify the increases in sediment production and delivery resulting from unpaved roads; and (3) compare model predictions to pre-existing sediment yield data.

At the most basic level, a sediment budget quantitatively describes the production, movement, and storage of sediment for a single landscape unit (Dietrich et al, 1982). The sediment budget approach is useful because it quantifies the absolute and relative contributions of different sediment sources in a watershed (Reid and Dunne, 1996). In this paper a landscape unit is defined as a surface area in a drainage basin where similar erosional processes act at a spatially-uniform rate. Initial field observations made in St. John led to the identification of the following landscape units:

- erodible streambanks;
- stream margins subjected to soil disturbance by treethrow;
- unchannelled (zero-order) catchments;

- road travelways; and
- road cutslopes.

Sediment production data were collected for each of these landscape units (Chapters 2 and 4).

To route sediment through a watershed it is necessary to quantify the rate of sediment movement between temporary storage sites (Swanson and Fredriksen, 1982). The STJ-EROS model uses a simple routing routine based on two storage units: (1) a terrestrial unit composed of hillslopes, the fluvial network, and associated wetlands; and (2) the marine environment. The rate at which terrestrial sediment is transferred to the marine environment is controlled by a user-defined sediment delivery ratio (SDR). The SDR is defined as the ratio of watershed sediment yield divided by the gross erosion within the basin (Walling, 1983). The alternative to SDRs is a more physically-based approach, but physical models carry a high degree of uncertainty and require much more detailed input data. The SDR approach is conceptually simple and easy to implement, and it is preferred for STJ-EROS given the model objectives and the intended users.

STJ-EROS is intended to guide land management decisions on St. John, as the model can quantify sediment delivery rates for both undisturbed and current conditions. It also can be used to predict sediment yields from different management scenarios. Actual or potential changes can be evaluated by making changes to one or more GIS data layers or user-defined variables. Since the focus of STJ-EROS is on road-related sediment sources, some of the changes that might be evaluated include paving selected road segments or comparing alternative routes for new roads. The model also can evaluate the effect of changes in the fluvial network or sediment trapping efficiency of coastal wetlands. An improved prediction tool will help managers choose alternatives that minimize the amount of sediment being delivered to the marine environment or other locations of particular concern.

5.2 Study Area

The U.S. and British Virgin Islands constitute the eastern extremity of the Greater Antilles, and St. John is the third largest island within the U.S. Virgin Islands (Figure 1). St. John lies on the Puerto Rico-Virgin Islands microplate, which is between the Caribbean and North American plates (Rankin, 2002). The resultant folding and faulting has created a very rugged topography, as more than 60% of St. John has slopes greater than 30%. St. John's lithology is dominated by volcanic rocks that have undergone periods of deformation, magmatic intrusions, and hydrothermal alterations (Donnelly, 1966; Rankin, 2002). The soils developed from these rocks are predominantly gravelly clay loams (Soil Conservation Service, 1970; USDA, 1995), and they tend to be shallow, moderately permeable, well-drained, and underlain by nearly impervious material.

The climate of St. John is characterized as dry tropical. Bowden et al. (1970) identified five precipitation zones ranging from 90 to 100 cm yr⁻¹ on the drier east end to a high of 130 to 140 cm yr⁻¹ near Bordeaux Mountain. Easterly waves, which can develop into tropical storms and hurricanes, generate most of the rainfall from May through November, while cold fronts are important sources of rainfall from December through April (Calversbert, 1970). There are no sharply defined wet and dry seasons in St. John, but a relatively dry season extends from about February to July, and a relatively wet season lasts from August until January (Bowden et al., 1970).

Precipitation in St. John can be highly erosive. The average erosivity at Caneel Bay was estimated to be 13,500 MJ mm ha⁻¹ hr⁻¹ (Sampson, 2000). Fifteen-minute precipitation intensities at Caneel Bay exceeded 100 cm hr⁻¹ sixteen times between 1979 and 1995.

Mean monthly potential evapotranspiration (PET) exceeds mean monthly precipitation for most of the year (Bowden et al., 1970). There is little ground water storage and no perennial streams (known locally as "guts") on St. John (MacDonald et al., 1997). The combination of steep slopes, small drainage areas, shallow soils with low-water holding capacities, and

occasional intense storm events result in “flashy” runoff hydrographs with very steep rising and recession limbs.

The history of land use in St. John is similar to most of the other islands in the eastern Caribbean. It was originally forested and subjected to only minor disturbance by Amerindian groups. During the 1700’s and 1800’s, approximately 90% of the forests were removed and replaced by sugarcane fields (Tyson, 1987). The agricultural fields were largely abandoned in the late 19th century as a result of the decline in the sugarcane industry, and this marked the beginning of the forest recovery period. The United States purchased the Virgin Islands from Denmark in 1917, and in 1956 Virgin Islands National Park (VINP) was established. The park was designated an International Biosphere Reserve in 1976, and it is one of the few reserves that has both marine and terrestrial resources (Rogers, 1992). In 2001 an additional 47 km² of offshore waters were included in VI Coral Reef National Monument.

Current sediment yields on St. John are believed to be higher than at any point in its recent history (MacDonald et al., 1997). Rapid development over the past 30 years has resulted in a dense network of unpaved roads, particularly on the private lands outside of VINP. Maps developed for this study show that the road network in the 6 km² Fish Bay basin nearly tripled in length between 1971 and 2000, and that 56% or 13.1 km of roads are still unpaved. The unpaved road density of 2.2 km km⁻² in this basin is nearly three times the density of unpaved roads in the Greater Lameshur Bay basin, which lies mostly within VINP. The unpaved road network is believed to be the single most important sediment source on St. John (Anderson and MacDonald, 1998), but there are no locally-calibrated, spatially-explicit models for estimating the effects of unpaved roads on sediment production and delivery rates at the watershed scale.

5.3 Field Methods and Results

Sediment production rates from natural and anthropogenic sources were measured by various field methods (Chapters 2 and 4). Streambank erosion was quantified by use of erosion pins

(Lawler, 1993). The amount of sediment delivered to the fluvial network by treethrow was determined by estimating the frequency of treethrow events and the volume of soil in rootwads along selected stream reaches (Reid, 1981). Sediment fences (Robichaud and Brown, 2002) were used to quantify sediment production rates from undisturbed hillslopes, zero-order catchments, unpaved road segments, and cutslopes.

Measured sediment production rates ranged over five orders of magnitude (Figure 2; Table 1; Chapter 4). The mean streambank erosion rate was $10 \text{ kg m}^{-2} \text{ yr}^{-1}$. Uprooting of trees along stream margins was estimated to deliver 0.17 tons of sediment per kilometer of stream per year, or $11 \text{ g m}^{-2} \text{ yr}^{-1}$ for a 15-meter wide stream corridor. The mean sediment yield for zero-order catchments was $1.0 \text{ g m}^{-2} \text{ yr}^{-1}$. This value was used for undisturbed areas because plot-scale measurements do not account for hillslope sediment storage, and measurements from first-order basins include streambank erosion and treethrow (Chapter 4). In STJ-EROS streambank erosion and treethrow are treated independently of surface erosion from undisturbed areas.

Surface erosion rates from unpaved road segments were found to vary with rainfall, road slope, and frequency of grading (Figure 2; Table 1; Chapter 4). Sediment production rates for roads that were graded once every two years ranged from 0.57 to $58 \text{ kg m}^{-2} \text{ yr}^{-1}$ for roads with mean slopes of 1% and 21%, respectively. Ungraded roads had sediment production rates ranging from 5.1 to $14 \text{ kg m}^{-2} \text{ yr}^{-1}$ for roads with slopes of 10% and 16%, respectively. Abandoned roads with 15% slopes had a mean erosion rate of $1.1 \text{ kg m}^{-2} \text{ yr}^{-1}$. Although cutslopes eroded at rates ranging from 2 to $17 \text{ kg m}^{-2} \text{ yr}^{-1}$, their estimated contribution to sediment yields at the road-segment scale is $0.9 \text{ kg m}^{-2} \text{ yr}^{-1}$, or only about 11% of the total sediment yield from unpaved roads (Chapter 4).

5.4 St. John Sediment Budget Model (STJ-EROS)

5.4.1 Overview

STJ-EROS uses the capabilities of GIS software to develop spatially-variable sediment budgets. The program is written in Arc Macro Language (AML) for Arc/Info version 8.2 and uses the spatial analysis capabilities provided by Arc and the relational database commands available in the Tables module. The model is designed to calculate the amount of sediment from different sources that reaches the marine environment on a watershed scale.

The STJ-EROS model contains six input routines and five routines that calculate sediment production and delivery (Figure 3). The six input routines have user interfaces that allow the user to adjust some of the variables controlling sediment production and delivery (Table 2a). The remaining five routines use pre-set erosion rate constants, user-defined variables, and item values stored in nine data layers to calculate watershed scale sediment yields (Table 2b). Appendix IV-B describes the GIS data layers needed to run the model, Appendix IV-C provides flowcharts of the most important routines, and Appendix IV-D displays the program code.

5.4.2 Input Routines

STJ-EROS begins with the 'set_sdr' routine (Figure 3; Table 2a). This routine prompts the user to choose the sediment delivery ratios (SDRs) used by STJ-EROS to route sediment into the marine environment. A strict application of SDRs requires knowledge of the type and location of sediment sources, the particle-size distribution of the sediment being eroded, and both the transport and sediment storage capacity of the fluvial network (Bunte and MacDonald, 1999). Use of the SDR approach by STJ-EROS is a simplification of sediment transport dynamics, as SDR values only vary according to the interaction of the fluvial network with coastal wetlands and salt ponds.

SDRs for catchments with drainage areas of 0.1 to about 5 km² are generally between 40 and 100% (Walling, 1983). In STJ-EROS sediment delivery ratios of 50-100% are used for

with a high sediment delivery potential. These areas drain directly to the sea without an intervening coastal wetland or salt pond.

The presumed SDR values of 50-100% imply a fluvial system with a high sediment transport capacity, and this is consistent with measured runoff rates and sediment transport calculations. The sediment transport capacity of Fish Bay Gut was estimated at 12 different locations based on the ratio of particle settling velocities to shear flow velocities (Middleton, 1976) (Appendix IV-A). On average, flow depths that were only 12% of the estimated bankfull depth were needed to maintain particles smaller than 2 mm in suspension. Flows exceeding bankfull depth were needed to transport particles larger than 2 mm in suspension. This indicates that particles smaller than 2 mm are readily transported as suspended load along the Main Fish Bay Gut, and presumably along the other guts in St. John. Particles larger than 2 mm are assumed to be transported as bed load and are likely to remain within the fluvial system for longer time periods.

STJ-EROS refines the SDR approach by partitioning sediment production and delivery into two size classes. The fine fraction is defined as particles smaller than or equal to 2 mm, while the coarse fraction consists of particles larger than 2 mm. Although the SDR values are applied to both size classes, this partitioning allows STJ-EROS to calculate a range of long-term sediment yield rates. The minimum value simply assumes that none of the coarse sediment but all of the fine sediment that reaches the guts is delivered to the watershed outlet. The maximum value assumes that all of the particles from clays to coarse gravel (about 30 mm) are delivered to the watershed outlet. The upper limit of 30 mm corresponds to the largest particles found in the sediment traps below unpaved roads and undisturbed hillslopes (Appendices I-D, III).

The delivery of sediment from catchments with an intervening wetland or salt pond is more complicated. These wetlands vary in size, the magnitude of fresh water versus tidal inflows, and their sensitivity to natural and human disturbance. Some wetlands become inundated during extreme storms due to the rise in sea level, while others remain separated from

the sea by a berm. Field observations of the wetlands at Fish Bay and Lameshur Bay indicate that these wetlands were not inundated by the sea during Hurricane Georges in 1998 or Hurricane Lenny in 1999. Maps of the 100-yr high tide show that seawater intrusions on St. John are limited to a very narrow area (U.S. Army Corps of Engineers, 1975). On the other hand, large runoff events flood the wetlands and flow into the sea. It is these events that give the water in some bays a brown color, indicating that terrestrial sediment is being delivered to the marine environment up to several times each year.

Data on the trapping efficiency of mangrove wetlands are mostly qualitative (Augustinus, 1995). In the absence of specific data, the SDRs for areas draining into coastal wetlands are assumed to range from 0 to 50%. These catchments are defined as having a moderate potential for sediment delivery.

Other catchments are assumed to have a SDR of 0. These catchments drain to a wetland or pond that lacks any surface pathway to the marine environment, implying a sediment trapping efficiency of 100%.

The polygons representing the areas with a given SDR are stored in the SED_DEL layer (Table 3). An item in the attribute table named "potential" identifies each polygon as having a high, moderate, or no potential for delivering sediment into the sea. The SDR values chosen by the user during the 'set_sdr' routine for high and moderate delivery potential areas are stored as variables named "hi_pot" and "mod_pot", respectively.

The next step in the 'del_potential' routine prompts the user to choose the basin for which the sediment budget is to be estimated (Figure 3). The chosen name is assigned to a variable called "basin" (Table 2a). At this point a complete set of data layers to run STJ-EROS are available only for the Cinnamon Bay (CB), Fish Bay (FB), and Lameshur Bay (LB) basins on St. John (Figure 1), so these are the only choices available.

The 'del_potential' routine constructs a new data layer called DEL_BD. This new layer is created by clipping the SED_DEL layer with the boundaries of the selected area as defined by

the variable “basin” (Table 3). The routine assigns the values of “hi_pot” and “mod_pot” to the polygons in DEL_BD with high and moderate sediment delivery potentials, respectively.

The next routines are ‘set_years’, ‘set_rain’, ‘roads_name’, and ‘nat_name’ (Figure 3; Table 2a). These routines prompt the user to enter the total number of years over which the model is to be applied, an annual rainfall rate, and names for the text files and GIS data layers that will contain the model results. User choices are assigned as values to the “years”, “rain_rate”, “road_name”, and “nat_name” variables.

5.4.3 Sediment Yield Calculation Routines

Once these user-defined inputs have been specified, the model calculates sediment production from each unpaved road segment using the ‘rd_erosion’ routine (Figure 3). This routine uses four input layers and four user-defined variables to estimate sediment yields resulting from unpaved roads (Table 2b). To run rd_erosion, the user must have a line layer (GPS_RDS) that defines each road segment along with its road surface type, grading frequency, slope, length, and width (Table 2b). Road segments are distinguished by having different distinct drainage locations, and the point coordinates of road drainage structures are in GPS_DRA (Table 3).

The first step in the rd_erosion routine creates a data layer called DRAIN by clipping GPS_DRA with “BASIN”_BD (Table 3). DRAIN contains the spatial and attribute data of road drainage points within the chosen basin. The routine intersects DRAIN with DEL_BD to assign SDR values to each individual road drainage point. A ‘joinitem’ command then incorporates these segment-specific SDRs to a copy of the original road data layer (GPS_RDS).

The Tables module calculates sediment production and delivery from each unpaved road segment that delivers sediment into the chosen basin. Although paved roads may also contribute sediment from cutslope and ditch erosion, there were not enough data to incorporate paved roads into STJ-EROS.

Road sediment production is calculated from the “rain_rate” and “years” variables, as well as the road segment characteristics stored in GPS_RDS (Tables 1 and 3). The empirical sediment production functions used in STJ-EROS (Table 1) were derived from data collected by sediment traps placed at road drainage outlets. These measurements integrate sediment production at the road-segment scale, but they do not consider how much of this sediment reaches the stream channel. The hillslope-scale routing of road-related sediment is an important control on sediment yields. Field assessments showed that only 70 of the 338 road-drainage structures mapped on St. John were within 50 m of the stream network (Appendix IV-B). From a practical point of view, it is extremely difficult to measure the proportion of sediment from unpaved roads that reaches the stream network. As a result, the only means to account for hillslope storage is to incorporate this with the selection of SDR values for each polygon or basin using the ‘del_potential’ routine.

The use of sediment trap data to develop empirical road erosion models poses another problem. The trapping efficiency of sediment traps generally decreases with decreasing particle size (Ice, 1986). Runoff and suspended sediment data for a road segment in St. John yielded nine times more silt (defined as 0.004-0.062 mm) than measured with a sediment trap (Chapter 3). Surprisingly, there were no differences between the two measurement methods for the amount of clay-sized (< 0.004 mm) sediment. This difference in the amount of silt-sized particles appears to be of little practical significance since both methods showed that less than 5% of the sediment from the road fell into this size class. Nevertheless, a factor has been integrated into the ‘rd_erosion’ routine to compensate for this apparent underestimation of the silt-size fraction (Tables 1, 2b).

The delivery of sediment from each road segment is partitioned into that originating from the travelway and that being produced from cutslopes. A visual classification system determined that on average cutslopes account for only 9% of road-segment scale sediment yield (Chapter 4). This has been incorporated into the ‘rd_erosion’ routine by subtracting 9% from the total

sediment estimated for each road segment and assigning it to cutslopes. The remaining 91% of the estimated sediment is assigned to travelways.

The delivery of sediment from individual road segments is calculated as the product of the estimated sediment produced by its SDR. The sediment delivery rate is then partitioned into suspended load (≤ 2 mm) and bed load (> 2 mm) based on the particle-size distributions on Table 4. The final results of the 'rd_erosion' routine are stored in a text file and a GIS data layer both given the name stored in the user-defined "road_name" variable.

The next routine in the model is the 'streambank' routine (Figure 3). This routine calculates sediment production and delivery rates from streambank erosion. The streambank attribute data needed to estimate sediment production are stored in the BANKS data layer (Table 3). BANKS was developed based on stream surveys and distinct stream sections in this data layer were defined according to streambank height. Erodible banks on St. John are generally restricted to areas where streams intersect alluvial or colluvial deposits. These deposits are found primarily along the larger channels that drain to the southern coast of St. John, as the lower portions of these basins are not nearly as steep as the smaller basins draining to the north. The alluvial deposits are composed of loose, angular, gravel-sized fragments supported by a fine sand-silt matrix. The deposits show little layering or weathering and are poorly sorted. Streambanks in these areas are very steep, mostly unvegetated, and range from 0.6 to 2.5 m in height.

The 'streambank' routine begins by intersecting BANKS with DEL_BD to create BANK_DEL (Table 2b). BANK_DEL contains the bank height information in BANKS in addition to the user-defined SDR values. Total sediment production from streambanks is calculated as a function of the total length of streams with erodible banks (approximated as half of the stream section perimeter), bank height, the "streambank" variable that defines the sediment production rate (Table 1), and the user-defined "years" variable (Table 2b). Sediment delivery for individual stream sections is calculated as the product of sediment production by SDR. Sediment delivery is then partitioned into suspended load (≤ 2 mm) and bed load (> 2 mm)

according to the particle-size distribution of streambanks shown in Table 4. The results of the streambank routine are stored in a polygon data layer called BANK_DEL.

The next routine is the 'stream_total' routine (Figure 3). The first part of this routine calculates sediment from treethrow based on the "treethrow" variable, the total channel length in the basin being modeled, and the user-defined variable "years" (Table 2b). "Treethrow" defines the sediment production rates from treethrow in tons per kilometer of stream per year (Table 1). The length of stream in the chosen basin is determined by clipping STJ_STR with DEL_BD. In this study the fluvial network in STJ_STR was developed from field reconnaissance, so this data layer represents a longer stream network than that represented by standard topographical maps. Channels were identified in the field as features along which runoff and sediment is transported between well-defined banks (Dietrich and Dunne, 1993). Although it might be possible to use a GIS flow accumulation algorithm to generate a stream data layer similar to STJ_STR, the lack of appropriate data prevented the definition of a source area threshold for channel initiation in St. John.

Sediment delivery from treethrow is calculated by the 'stream_total' routine by multiplying the estimated sediment production of each stream arc by its respective SDR. The routine partitions treethrow sediment delivery into the portion presumed to be transported as suspended load (≤ 2 mm) and that transported as bed load (> 2 mm) based on the particle-size distribution shown in Table 4. Treethrow sediment delivery estimates are stored in the TR_DEL polygon data layer. The 'stream_total' routine uses a union command to combine the sediment delivery from streambanks (BANK_DEL) with that from treethrow (TR_DEL) into a new polygon layer called STR_DEL.

The next routine in the model is 'surf_erosion' (Figure 3). This routine estimates sediment production and delivery from undisturbed areas by surface erosion. This routine requires the STJ_BD, "BASIN"_BD, and DEL_BD data layers, the user-defined "basin", "years" and "rain" variables, and a variable called "undisturbed" (Table 2b). The variable "undisturbed"

defines sediment production as a function of the rainfall from large storms and the total area. Field data showed that sediment was produced from undisturbed zero-order catchments only from storms with 6 or more centimeters of rainfall (Chapter 4). Long-term rainfall data from Caneel Bay shows that events larger than 6 cm account for about 14% of the annual rainfall. This proportion of the effective rainfall was incorporated into the empirical sediment production model for undisturbed hillslopes (Table 1).

It is important to point out that the value of the “undisturbed” variable was developed with data collected from sediment traps. As it was the case for unpaved roads, the erosion rate for undisturbed catchments defined by this variable is likely to underestimate erosion rates for the silt-sized sediment fraction. A multiplication factor based on the mass-weighted average particle-size distribution data has been integrated into the ‘surf_erosion’ routine to compensate for underestimation of the silt-size fraction (Tables 1 and 2b). The ‘surf_er’ routine partitions the sediment into suspended (≤ 2 mm) and bed load (> 2 mm) based on the particle-size distribution values shown in Table 4. The sediment yield rate for each polygon in the final data layer (SE_BD) is calculated by multiplying the sediment production by its respective SDR.

The ‘nat_erosion’ routine (Figure 3) uses a union command to join the sediment production and delivery estimates contained in the STR_DEL and SE_BD data layers. The final text file and GIS data layer are given the name stored in the user-defined “nat_name” variable. The file and data layer contain the sediment delivery estimates from streambank, treethrow, and surface erosion on undisturbed hillslopes. The ‘summary_results’ routine is the final routine in STJ-EROS, and this displays a table of sediment delivery estimates from roads and undisturbed areas.

5.5 Model Application

5.5.1 Basin Description

The STJ-EROS model was applied to three basins on St. John: Lameshur Bay, Fish Bay, and Cinnamon Bay (Figure 1). These three basins were chosen for analysis because they have

been the target of several road rehabilitation projects conducted by the VI National Park, the VI Department of Planning and Natural Resources, and several homeowner associations. Lameshur Bay and Fish Bay have also been the subject of previous sediment yield and bay sedimentation studies. Previous sediment yield estimates provide a baseline to compare STJ-EROS results.

The Lameshur Bay basin is defined as those areas that drain to Little Lameshur, Greater Lameshur, and Europa Bays on the south coast of St. John. This 4.3 km² basin is relatively undisturbed, as it mostly lies within VINP (Figure 1). The basin has an average slope of 41%. Approximately 70% of the basin has a moderate sediment delivery potential, while 7% has a high delivery potential (Table 5). Twenty-three percent of the basin is classified as having no sediment delivery potential because sediment produced from this area gets deposited in a large capacity detention pond. There are 6.4 km of streams with 40% of these having erodible banks. The road network in 1999 consisted of 3.2 km of unpaved and actively-used roads, 0.2 km of abandoned unpaved roads, and 0.1 km of paved segments (Table 5). Unpaved roads had an average slope of 5%. Among actively-used roads only 10% were classified as graded and 90% ungraded.

The Fish Bay basin drains to the south coast of St. John and has a total area of 6.0 km² (Figure 1). The basin has an average slope of 32%. Approximately 68% of the basin has a high sediment delivery potential (Table 5). Much of the area with a high potential for sediment delivery feeds into the Main Fish Bay Gut or its Battery Gut tributary, which deliver runoff and sediment to the marine environment without any intervening wetlands. The other 32% of the basin has a moderate potential for sediment delivery. Of the 12.7 km of streams in the basin, 5.2 km or 41% have actively eroding banks. The Fish Bay basin has one of the highest road densities on the island. In 1999 there were 22 km of roads, with 9.5 km classified as paved, 9.2 km as actively-used unpaved roads, and 3.2 km as unpaved roads that had been abandoned for over 15 years (Table 5). The average slope for unpaved roads was 7%. Among the 9.2 km of actively-used unpaved roads 57% were classified as graded and 43% as ungraded.

STJ-EROS was applied to 1.6 km² or 90% of the 1.8 km² Cinnamon Bay basin. The highly-developed Peter Bay area was not included because there is no public access and we could not collect the necessary field data. The average slope in the area modeled was 41%. Seventy-six percent of the catchment is in wetlands or areas that drain through wetlands, so these areas were classified as having a moderate sediment delivery potential (Table 5). The remaining 24% of the area was designated as having a high potential for sediment delivery. There were 4.1 km of streams, and none of the reaches had banks composed of erodible alluvial material. In 1999 there were 3.6 km of paved roads and 1.6 km of unpaved roads (Table 5). The main unpaved road is the John Head road, which appears as a cartway in a 1919 Geodetic survey and was expanded to its current width during the 1960's (Gibney and Ray, 1993). The mean slope of all roads was 11%. Ninety-six percent of the unpaved roads are ungraded, while only 4% are graded at least once every two years. No abandoned roads were found in the basin.

5.5.2 Predicted Sediment Yields

In the absence of specific data on basin-scale sediment delivery ratios and the trapping efficiency of coastal wetlands in St. John, long-term sediment delivery ratios of 80% were assigned for high potential areas and 30% for areas with moderate potential. The estimated sediment delivery rates to each of the three bays under undisturbed conditions were 9 to 12 tons yr⁻¹ (2-3 tons km⁻² yr⁻¹) for Lameshur Bay, 32 to 44 tons yr⁻¹ (5-7 tons km⁻² yr⁻¹) for Fish Bay, and 0.6 to 1.0 ton yr⁻¹ (0.004-0.6 tons km⁻² yr⁻¹) for Cinnamon Bay (Figure 4). While the lower values in these estimates exclusively represent sediment finer than 2 mm, the higher value refers to sediments ranging from clay to coarse gravel (roughly 32 mm). In the Lameshur Bay and Fish Bay basins approximately 90% of the sediment yield in undisturbed conditions originates from streambanks. In contrast, in Cinnamon Bay approximately 60% of the estimated sediment yield under natural conditions originates from undisturbed hillslopes, and about 40% is produced by treethrow.

The addition of unpaved roads increases the estimated sediment yields by a factor of 4.7 to 40, depending on the estimated sediment yield from natural sources and road characteristics (Figure 4). When unpaved roads are included, STJ-EROS estimates sediment yields ranging from 50 to 80 tons yr⁻¹ into Lameshur Bay. These sediment yield rates are 5-6 times above undisturbed conditions. Current sediment yields into Fish Bay are estimated to be from 240 to 376 tons yr⁻¹, or 7-8 times above background. Current sediment yields into Cinnamon Bay are estimated to have increased to 24 to 40 tons yr⁻¹, or 24-40 times relative to undisturbed conditions.

The contributions of individual road segments to sediment yield rates, as well as the spatial distribution of the sediment delivery potential zones in the Lameshur Bay, Fish Bay, and Cinnamon Bay basins are shown in Figures 5a, 5b, and 5c, respectively. Sediment yield rates from road segments in these figures refer to all sediment sizes ranging from clays to coarse gravel. Individual road segments are color coded in Figures 5a-5c according to their sediment yield contributions. The color code permits easy identification of individual road segments that are contributing high quantities of sediment to the marine environment. Road segments in white indicate paved road segments for which no sediment yield was estimated, unpaved roads with a negligible slope, or roads that are not contributing sediment to the selected basin. Road segments in yellow and orange indicate road segments that contribute 0-3 tons yr⁻¹ and 3-5 tons of sediment per year to the marine environment, respectively. Road segments contributing 5-10 and 10-45 tons yr⁻¹ are shown in purple and red, respectively. Figures 6a, 6b, and 6c show how sediment delivery rates are distributed by sediment source and particle-size class for the Lameshur Bay, Fish Bay, and Cinnamon Bay, respectively. Sediment finer than 2 mm represents 60-65% of the total sediment yield in each of the three study basins.

Unpaved roads account for approximately 83% of the 50-80 tons of sediment delivered to Lameshur Bay every year (Figure 6a). Graded roads are responsible for 55% of the sediment being delivered into Lameshur Bay. All of this sediment comes from a 330-m long road segment

with an average slope of 20% (shown in red in Figure 5a). Ungraded roads account for about 18% of sediment yield, cutslopes 10%, streambanks 15%, while undisturbed hillslopes and treethrow account for less than 2 percent of the total sediment yield.

Sediment produced from unpaved roads is responsible for about 88% of the 240-380 tons of sediment being delivered to Fish Bay per year. Graded roads account for about 56% of the total sediment yield into Fish Bay, while ungraded roads are responsible for 20% (Figure 6b). Individual road segments contributing an excess of 5 tons of sediment per year contribute about 200 tons of sediment per year, or about 52% of the total sediment yield. Most of these roads deliver their sediments directly to the Main Fish Bay Gut in the lower portions of the basin or to the Battery Gut tributary in the upper portion of the basin (Figure 5b). These unpaved road segments represent 2.1 km of the 12.4 km of unpaved roads in the basin. Bank erosion produces roughly 11% of the annual sediment yield, while ungraded roads and cutslopes represent approximately 20 and 10%, respectively. The total contributions from surface erosion of undisturbed hillslopes, treethrow, and erosion from abandoned road surfaces are less than 1% of the sediment yield.

In the Cinnamon Bay basin unpaved roads account for 98% of a total sediment yield of 25-40 tons per year. An unpaved private driveway and several ungraded road segments along John Head road account for 80% of the total sediment yield into Cinnamon Bay (Figure 6c). The ungraded 80-m long driveway has a slope of 27% and is the only road segment in this basin producing an excess of 10 tons of sediment per year. Although this driveway represents only 5% of the unpaved road network in Cinnamon Bay, it is estimated to contribute a total of 11 tons of sediment per year, or 27% of the total sediment yield. Even though individual road segments along John Head road contribute sediment at rates lower than 5 tons per year (Figure 5c), they represent 1.5 km of the 1.6 km of unpaved roads in the basin. As a result these road segments are responsible for 57% of the total sediment yield into Cinnamon Bay. Cutslopes are responsible for

another 12% of the total sediment delivered, while surface erosion from undisturbed hillslopes and treethrow account for 5% of the total sediment yield.

In summary, application of STJ-EROS to Lameshur Bay, Fish Bay, and Cinnamon Bay indicates that unpaved roads are the dominant sediment source in these basins and are responsible for 83-98% of the total sediment yield. The results summarized in Figures 5a-5c can be used in evaluating the effectiveness of various road erosion control programs. For example, paving road segments delivering more than 5 tons of sediment per year could reduce sediment yields into Lameshur Bay and Fish Bay by 55 and 52%, respectively. This considerable reduction in sediment yields is achieved by paving only 0.3 km and 2.1 km of roads, or 10% and 17% of the unpaved roads in Lameshur Bay and Fish Bay, respectively. In contrast, paving road segments in Cinnamon Bay that are producing more than 5 tons of sediment per year would result in only a 27% reduction in sediment yields. A sediment yield reduction of 57% can be achieved in Cinnamon Bay if 1.5 km of unpaved road segments are paved. These road segments represent 94% of the total unpaved roads in the basin.

5.5.3 Effects of Varying Sediment Delivery Ratios in Basin-scale Sediment Yields

The sensitivity of sediment yields to varying sediment delivery ratios was estimated for the STJ-EROS model. SDRs were varied from zero to 50% for moderate potential areas, and high potential areas were assigned SDRs from 50 to 100%. Sediment yields defined as a percentage of the yield estimated using SDR values of 50 and 100% for moderate and high potential areas were used to evaluate sensitivity. Differences in the slope and spacing of the lines shown in Figures 7a-7c indicate that the sensitivity of sediment yields to varying SDR values varied from basin to basin.

In the Lameshur Bay basin 130 tons per year was the total sediment yield estimated using 50 and 100% SDR values for moderate and high potential areas, respectively. Sediment yields in Lameshur Bay were very sensitive to the SDR values assigned to the moderate potential areas

(Figure 7a). Reducing SDR values for moderate potential areas from 50 to 0% induced a 94% decline in sediment yields. In contrast, dropping the SDR value of high potential areas from 100 to 50% caused only a 3% reduction in sediment yields. The Lameshur Bay basin is very sensitive to moderate potential SDRs because these areas represent 74% of the total basin (Table 5). A moderate potential area is also the recipient of sediment produced from an unpaved road that accounts for approximately 55% of the total basin sediment yield (Figure 5a).

A sediment yield of 520 tons per year was estimated for the Fish Bay basin using SDR values of 50 and 100% for moderate and high delivery potential areas, respectively. Sediment yield estimates for the Fish Bay basin were slightly more sensitive to SDR values of high potential areas than SDRs of moderate areas. A reduction from 100 to 50% in the SDR for high potential areas decreased sediment yield by 37%, while reducing SDR for moderate potential areas from 50 to 0% caused a 25% drop in sediment yields (Figure 7b). The slightly higher sensitivity to values assigned to high potential areas is due to the fact that high potential areas cover 68% of the total basin, while those with moderate delivery potential cover only 29% (Table 5).

A sediment yield of 59 tons per year was estimated for the Cinnamon Bay basin using a SDR of 50% for moderate potential areas and a SDR of 100% for high potential areas. Estimated sediment yields into Cinnamon Bay were more sensitive to changes in SDR values assigned to moderate potential areas than those assigned to high potential areas (Figure 7c). A reduction in SDRs for moderate areas from 50 to 0% caused sediment yields estimates to decline by 55%. Reducing the SDR value for high potential areas from 100 to 50% induced a 23% decline in the estimated sediment yields. Sediment yields are more sensitive to the SDR values of moderate potential areas because they cover 74% of the total basin area, while areas with high delivery potential make up 23% of the basin (Table 5).

5.5.4 Comparison of Model Results to Other Sources of Data

Sediment yields estimated by STJ-EROS were compared to other measured or estimated values. Runoff and suspended sediment data was collected from the Main Fish Bay Gut from October 1998 and November 2001. A runoff record longer than 3 years was deemed necessary to estimate long-term suspended sediment yields from the Main Fish Bay Gut drainage area (Figure 5b). A fifteen-year long runoff record existed for the Guinea Gut US Geological Survey stream gaging station (USGS station 50295000) located only two kilometers west of the Main Fish Bay Gut station. A flow duration curve developed from the Guinea Gut runoff data and the mean suspended sediment concentration of 35 samples collected from the Main Fish Bay Gut were used to calculate an average annual suspended sediment yield for the Main Fish Bay Gut (Appendix IV-E). The estimated annual suspended sediment yield for the 3.5 km² Main Fish Bay catchment was 65 tons yr⁻¹ (18 tons km² yr⁻¹) (Table 6). Assuming an annual rainfall of 115 cm yr⁻¹ and a sediment delivery ratio of 80%, STJ-EROS estimated a suspended sediment yield of 190 tons yr⁻¹ (54 tons km⁻² yr⁻¹).

The higher sediment yield estimates resulting from STJ-EROS relative to the suspended sediment yield data might be explained in part by the limited number of suspended sediment samples. Suspended sediment yield estimates from STJ-EROS assume that all material finer than 2 mm will be transported in suspension. This assumption could not be corroborated as no particle-size distribution analysis was performed on the 35 suspended sediment samples. The mean flow rate represented by the 35 samples was 0.59 m³ s⁻¹ or 0.06 cm hr⁻¹, and only three of these samples represented flows higher than 1 m³ s⁻¹ (0.1 cm hr⁻¹) (Appendix IV-E). Between October 1998 and October 2001 flow rates up to 41 m³ s⁻¹ (4.3 cm hr⁻¹) were recorded at Main Fish Bay Gut. It is then possible that the mean sediment concentration is lower than the actual average, as it might be biased towards low-flow conditions during which only the finest particle sizes are being transported.

The limited number of samples also questions its true representation of long-term sediment transport rates, considering that sediment yields are a function of the amount of sediment available for transport and the sediment transport capacity of the fluvial network. A stream profile of Main Fish Bay Gut and its Battery Gut tributary surveyed in February 2000 estimated that approximately 380 tons of sediment finer than 2 mm were stored on the streambed surface (Appendix IV-A). This mass of sediment represents approximately two-year's worth of sediment yield as estimated by STJ-EROS. The presence of this significant amount of sediment just two months after flow rates up to 4.3 cm hr^{-1} were recorded on the Main Fish Bay Gut seems to contradict the high suspended sediment transport capacity estimated for this gut (Appendix IV-A). We postulate that the reason for the large amount of fine sediment in storage is because runoff rates capable of transporting sediment did not last for very long prior to the stream survey. This assumption is supported by the fact that between October 1998 and February 2000 runoff rates exceeding $1.0 \text{ m}^3 \text{ s}^{-1}$ (0.1 cm hr^{-1}) lasted only a total of 17 hours. Therefore, it seems possible that most of the fine sediment that will eventually be transported as suspended sediment still remained in storage along the fluvial network between 1998 and 2001, as flows capable of transporting it did not last long enough to allow this sediment to reach Fish Bay.

Sediment yields predicted by STJ-EROS are within the same order of magnitude as those measured in previous studies on St. John (Table 6). Direct comparisons are confounded by differences in methodology, spatial scale (Walling, 1983), and temporal scales (Kirchner et al., 2001). The sediment yield rates estimated by STJ-EROS for current conditions are 25-50% lower than bay sedimentation rates measured over two years with sediment traps at the bottom of Lameshur Bay and 10-70% higher than sedimentation rates measured in Fish Bay (Nemeth et al., 2001) (Table 5). Although there are discrepancies between STJ-EROS sediment yield estimates and bay sedimentation rates, the similar order of magnitude is encouraging and supports the validity of the model.

Previous sediment yields estimated over time-scales exceeding 40 years suggest that watershed-scale sediment yield rates for undisturbed basins on St. John range between 7 and 35 tons km⁻² yr⁻¹ (Table 6). These baseline sediment yields are between 1% and 730% of those estimated by STJ-EROS for the three study basins. Sediment yields ranging from 1 to 35 tons km⁻² yr⁻¹ were used as a baseline rate to compare road-related sediment yields estimated by the ROADMOD model for the Lameshur Bay and Fish Bay basins (MacDonald et al., 1997).

ROADMOD estimated sediment yields ranging from 19 to 52 tons km² yr⁻¹ for Lameshur Bay (Table 6). Unpaved roads were responsible for 9.8 tons km² yr⁻¹, or roughly 20-50% of the total sediment yield (Anderson and MacDonald, 1998). STJ-EROS estimated sediment yields ranging from 12-19 tons km⁻² yr⁻¹ into Lameshur Bay (Table 6), or 23-100% of that estimated by ROADMOD. STJ-EROS estimated that unpaved roads contribute a total of 10-16 tons km⁻² yr⁻¹. The disparity in the sediment yield estimates were attributed to differences in baseline sediment yields and discrepancies in the road data layers used by the models. STJ-EROS was applied to 3.2 km of unpaved roads (Table 5). Sediment produced from these roads was delivered to areas that drained into Europa Bay, Little Lameshur Bay, and Greater Lameshur Bay (Figure 4a). In contrast, ROADMOD was applied only to the 1.4 km of roads contributing to the Greater Lameshur Bay.

Current sediment yields into Fish Bay estimated by ROADMOD ranged from 72-104 tons km² yr⁻¹ (Anderson and MacDonald, 1998) (Table 6). STJ-EROS estimated a range of 42-65 tons km² yr⁻¹, or 40-90% of the rates estimated by ROADMOD. The discrepancies in sediment yields are mostly due to differences in the estimation of baseline sediment yields, as those used by ROADMOD are from 14% to 660% of those estimated by STJ-EROS. Even though there are differences in the road data layers used by the models, both were applied to approximately 9 km of unpaved roads. Road-related sediment yield according to ROADMOD was 63 tons km² yr⁻¹. This estimate is only 1.1-1.7 times higher than the 36-57 tons km² yr⁻¹ estimated by STJ-EROS.

The results presented in this study represent one of the few attempts to quantify sediment yields in a dry tropical environment. The sediment yield rates estimated for St. John were up to two orders of magnitude lower than world-wide yields for watersheds with similar drainage areas (Milliman and Syvitski, 1992). None of the data sources in Milliman and Syvitski (1992) depicts a dry tropical climate such as that found on St. John. It is likely that the yield rates reported in the literature are influenced by mass wasting events occurring on steep slopes of small watersheds, whereas this process is generally absent on St. John. Therefore, the sediment yield estimates presented in this study begin to fill a gap in the representation of dry tropical climates in world-wide sediment yield data.

5.6 Conclusions

A GIS-based sediment budget model, STJ-EROS, was developed for use on the island of St. John in the Eastern Caribbean. STJ-EROS estimates annual sediment delivery to the marine environment from unpaved roads and natural sediment sources. While sediment production is estimated by using empirical erosion data and models, sediment delivery is calculated as the product of the estimated sediment production and spatially-variable sediment delivery ratios. The STJ-EROS program code is organized in six input routines and five routines that calculate sediment production and delivery. The six input routines allow the user to adjust variables controlling sediment production and delivery, such as rainfall rates and sediment delivery ratios. The remaining five routines use pre-set erosion rate constants, user-defined variables, and item values stored in nine GIS data layers to calculate watershed scale sediment yields.

The model was applied to three different basins in St. John. Predicted sediment delivery rates under natural conditions are on the order of 9-12 tons yr⁻¹ into Lameshur Bay (2-3 tons km⁻² yr⁻¹), 32-44 tons yr⁻¹ into Fish Bay (5-7 tons km² yr⁻¹), and roughly 1 ton yr⁻¹ into Cinnamon Bay (0.6 tons km⁻² yr⁻¹). These rates are within the range of sediment yields estimated from previous

bay and wetland sedimentation studies on St. John. The results indicated that streambank erosion was generally more important than treethrow and undisturbed hillslopes.

Unpaved roads are responsible for increasing sediment delivery rates by 5-6 times for Lameshur Bay, 7-8 times for Fish Bay, and 24-40 times for Cinnamon Bay. These results agree with previous studies in that the unpaved road network is currently the main source of sediment on St. John.

STJ-EROS sediment yield estimates were 25-50% lower and 10-70% higher than bay sedimentation rates measured at Lameshur Bay and Fish Bay, respectively. Although there are discrepancies between STJ-EROS sediment yield estimates and bay sedimentation rates, the similar order of magnitude is encouraging and supports the validity of the model. STJ-EROS estimated sediment yields were 23-100% and 40-90% of sediment yields estimated by the ROADMOD model for Lameshur Bay and Fish Bay, respectively. The disparity in the sediment yield estimates were attributed to differences in the baseline sediment yields and discrepancies in the road data layers used by the models.

5.7 References Cited

- Acevedo R, Morelock J, Olivieri RA. 1989. Modification of coral reef zonation by terrigenous sediment stress. *Palaios* 4: 92-100.
- Ahmad N, Breckner E. 1974. Soil erosion on three Tobago soils. *Tropical Agriculture (Trinidad)* 51(2): 313-324.
- Anderson DM. 1994. Analysis and modeling of erosion hazards and sediment delivery on St. John, U.S. Virgin Islands, US National Park Service Water Resources Division, Technical Report NPS/NRWRD/NRTR-94-34, Fort Collins, Colorado; 153 p.
- Anderson DM, MacDonald LH. 1998. Modelling road surface sediment production using a vector geographic information system. *Earth Surface Processes and Landforms* 23: 95-107.
- Augustinus PGEF. 1995. Geomorphology and sedimentology of mangroves. In Geomorphology and Sedimentology of Estuaries, Developments in sedimentology series 53: 333-357.
- Bowden MJ, Fischman N, Cook P, Wood J, and Omasta E. 1970. Climate, water balance, and climatic change in the north-west Virgin Islands. Caribbean Research Institute, College of the Virgin Islands, 127 p.
- Bunte K, MacDonald LH. 1999. Scale considerations and the detectability of sedimentary cumulative watersheds effects. NCASI, Technical Bulletin No. 776, 327 p.
- Calversbert RJ. 1970. Climate of Puerto Rico and the U.S. Virgin Islands. Climatography of the United States No. 60-52, US Dept. of Commerce, 29 p.
- DeGraff JV, Bryce R, Jibson RW, Mora S, Rogers CT. 1989. Landslides: Their extent and significance in the Caribbean. In Landslides: Extent and economic significance. Brabb EE, Harrod BL (eds.): 51-80.
- Del Mar-López T, Mitchell T, Scatena FN. 1998. The effect of land use on soil erosion in the Guadiana Watershed in Puerto Rico. *Caribbean Journal of Science* 34(3-4): 298-307.
- Dietrich WE, Dunne T, Humphrey N, Reid L. 1982. Construction of sediment budgets for drainage basins. In, FJ Swanson et al. (eds.), *Sediment Budgets and Routing in Forested Drainage Basins*. US Forest Service General Technical Report PNW-141, Corvallis, OR; 5-23.
- Dietrich WE, Dunne T. 1993. The channel head. In, K Beven and MJ Kirkby (eds.), *Channel network hydrology*, John Wiley and Sons, England.
- Donnelly TW. 1966. Geology of St. Thomas and St. John. *Geological Society of America, Memoir* 98: 85-176.
- Gardner TA, Côte I, Gill J, Grant A, Watkinson A. 2003. Long-term region-wide declines in Caribbean corals. *Science* 301: 958-960.

- Gibney E, Ray G. 1993. Vegetation inventory for proposed road construction of John Head Road, St. John. Unpublished report to D.L. Hamlin Consulting Engineers, Inc. St. Thomas, USVI, 9 p.
- Hernández-Delgado EA. 2001. Enfermedades, competencia por sobrecrecimiento y otras causas de mortalidad en el coral (*Monastrea annularis*). Paper presented at the XXIV Symposium of Natural Resources, Univ. Politécnica, San Juan-Puerto Rico, 16 November 2001.
- Hubbard DK. 1986. Sedimentation as a control of reef development: St. Croix, U.S.V.I. *Coral Reefs* 5: 117-125.
- Hubbard DK. 1987. A general review of sedimentation as it relates to environmental stress in the Virgin Islands Biosphere Reserve and the eastern Caribbean in general. Biosphere Reserve Report no. 20, Virgin Islands Resource Management Cooperative, St. Thomas, 42 p.
- Ice G. 1986. A study of the effectiveness of sediment traps for the collection of sediment from small plot studies. NCASI Technical Bulletin 483, New York, NY, 27 p.
- Jibson, R.W. 1989. Debris flows in southern Puerto Rico. *Geological Society of America, Special Paper* 236: 29-55.
- Kirchner JW, Finkel RC, Riebe CS, Granger DE, Clayton JL, King JG, Megahan WF. 2001. Mountain erosion over 10 yr, 10 k.y., and 10 m.y. time scales. *Geology* 29(7): 591-594.
- Lal R. 1990. Soil Erosion in the Tropics: Principles and Management. McGraw-Hill, New York, NY, 580 p.
- Larsen MC, Parks J. 1997. How wide is a road? The association of roads and mass-wasting in a forested montane environment. *Earth Surface Processes and Landforms* 22: 835-848.
- Larsen MC, Torres-Sánchez AJ. 1998. The frequency and distribution of recent landslides in three montane tropical regions of Puerto Rico. *Geomorphology* 24: 309-331.
- Lawler DM. 1993. The measurement of river bank erosion and lateral channel change: A review. *Earth Surface Processes and Landforms* 18: 777-821.
- Lugo AE, Schmidt R, Brown S. 1981. Tropical forests in the Caribbean. *Ambio* 10: 318-324.
- MacDonald LH, Anderson DM, Dietrich WE. 1997. Paradise threatened: Land use and erosion on St. John, U.S. Virgin Islands. *Environmental Management* 21(6): 851-863.
- MacDonald LH, Sampson RW, Anderson DM. 2001. Runoff and road erosion at the plot and road segment scales, St. John, US Virgin Islands. *Earth Surface Processes and Landforms* 26: 251-272.
- Middleton G. 1976. Hydraulic interpretation of sand size distributions. *Journal of Geology* 84: 405-426.
- Milliman JD, Syvitski JPM. 1992. Geomorphic/tectonic control of sediment discharge to the ocean: The importance of small mountainous rivers. *Journal of Geology* 100: 525-544.

- McGregor DF. 1988. An investigation of soil status and landuse on a steeply sloping hillside, Blue Mountains, Jamaica. *Singapore Journal of Tropical Geography* 9(1): 60-71.
- Nemeth RS, MacDonald LH, Ramos-Scharrón CE. 2001. Delivery, deposition, and effects of land-based sediments on corals in St. John, U.S. Virgin Islands. Water Resources Research Institute-University of the Virgin Islands, St. Thomas, Report on Project No. VI99-2, 24 p.
- Nemeth RS, Nowlis JS. 2001. Monitoring the effects of land development on the near-shore marine environment of St. Thomas, USVI. *Bulletin of Marine Science* 69(2): 759-775.
- Nichols MN, Brush GS. 1988. Man's long-term impact on sedimentation: Evidence from salt pond deposits. Biosphere Reserve Research Rep. No. 23, Virgin Islands Resource Management Cooperative, St. Thomas, 26 p.
- Radke J. 1997. Detecting potential erosion threats to the coastal zone: St. John, USVI. *Marine Geodesy* 20: 235-254.
- Ramsarran C. 1992. Simulation of the effects of urbanization on soil loss and runoff from a small tropical watershed using the ANSWERS model. MS thesis, Colorado State University, Fort Collins, CO, 119 p.
- Rankin DW. 2002. Geology of St. John, U.S. Virgin Islands. U.S. Geological Survey professional paper 1631, 36 p.
- Reid LM. 1981. Sediment production from gravel-surfaced roads, Clearwater Basin, Washington. University of Washington Fisheries Research Institute, Seattle, WA. Pub. FRI-UW-8108, 301 p.
- Reid LM, Dunne T. 1996. Rapid evaluation of sediment budgets. Reiskirchen, Germany: Catena Verlag, 164 p.
- Robichaud PR, Brown RE. 2002. Silt fences: An economical technique for measuring hillslope soil erosion. General Technical Report RMRS-GTR-94, Fort Collins, CO: US Forest Service, Rocky Mountain Research Station, 24 p.
- Rogers CS 1990. Responses of coral reefs and reef organisms to sedimentation. *Marine Ecology Progress Series* 62: 185-202.
- Rogers CS. 1992. An integrated approach to marine and terrestrial research in Virgin Islands National Park and Biosphere Reserve. *Park Science* 12(2): 1,27.
- Rogers CS. 1998. Coral reefs of the U.S. Virgin Islands. In: Status and Trends of the Nation's Biological Resources, Vol. I. P. Haeker & P.D. Doran (eds.). U.S. Department of the Interior, U.S. Geological Survey, Reston, VA, pp. 322-324.
- Rogers CS, Teytaud R. 1988. Marine and terrestrial ecosystems of the Virgin Islands National Park and Biosphere Reserve: St. Thomas, U.S. Virgin Islands: Washington, D.C., USDA, Natural Resources Conservation Service.

- Sampson RW. 2000. Road runoff and erosion at the plot and road segment scales on St John US Virgin Islands. MS thesis, Department of Earth Resources, Colorado State University, Fort Collins, 189 p.
- Smith RM, Abruña F. 1955. Soil and water conservation research in Puerto Rico, 1938 to 1947. Bulletin no. 124, Univ. of Puerto Rico Agricultural Experiment Station, Rio Piedras, PR, 51 p.
- Soil Conservation Service. 1970. Soil Survey, Virgin Islands of the United States. 78 p.
- Swanson FJ, Fredriksen RL. 1982. Sediment routing and budgets: Implications for judging impacts of forestry practices. In, F.J. Swanson et al., eds., *Sediment Budgets and Routing in Forested Drainage Basins*. US Forest Service General Technical Report PNW-141, Corvallis, OR; 129-137.
- Torres J. 2001. Impacts of sedimentation on the growth rates of *Montastraea annularis* in Southwest Puerto Rico. *Bulletin of Marine Science* 69(2): 631-637.
- Torres R, Chiappone M, Geraldles F, Rodríguez Y, Vega M. 2001. Sedimentation as an important environmental influence on Dominican Republic reefs. *Bulletin of Marine Science* 69(2): 805-818.
- Tyson GF. 1987. Historic land use in the Reef Bay, Fish Bay and Hawknest Bay watersheds, St. John, US Virgin Islands, 1718-1950. Virgin Islands Resource Management Cooperative, Biosphere Reserve Report No. 19; 54 p.
- UNEP. 1994. Regional overview of land-based sources of pollution in the Wider Caribbean Region. CEP-Technical Report No. 33; 56 p.
- USDA. 1995. Classification and Correlation of the Soils of the Virgin Islands of the United States. US Department of Agriculture: Hato Rey, Puerto Rico.
- U.S. Army, Corps of Engineers. 1975. Flood plain information-Tidal areas. St. Thomas, St. Croix, and St. John, U.S. Virgin Islands.
- Walling DE. 1983. The sediment delivery problem. *Journal of Hydrology* 65: 209-237.
- Walling DE. 1997. The response of sediment yields to environmental change. In *Human Impact on Erosion and Sedimentation*. IAHS Publication 245: 77-89.
- Woodbury RO, Weaver PL. 1987. The vegetation of St. John and Hassel Island, USVI. National Park Service, Southeast Region, Research/Resources Management Report SER-83, Atlanta, GA, 26 p.

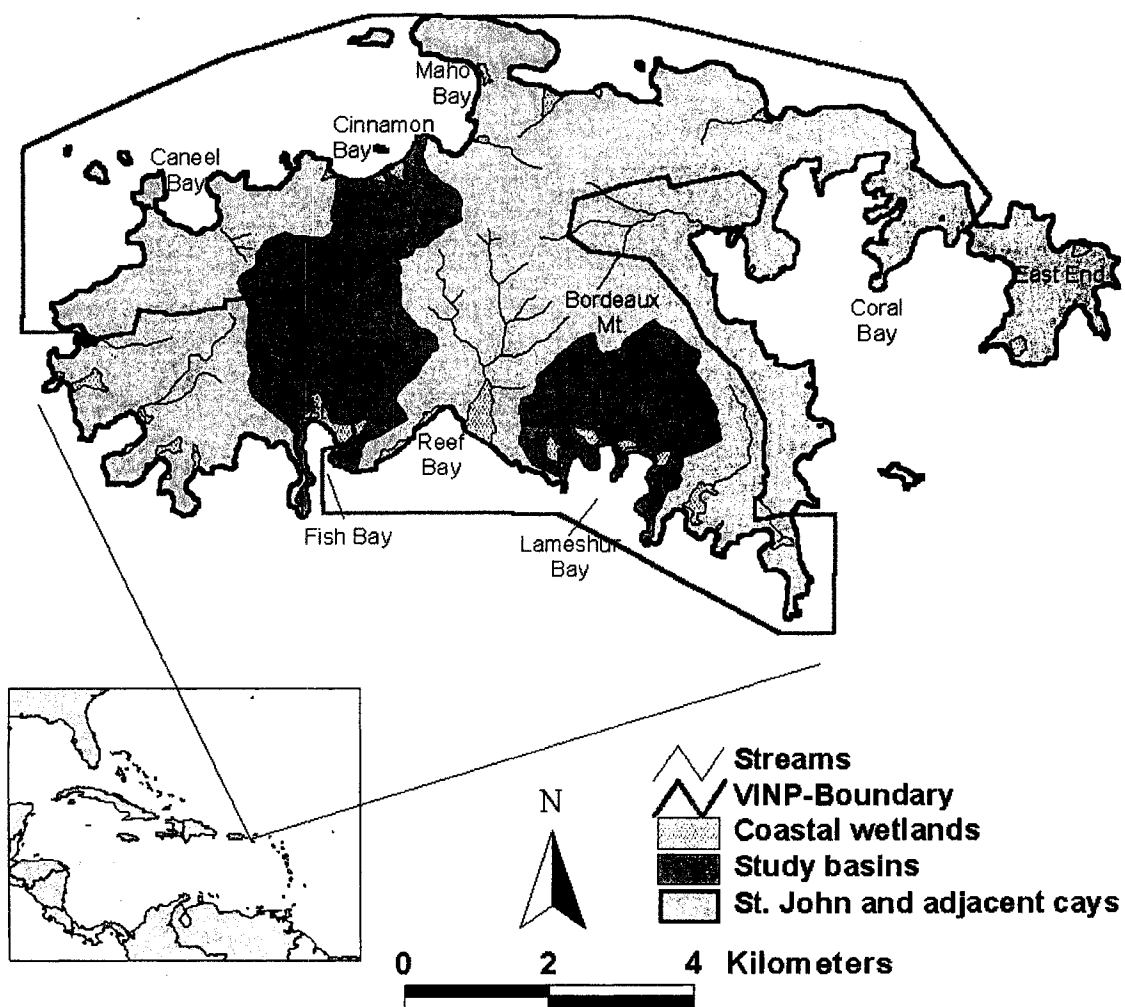


Figure 1. Map of St. John showing the location of the VINP boundary and study basins.

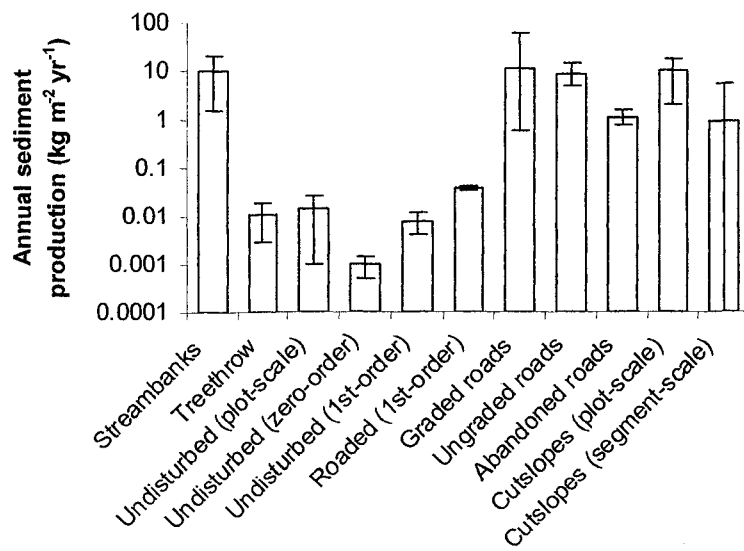
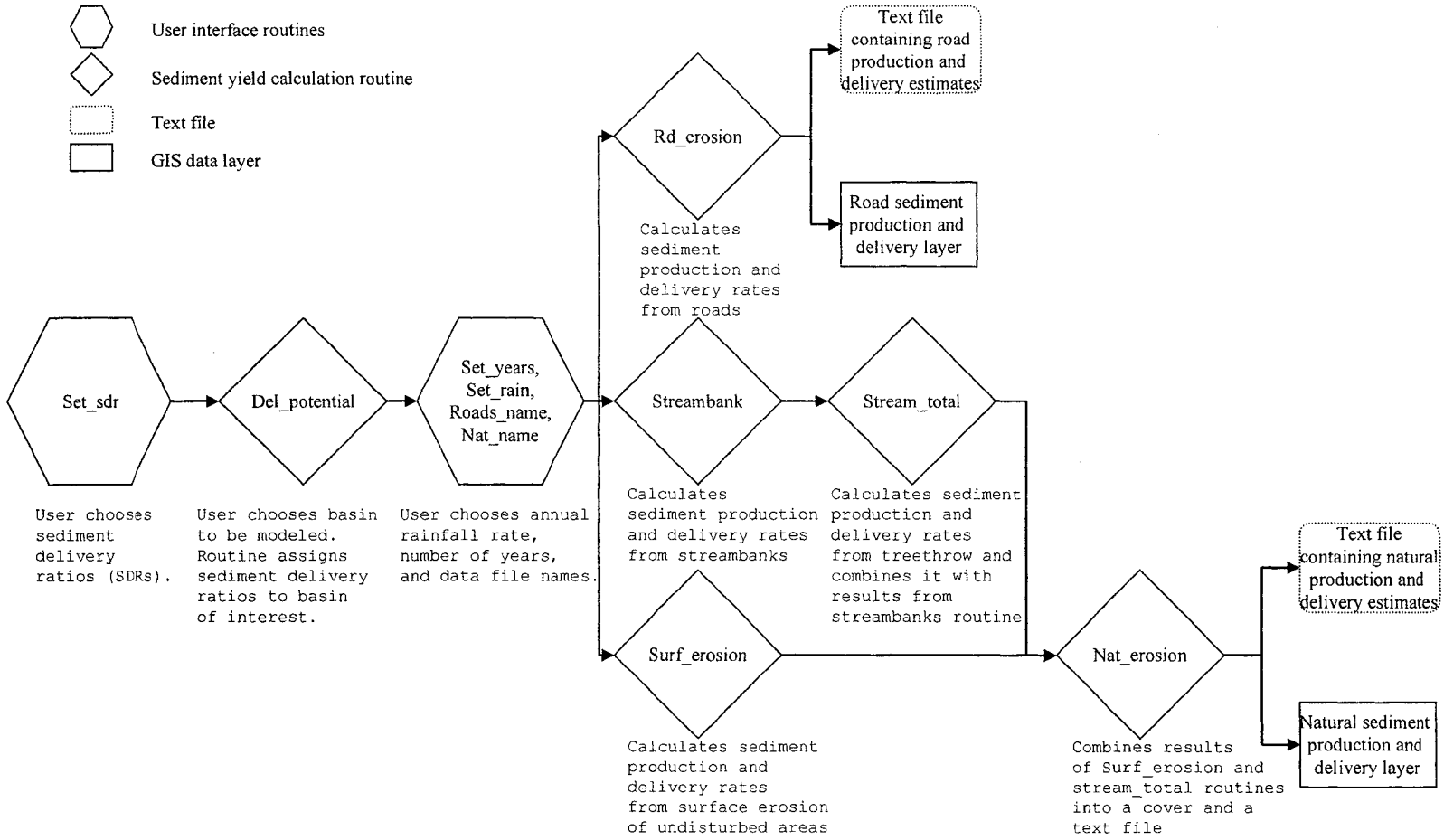


Figure 2. Annual sediment production rates from natural and anthropogenic sediment sources on St. John. Columns show average values, and bars indicate the range of values.

Figure 3. Flowchart of the STJ-EROS model.



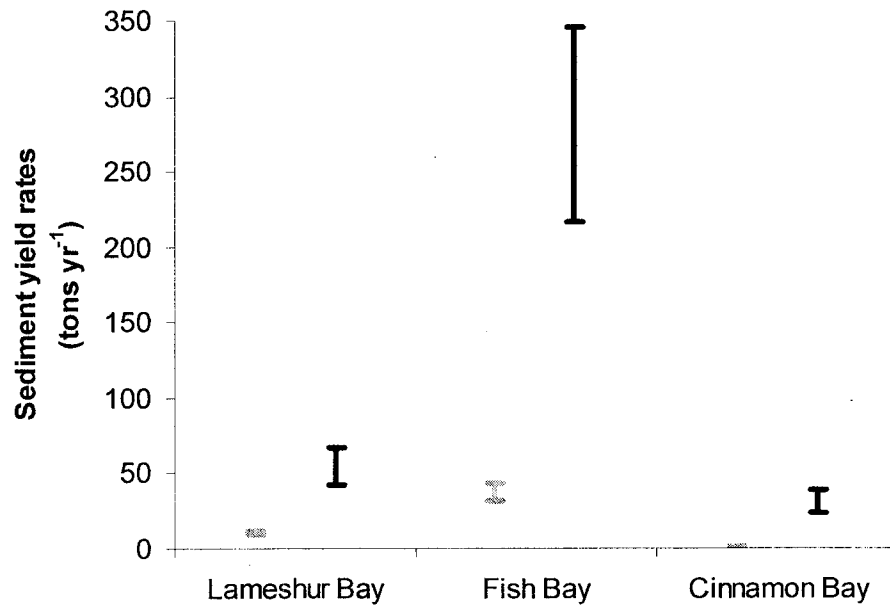


Figure 4. Calculated sediment yields for the Lameshur Bay, Fish Bay, and Cinnamon Bay basins. Gray bars are for natural sources and those in black are for unpaved roads. The lower values are for sediment finer than 2 mm and the higher values are for all sediment sizes from clays to coarse gravel (32 mm).

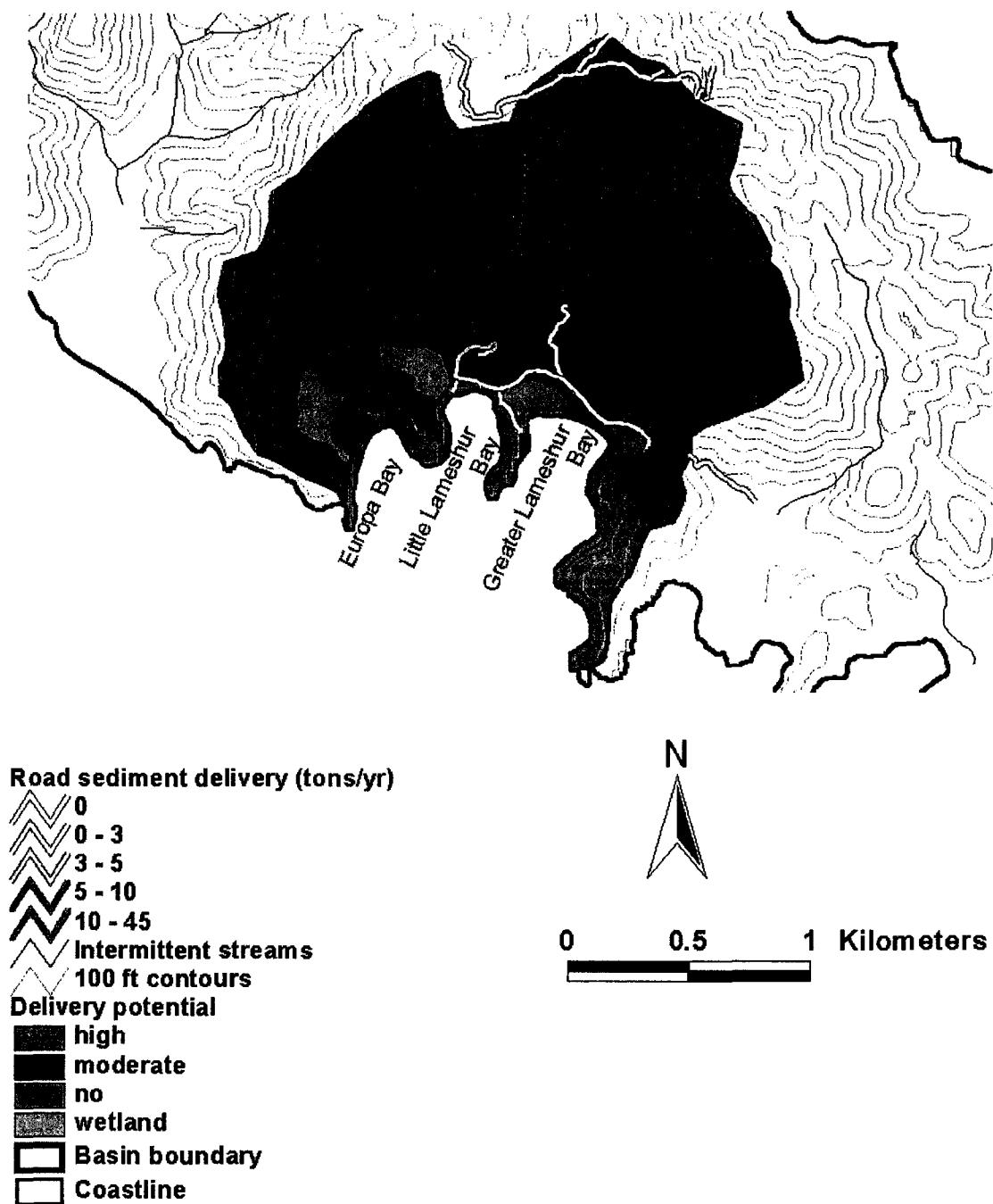


Figure 5a. Map of road segments and hillslopes in the Lameshur Bay basin classified by sediment delivery rates and sediment delivery potential, respectively.

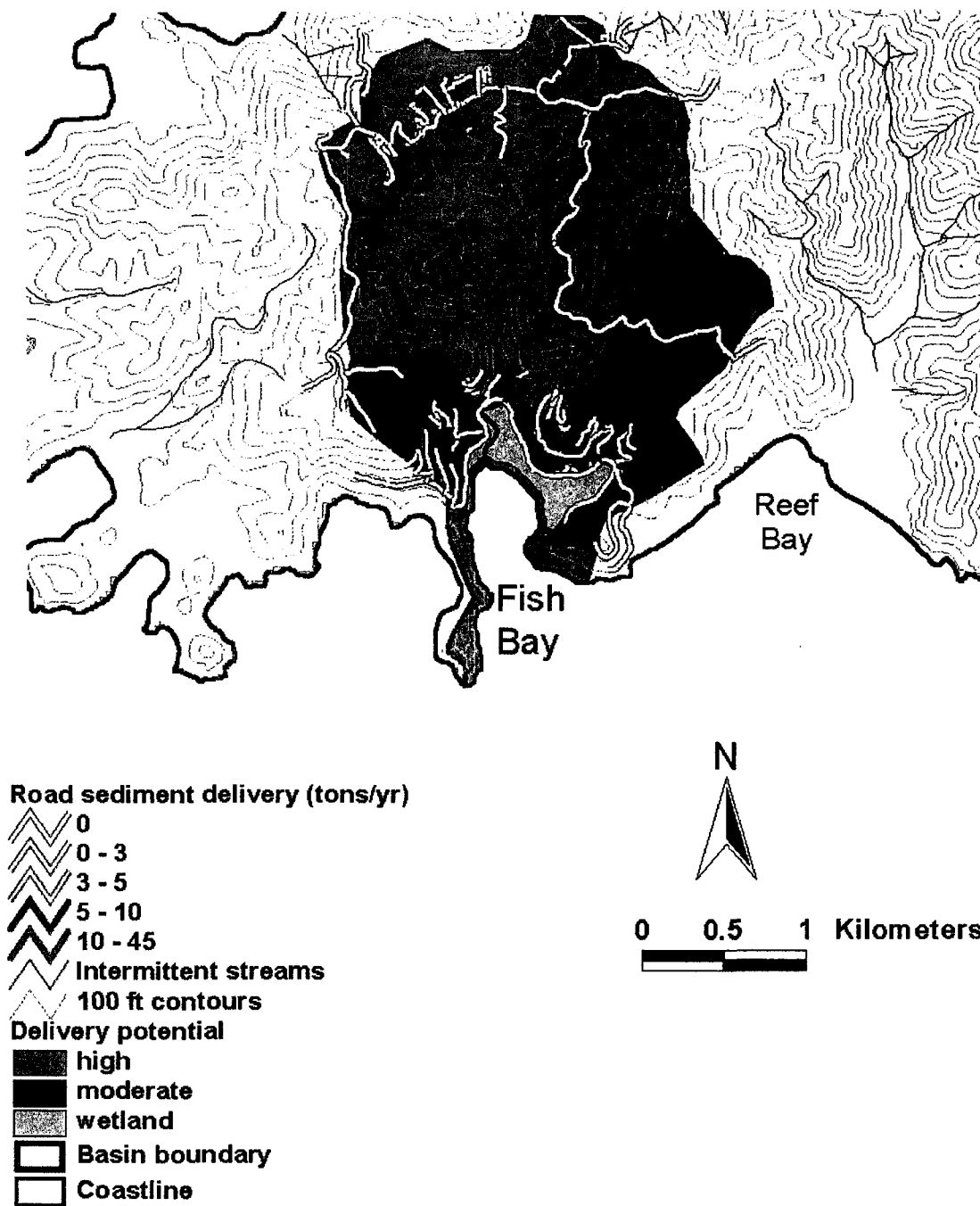


Figure 5b. Map of road segments and hillslopes in the Fish Bay basin classified by sediment delivery rates and sediment delivery potential, respectively.

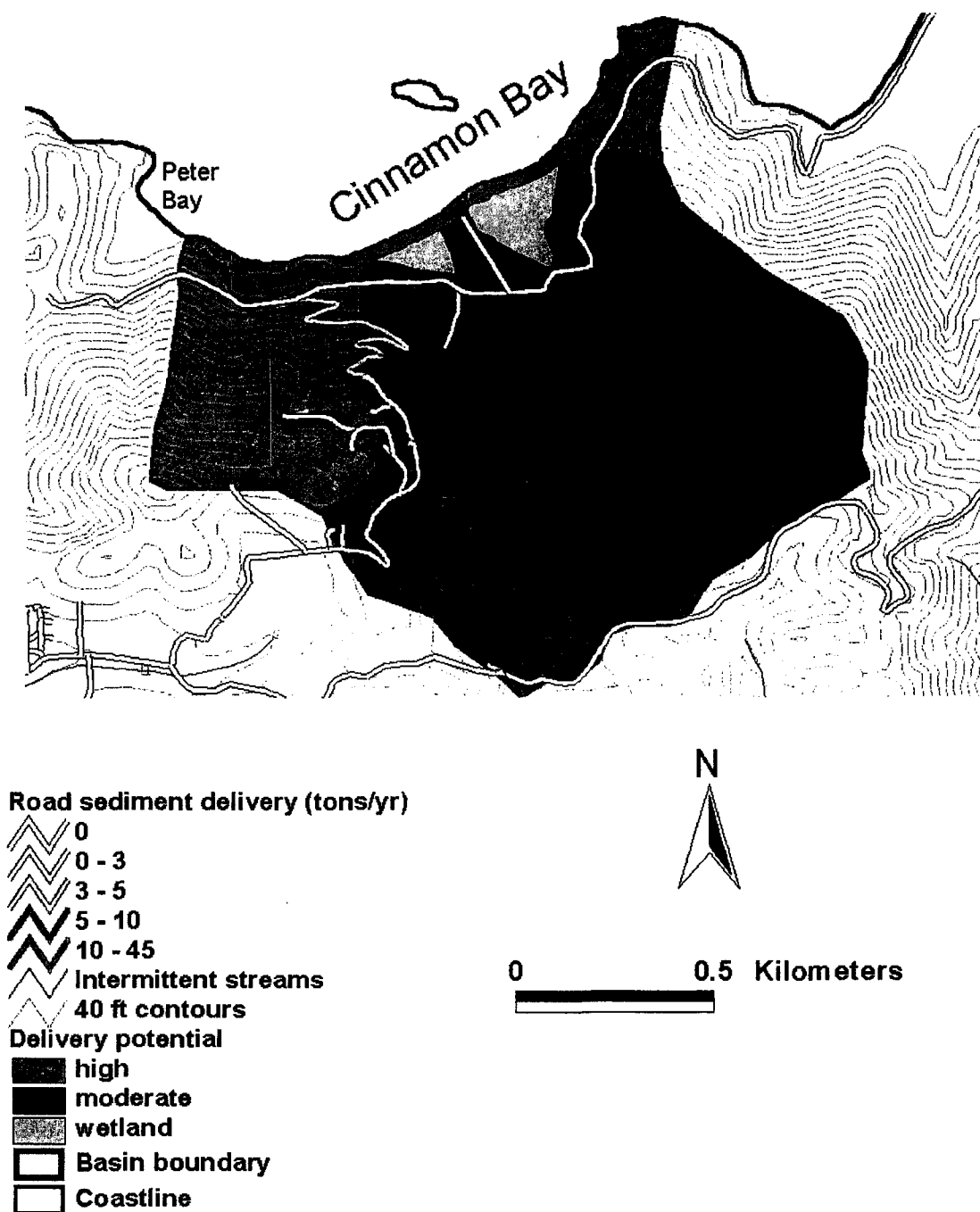


Figure 5c. Map of road segments and hillslopes in the Cinnamon Bay basin classified by sediment delivery rates and sediment delivery potential, respectively.

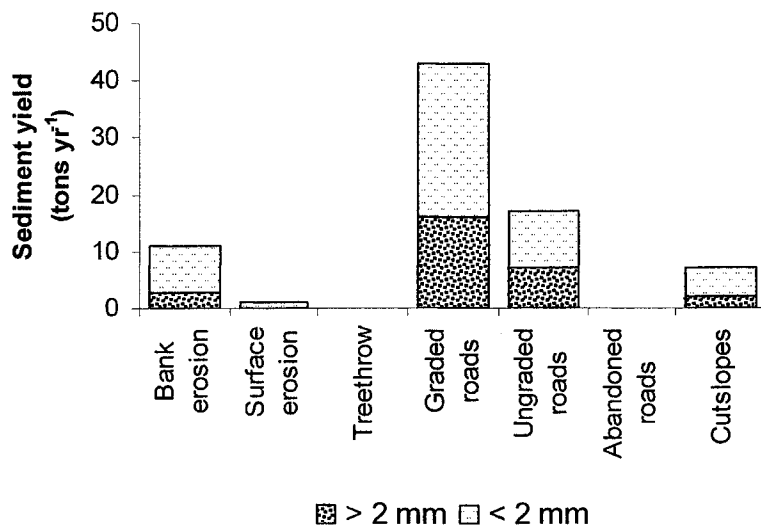


Figure 6a. Predicted contribution of different sediment sources by particle-size class for the Lameshur Bay basin.

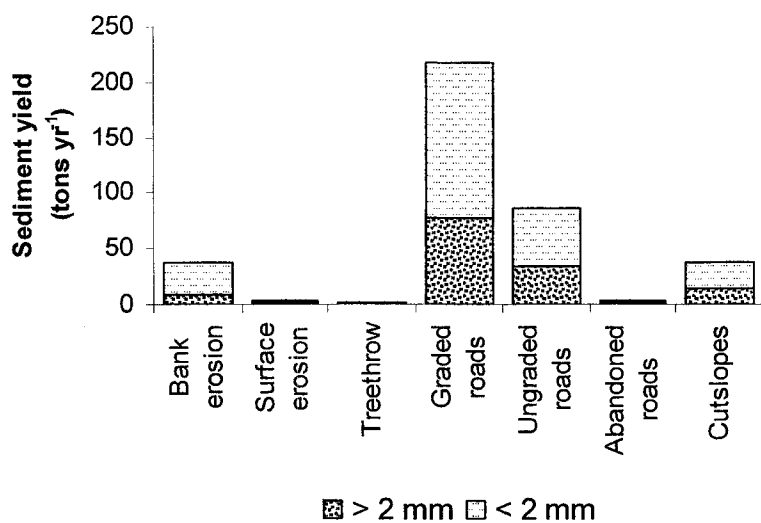


Figure 6b. Predicted contribution of different sediment sources by particle-size class for the Fish Bay basin.

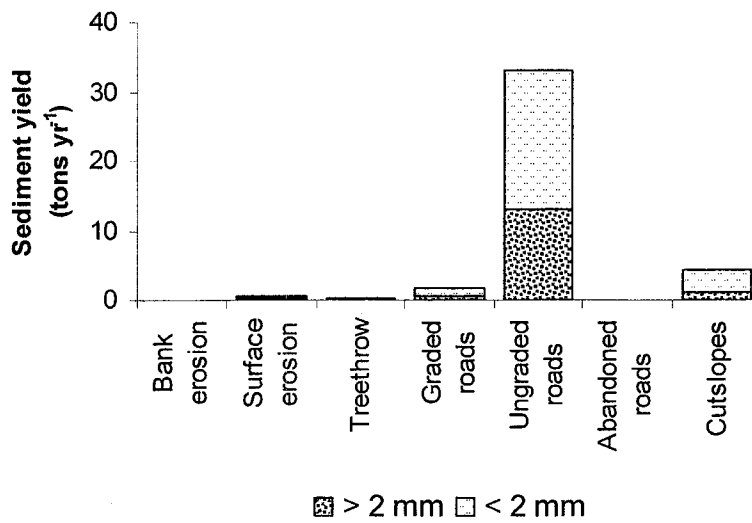


Figure 6c. Predicted contribution of different sediment sources by particle-size class for the Cinnamon Bay basin.

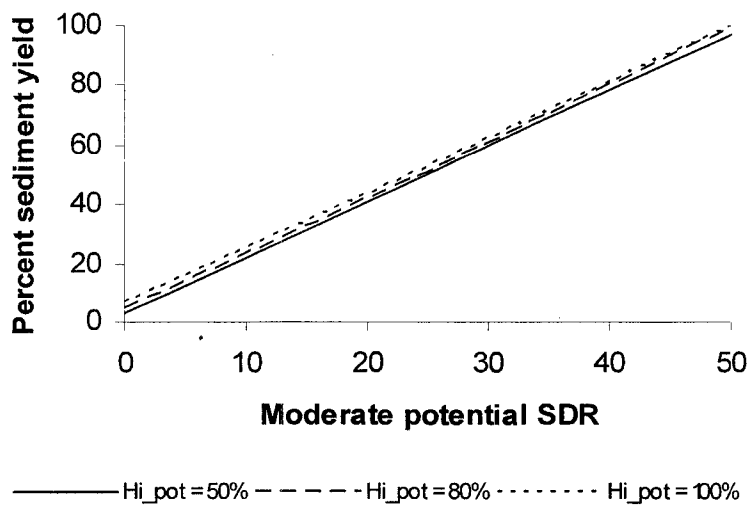


Figure 7a. Changes in percent sediment yield with varying sediment delivery ratios for the Lameshur Bay basin. One-hundred percent refers to sediment yields estimated using sediment delivery ratios of 50 and 100% for areas with moderate and high sediment delivery potential, respectively.

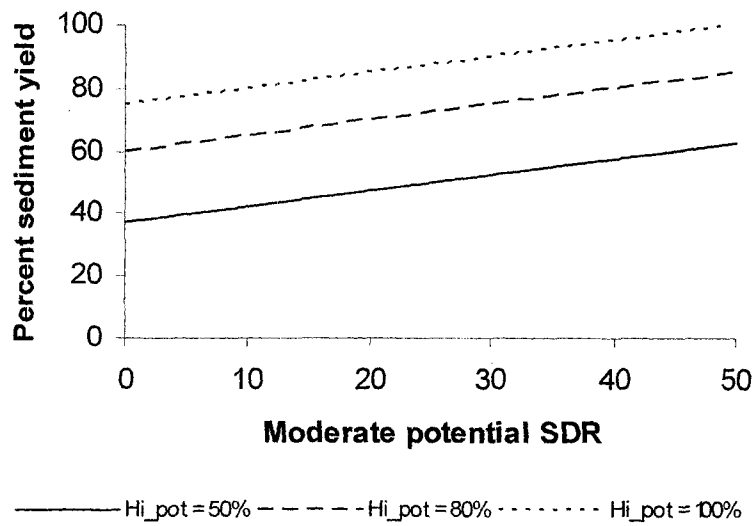


Figure 7b. Changes in percent sediment yield with varying sediment delivery ratios for the Fish Bay basin. One-hundred percent refers to sediment yields estimated using sediment delivery ratios of 50 and 100% for areas with moderate and high sediment delivery potential, respectively.

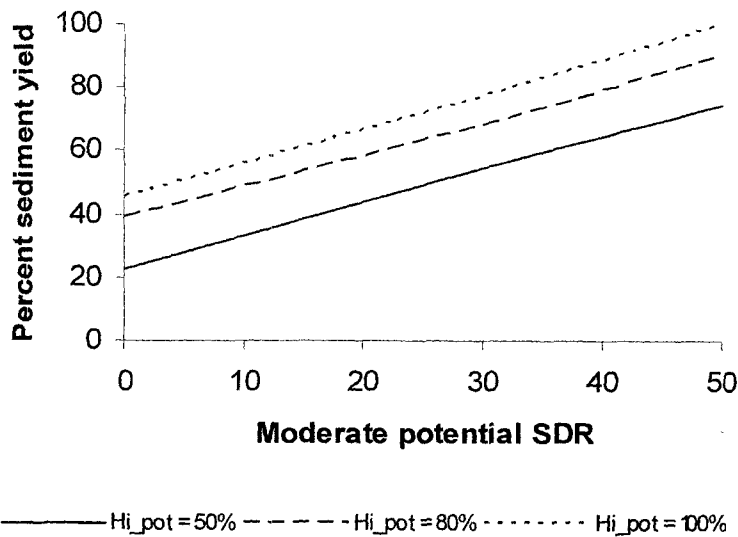


Figure 7c. Changes in percent sediment yield with varying sediment delivery ratios for the Cinnamon Bay basin. One-hundred percent refers to sediment yields estimated using sediment delivery ratios of 50 and 100% for areas with moderate and high sediment delivery potential, respectively.

Table 1. Sediment production functions used in STJ-EROS.

Sediment source	Annual erosion rate (kg m ⁻² yr ⁻¹)	Sediment production function
Streambank	10	[10] * 2 * <i>channel length w. erodible banks</i> * <i>bank height</i> * time
Treethrow	0.01 [0.17 kg m ⁻¹ yr ⁻¹]	[0.17] * <i>channel length</i> * time
Undisturbed hillslopes	0.001	[6.4 x 10 ⁻⁵] * 14% rainfall * <i>area</i> * { 1 + 9 * 0.004 ^A }
Graded roads	0.1 – 52 (slopes from 1 to 21%)	[-0.432 + 4.73 * slope ^{1.5} * rainfall] * <i>road length</i> * <i>width</i> * { 1 + 9 * 0.06 ^A }
Ungraded roads	0.0 – 20 (slopes from 1 to 21%)	[-0.432 + 1.88 * slope ^{1.5} * rainfall] * <i>road length</i> * <i>width</i> * { 1 + 9 * 0.04 ^A }
Abandoned roads	0.08 – 1.7 (slopes from 1 to 21%)	[0.071] * slope * rainfall * <i>road length</i> * <i>width</i> * { 1 + 9 * 0.001 ^A }
Cutslopes	0.0 – 5.7	[0.09] * road segment sediment production

Sediment production is in kg, all lengths, widths, and heights are in meters, time is in years, slope is in percent, area is in m², and rainfall is in centimeters.

Empirical sediment production functions are in square brackets; corrections for the loss of silt-sized particles are between {}. Items in italics are taken from GIS data layers, and rainfall equals the product of the user-defined annual rainfall rate and time in years.

Road surface erosion accounts for 91% of the sediment yield from road segments, and cutslopes account for the remaining 9%.

^ARefers to the percent of silt from Table 4.

Table 2a. Variables and GIS data layers used by the six input routines in STJ-EROS.

Routine	Required pre-defined variable(s)	New variable(s) created	Required input layer(s)	New GIS data layer(s) created
Set_sdr	None	<u>Hi_pot</u> - The user-defined sediment delivery ratio (SDR) for areas with high delivery potential. Range of accepted values: 50-100%. <u>Mod_pot</u> - The user defined SDR for areas with moderate delivery potential. Range of accepted values: 0-50%.	None	None
Del_potential	<u>Hi_pot</u> , <u>mod_pot</u>	<u>Basin</u> - The name of the basin chosen by the user for analyses.	<u>BASIN_BD</u> , <u>SED_DEL</u>	<u>DEL_BD</u> - Contains the SDR values for the sediment delivery potential areas in <u>basin</u> .
Set_years	None	<u>Years</u> - The user-defined number of years for which sediment yield is to be estimated. Range of accepted values: 1-50 years.	None	None
Set_rain	<u>Years</u>	<u>Rain_rate</u> -The user-defined annual rainfall rate. Range of accepted values: 70-160 cm yr ⁻¹ . <u>Rain</u> -Total rainfall in cm calculated as the product of <u>rain_rate</u> and <u>years</u> .	None	None
Roads_name	<u>Basin</u>	<u>Road_name</u> *-The user-defined name of the layer containing road-related sediment yield estimates.	None	None
Nat_name	<u>Basin</u>	<u>Nat_name</u> *-The user-defined name of the layer containing sediment yield estimates from natural sources.	None	None

Underlined names indicate variables with values established by the user. Names in italics refer to variables with constant values established in the program code or those that are automatically calculated. Names in small caps indicate GIS data layer names.

* Alpha-numerical names cannot exceed 8 characters in length.

Table 2b. Variables and GIS data layers used by five routines in STJ-EROS used to calculate sediment yields.

Routine	Required pre-defined variable(s)	New variable(s) created	Required input layer(s)	New GIS data layer(s) created
Rd_erosion	<u>Basin</u> , <u>years</u> , <u>road_name</u> , <u>rain</u> , <i>silt_loss^A</i> , <i>silt_u_rd_fr^B</i> , <i>silt_g_rd_fr^B</i> , <i>silt_a_rd_fr^B</i> , <i>un_sus_fr^C</i> , <i>gr_sus_fr^C</i> , <i>ab_sus_fr^C</i>	None	GPS_DRA, <u>BASIN_BD</u> , GPS_RDS, DEL_BD	<u>ROAD_NAME</u> - A line layer containing road-related sediment yield estimates.
Streambank	<u>Years</u> , <u>bank_er</u> , <u>bank_sus_fr^C</u>	None	BANKS, DEL_BD	<u>BANK_DEL</u> - A polygon layer containing streambank sediment yield estimates.
Stream_total	<u>Years</u> , <u>treethrow</u> , <u>tree_sus_fr^C</u>	None	STJ_STR, DEL_BD, <u>BANK_DEL</u>	<u>STR_DEL</u> - A polygon layer containing streambank and treethrow sediment yield estimates.
Surf_er	<u>Years</u> , <u>undisturbed</u> , <u>rain</u> , <i>silt_loss^A</i> , <i>silt_se_fr^B</i> , <i>se_sus_fr^C</i>	None	STJ_BD, DEL_BD, <u>BASIN_BD</u>	<u>SE_BD</u> - A polygon layer containing sediment yield estimates for undisturbed hillslopes.
Nat_erosion	<u>Years</u>	None	<u>SE_BD</u> , <u>STR_DEL</u>	<u>NAT_NAME</u> - A polygon layer containing streambank, treethrow, and undisturbed hillslope sediment yield estimates.

Underlined names indicate variables with values established by the user. Names in italics refer to variables with constant values established in the program code or those that are automatically calculated. Names in small caps indicate GIS data layer names.

^A Refers to the ratio of actual sediment production rates to that measured from sediment traps for the silt-size sediment fraction (Chapter 3).

^B Refers to the silt fraction from ungraded roads (u), graded roads (g), abandoned roads (a), and undisturbed hillslopes (se) from Table 4.

^C Refers to the sediment believed to be transported as suspended load by streams in St. John. It is estimated as the sum of the sand, silt, and clay fractions for ungraded roads (un), graded roads (gr), abandoned roads (ab), streambanks (bank), treethrow (tree), and undisturbed hillslopes (se) from Table 4.

Table 3. Description of the nine input layers used by STJ-EROS.

Data layer	Type	Description	Key items	Routine(s) using data layer
SED_DEL	Polygon	Sediment delivery potential areas	<i>Potential</i> -Qualitative classifies sediment delivery potential into three types: no, moderate/wetlands, high	Del_potential
CB_BD	Polygon	Boundaries of the Cinnamon Bay basin	None	Del_potential, rd_erosion, and surf_er
FB_BD	Polygon	Boundaries of the Fish Bay basin	None	Del_potential, rd_erosion, and surf_er
LB_BD	Polygon	Boundaries of the Lameshur Bay basin	None	Del_potential, rd_erosion, and surf_er
GPS_DRA	Point	Road drainage structures	<i>Drain_id</i> - Identification code used to link individual road segments in GPS_RDS to their respective drainage structures.	Rd_erosion
GPS_RDS	Line	Roads	<i>Drain_id</i> - Identification code used to link individual drainage structures in GPS_DRA to their respective road segments. <i>Surface</i> -Describes whether the road segment is paved or unpaved. <i>Length_m</i> and <i>width_m</i> -Road segment length and width in meters. <i>Slope</i> - Road segment slope in percent. <i>Grading</i> -Defines road grading type: graded, ungraded, or abandoned.	Rd_erosion
BANKS	Polygon	Streambanks	<i>Bank_ht_m</i> - Bank height in meters.	Streambank
STJ_STR	Line	Streams	<i>Length</i> - Length of stream segments in meters.	Stream_total
STJ_BD	Polygon	Coastal boundaries	None	Surf_er

Names in italics are for item names in GIS data layers.

Table 4. Proportion of sediment by particle-size class for different sediment sources on St. John.

Sediment source (source of size distribution estimate)	Gravel (%) (> 2mm)	Sand (%) (0.062-2 mm)	Silt and clay (%) (< 0.062 mm)
Streambanks (Nichols & Brush, 1988)	25	25	50
Treethrow (USDA, 1995)	25	25	50
Undisturbed hillslopes (Chapter 4)*	42	57	0.4 (0.4)
Graded roads (Chapter 2)*	35	58	7 (6)
Ungraded roads (Chapter 2)*	41	53	6 (4)
Abandoned roads (Chapter 2)*	73	27	0.1 (0.1)

*Size distribution for these sources were from analyzing samples of the material collected in sediment fences. Values in parentheses are the proportion of silt (0.004-0.062 mm)

The sediment from cutslopes is assumed to have the same particle-size distribution as the sediment from the road surface.

Table 5. Characteristics of the three basins where STJ-EROS was applied.

Basin	Basin area (km ²)	No delivery potential (% of basin)	Wetland (% of basin)	Moderate delivery potential (% of basin)	High delivery potential (% of basin)	Length of fluvial network (km)	Percent streams with erodible banks	Length of paved roads (km)	Length of unpaved roads (km)	Graded roads (% of unpaved)	Ungraded roads (% of unpaved)	Abandoned roads (% of unpaved)
Lameshur Bay	4.28	24	4	64	8	6.45	41	0.11	3.2	9	84	7
Fish Bay	6.01	0	3	29	68	12.7	41	9.5	9.2	42	32	26
Cinnamon Bay	1.58	0	2	74	23	4.11	0	3.6	1.6	4	96	0

Table 6. Comparison of sediment yield values from St. John.

Reference	Location	Time scale (years)	Spatial scale (km ²)	Undisturbed sediment yields (tons km ⁻² yr ⁻¹) [tons yr ⁻¹]	Sediment yield disturbed conditions (tons km ⁻² yr ⁻¹) [tons yr ⁻¹]
<i>WATERSHED-SCALE SUSPENDED SEDIMENT YIELDS</i>					
Appendix IV-E	Main Fish Bay Gut	3	3.5	--	18 [65]
<i>BAY SEDIMENTATION RATES</i>					
Nemeth et al. (2001)	Great Lameshur Bay	2	2.3	--	24 [55]
Nemeth et al. (2001)	Fish Bay	2	6.0	--	36 [216]
Anderson (1994)	Fish Bay	~3,000	6.0	35 [210]	--
<i>WETLAND SEDIMENTATION RATES</i>					
Nichols and Brush (1988)	Mandal Pond	~3,000	1.33	29 [39]	--
Nichols and Brush (1988)	Reef Bay swamp	~3,000	5.63	8 [45]	--
Anderson (1994)	Lameshur Bay Gut detention pond	~40	0.97	7-10 [7-10]	--
<i>MODEL APPLICATIONS</i>					
ROADMOD (Anderson and MacDonald, 1998)	Lameshur Bay	n/a	4.3	--	19 – 52 [84 – 220]
ROADMOD (Anderson and MacDonald, 1998)	Fish Bay	n/a	6.0	--	72 – 104 [440 – 630]
STJ-EROS (This study)	Lameshur Bay	10	4.3	2.0 – 2.8 [9 – 12]	12 – 19 [50 – 80]
STJ-EROS (This study)	Fish Bay	10	6.0	5.3 – 7.3 [32 – 44]	42 – 65 [250 – 390]
STJ-EROS (This study)	Cinnamon Bay	10	1.6	0.4 – 0.6 [0.6 – 1.0]	15 – 25 [24 – 40]

CHAPTER 6.

CONCLUSIONS, FUTURE RESEARCH, AND MANAGEMENT RECOMMENDATIONS

6.1 Runoff generation from hillslope plots and roads

Runoff volumes were measured from three 40 m² plots on undisturbed planar hillslopes and runoff rates were measured from a 230-m long, partially-paved road segment. The undisturbed hillslopes only generated runoff from precipitation events with at least 2.5-3.0 cm of rainfall (Figure 1; Chapter 4). In contrast, only 0.3 cm of rainfall generated runoff from the unpaved road segment (Chapter 3). The low runoff coefficients for the undisturbed hillslopes show that runoff represented less than 10% of the total rainfall, at least for the smaller storm events where all the runoff was captured. The runoff coefficients from the road segment often exceeded 10% and were as high as 70% for storms with at least 2 cm of rainfall (Figure 1).

Storm precipitation is a major control on the amount of runoff from undisturbed areas, but the amount of runoff varies among storm events with similar rainfall totals. The predictability of runoff volumes was improved when storm rainfall (P) was combined with an antecedent precipitation index (API). Runoff was generated from the hillslope plots only when storm precipitation exceeded 2.5-3.0 cm and the sum of P and API was at least 5 cm. Runoff from the road segment was strongly correlated with total precipitation regardless of the antecedent conditions.

These differences in the initiation and amount of runoff help explain the observed differences in sediment production. First, the amount of precipitation needed to initiate surface runoff from roads is at least an order of magnitude less than for planar hillslopes, and this greatly

increases the frequency of surface runoff. Second, the higher flows on the road segment greatly increase the shear stress on the relatively erodible road surface.

Precipitation and runoff rate data from the partially-paved road were used to develop, calibrate, and validate two runoff models (Chapter 3). The first model (GA-UH) predicted runoff using the Green-Ampt infiltration equation and an empirically-derived unit hydrograph. The second model (GA-KW) used the Green-Ampt infiltration equation to calculate precipitation excess and a kinematic wave to route the resulting runoff. Model development and calibration were based on eight runoff events and yielded parameter sets with physically realistic values.

The two runoff models were validated by comparing predicted and measured hydrographs for 18 storms. Predicted hydrographs from the two models were very similar, but the GA-KW model performed slightly better than the GA-UH model. Both models predicted no runoff for most events with less than 0.7 cm of rainfall, and tended to underestimate peak flows. The absolute errors in predicted discharge did not increase with increasing storm size. Much of the error in estimating storm runoff was attributed to the difficulty of predicting the initial infiltration rate.

6.2 Measuring and predicting sediment production and delivery

A sediment budget provided the conceptual framework for measuring and modeling sediment production from both natural and anthropogenic sources on St. John. Estimated annual erosion rates at the plot, hillslope, and road-segment scale ranged over five orders of magnitude (Chapter 4). Mean sediment production rates from undisturbed areas were $27 \text{ g m}^{-2} \text{ yr}^{-1}$ at the plot scale, $0.5 \text{ g m}^{-2} \text{ yr}^{-1}$ at the zero-order catchment scale, and $8 \text{ g m}^{-2} \text{ yr}^{-1}$ for first-order catchments (Figure 2). The highest erosion rate for natural sediment sources was $10 \text{ kg m}^{-2} \text{ yr}^{-1}$ for streambank erosion. The uprooting of trees along stream margins was estimated to deliver 0.17 tons per kilometer of stream length per year, or $11 \text{ g m}^{-2} \text{ yr}^{-1}$ for a 15-m wide stream corridor.

Differences in the magnitude of sediment yields for undisturbed catchments are attributed in part to the scale at which the rates were measured or predicted. For example, the drop in sediment yields from the undisturbed plot ($0.027\text{-}0.77\text{ g m}^{-2}\text{ yr}^{-1}$) to the zero-order scale ($0.010\text{-}0.085\text{ g m}^{-2}\text{ yr}^{-1}$) stems in part from the higher potential for sediment storage on zero-order catchments relative to 40 m^2 plots. The addition of streambank and treethrow erosion appears to account for the higher sediment yields from first-order catchments relative to zero-order catchments.

Sediment production from 21 unpaved road segments with varying contributing areas, slopes, and traffic loads was measured with sediment traps over the two-year study period. The mean sediment production rate from these road segments was 0.064 kg m^{-2} per centimeter of precipitation. Sediment production was related to total precipitation and to road segment slope. Sediment production rates for roads that had been graded within the last two years ranged from 0.57 to $58\text{ kg m}^{-2}\text{ yr}^{-1}$ (Figure 2), depending on slope. Sediment production from ungraded roads ranged from 5.1 to $14\text{ kg m}^{-2}\text{ yr}^{-1}$ for roads with slopes of 10 and 16%, respectively (Figure 2). The mean erosion rate for abandoned roads with a slope of 15% was $1.1\text{ kg m}^{-2}\text{ yr}^{-1}$. Although cutslopes eroded at rates ranging from 2 to $17\text{ kg m}^{-2}\text{ yr}^{-1}$, they were estimated to be responsible for only 9% of sediment measured at the road segment scale.

These annual erosion rates indicate that unpaved roads on St. John produce sediment at a rate that is up to four orders of magnitude higher than undisturbed plots and zero-order catchments. First-order catchments receiving sediment from unpaved roads had a mean sediment yield of $38\text{ g m}^{-2}\text{ yr}^{-1}$, or about five times the rate of comparable undisturbed first-order catchments (Figure 2).

STJ-EROS is an Arc/Info-based system that quantifies watershed-scale sediment yields based on empirically-derived sediment production functions and delivery ratios. Sediment delivery ratios are meant to reflect the retention of sediment by hillslopes, fluvial networks, and coastal wetlands. The STJ-EROS Arc Macro Language program code consists of six input

routines and five routines that calculate sediment production and delivery (Chapter 5). Interfaces for the six input routines allow users to adjust the values of the variables controlling sediment production and delivery (e.g., rainfall rates and sediment delivery ratios). The remaining five routines use pre-set erosion rate constants, user-defined variables, and item values stored in nine input GIS data layers to calculate watershed-scale sediment yields from the combination of streambanks, treethrow, undisturbed hillslopes, unpaved road travelways, and road cutslopes.

Simulations with STJ-EROS indicate that sediment yields for undisturbed conditions would be 2.8 tons km⁻² yr⁻¹ for the Lameshur Bay basin, 7.3 tons km⁻² yr⁻¹ for the Fish Bay basin, and 0.6 tons km⁻² yr⁻¹ for the Cinnamon Bay basin (Figure 2). Estimated sediment yields under current conditions are 19 tons km⁻² yr⁻¹ for the Lameshur Bay basin, 65 tons km⁻² yr⁻¹ for the Fish Bay basin, and 25 tons km⁻² yr⁻¹ for the Cinnamon Bay basin (Figure 2). The latter values are 7-40 times higher than under undisturbed conditions, and in each case unpaved roads were the main source of sediment. The differences in the estimated sediment yields are mostly a response to differences in the amount of unpaved roads in each basin. The modeled sediment yields for undisturbed and current conditions are within the range of sediment yield and bay sedimentation rates measured by previous studies on St. John.

6.3 Recommendations for future research

STJ-EROS is a useful tool for estimating erosion rates and the delivery of sediment to the marine environment. The accuracy of these estimates is limited by the available hydrologic and geomorphic data. One of the most important limitations is the potential underestimate of sediment production rates by the sediment traps used in this study. The analysis in Chapter 3 showed that the sediment traps underestimate sediment production rates because they do not capture all of the silt-sized particles. An accurate estimate of the amount of these particles is important because these particles generally are suspended in the surface runoff and are readily

delivered to the marine environment. A more detailed study is needed to quantify the trap efficiency of the sediment fences for different-sized particles.

The movement of sediment through the fluvial network and coastal wetlands is treated as a black-box in STJ-EROS due to the lack of data on sediment storage and transport rates. Predicted sediment yields are very sensitive to the user-defined sediment delivery ratios (Chapter 5). Additional measurements and theoretical analyses are needed to improve the predictions of land-use changes on watershed-scale sediment yields.

Runoff data for St. John are very limited and this restricts the ability to develop, calibrate, and validate models. Government agencies and researchers should collaborate to develop a long-term program to collect data on runoff and sediment yields at spatial scales ranging from zero-order catchments to the larger watersheds such as Fish Bay. Quantifying runoff initiation, peak flows, and runoff coefficients at different spatial scales is a necessary first step towards modeling sediment entrainment and transport through the fluvial network. Similar efforts are needed to quantify the hydrology and sediment retention capacity of coastal wetlands.

Additional research is also needed to determine the ultimate fate of the sediment from terrestrial sources that is being delivered to the marine environment. Given the ephemeral nature of surface runoff on St. John, the delivery of sediment into the bays is very sporadic. Data on the residence time of sediment in different bays will help determine whether the effects of sediment on coral reef organisms are only present when a pulse of sediment is being delivered to the bays, or whether the effects of terrestrial sediment inputs are more chronic and persistent because the sediment remains in the bays over longer time periods.

6.4 Management recommendations

The findings from Chapter 2 can be translated into specific recommendations for reducing sediment production rates from unpaved roads. The steep, frequently-graded road segments should be the first target for implementing erosion control practices, as increasing slope and more

frequent grading significantly increase sediment production rates. Roads and driveways with steep slopes should be paved immediately after construction. The frequency and amount of road grading should be kept to a minimum.

STJ-EROS can be a valuable tool for land managers. The model can compare sediment delivery rates from natural versus current conditions. As shown in Chapter 5, STJ-EROS can generate color-coded maps to identify the individual road segments that are contributing high quantities of sediment to the marine environment. STJ-EROS also may be used to assess the effect of different management scenarios, such as new road developments or proposed mitigation projects, on sediment production and delivery. The proposed changes can be readily evaluated by making the appropriate changes to the GIS data layers or user-defined input parameters. The ability to predict the effects of different management scenarios will allow managers to optimize sediment reduction efforts.

Potential users should recognize that the model results depend on the completeness and accuracy of the GIS data layers. On St. John, the data layers needed by STJ-EROS have been developed only for the Lameshur Bay, Fish Bay, and the Cinnamon Bay basins. Development of the data layers takes time, as some of the data must be collected in the field. Aerial photos or automated methods, such as combining a DEM with the road layer to calculate road segment slope, could be used to create or update the layers, but such approaches need to be validated before they can be more widely applied. The rapid expansion and alteration of the road networks on St. John also means that the road data layers must be updated at least every five years.

Both model users and land managers must understand the limitations of STJ-EROS. Many of the predictive equations were empirically derived from field data collected on St. John, so they are calibrated to the erosion rates and processes observed during the study period. Since the nearby islands of Culebra, St. Thomas, Tortola, and Virgin Gorda have similar geologic, topographic, and climatic conditions, STJ-EROS can probably be applied to these islands with minimal changes. The application of STJ-EROS to areas with physical characteristics different

from St. John is only possible if the model is used in a relative sense—e.g., identifying road segments that have relatively high erosion rates. The use of STJ-EROS to estimate absolute erosion rates or sediment yields must be preceded by a field-based calibration. The field data can then be used to adjust or modify the sediment production and delivery functions currently in STJ-EROS.

Finally, it is important to recognize that STJ-EROS does not incorporate any anthropogenic sediment sources other than unpaved roads. Other changes in the type and intensity of land use can increase erosion rates and cause unpaved roads to play a relatively smaller role compared to other sediment sources. Any attempt to expand the sediment budgeting capabilities of STJ-EROS should consider incorporating other sediment sources, such as grazing, agriculture, and land clearing for residential or commercial development.

This study has shown that the expanding network of unpaved roads is significantly increasing the delivery of sediment to the marine environment around St. John. This increase should concern all who are interested in the conservation of the nearshore coral reef communities. Land development is inevitable in the Virgin Islands and most of the rest of the Caribbean, but stricter controls on land development must be enacted and enforced to reduce the amount of sediment being delivered to the marine environment. Land developers and local residents also must accept more of the moral and economic responsibility for limiting the adverse impacts of development. Collaborations, such as the Fish Bay Road Stabilization Program between the Virgin Islands Department of Planning and Natural Resources and the Fish Bay Homeowners Association, should be encouraged. Only through the widespread development of such collaborations will land development be able to coexist with a healthy, diverse, and visually appealing marine environment in the Virgin Islands and elsewhere.

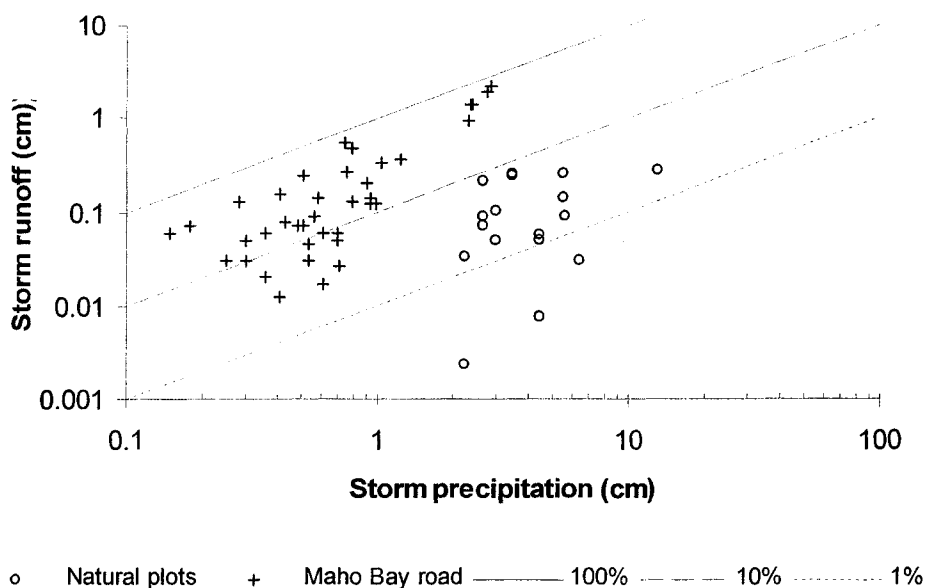


Figure 1. Relationship between storm precipitation and runoff for hillslope plots and road surfaces in St. John. Lines represent 100%, 10%, and 1% runoff coefficients.

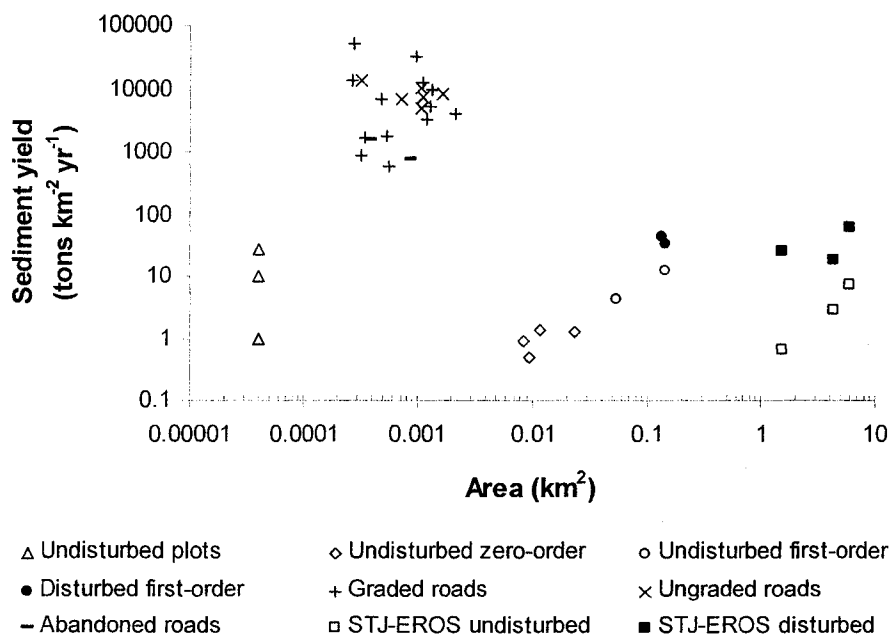
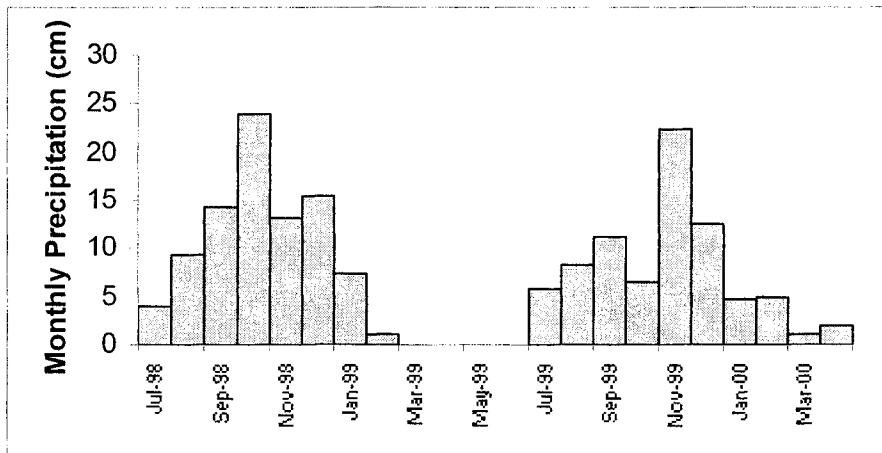


Figure 2. Relationship between sediment yields and contributing area for different landscape units on St. John.

APPENDIX I-A
MONTHLY PRECIPITATION MEASURED IN ST. JOHN BETWEEN
JULY 1998 AND MAY 2001

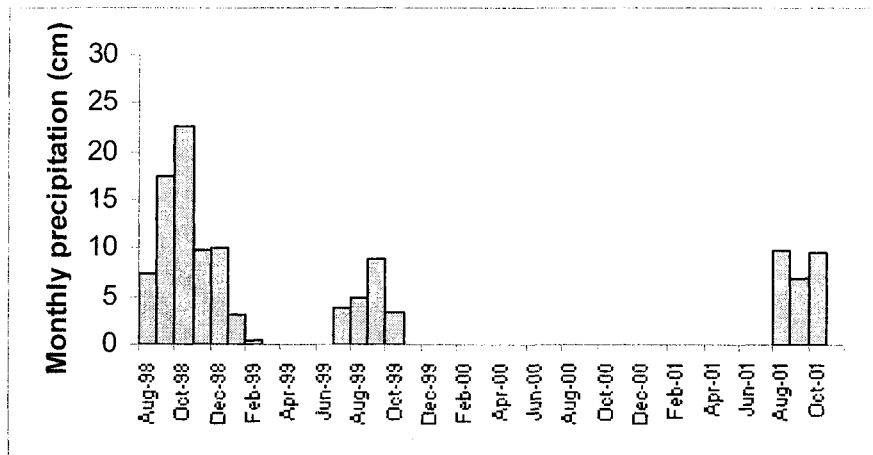
Appendix I-A. Monthly precipitation at Fish Bay.

Month	Precipitation (cm)	Comments
Jul-98	4.0	starting July 20th
Aug-98	9.4	
Sep-98	14.3	
Oct-98	24.0	
Nov-98	13.1	
Dec-98	15.5	
Jan-99	7.4	
Feb-99	1.1	until Feb 8th
Mar-99	0.0	no data
Apr-99	0.0	no data
May-99	0.0	no data
Jun-99	0.0	no data
Jul-99	5.8	starting July 8th
Aug-99	8.2	
Sep-99	11.2	
Oct-99	6.6	missing Oct 19 1900 to end of month
Nov-99	22.4	missing Nov 1 to Nov 8 1530hrs
Dec-99	12.6	
Jan-00	4.6	
Feb-00	5.0	
Mar-00	1.2	
Apr-00	1.9	



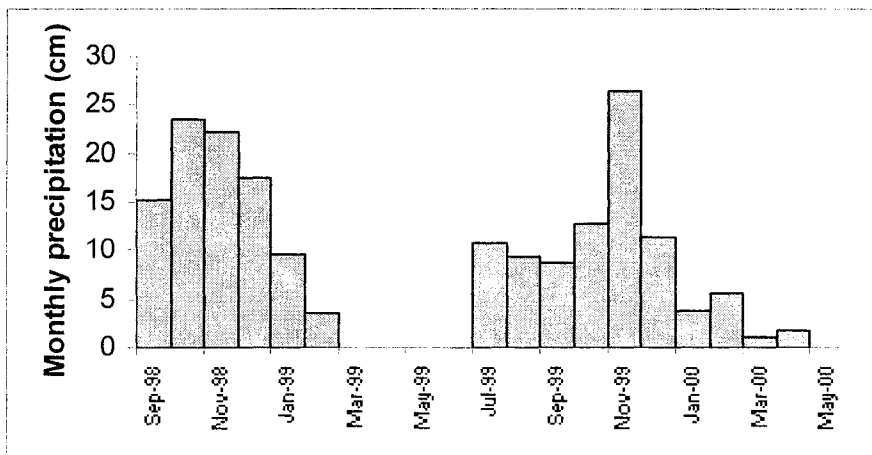
Appendix I-A. Monthly precipitation at Lameshur Bay.

Month	Precipitation (cm)	Comments
Aug-98	7.4	from Aug 19th on
Sep-98	17.5	
Oct-98	22.6	
Nov-98	9.9	
Dec-98	10.2	
Jan-99	3.0	
Feb-99	0.5	up to Feb 8
Mar-99	no data	
Apr-99	no data	
May-99	no data	
Jun-99	no data	
Jul-99	3.8	starting July 12th
Aug-99	4.8	
Sep-99	8.9	
Oct-99	3.3	up to Oct 19
Nov-99	no data	
Dec-99	no data	
Jan-00	no data	
Feb-00	no data	
Mar-00	no data	
Apr-00	no data	
May-00	no data	
Aug-01	9.78	
Sep-01	6.91	
Oct-01	9.58	
Nov-01		



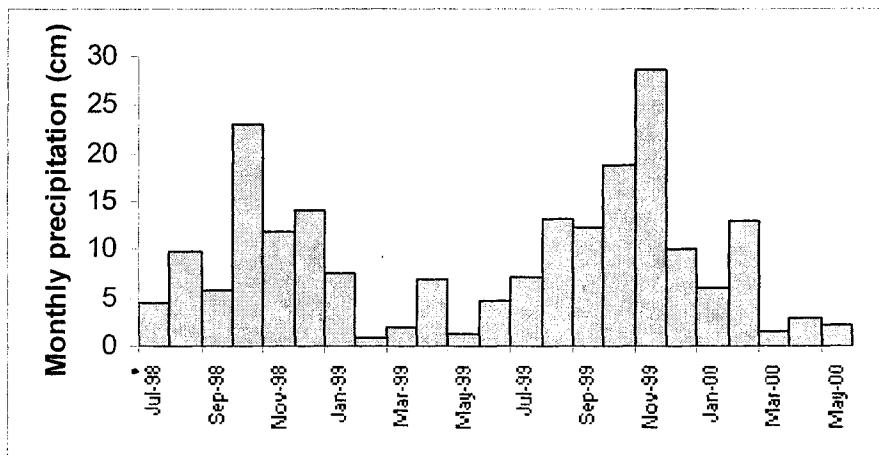
Appendix I-A. Monthly precipitation at Bordeaux Mountain.

Month	Precipitation (cm)	Comments
Sep-98	15.2	Starting Sept. 14th
Oct-98	23.5	
Nov-98	22.3	
Dec-98	17.4	
Jan-99	9.7	
Feb-99	3.6	Until Feb 28th
Mar-99	no data	
Apr-99	no data	
May-99	no data	
Jun-99	0.1	Starting June 28th
Jul-99	10.6	
Aug-99	9.3	
Sep-99	8.7	
Oct-99	12.7	
Nov-99	26.4	includes H. Lenny
Dec-99	11.4	
Jan-00	3.7	
Feb-00	5.6	
Mar-00	1.1	
Apr-00	1.7	
May-00	0.0	taken down May 3



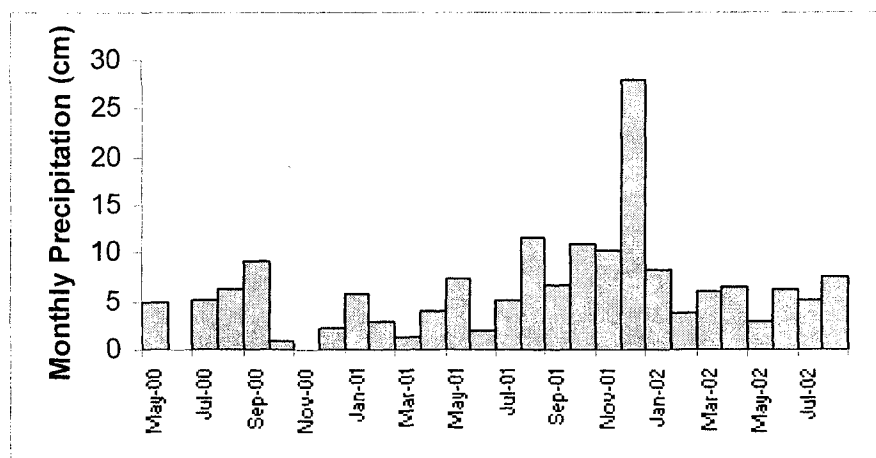
Appendix I-A. Monthly precipitation at Maho Bay.

Precipitation		
Month	(cm)	Comments
Jul-98	4.4	Started on July 13
Aug-98	9.8	
Sep-98	5.7	Does not include H. Georges
Oct-98	23.2	
Nov-98	11.9	
Dec-98	14.1	
Jan-99	7.7	
Feb-99	0.9	
Mar-99	2.0	No data 23rd 1800hrs to 29th 1300hrs
Apr-99	7.0	
May-99	1.4	
Jun-99	4.7	
Jul-99	7.2	No data 29th 1200 hrs to end of month
Aug-99	13.2	No data 1st to 3rd 0700 hrs
Sep-99	12.3	New raingage set 02-Sept
Oct-99	18.89	
Nov-99	28.6	
Dec-99	10.18	
Jan-00	5.94	
Feb-00	12.95	
Mar-00	1.55	
Apr-00	2.82	
May-00	2.16	Station taken down May 19th



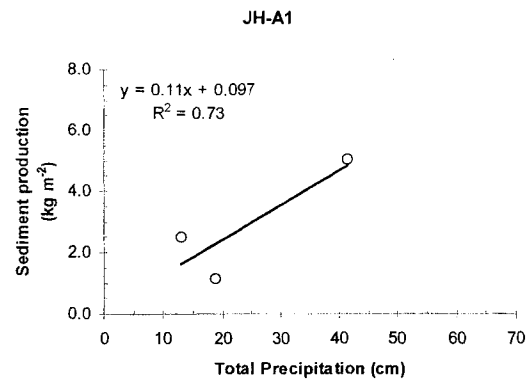
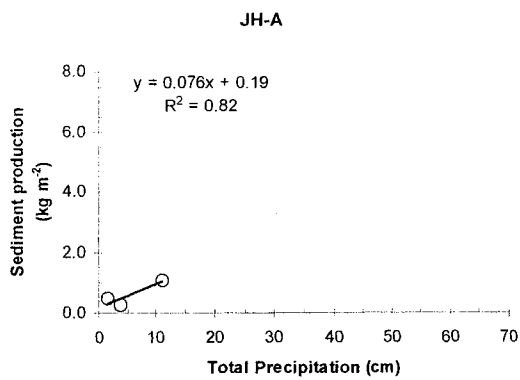
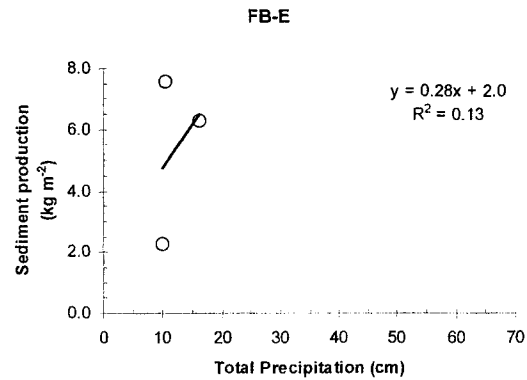
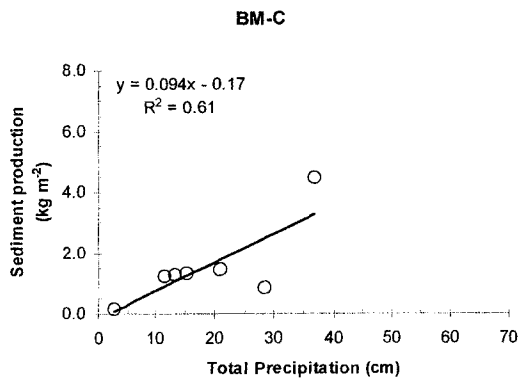
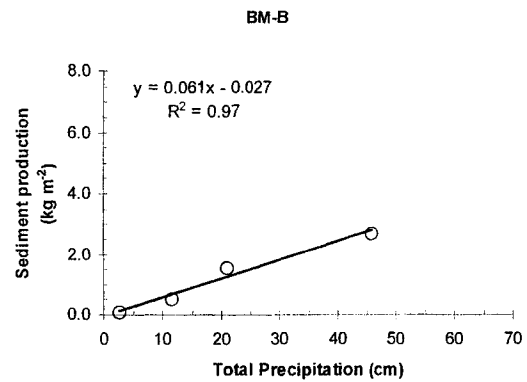
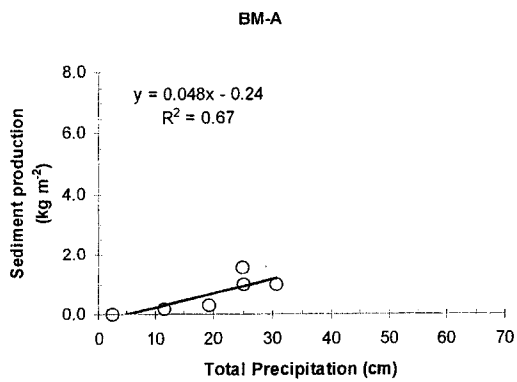
Appendix I-A. Monthly precipitation at L'Esperance.

Month	Precipitation (cm)	Comments
May-00	4.9	Beginning on May 19th
Jun-00	0.0	
Jul-00	5.1	
Aug-00	6.2	
Sep-00	9.2	
Oct-00	0.8	
Nov-00	0.0	
Dec-00	2.3	
Jan-01	5.8	
Feb-01	2.9	
Mar-01	1.4	
Apr-01	3.9	
May-01	7.4	
Jun-01	2.0	
Jul-01	5.2	
Aug-01	11.8	
Sep-01	6.7	
Oct-01	11.0	
Nov-01	10.3	
Dec-01	28.0	
Jan-02	8.2	
Feb-02	3.8	
Mar-02	6.1	
Apr-02	6.6	
May-02	2.9	
Jun-02	6.3	
Jul-02	5.2	
Aug-02	7.7	Until 20th August

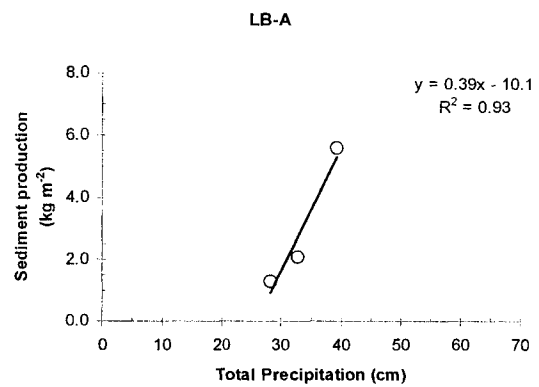
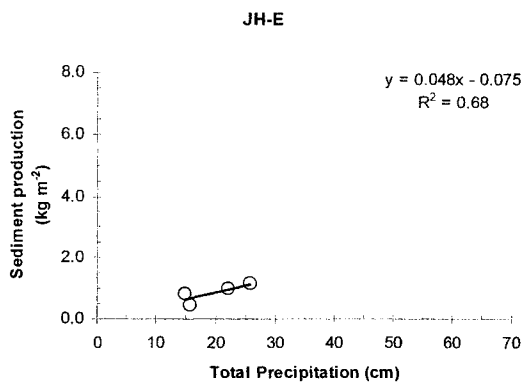
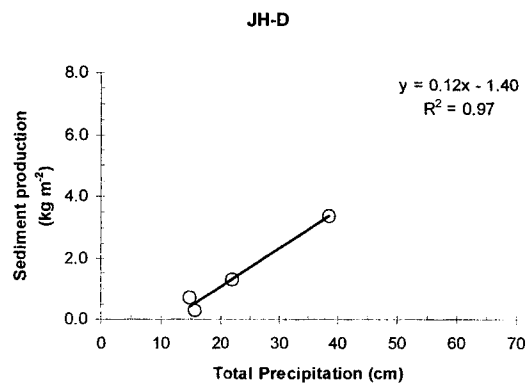
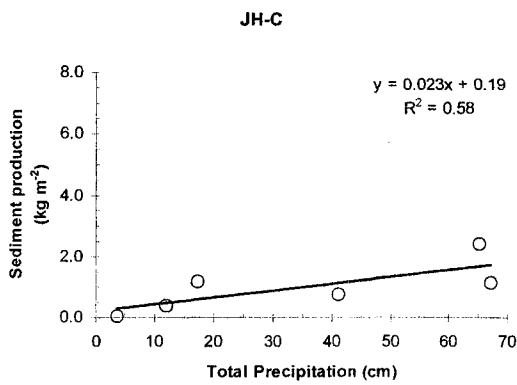
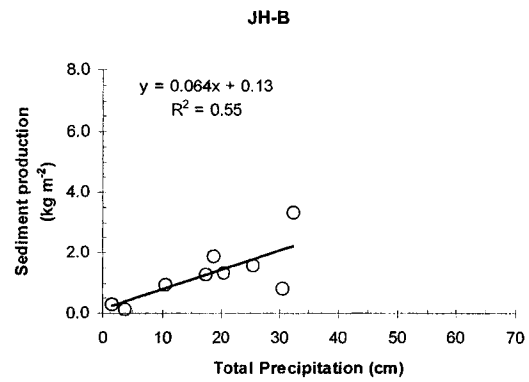
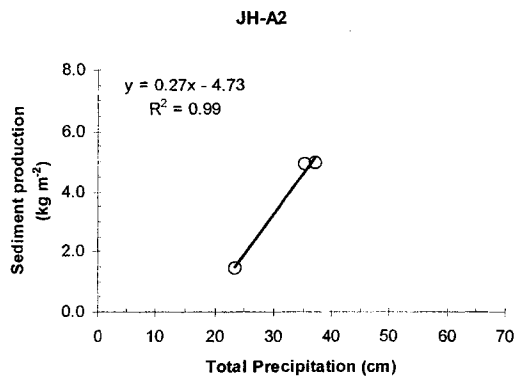


APPENDIX I-B
RELATIONSHIP BETWEEN PRECIPITATION AND SEDIMENT PRODUCTION
FOR FOURTEEN ROAD SEGMENTS

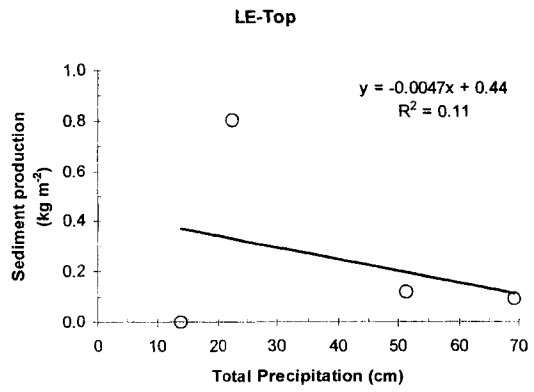
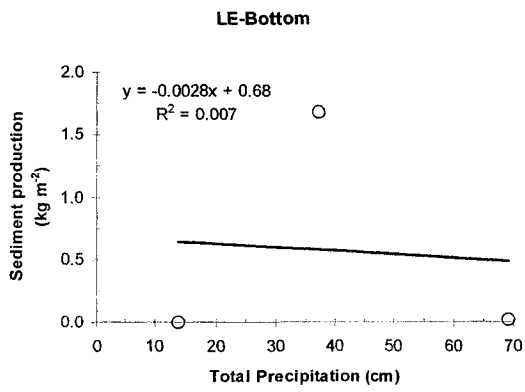
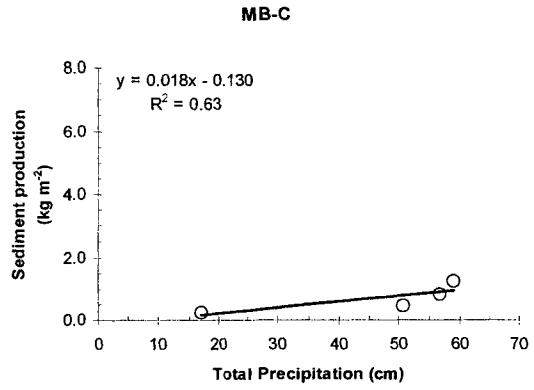
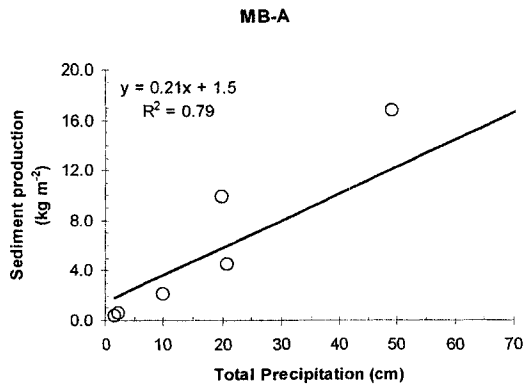
Appendix I-B. Relationship between precipitation and sediment production for each of the 14 road segments with at least three measurements.



Appendix I-B (cont.)



Appendix I-B (cont.).

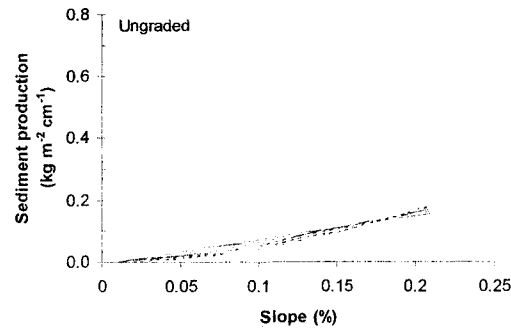
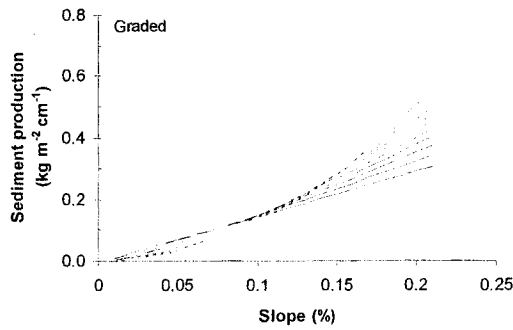
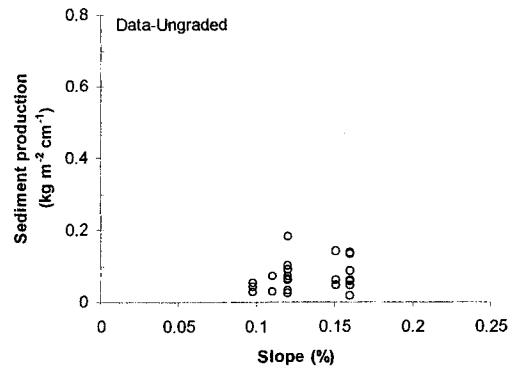
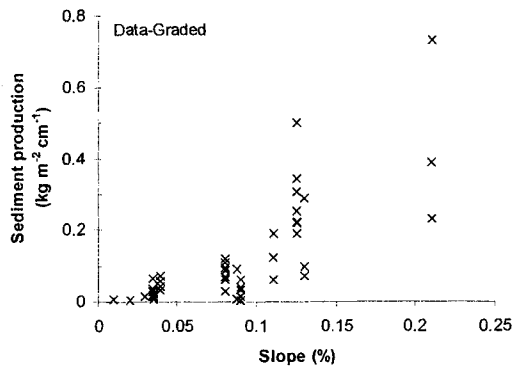


APPENDIX I-C
SUMMARY OF MULTIPLE REGRESSION ANALYSIS
FOR ROAD EROSION MODEL

Appendix I-C. Summary of multiple regression analysis for the relationship between precipitation, slope, area-slope, and grading.

Model	Model R ²	Model p value	Intercept (p value)	Slope ¹ * Precipitation parameter (p value)	Slope ¹ * Precipitation * Grading Parameter (p value)
Slope ^{1.0}	0.61	<0.0001	-0.635 (0.0801)	0.772 (<0.0001)	0.714 (<0.0001)
Slope ^{1.1}	0.66	<0.0001	-0.651 (0.0529)	0.941 (<0.0001)	0.988 (<0.0001)
Slope ^{1.2}	0.69	<0.0001	-0.627 (0.0453)	1.13 (<0.0001)	1.33 (<0.0001)
Slope ^{1.3}	0.72	<0.0001	-0.576 (0.0501)	1.35 (<0.0001)	1.743 (<0.0001)
Slope ^{1.4}	0.74	<0.0001	-0.509 (0.0678)	1.60 (<0.0001)	2.24 (<0.0001)
Slope ^{1.5}	0.75	<0.0001	-0.433 (0.1047)	1.88 (<0.0001)	2.85 (<0.0001)
Slope ^{1.6}	0.76	<0.0001	-0.353 (0.1709)	2.21 (<0.0001)	3.59 (<0.0001)
Slope ^{1.7}	0.76	<0.0001	-0.272 (0.2779)	2.60 (<0.0001)	4.48 (<0.0001)
Slope ^{1.8}	0.76	<0.0001	-0.193 (0.4321)	3.06 (<0.0001)	5.55 (<0.0001)
Slope ^{1.9}	0.76	<0.0001	-0.117 (0.6297)	3.59 (<0.0001)	6.84 (<0.0001)
Slope ^{2.0}	0.76	<0.0001	-0.044 (0.8547)	4.22 (<0.0001)	8.39 (<0.0001)
Area*slope	0.68	<0.0001	-0.202 (0.4929)	0.0029 (<0.0001)	0.00099 (0.0673)

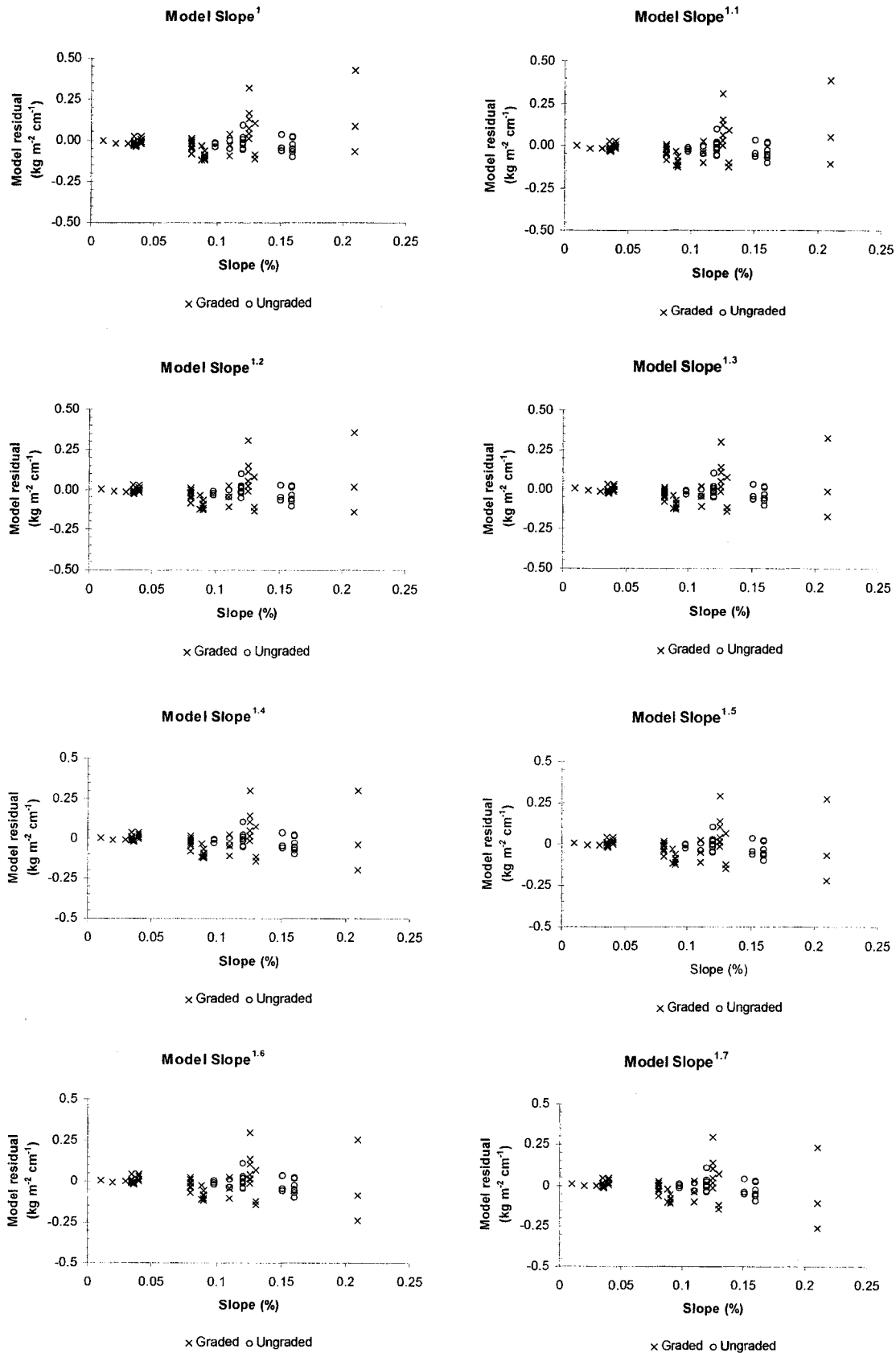
Appendix I-C. Graphs showing the relationship between sediment production and slope for sediment trap data and different empirical erosion models.



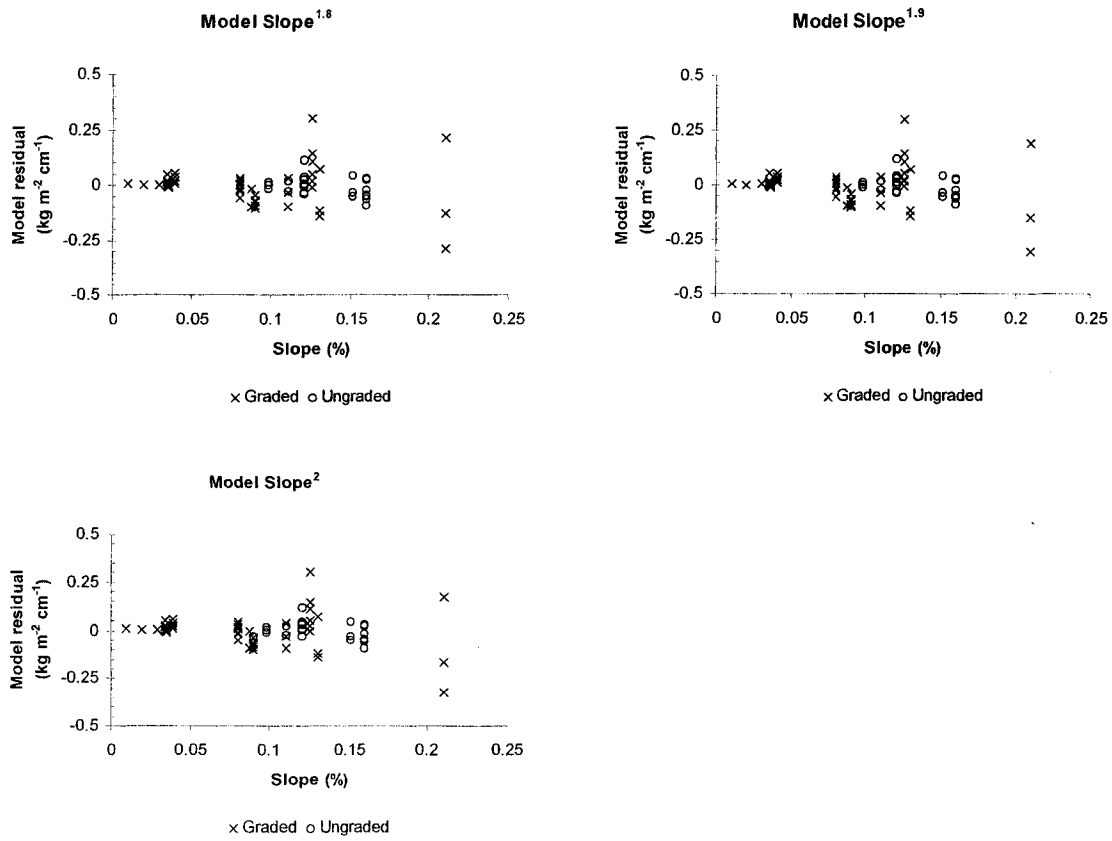
----- S1 ----- S11 ----- S12 ----- S13 ----- S14 ----- S15
 ----- S16 ----- S17 ----- S18 ----- S19 ----- S2

----- S1 ----- S11 ----- S12 ----- S13 ----- S14 ----- S15
 ----- S16 ----- S17 ----- S18 ----- S19 ----- S2

Appendix I-C. Graphs showing the relationship between residual sediment production and slope for different empirical erosion models.

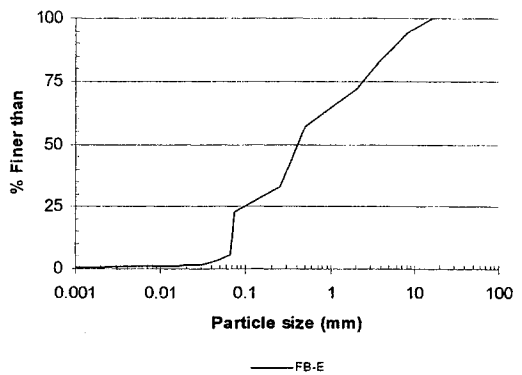
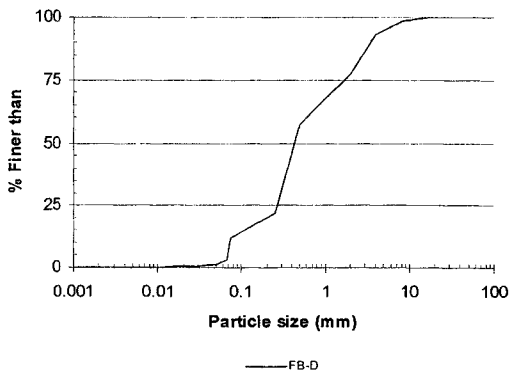
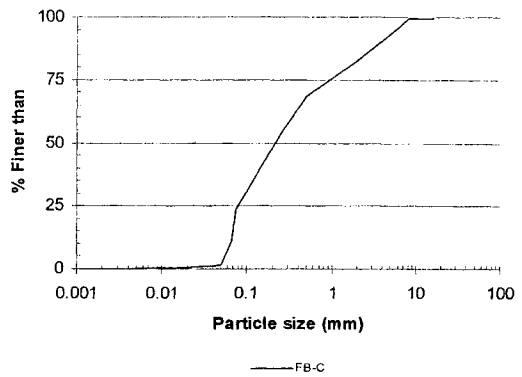
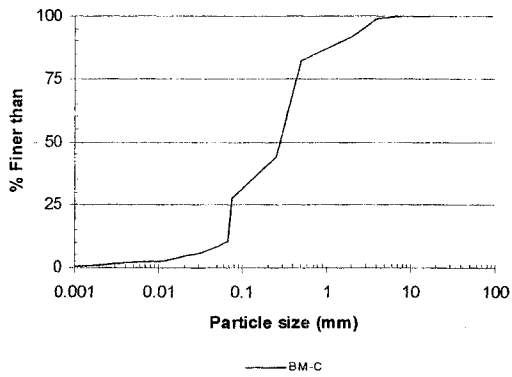
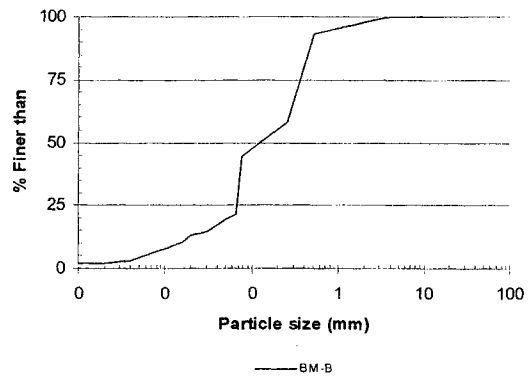
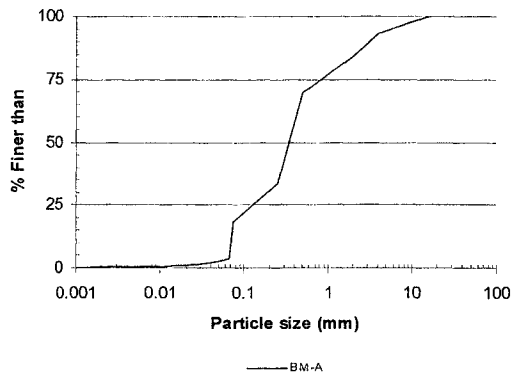


Appendix I-C. Graphs showing the relationship between residual sediment production and slope for different empirical erosion models.

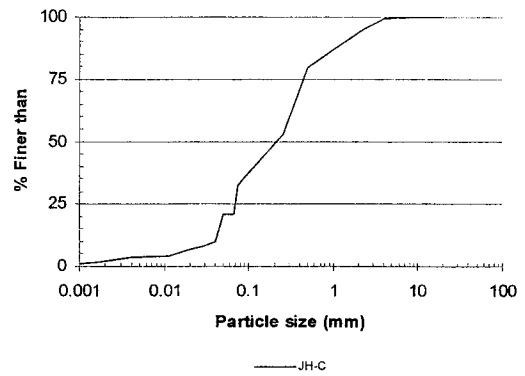
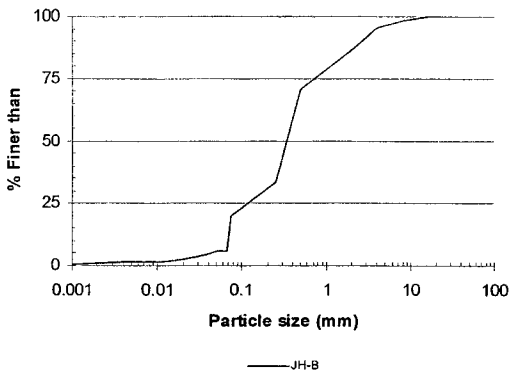
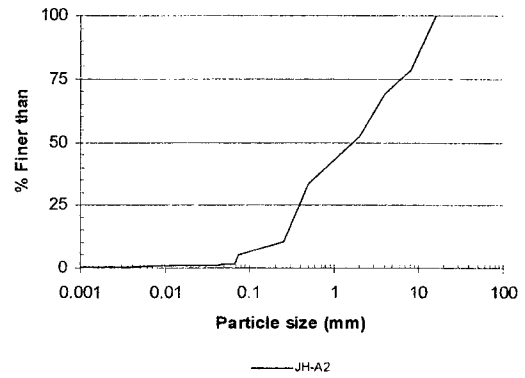
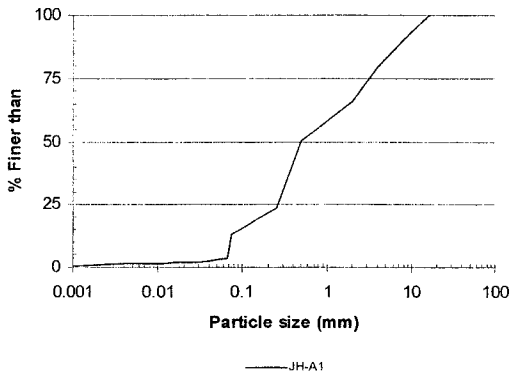
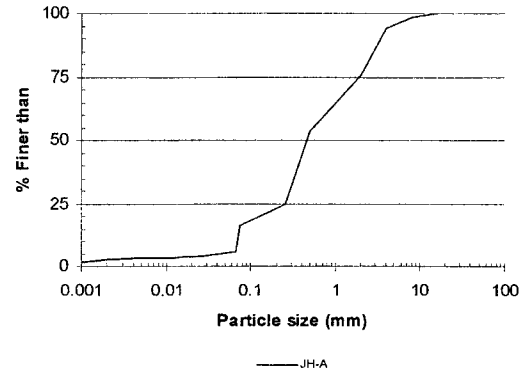
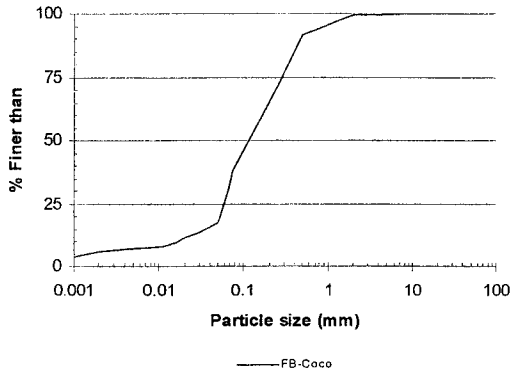


APPENDIX I-D
PARTICLE-SIZE DISTRIBUTIONS FOR SEDIMENT PRODUCED FROM
TWENTY ROAD SEGMENTS

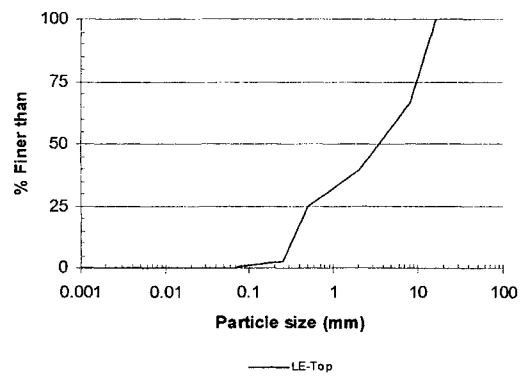
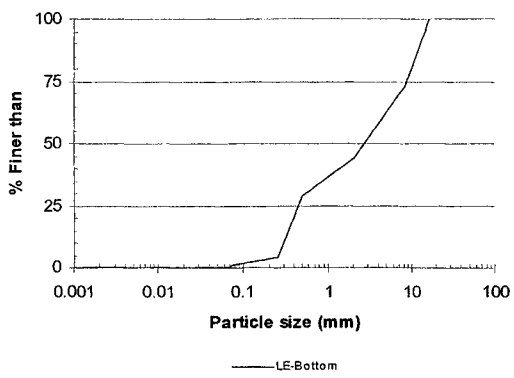
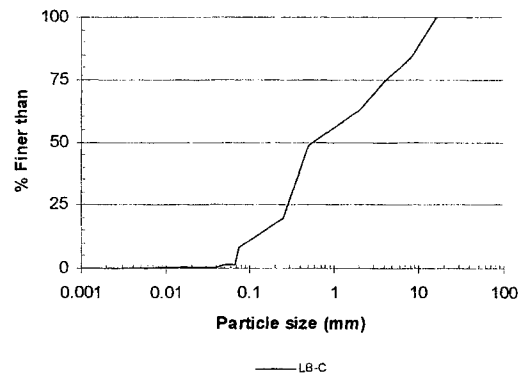
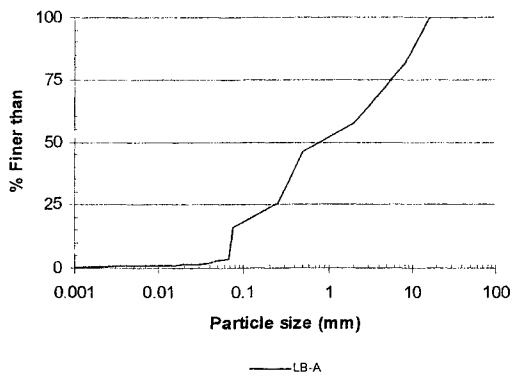
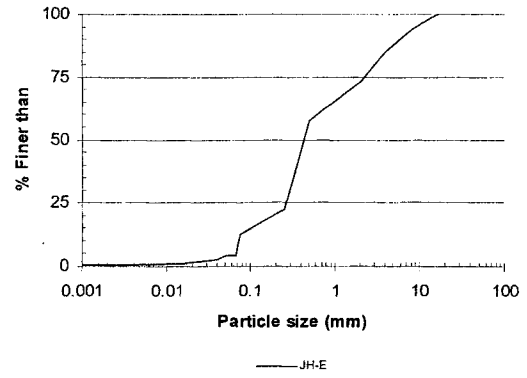
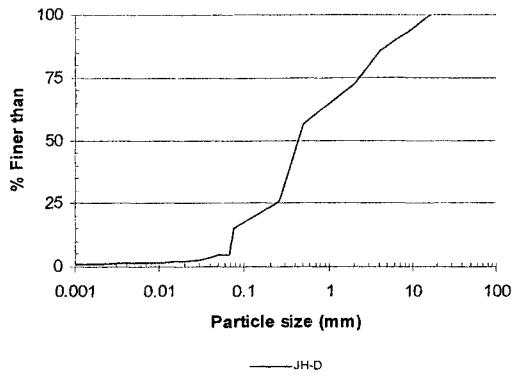
Appendix I-D. Mass-weighted average particle size distributions for 20 road segments.



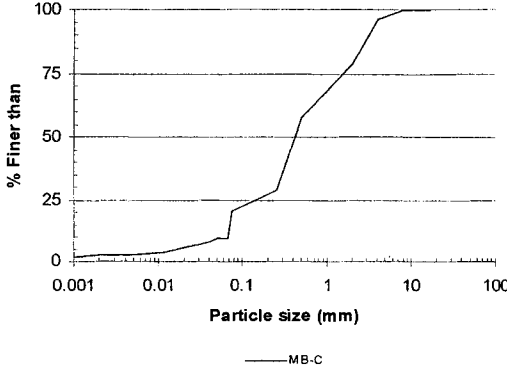
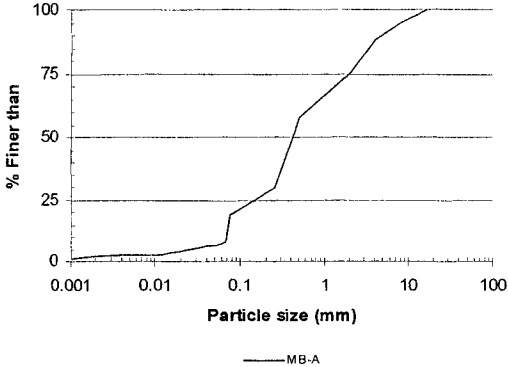
Appendix I-D (cont.).



Appendix I-D (cont.).

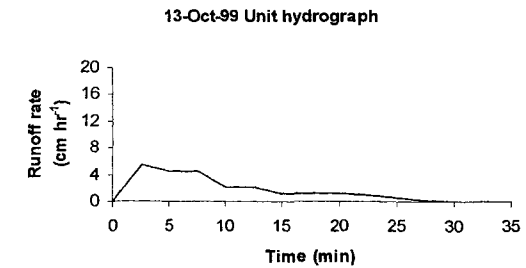
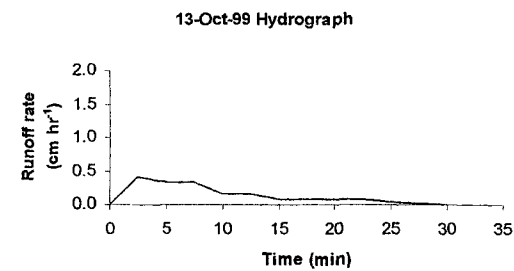
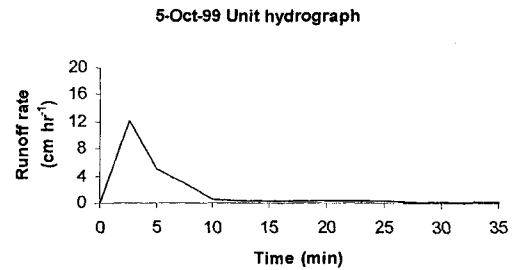
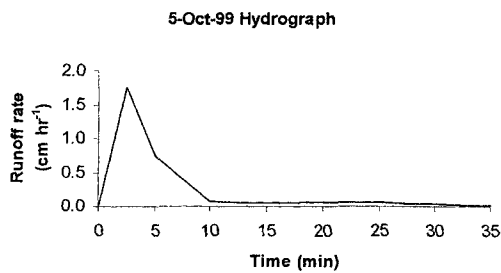
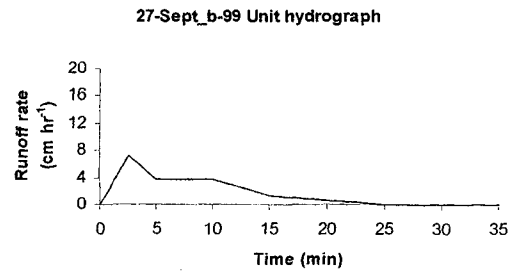
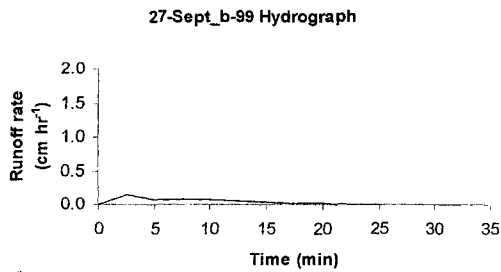
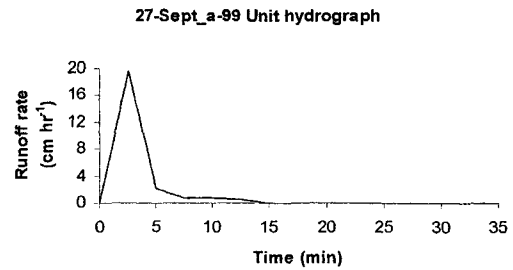
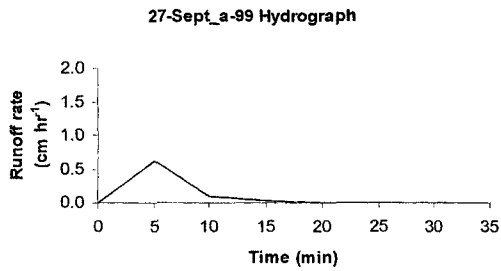


Appendix I-D (cont.).



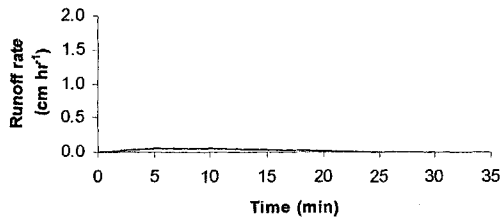
APPENDIX II-A
HYDROGRAPHS AND UNIT HYDROGRAPHS USED FOR CALIBRATION OF
THE GA-UH AND GA-KW MODELS

Appendix II-A. Hydrographs and unit hydrographs of eight events used for model calibration.

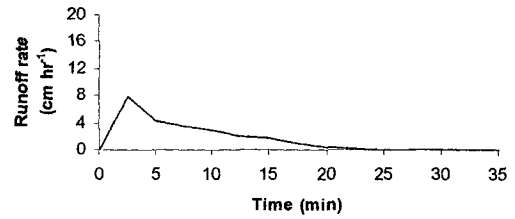


Appendix II-A (cont.).

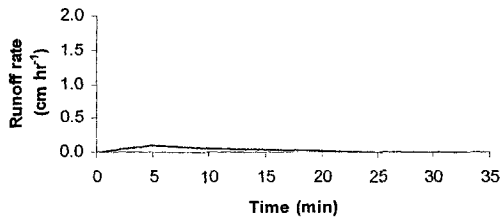
4-Jan-00 Hydrograph



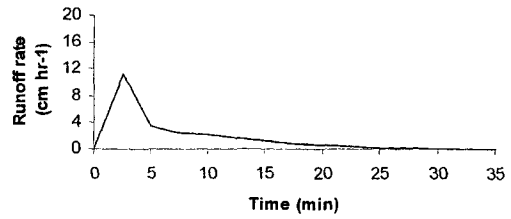
4-Jan-00 Unit hydrograph



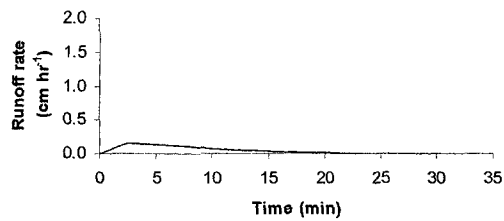
29-Jan-00 Hydrograph



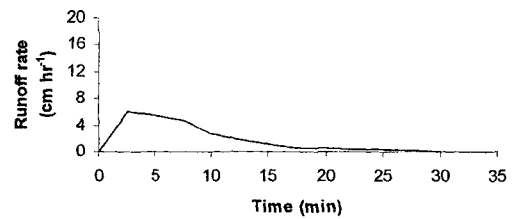
29-Jan-00 Unit hydrograph



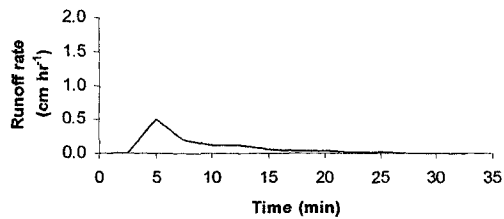
22-Apr-00 Hydrograph



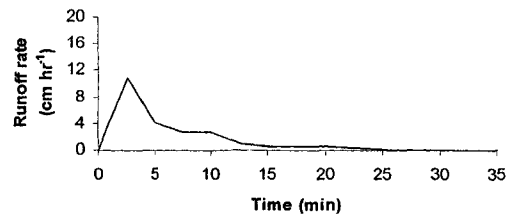
22-Apr-00 Unit hydrograph



29-Apr-00 Hydrograph



29-Apr-00 Unit hydrograph

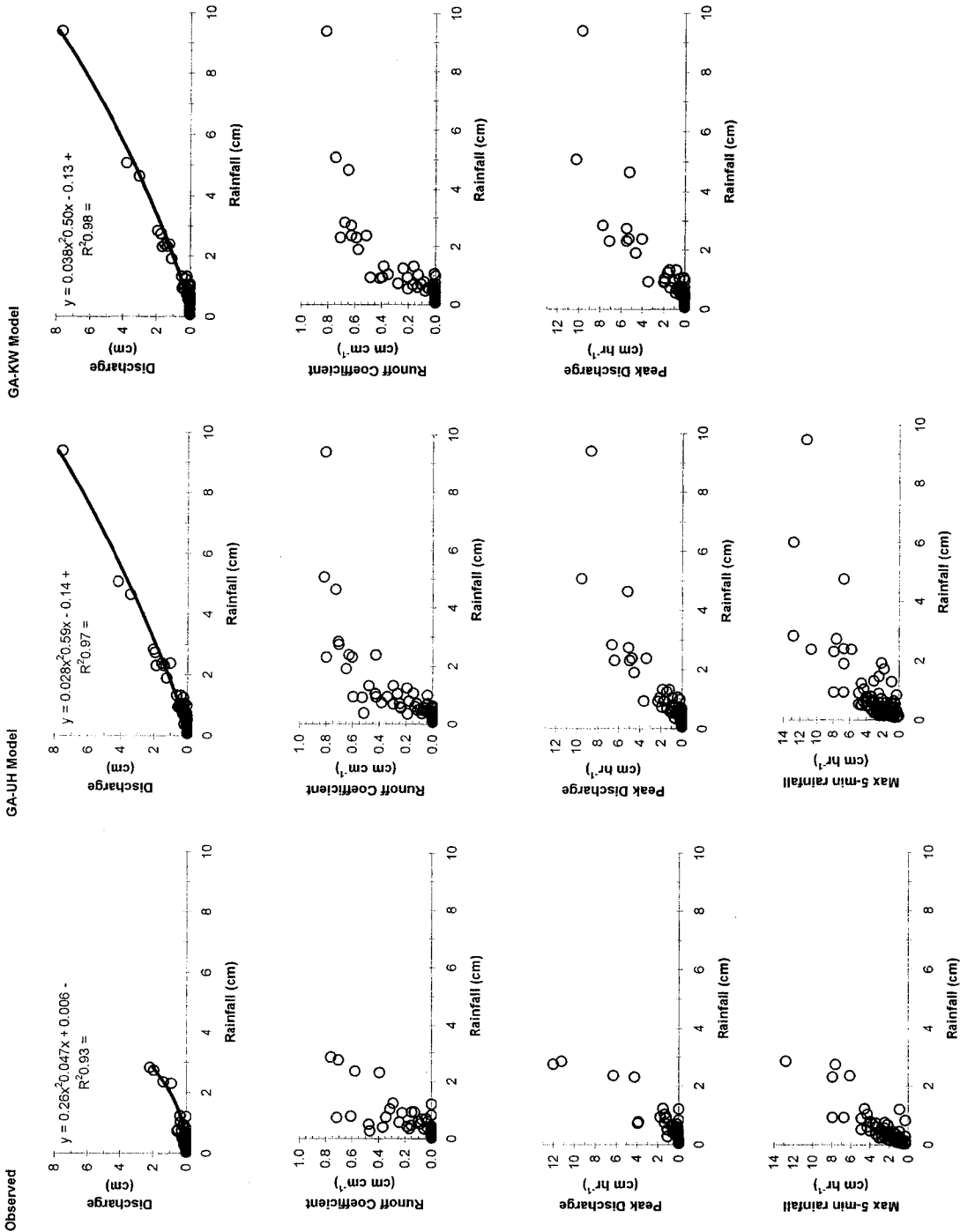


APPENDIX II-B

SUMMARY OF RUNOFF DATA AND MODEL RESULTS FOR THE MAHO BAY

ROAD SEGMENT

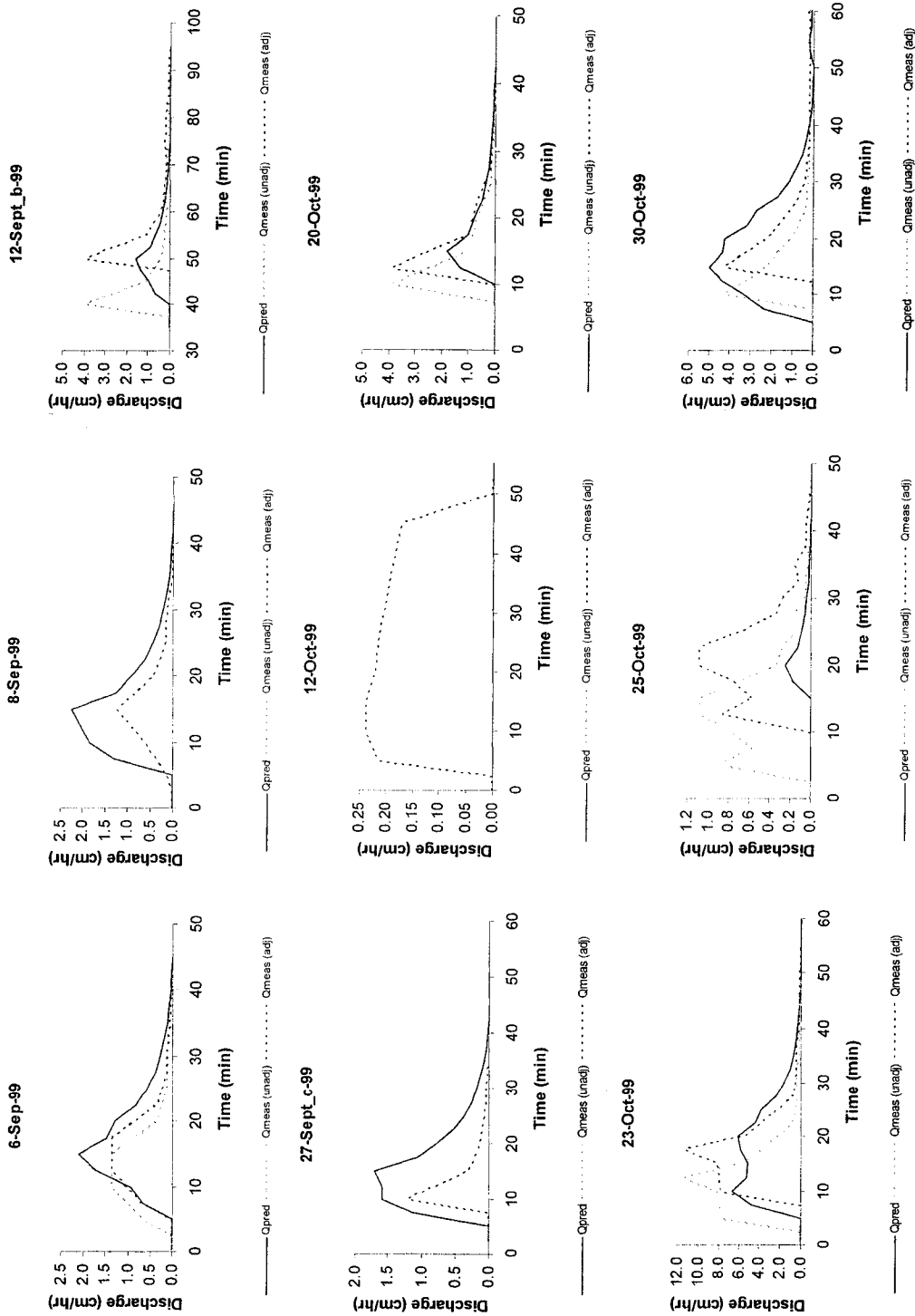
Appendix II-B. Relationship between discharge, runoff coefficient, peak discharge, and maximum 5-min rainfall intensity against storm precipitation. Observed data originates from 135 rainfall events. GA-UH and GA-KW estimates were based on rainfall data from 160 events.



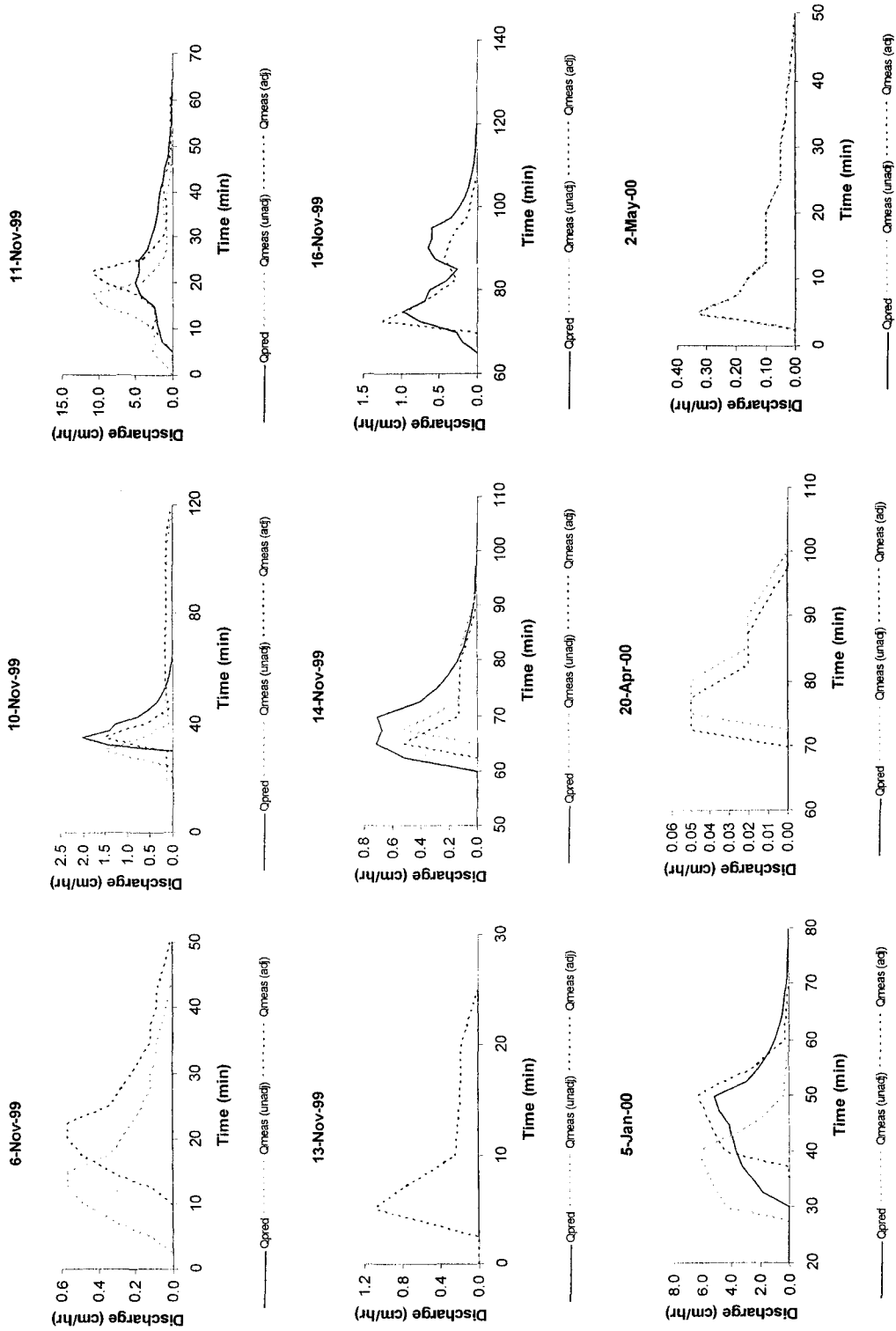
APPENDIX II-C

COMPARISON BETWEEN OBSERVED HYDROGRAPHS AND HYDROGRAPHS
PREDICTED BY THE GA-UH MODEL

Appendix II-C. Comparison between observed and predicted hydrographs for events used in GA-UH model validation. Q_{meas} (unadj) refers to unadjusted measured hydrographs. Q_{meas} (adj) refers to measured hydrographs for which the time axis was adjusted to compensate for timing errors in the measurements.



Appendix II-C (cont.).

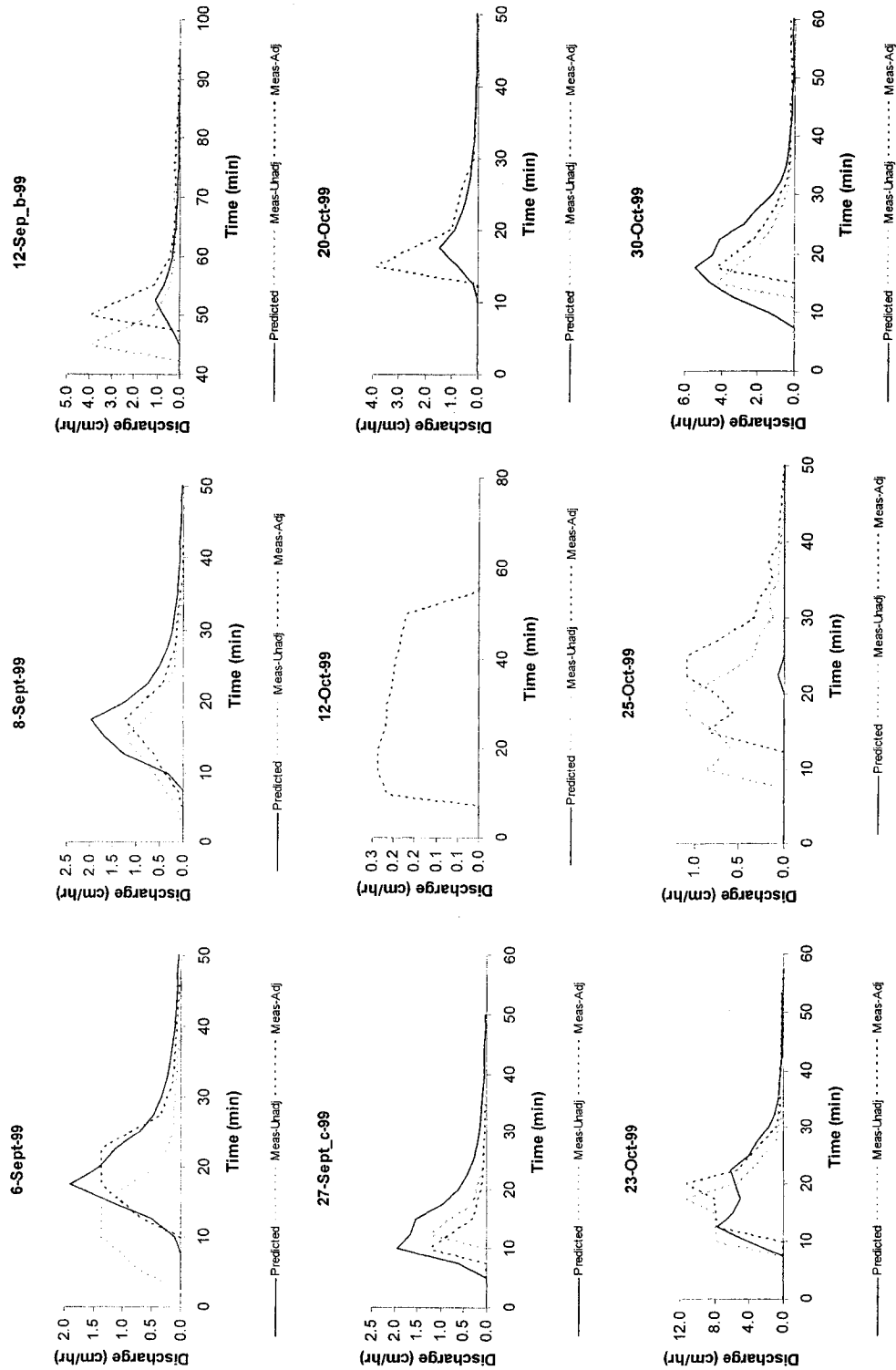


APPENDIX II-D

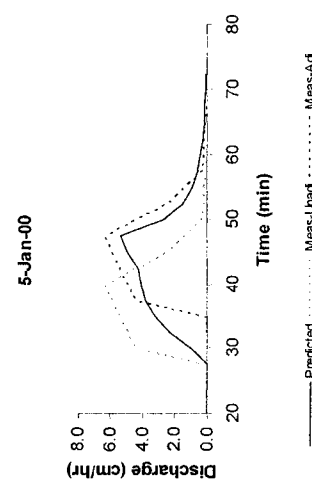
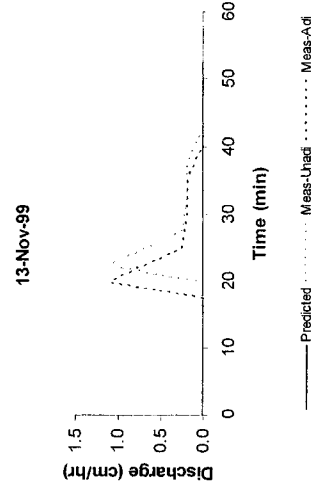
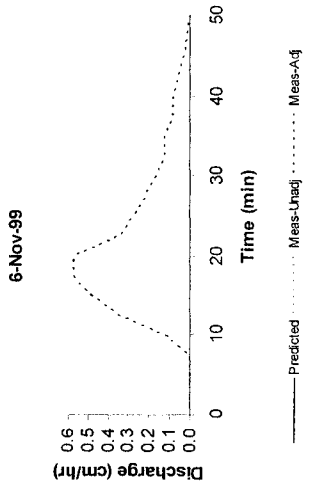
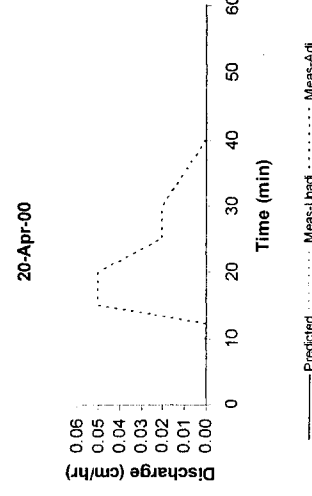
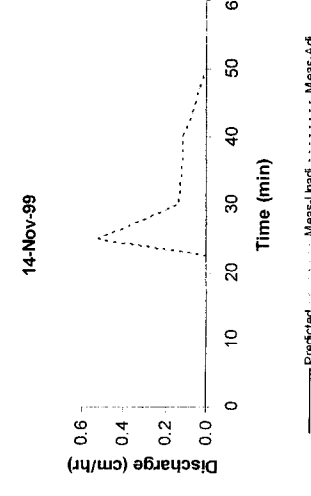
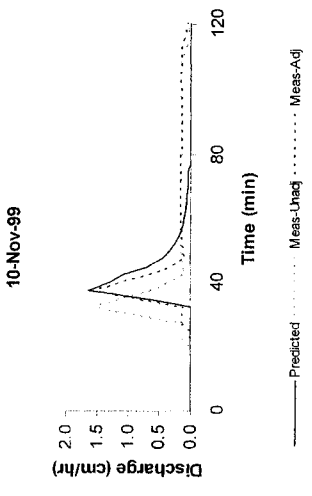
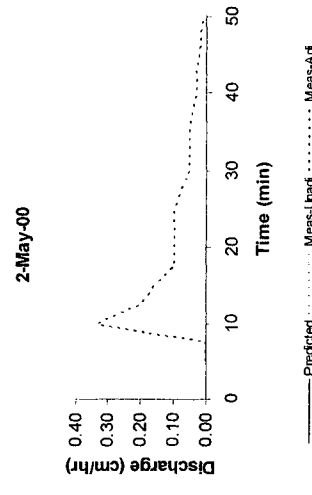
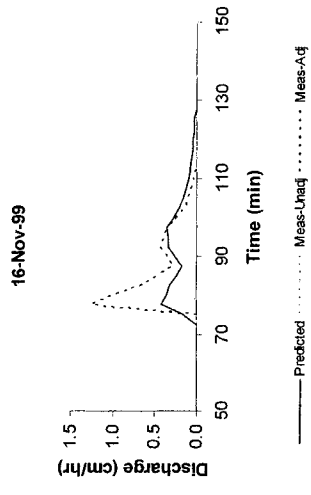
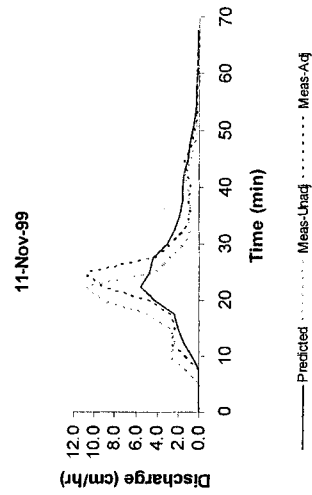
COMPARISON BETWEEN OBSERVED HYDROGRAPHS AND HYDROGRAPHS

PREDICTED BY THE GA-KW MODEL

Appendix II-D. Comparison between observed and predicted hydrographs for events used in GA-KW model validation. Q_{meas} (unadj) refers to unadjusted measured hydrographs. Q_{meas} (adj) refers to measured hydrographs for which the time axis was adjusted to compensate for timing errors in the measurements.

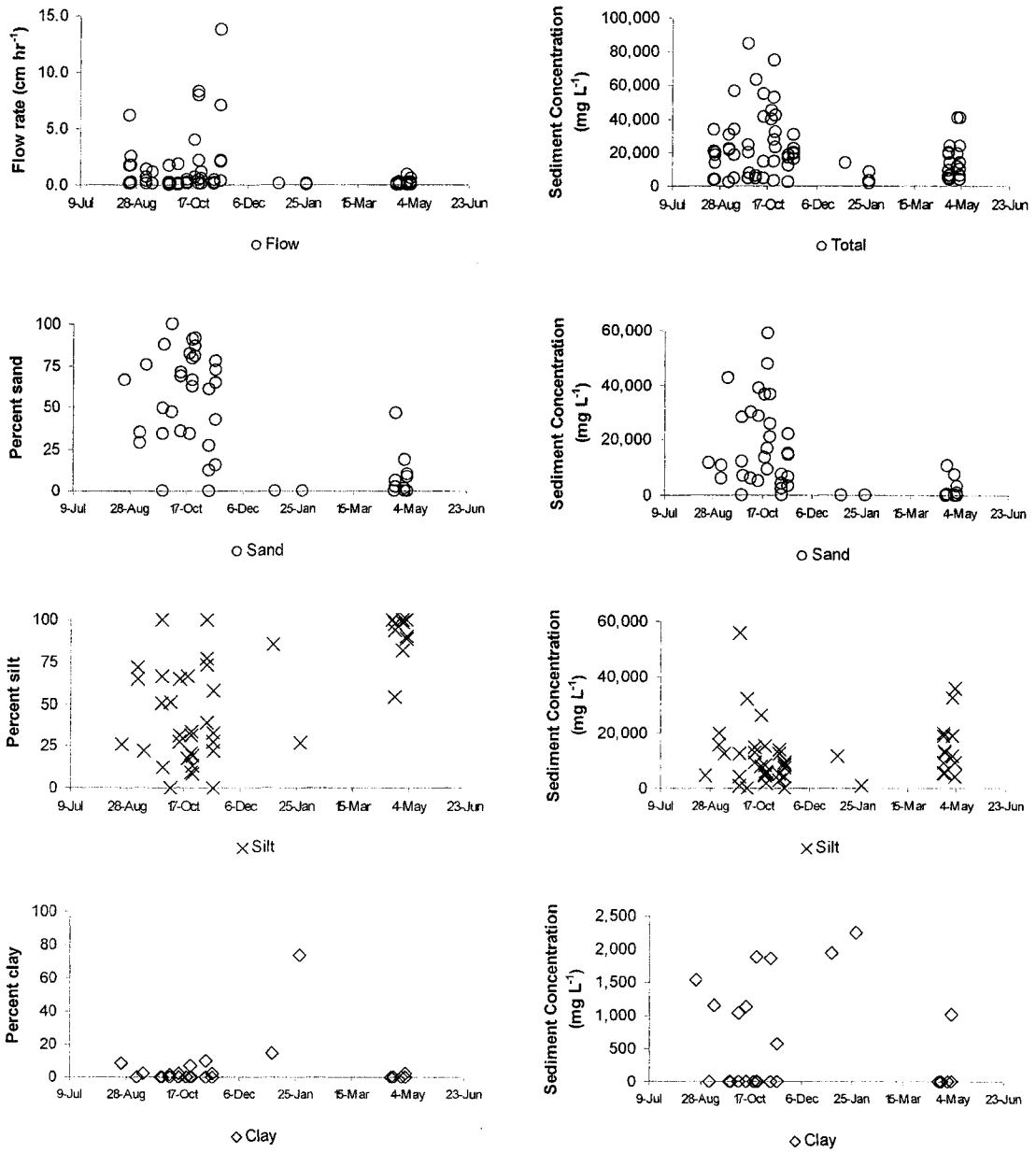


Appendix II-D (cont.).



APPENDIX II-E
CONCENTRATION OF SEDIMENT IN RUNOFF SAMPLES COLLECTED
FROM THE MAHO BAY ROAD SEGMENT

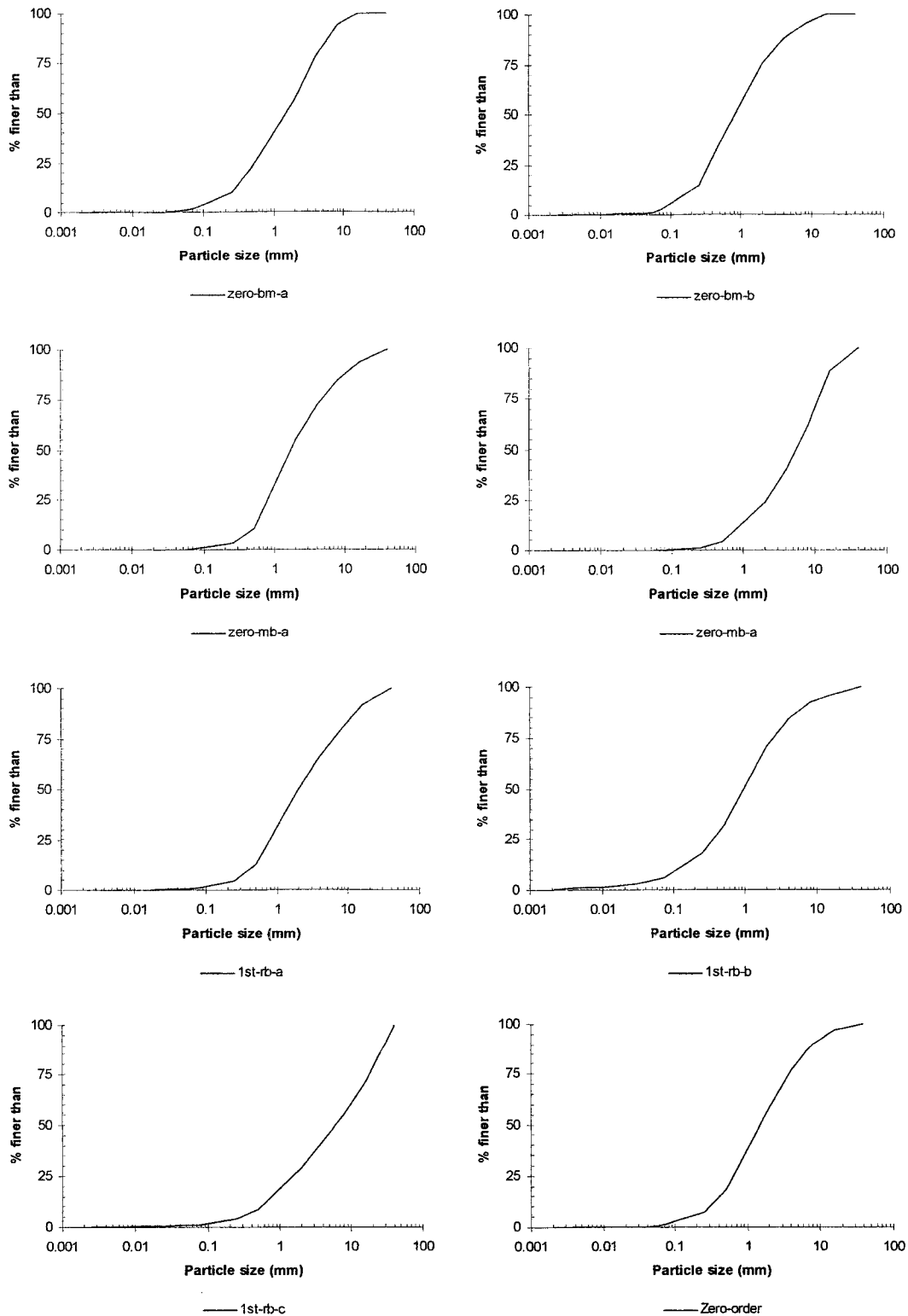
Appendix II-E. Changes in the concentration and relative proportion of sand, silt, and clay in the suspended sediment samples from the Maho Bay road segment over time.



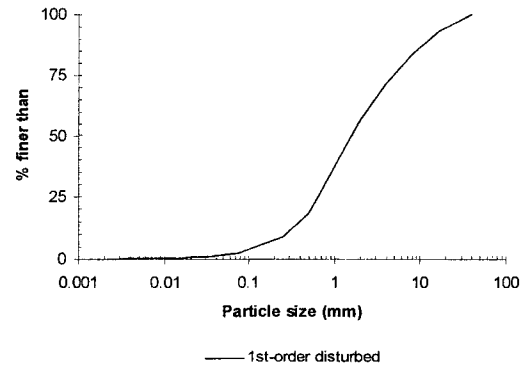
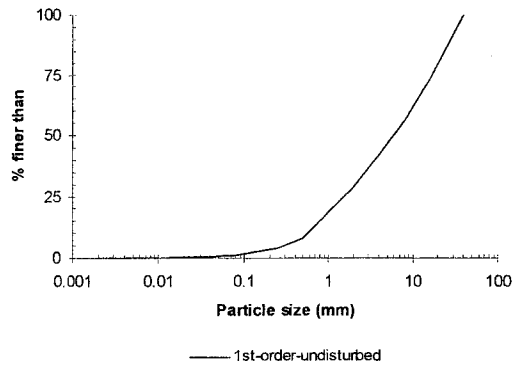
APPENDIX III

PARTICLE-SIZE DISTRIBUTIONS OF SEDIMENT PRODUCED FROM ZERO-
AND FIRST-ORDER CATCHMENTS

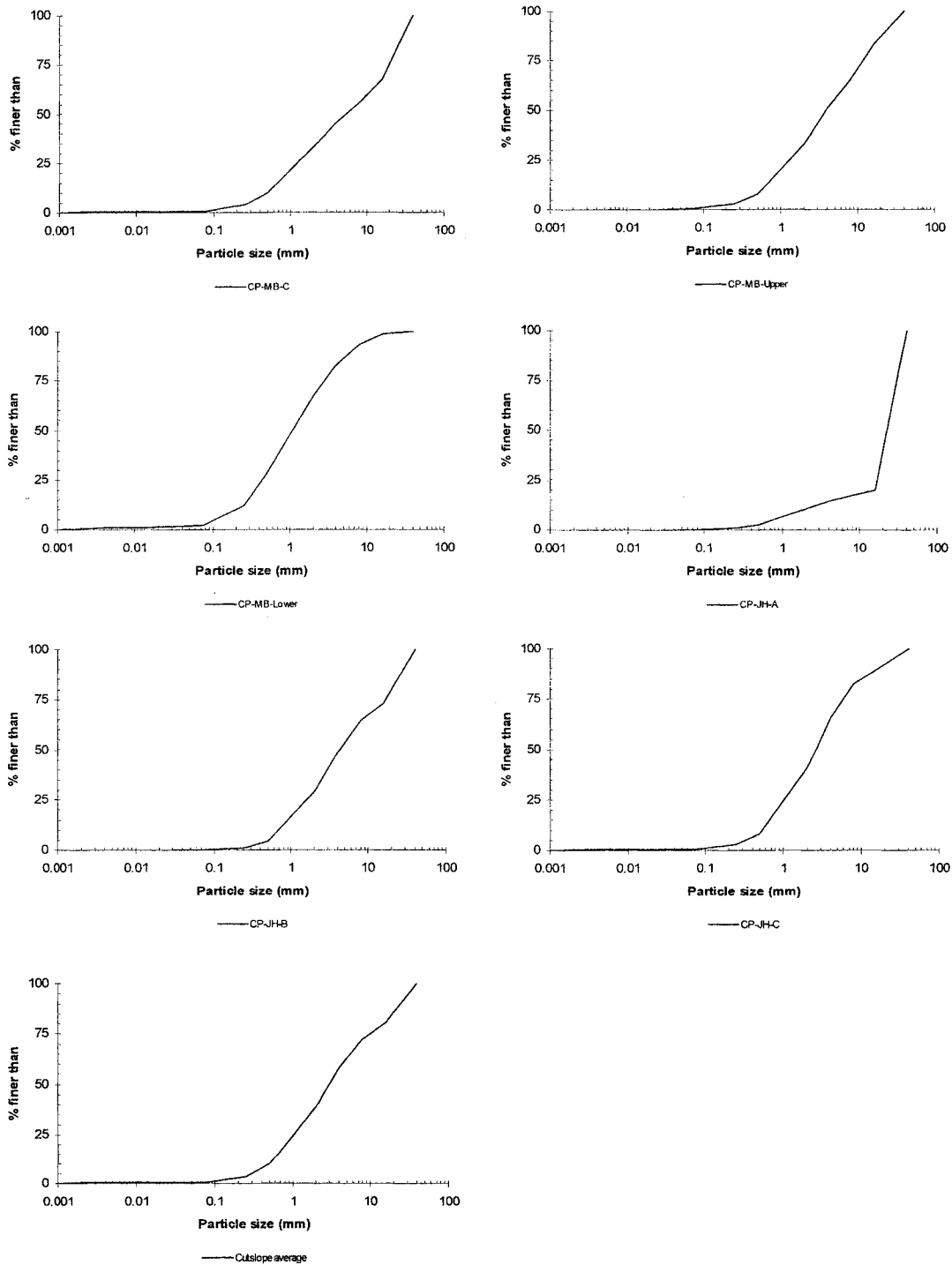
Appendix III. Particle-size distributions of the sediment collected in the zero- and first-order sediment traps.



Appendix III. Particle-size distributions of the sediment collected in the zero- and first-order sediment traps.



Appendix III. Particle-size distributions of the sediment collected from the cutslope sediment traps.



APPENDIX IV-A

CHARACTERIZATION OF THE STREAM NETWORK IN ST. JOHN

CHARACTERIZATION OF THE STREAM NETWORK IN ST. JOHN

Purpose

The storage and transport capacity of sediment along stream channels is an important component of a sediment budget (Reid and Dunne, 1996). The routing component of the St. John sediment budget model (STJ-EROS) is based on sediment delivery ratios. The use of this method requires making some assumptions related to processes controlling the storage and transport of sediment through the fluvial network on St. John. The purpose of this appendix is to present a qualitative and quantitative geomorphic description of several stream reaches on the island that support the assumptions made for STJ-EROS.

Methods

Three first-order streams on the Reef Bay basin, and two second- to third-order streams in the Main Fish Bay and Greater Lameshur Bay guts are described in this Appendix. Longitudinal profiles and channel cross-sections were measured with a measuring tape and hand level (Ramos, 1996). The particle-size distribution of the streambed surface was determined on several stream reaches by the pebble-count method (Wolman, 1954). The location and height of eroding banks and the channel type (Montgomery and Buffington, 1997) were also noted. These surveys were used to determine channel slope, sediment transport capacity, and the total volume of fine sediment (≤ 2 mm) stored on the surface of the streambed.

Results

The three first-order in the Reef Bay basin had average slopes ranging of 20 to 30%, a predominantly cobble and boulder streambed, and a cascade-type morphology with pools that have been completely filled in by clay to medium gravel-sized sediment (Figures 1a-1c). These characteristics make them highly capable of transporting additional fine sediment (roughly ≤ 2

mm) delivered to them (Montgomery and Buffington, 1997). This suggests that fine sediments being delivered to low-order (first to second order) channels in St. John have a high potential of being transported downstream to higher order streams.

A longitudinal profile was surveyed along the third to fourth-order Main Fish Bay Gut and its tributary, Battery Gut (Figure 2). The Main Fish Bay and Battery guts can be divided into three distinct sections based on breaks in slope and changes in channel morphology. The first section is in the lower Fish Bay area where a 0.37-km long channel with an average slope of 2% cuts through alluvial fan deposits. This portion of the channel appears to have been created in the 1970's when the Fish Bay Estate area was starting to be developed. The apparent goal of this work was to prevent flooding of the low-lying areas by channeling the runoff directly into Fish Bay. The channel appears to have developed morphologies that can be described as step-pool and planar (Montgomery and Buffington, 1997).

The 1.6-km middle portion of the channel is characterized by an average slope of 7%, cascade and step-pool morphologies, a general absence of fine sediment deposits, and an abundance of bedrock exposures and large boulders. The change from a gently-sloped channel in the low-lying areas to a steep channel in the headwater areas is considered to be representative of the third-order streams draining to the southern coast of St. John.

The 1.4-km uppermost section of the channel has an average slope of 4%, step-pool and plane-bed morphologies, and a streambed dominated by cobbles and boulders with occasional patches of fine sediment.

Figure 2 shows the location of stream segments where the particle-size distribution of the streambed surface was determined. Points with significant sediment inputs are also shown. On average, 21% of the streambed surface in the upper and lower reaches is composed of particles finer than 2 mm (Figures 3a and 3b). The volume of fine sediment stored on the streambed was calculated assuming: (1) sediment storage only occurred along the 0.37-km lower reaches and 1.4-km upper reaches of the channel; (2) fine sediment occupies 21% of the 1.8-km of streambed

where sediment was present; (3) a channel average width of 9 m can be approximated as the mean width of the surveyed cross-sections; and (4) the depth of the fine sediment deposits is 0.08 m, which equals the mean D_{84} of the streambed sediment. On this basis an estimated 270 m^3 of fine sediment is stored on the streambed surface. Assuming a dry bulk density of 1.4 tons m^{-3} , this converts to 380 tons of fine sediment.

A closer look at the spatial distribution of fine sediment stored on the channel streambed shows that it is not evenly distributed throughout the entire length of the fluvial network and that these deposits are likely to be only temporary features of the channel. Channels in steady-state experience no net deposition or scour as the amount of sediment being delivered is balanced by the mass being transported out. An increase in the amount of fine sediment being stored on the streambed indicates an increase in the amount of sediment being delivered into the fluvial system (Kinnerson, 1990).

Sections with anomalously high quantities of fine sediment can be identified by plotting selected particle-size percentiles against stream gradient. Figure 4 shows the relationship between three particle-size percentiles (D_{16} , D_{50} , and D_{84}) and channel slope for the Main Fish Bay Gut and Battery Gut. This shows that the expected positive relationship between slope and particle size is disrupted at three locations. At these three sites the streambed is finer than other sites with similar slopes. The excess of fine sediment in these reaches appears to be related to their downstream location relative to very important inputs of sediment into the main channel. These inputs include sediment produced from several steep and unpaved roads on the upper portions of the Fish Bay basin.

The storage of fine sediment along the channel reaches with anomalously fine streambeds is expected to be temporary due to the ephemeral nature of channel flows that permits the accumulation of sediment during periods with little or no flow. The sediment transport capacity was estimated at 12 different stream reaches from the ratio of particle settling velocities (ω_o) to shear flow velocities (u^*). While settling velocities are proportional to particle size, shear

velocities equal the square root of the product of gravitational acceleration, flow depth, and channel slope. Laboratory experiments have shown that when ω_o/u^* equals or exceeds 1.0, flows can suspend those particles with settling velocities slower than ω_o (Middleton, 1976). Settling velocities for coarse sand (2 mm) and medium gravel (8 mm) at water temperatures of 20° Celsius are 0.112 and 0.338 m s⁻¹, respectively (Julien, 1995). Calculated u^* values calculated for 12 reaches stream segments along the Main Fish Bay and Battery Guts show that even on stream segments with a 1% slope, a flow depth of 0.10 m is sufficient to keep material finer than coarse sand in suspension (Table 1). For the 12 stream reaches these flow depths represent on average only 12% of the channel depth at bankfull stage, which indicates that the entire fluvial network is capable of transporting sediment finer than 2 mm in suspension even during low flows. The relatively low flows required to transport fine sediment (< 2 mm) along the entire stream network leads to the conclusion that the anomalous abundance of fine sediments along several stream segments represent only temporary storage of sediment that has occurred after the last flow event.

Table 1 also shows that critical flow depths needed to transport medium gravel in suspension are much higher than those for coarse sand and they generally represent flow depths greater than bankfull. Hence particles coarser than 2 mm will tend to be transported as bed load and are likely to remain in the fluvial system for much longer than the sediment finer than 2 mm.

References cited

- Julien PY. 1995. Erosion and Sedimentation. Cambridge Univ. Press, New York, NY, 280 p.
- Kinnerson D. 1990. Bed surface response to sediment supply. MS thesis, University of California, Berkeley, CA.
- Middleton G. 1976. Hydraulic interpretation of sand size distributions. *Journal of Geology* 84: 405-426.
- Montgomery DR, and Buffington J. 1997. Channel reach morphology in mountain drainage basins. *GSA Bulletin* 109(5): 596-611.
- Reid LM, Dunne T. 1996. Rapid evaluation of sediment budgets. Reiskirchen, Germany: Catena Verlag, 164 p.
- Ramos CE. 1996. Quantification of Stream Channel Morphological Features: Recommended Procedures for Use in Watershed Analysis and TFW Ambient Monitoring. Timber-Fish & Wildlife, TFW-AM 9-96-006, 89 p.
- Wolman, G. (1954) A method of sampling coarse river-bed material. *Transactions American Geophysical Union* 35(6):951-956.

Figure 1a. Longitudinal profile of Reef Bay 1st-order Gut-A.

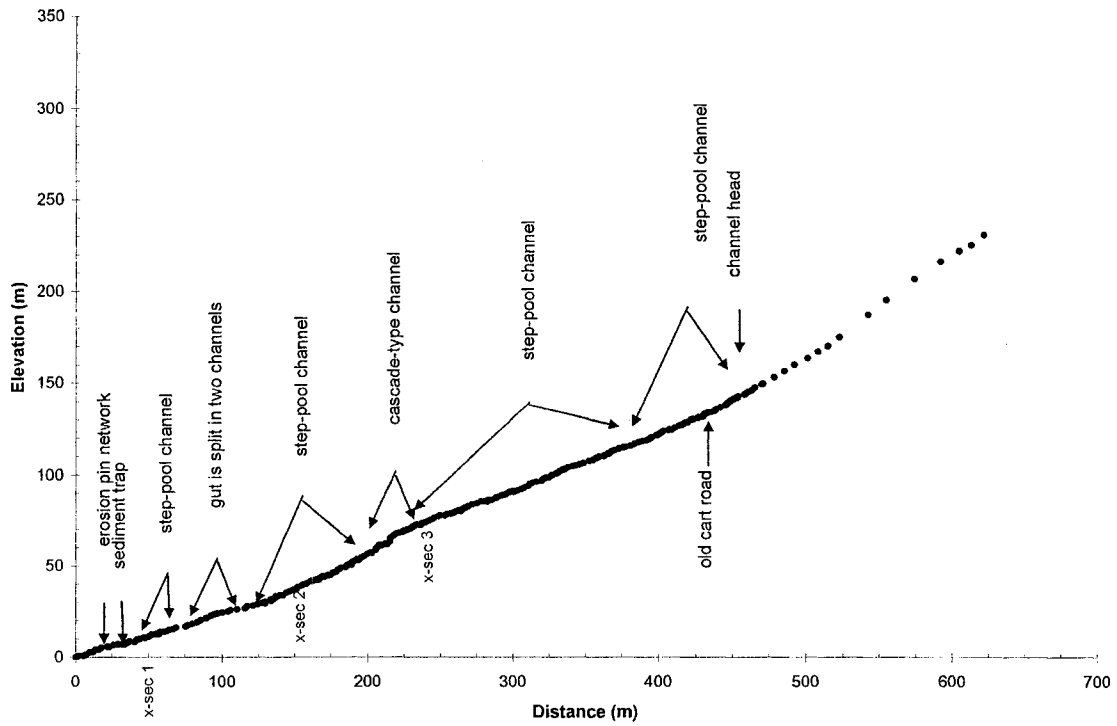


Figure 1b. Longitudinal profile of Reef Bay 1st-order Gut-B.

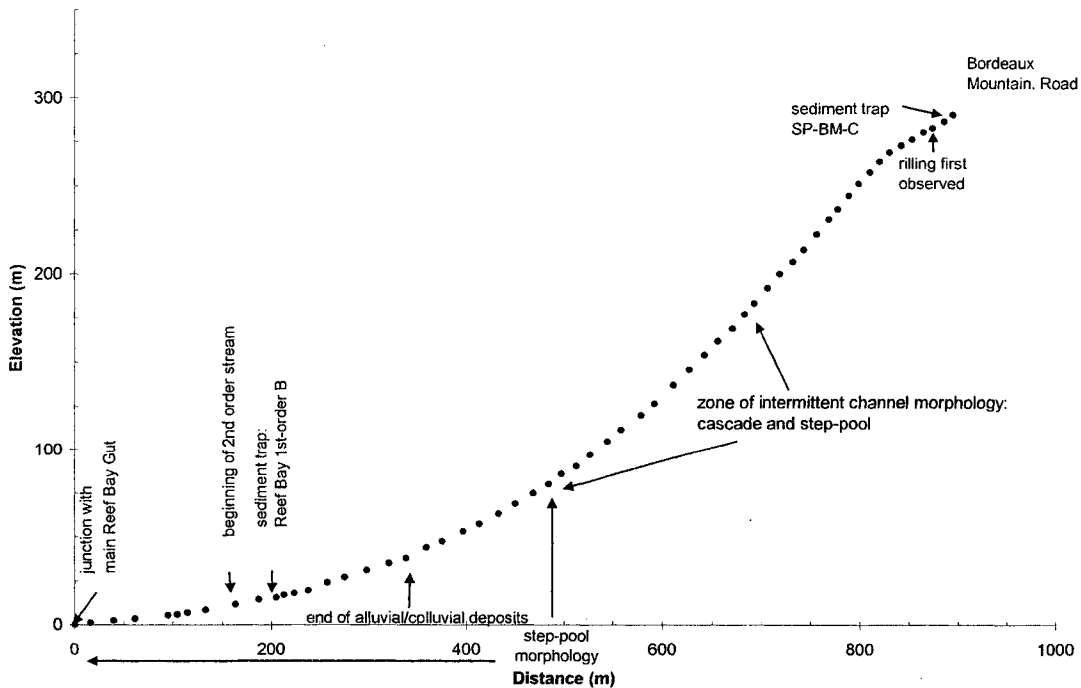


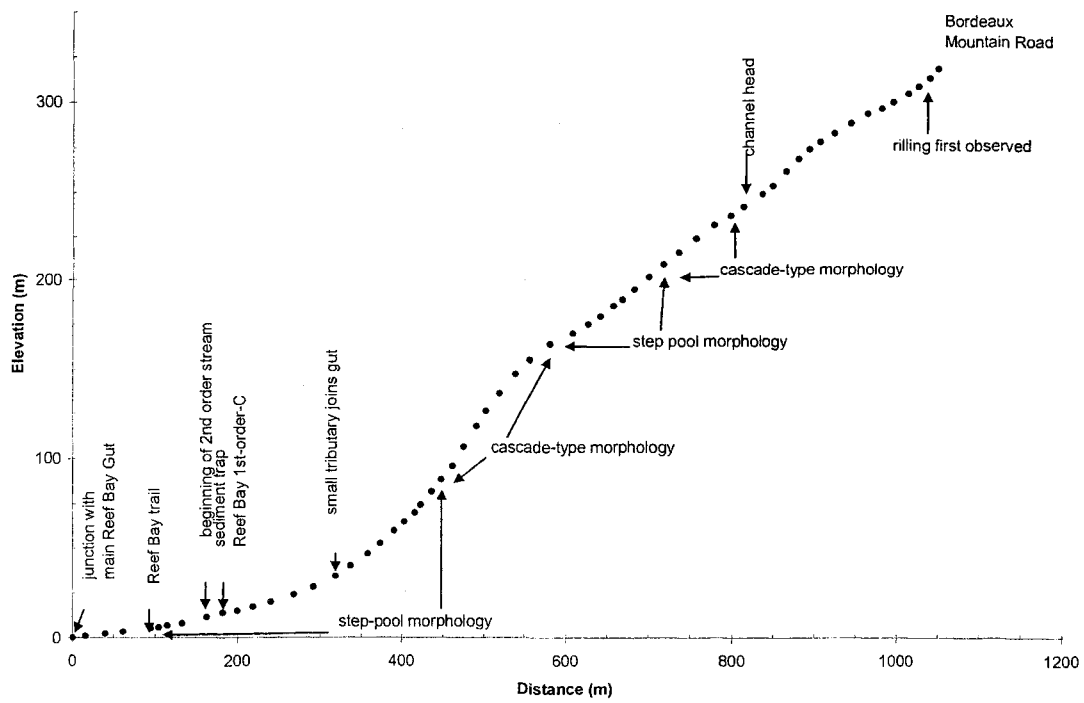
Figure 1c. Longitudinal profile of Reef Bay 1st-order Gut-C.

Figure 2. Longitudinal profile of Fish Bay Gut and Battery Gut. Solid arrows indicate points where the particle-size distribution of the streambed surface was determined, while dashed arrows signal the location of important sediment inputs.

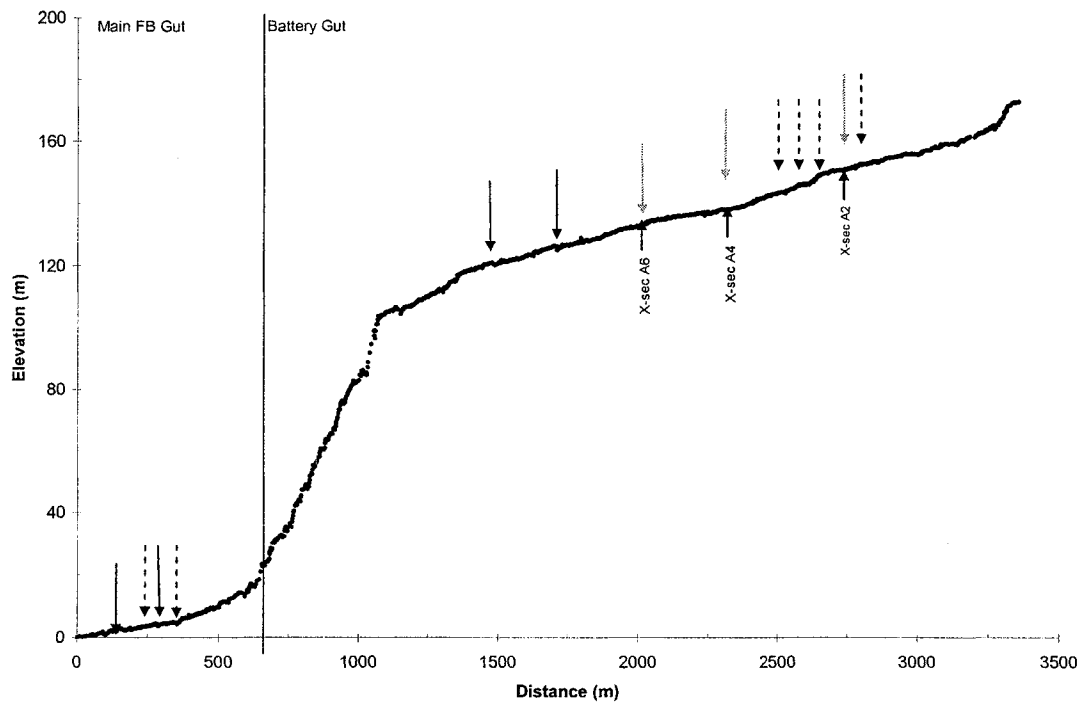


Figure 3a. Streambed surface particle-size distribution measured at several cross-sections along the Main Fish Bay Gut and Battery Gut. Distributions shown in this figure appear to be correlated with channel slope (Figure 4).

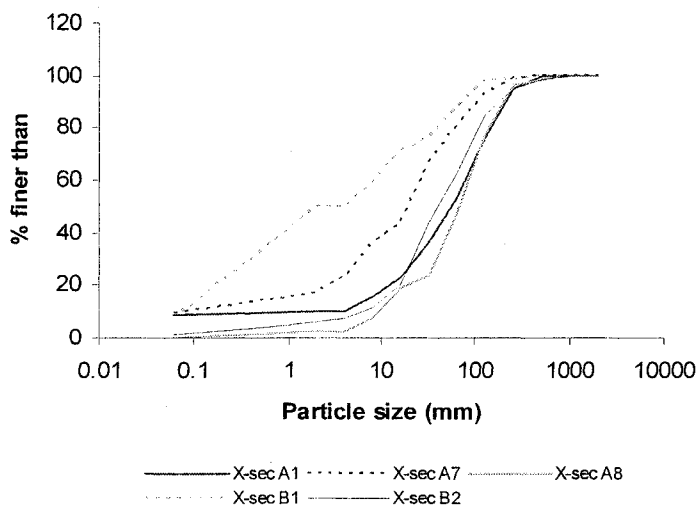


Figure 3b. Streambed surface particle-size distribution measured at several cross-sections along the Main Fish Bay Gut and Battery Gut. Distributions shown in this figure appear to be anomalously fine for their channel slope (Figure 4).

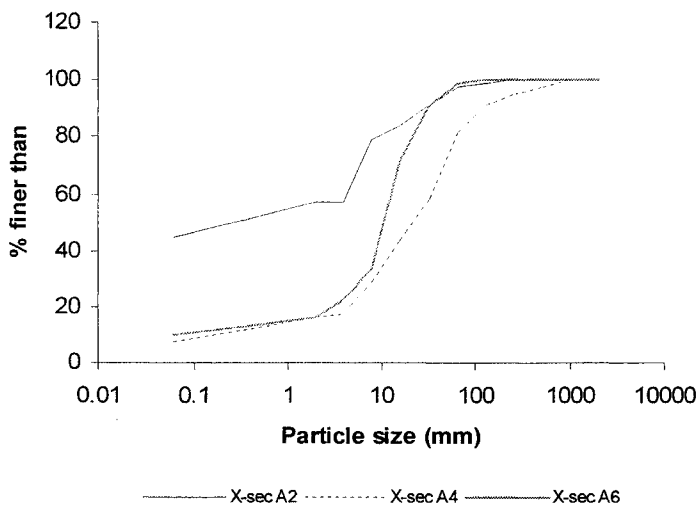


Figure 4. Relationship between slope and the 16th, 50th, and 84th percentile of the particle-size distributions from Main Fish Bay Gut. Points in gray refer to the gray arrows in Figure 2.

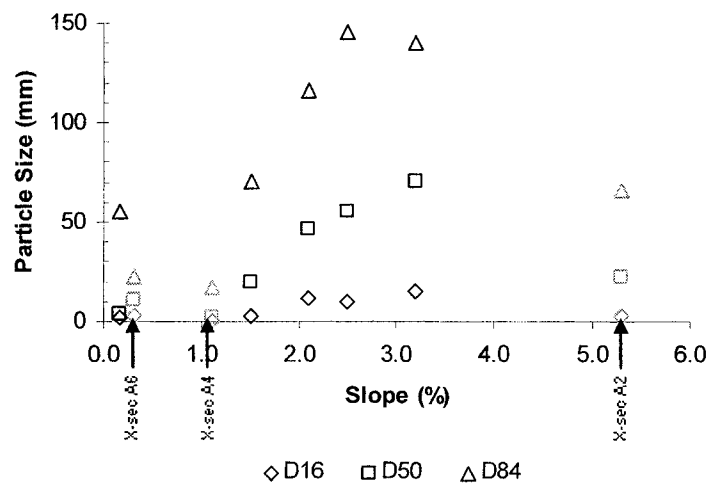


Figure 5. Longitudinal profile for the Greater Lameshur Bay Gut.

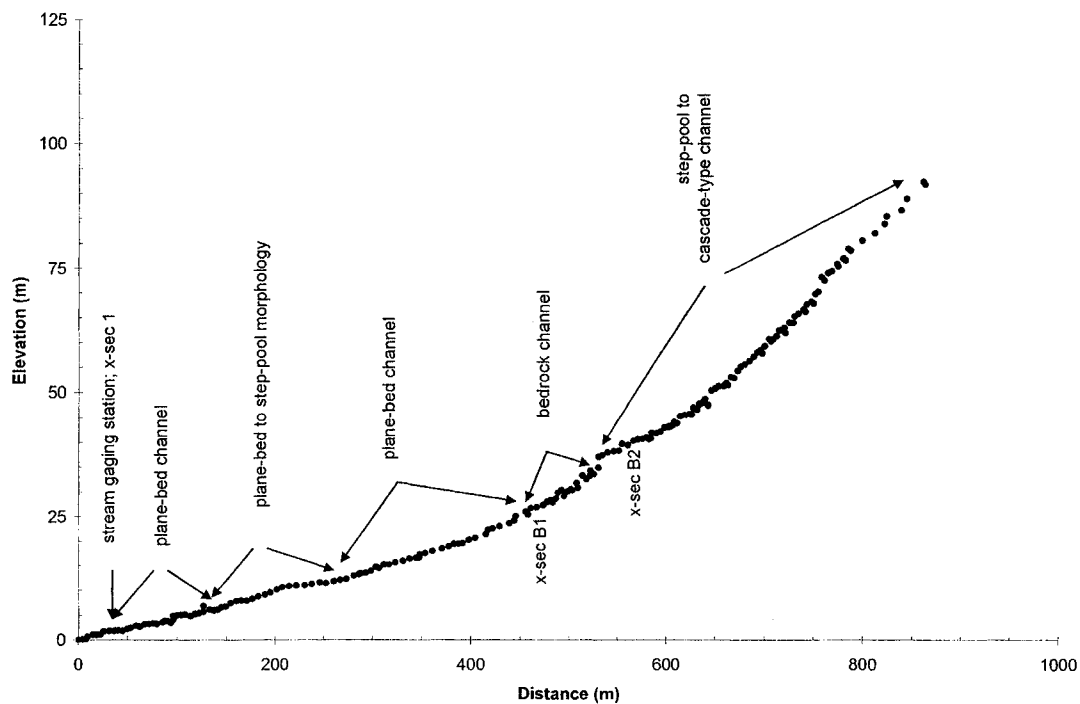


Figure 6. Particle-size distribution at three cross-sections surveyed along Greater Lameshur Bay Gut.

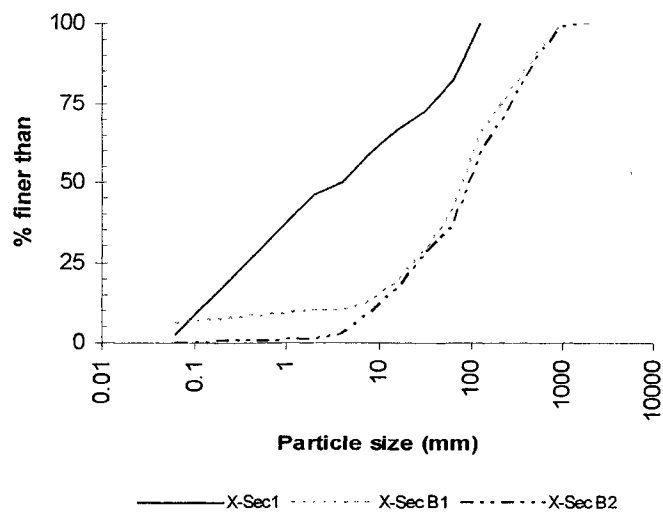


Table 1. Channel characteristics and critical flow depths for twelve reaches along the Main Fish Bay Gut and Battery Gut.

Long-Profile distance* (km)	Slope (m m ⁻¹)	Channel depth at bankfull (m)	Critical flow depth to maintain sand in suspension (m)	Critical flow depth to maintain medium gravel in suspension (m)
3.26	0.03	0.64	0.05	0.47
3.12	0.01	0.42	0.12	1.06
2.80	0.01	0.38	0.09	0.83
2.65	0.05	0.51	0.02	0.22
2.48	0.02	0.34	0.05	0.49
2.30	0.01	0.46	0.10	0.90
1.98	0.02	0.44	0.06	0.56
1.70	0.04	0.38	0.03	0.31
1.33	0.08	0.50	0.02	0.14
0.73	0.13	1.04	0.01	0.10
0.36	0.02	0.81	0.06	0.56
0.18	0.02	1.21	0.08	0.73

*Distances refer to those in Figure 2.

APPENDIX IV-B
SPATIAL DATABASE REQUIREMENTS FOR APPLICATION OF
ST. JOHN EROSION MODEL (STJ-EROS)

Attribute data descriptions and maps

for the following GIS data layers:

stj_bd, fb_bd, lb_bd, cb_bd, gps_dra, gps_rds, stj_str, banks, sed_del

ST. JOHN EROSION MODELING- SPATIAL DATABASE LAYER DEFINITION

Layer: **stj_bd**

Type: Polygon layer; UTM projection-Zone 20; Units in meters

Description: Contains the coastal boundaries of the island of St. John and adjacent cays as defined by USGS topographic maps.

Table Items:

<u>Name</u>	<u>Width</u>	<u>Type</u>	<u>Decimal Places</u>
AREA	13	N	0
PERIMETER	13	N	0
STJ_BD_	11	N	0
STJ_BD_ID	11	N	0

Item description:

<u>Name</u>	<u>Description</u>
AREA	ArcInfo item defining the total areal layerage of each polygon.
PERIMETER	ArcInfo item defining the total perimeter of each polygon.
STJ_BD_	ArcInfo identification number.
STJ_BD_ID	ArcInfo user identification number.

Uses in STJ-EROS: Used in the surf_erosion routine to create a 30 m coastline buffer. This buffer is created to avoid estimating sediment production rates from these areas as they are likely to be layered by beach deposits or rocky promontories.

ST. JOHN EROSION MODELING-- SPATIAL DATABASE LAYER DEFINITION

Layer: **fb_bd**

Type: Polygon layer; UTM projection-Zone 20; Units in meters

Description: Contains the boundaries of the entire Fish Bay basin as defined by 40 ft contours.

Table Items:

<u>Name</u>	<u>Width</u>	<u>Type</u>	<u>Decimal Places</u>
AREA	13	N	0
PERIMETER	13	N	0
FB_BD_	11	N	0
FB_BD_ID	11	N	0

Item description:

<u>Name</u>	<u>Description</u>
AREA	ArcInfo item defining the total areal layerage of each polygon.
PERIMETER	ArcInfo item defining the total perimeter of each polygon.
FB_BD_	ArcInfo identification number.
FB_BD_ID	ArcInfo user identification number.

Uses in STJ-EROS: If the user chooses to run the model for the Fish Bay basin this layer is used by the following routines: a) Del_potential- By using a clip command this routine uses this layer to exclude areas outside of the Fish Bay basin from sed_del (delivery potential data layer); b) Rd_erosion- By using a clip command this routine uses this layer to exclude all road drainage points in gps_dra outside of the Fish Bay basin; and c) Surf_erosion- By using a clip command this routine uses this layer to remove all buffered coastlines located outside of the Fish Bay basin.

ST. JOHN EROSION MODELING- SPATIAL DATABASE LAYER DEFINITION

Layer: **lb_bd**

Type: Polygon layer; UTM projection-Zone 20; Units in meters

Description: Contains the boundaries of the entire Lameshur Bay basin as defined by 40 ft contours.

Table Items:

<u>Name</u>	<u>Width</u>	<u>Type</u>	<u>Decimal Places</u>
AREA	13	N	0
PERIMETER	13	N	0
LB_BD_	11	N	0
LB_BD_ID	11	N	0

Item description:

<u>Name</u>	<u>Description</u>
AREA	ArcInfo item defining the total areal layerage of each polygon.
PERIMETER	ArcInfo item defining the total perimeter of each polygon.
LB_BD_	ArcInfo identification number.
LB_BD_ID	ArcInfo user identification number.

Uses in STJ-EROS: If the user chooses to run the model for the Lameshur Bay basin this layer is used by the following routines: a) Del_potential- By using a clip command this routine uses this layer to exclude areas outside of the Lameshur Bay basin from sed_del (delivery potential data layer); b) Rd_erosion- By using a clip command this routine uses this layer to exclude all road drainage points in gps_dra outside of the Lameshur Bay basin; and c) Surf_erosion- By using a clip command this routine uses this layer to remove all buffered coastlines located outside of the Lameshur Bay basin.

ST. JOHN EROSION MODELING– SPATIAL DATABASE LAYER DEFINITION

Layer: **cb_bd**

Type: Polygon layer; UTM projection-Zone 20; Units in meters

Description: Contains the boundaries of portions of the Cinnamon Bay basin as defined by 40 ft contours. The area defined under this layer does not include the sub-catchment draining into Peter Bay.

Table Items:

<u>Name</u>	<u>Width</u>	<u>Type</u>	<u>Decimal Places</u>
AREA	13	N	0
PERIMETER	13	N	0
CB_BD_	11	N	0
CB_BD_ID	11	N	0

Item description:

<u>Name</u>	<u>Description</u>
AREA	ArcInfo item defining the total areal coverage of each polygon.
PERIMETER	ArcInfo item defining the total perimeter of each polygon.
CB_BD_	ArcInfo identification number.
CB_BD_ID	ArcInfo user identification number.

Uses in STJ-EROS: If the user chooses to run the model for the Cinnamon Bay basin this layer is used by the following routines: a) Del_potential- By using a clip command this routine uses this layer to exclude areas outside of the Cinnamon Bay basin from sed_del (delivery potential data layer); b) Rd_erosion- By using a clip command this routine uses this layer to exclude all road drainage points in gps_dra outside of the Cinnamon Bay basin; and c) Surf_erosion- By using a clip command this routine uses this layer to remove all buffered coastlines located outside of the Cinnamon Bay basin.

ST. JOHN EROSION MODELING-- SPATIAL DATABASE LAYER DEFINITION

Layer: **gps_dra**

Type: Point layer, UTM projection-Zone 20; Units in meters

Description: Contains locations of all road drainage structures within the Lameshur Bay and Fish Bay basins, as well as portions of the Bordeaux Mountain road, Catherineberg, Maho Bay, and Susannaberg Estates, and Haulover Bay. Full description of all attributes currently exist only for those drainage structures within the Fish Bay basin, the Lameshur Bay basin, and those along John Head Road in the Catherineberg area draining into Cinnamon Bay.

Table Items:

<u>Name</u>	<u>Width</u>	<u>Type</u>	<u>Decimal Places</u>
AREA	13	N	6
PERIMETER	13	N	6
GPS_DRA_	11	N	0
GPS_DRA_ID	11	N	0
TYPE	20	C	0
DRAIN_ID	8	C	0

Item description:

<u>Name</u>	<u>Description</u>
AREA	Area of each drainage point. All areas will equal zero as the layer is built as a point layerage.
PERIMETER	Perimeter of each road drainage point. All perimeters will equal zero as the layer is built as a point layerage.
GPS_DRA_	ArcInfo identification number.
GPS_DRA_ID	ArcInfo user identification number.
TYPE	Describes the type of road drainage structure among the following options: swale, cemented or uncemented swale, culvert, ditch, gut crossing, or unknown.
DRAIN_ID	A user-defined drainage structure identification code. These identification codes correspond to codes in 'gps_rds' and serve to link an individual road segment with a specific road drainage structure. The relationship between a drainage structure and a road segment is not unique as a drainage point may drain more than one road segment. The code consists in two or three letters followed by a number. The letters identify the general location of the drainage point as follows: 'ufb'- Adrian Estate and portions of Catherineberg Estate in the upper Fish Bay basin; 'lfb'- Fish Bay Estate in the lower Fish Bay basin; 'le'- L'Esperance and Sieben Estates within the Fish Bay basin; 'cb'- Catherineberg Estate draining towards Cinnamon Bay; and 'lb'- entire Lameshur Bay basin. The numbers identify specific drains within each one of the zones.

Uses in STJ-EROS: Used by the rd_erosion routine. The location of each individual road drainage point is used in combination with the chosen basin boundary to eliminate points located outside of the area. This layer is also used to identify the sediment delivery potential of each drainage point. A joinitem command is used by this routine to link the delivery potentials of the drainage points with their respective road segments by way of the drain_id item.

ST. JOHN EROSION MODELING-- SPATIAL DATABASE LAYER DEFINITION

Layer: **gps_rds**

Type: Line layer; UTM projection-Zone 20; Units in meters

Description: Contains locations of all roads within the Lameshur Bay and Fish Bay basins, as well as portions of the Bordeaux Mountain road, Catherineberg, Maho Bay, and Susannaberg Estates, and Haulover Bay. Full description of all attributes currently exist only for those roads within the Fish Bay basin, the Lameshur Bay basin, and those along John Head Road in Catherineberg Estate.

Table Items:

<u>Name</u>	<u>Width</u>	<u>Type</u>	<u>Decimal Places</u>
FNODE_	11	N	0
TNODE_	11	N	0
LPOLY_	11	N	0
RPOLY_	11	N	0
LENGTH	13	N	6
GPS_RDS_	11	N	0
GPS_RDS_ID	11	N	0
SURFACE	16	C	0
LENGTH_M	8	N	0
WIDTH_M	8	N	1
SLOPE	8	N	2
GRADING	16	C	0
SOURCE	16	C	0
DRAIN_ID	8	C	0
BASIN	8	C	0

Item description:

<u>Name</u>	<u>Description</u>
FNODE_	ArcInfo topological item. All values equal to zero as the layer was built with line features.
TNODE_	ArcInfo topological item. All values equal to zero as the layer was built with line features.
LPOLY_	ArcInfo topological item. All values equal to zero as the layer was built with line features.
RPOLY_	ArcInfo topological item. All values equal to zero as the layer was built with line features.
LENGTH	ArcInfo item defining the map length of the linear feature.
GPS_RDS_	ArcInfo identification number.
GPS_RDS_ID	ArcInfo user identification number.
SURFACE	Describes whether the road surface is paved or unpaved.
LENGTH_M	Defines the field measured length of each individual road segment in meters.
WIDTH_M	Defines the field measured average width of each individual road segments in meters.

SLOPE	Defines the field measured areally-averaged slope of each individual road segment in percent ($m\ m^{-1}$).
GRADING	Describes the frequency at which unpaved road segments are regraded according to the following three categories: 1) graded- roads that are graded for more than two years; 2) ungraded- roads that have not been graded in the last two years; 3) abandoned- roads that are infrequently used by light vehicles and have not been graded in over fifteen years.
SOURCE	Describes whether spatial data was collected by a GPS unit or it was derived from an already existing road USGS layer.
DRAIN_ID	A user-defined drainage structure identification code. These identification codes correspond to codes in 'gps_dra' and serve to link an individual road segment with a specific road drainage structure. The relationship between a drainage structure and a road segment is not unique as a drainage point may drain more than one road segment. The code consists in two or three letters followed by a number (See 'gps_dra' layer description for explanation.).
BASIN	Defines the watershed where the sediment produced by the road is discharged. A two-letter code is used for this item: 'cb'- Cinnamon Bay sub-catchment; 'fb'- Fish Bay basin; and 'lb'- Lameshur Bay basin.

Uses in STJ-EROS: Used by the rd_erosion routine. A copy of gps_rds is created by this routine. The drain_id item in this new layer is used to determine the delivery potential for each road segment by way of a joinitem command with a newly created road drainage layer. The length_m, width_m, slope, grading, and del_ratio items are used to calculate road and outslope sediment production and delivery. At the end of the rd_erosion routine the gps_rds copy layer contains all of the models road-related sediment production and delivery estimates.

ST. JOHN EROSION MODELING-- SPATIAL DATABASE LAYER DEFINITION

Layer: **stj_str**

Type: Line layer; UTM projection-Zone 20; Units in meters

Description: Stream data layer for the entire island of St. John. The layer contains all stream features contained in USGS topographical maps, as well as stream extensions based on field reconnaissance. A channel was defined in the field by the presence of a morphological feature with a recognizable bank and a streambed composed of fluvial deposits.

Table Items:

<u>Name</u>	<u>Width</u>	<u>Type</u>	<u>Decimal Places</u>
FNODE_	11	N	0
TNODE_	11	N	0
LPOLY_	11	N	0
RPOLY_	11	N	0
LENGTH	13	N	6
STJ_STR_	11	N	0
STJ_STR_ID	11	N	0
SOURCE	16	C	0

Item description:

<u>Name</u>	<u>Description</u>
FNODE_	ArcInfo topological item. All values equal to zero as the layer was built as a line layer.
TNODE_	ArcInfo topological item. All values equal to zero as the layers was built as a line layer.
LPOLY_	ArcInfo topological item. All values equal to zero as the layers was built as a line layer.
RPOLY_	ArcInfo topological item. All values equal to zero as the layers was built as a line layer.
LENGTH	ArcInfo item defining the map length of the linear feature.
STJ_STR_	ArcInfo identification number
STJ_STR_ID	ArcInfo user identification number.
SOURCE	Describes whether the stream arc was derived from field reconnaissance or from an already existing stream layerage based on USGS maps.

Uses in STJ-EROS: Used by the stream_total routine. A clip command is used by the routine to maintain only the stream segments located within the basin chosen by the user. This new stream layer is then buffered so that it can be overlaid by way of an union command with the polygon layer resulting from the streambank routine. The perimeter of the final layer is used as a surrogate for length to calculate sediment production and delivery by treethrow.

ST. JOHN EROSION MODELING– SPATIAL DATABASE LAYER DEFINITION

Layer: **banks**

Type: Polygon layer; UTM projection-Zone 20; Units in meters

Description: Contains location and attribute data of streams with erodible banks within the Fish Bay, Lameshur Bay, and Reef Bay basins based on field reconnaissance. No significant stream segments with erodible banks were found in the Hawksnest or Cinnamon Bay catchments. Erodible banks are found in St. John in those areas where well-defined stream channel features cut through alluvial/colluvial deposits. Stream segments with erodible banks were isolated and buffered using a 0.25 m buffering distance. Such a short buffer was used so that the total length of stream segments with erodible banks could be approximated as being approximately half of their perimeters.

Table Items:

<u>Name</u>	<u>Width</u>	<u>Type</u>	<u>Decimal Places</u>
AREA	13	N	6
PERIMETER	13	N	6
BANKS_	11	N	0
BANKS_ID	11	N	0
INSIDE	11	N	0
BANK_HT_M	8	N	1

Item description:

<u>Name</u>	<u>Description</u>
AREA	ArcInfo item defining the total areal layerage of each individual stream polygon segment.
PERIMETER	ArcInfo item defining the total perimeter of each individual polygon segment.
BANKS_	ArcInfo identification number.
BANKS_ID	ArcInfo user identification number.
INSIDE	ArcInfo topological item. A value of 100 is assigned for stream polygons and no value is assigned to the universal polygon.
BANK_HT_M	Indicates the approximate height of erodible streambanks in meters. Average height of banks was determined during field surveys.

Uses in STJ-EROS: Used by the streambank routine. First, a new layer is created by an intersect command using this layer and a delivery potential layer created during the del_potential routine. This new layer contains bank segments within the basin chosen by the user with their corresponding perimeter, bank_ht_m, and del_ratio items. Table commands are used to calculate sediment production and delivery for each stream segment.

ST. JOHN EROSION MODELING- SPATIAL DATABASE LAYER DEFINITION

Layer: **sed_del**

Type: Polygon layer; UTM projection-Zone 20; Units in meters

Description: Displays the spatial distribution of the potential for terrestrial sediments to be delivered to the marine environments. The criteria used to develop the delivery potential zones is based on the interaction between guts draining a specific sub-catchment within a basin and detention ponds, salt ponds, or wetland areas (see description below). Sediment delivery potential zones have been defined for the entire Fish Bay and Lameshur Bay basins, and all sub-catchments draining into Cinnamon Bay with the exception of those draining directly into Peter Bay.

Table Items:

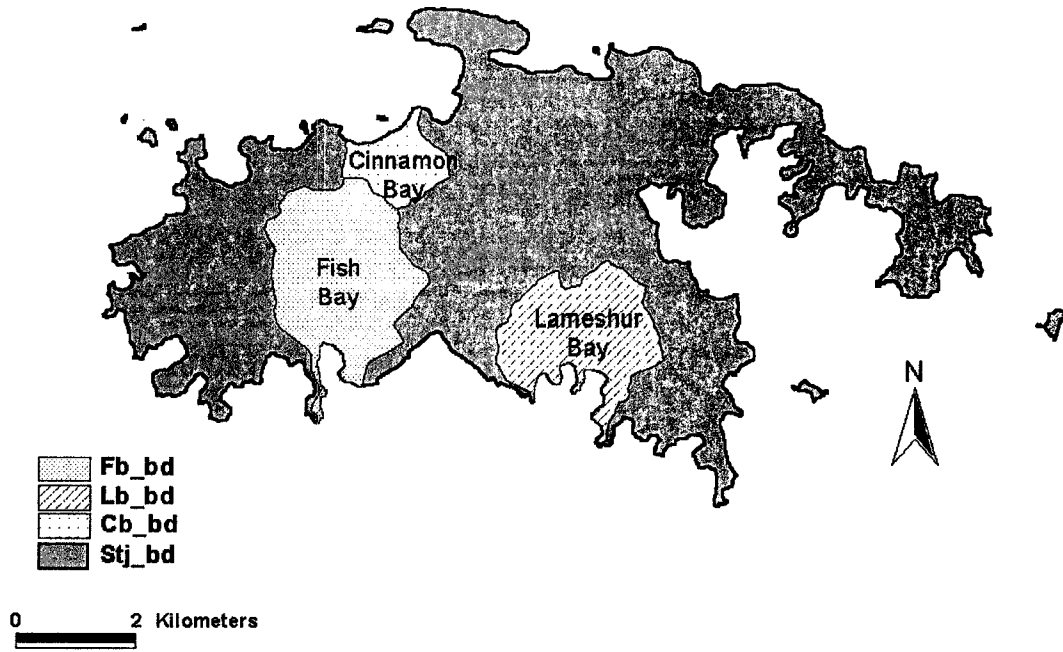
<u>Name</u>	<u>Width</u>	<u>Type</u>	<u>Decimal Places</u>
AREA	13	N	6
PERIMETER	13	N	6
SED_DEL_	11	N	0
SED_DEL_ID	11	N	0
POTENTIAL	10	C	0

Item description:

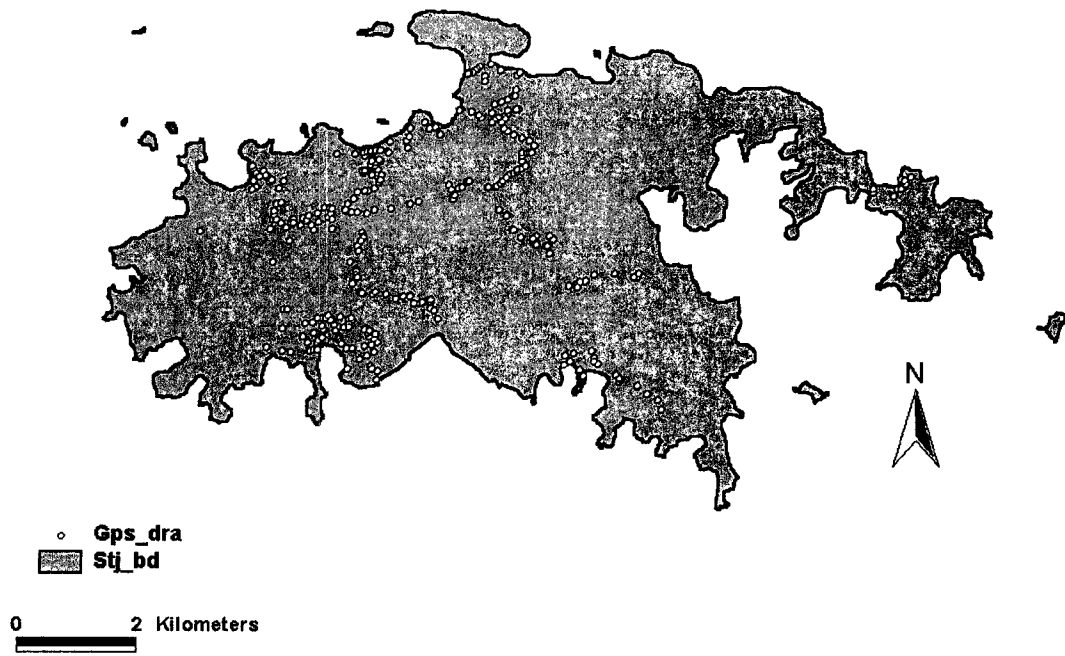
<u>Name</u>	<u>Description</u>
AREA	ArcInfo item defining the total areal layerage of each delivery potential polygon.
PERIMETER	ArcInfo item defining the total perimeter of each delivery potential polygon.
SED_DEL_	ArcInfo identification number.
SED_DEL_ID	ArcInfo user identification number.
POTENTIAL	A qualitative description of the potential for terrestrial sediment delivery into the marine environment based on the interaction between a gut draining an area and any detention ponds, salt ponds, or wetland areas. Areas are divided into one of the following four categories: 1) 'no'- Areas with no potential for sediment delivery include those drained by a gut that is interrupted by a pond or unchannelled area and lacks any surface pathway connecting it to the marine environment; 2) 'moderate'- areas that drain into a pond or wetland area that has a channel-like feature connecting it with the marine environment; 3) 'wetlands'- All wetland areas are identified separately, but they are considered to have the same delivery potential as moderate areas; and 4) 'high'- areas drained by a gut that is not interrupted by any pond or wetland area, so that it is able to directly deposit sediment into the marine environment.

Uses in STJ-EROS: Used by the del_potential routine. A clip command is used by this routine to select only those delivery potential areas within the basin chosen by the user. The newly created layer, del_bd, is then used by the rd_erosion, streambank, stream_total, and surf_er routines to assign sediment delivery ratios to numerous layers which allows the calculation of sediment yield rates

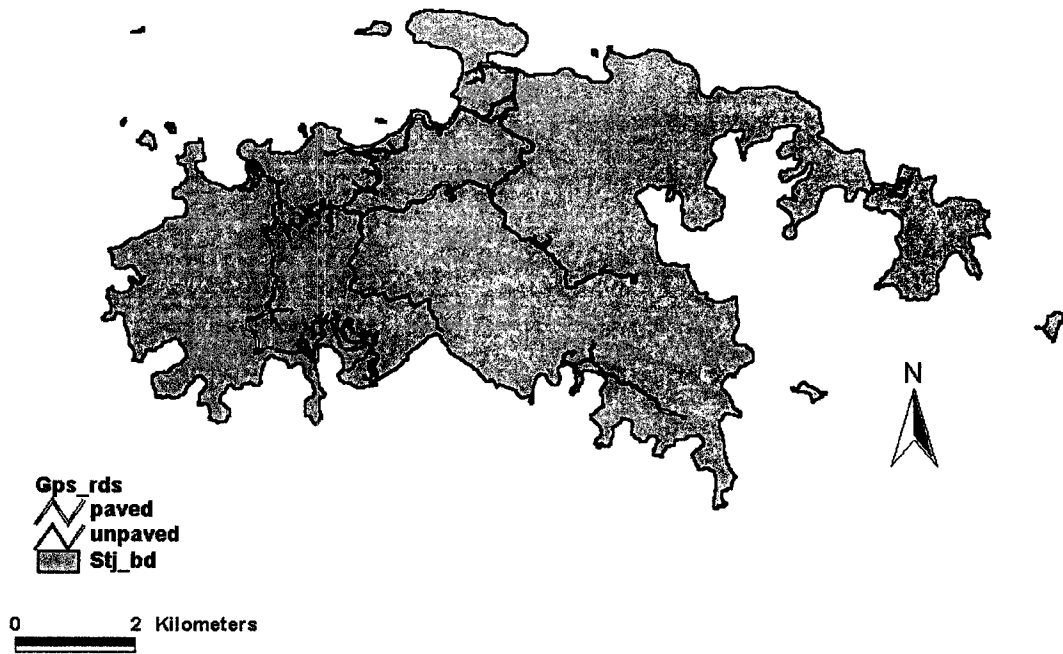
Layer names: fb_bd, lb_bd, cb_bd & stj_bd



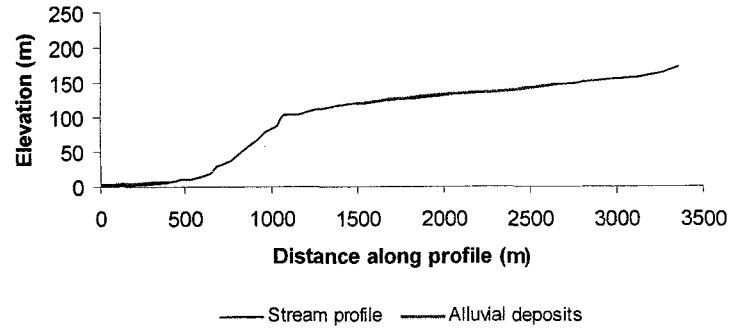
Layer names: gps_dra & stj_bd



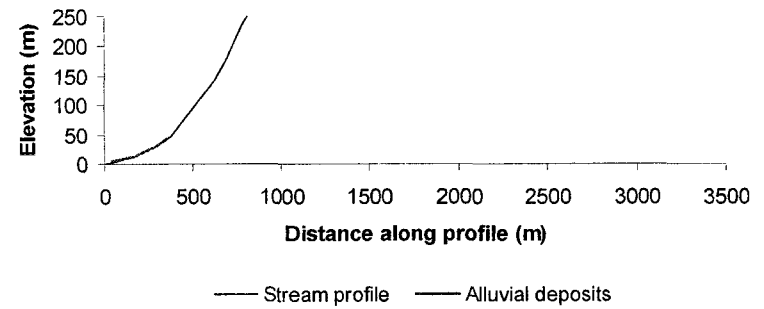
Layer names: gps_rds & stj_bd



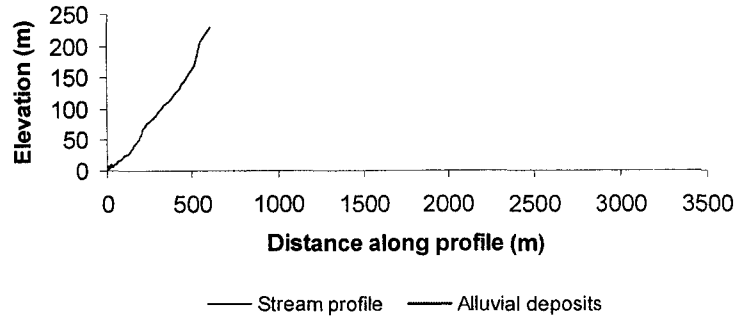
Appendix IV-B. Long profile of Fish Bay Gut and Battery Gut showing the location of eroding banks.



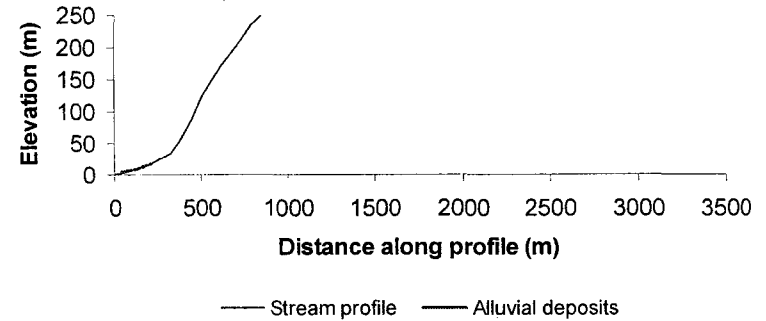
Appendix IV-B- Long profile of Reef Bay 1st-order B showing the location of eroding banks.



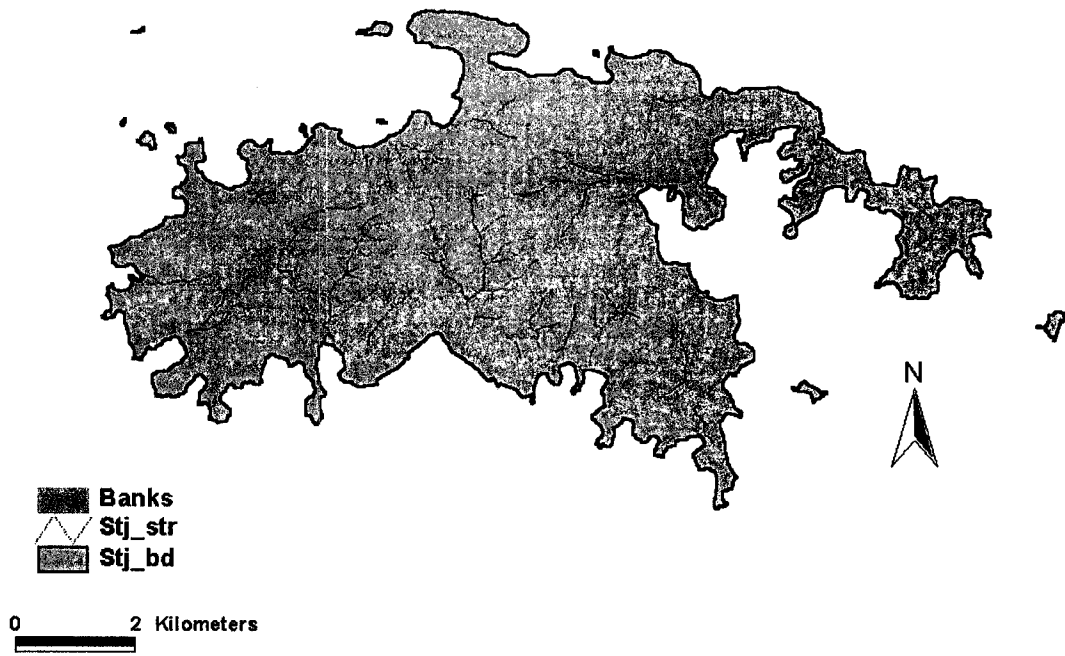
Appendix IV-B- Long profile of Reef Bay 1st-order A showing the location of eroding banks.



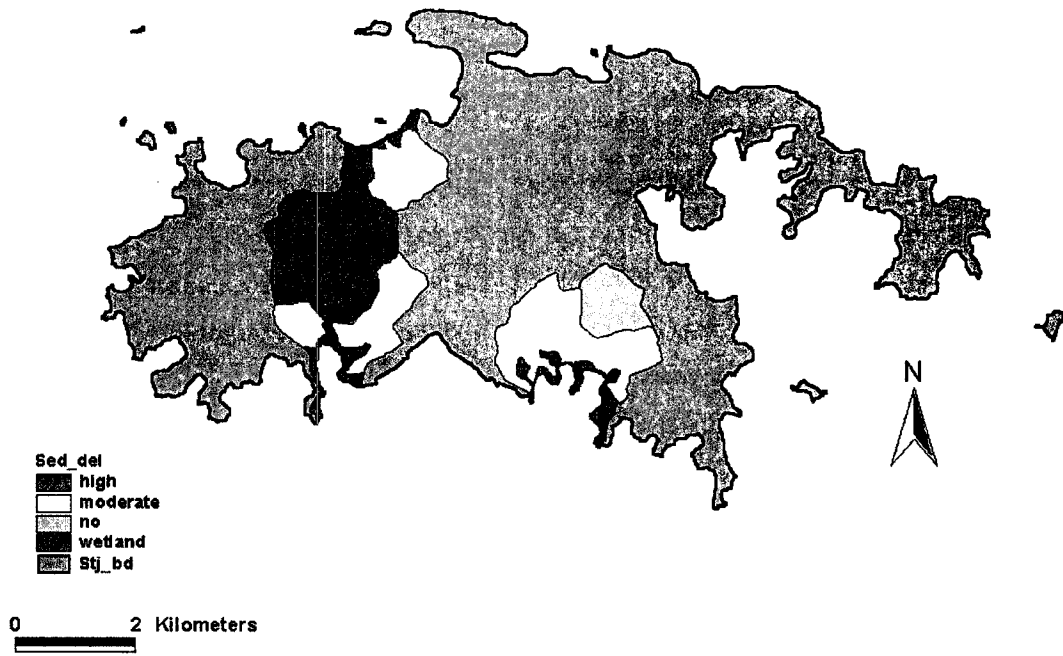
Appendix IV-B- Long profile of Reef Bay 1st and 2nd-order C showing the location of eroding banks.



Layer names: banks, stj_str & stj_bd



Layer names: sed_del & stj_bd



APPENDIX IV-C

ST. JOHN EROSION MODEL (STJ-EROS) ROUTINE FLOWCHARTS

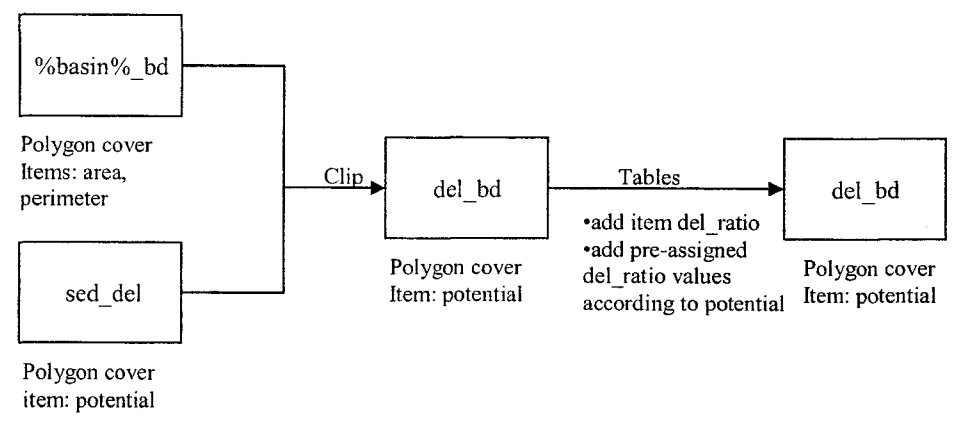
Pre-set variables:

- Treethrow: Defines sediment production from threethrow processes along streambanks at a rate of $0.17 \text{ tons km}^{-1} \text{ yr}^{-1}$
- Bank_er: Defines sediment production from streambank erosion at a rate of $10 \text{ kg m}^{-2} \text{ yr}^{-1}$
- Undisturbed: Defines surface erosion of undisturbed hillslopes at a rate of $0.001 \text{ kg m}^{-2} \text{ yr}^{-1}$
- Abandoned: Defines surface erosion of abandoned roads at $0.0067 \text{ kg m}^{-2} \text{ yr}^{-1}$
- Ungraded: Defines a linear regression term that defines surface erosion from ungraded roads at $1.88 \text{ kg m}^{-2} \text{ cm}^{-1} \text{ m m}^{-1}$
- Graded: Defines a linear regression term that defines surface erosion from graded roads at $4.73 \text{ kg m}^{-2} \text{ cm}^{-1} \text{ m m}^{-1}$
- Silt_loss: Ratio of actual sediment production rates to those measured from sediment traps for the silt-size sediment fraction. Value set equal to 9.
- Silt_u_rd_fr, silt_g_rd_fr, silt_a_rd_fr, silt_se_fr: The silt-size sediment fraction from ungraded roads (u), graded roads (g), abandoned roads (a), and undisturbed hillslopes (se).
- Un_sus_fr, gr_sus_fr, ab_sus_fr, bank_sus_fr, tree_sus_fr, se_sus_fr: Sediment finer than 2 mm measured or estimated for ungraded roads (un), graded roads (gr), abandoned roads (ab), streambanks (bank), treethrow (tree), and undisturbed hillslopes (se).

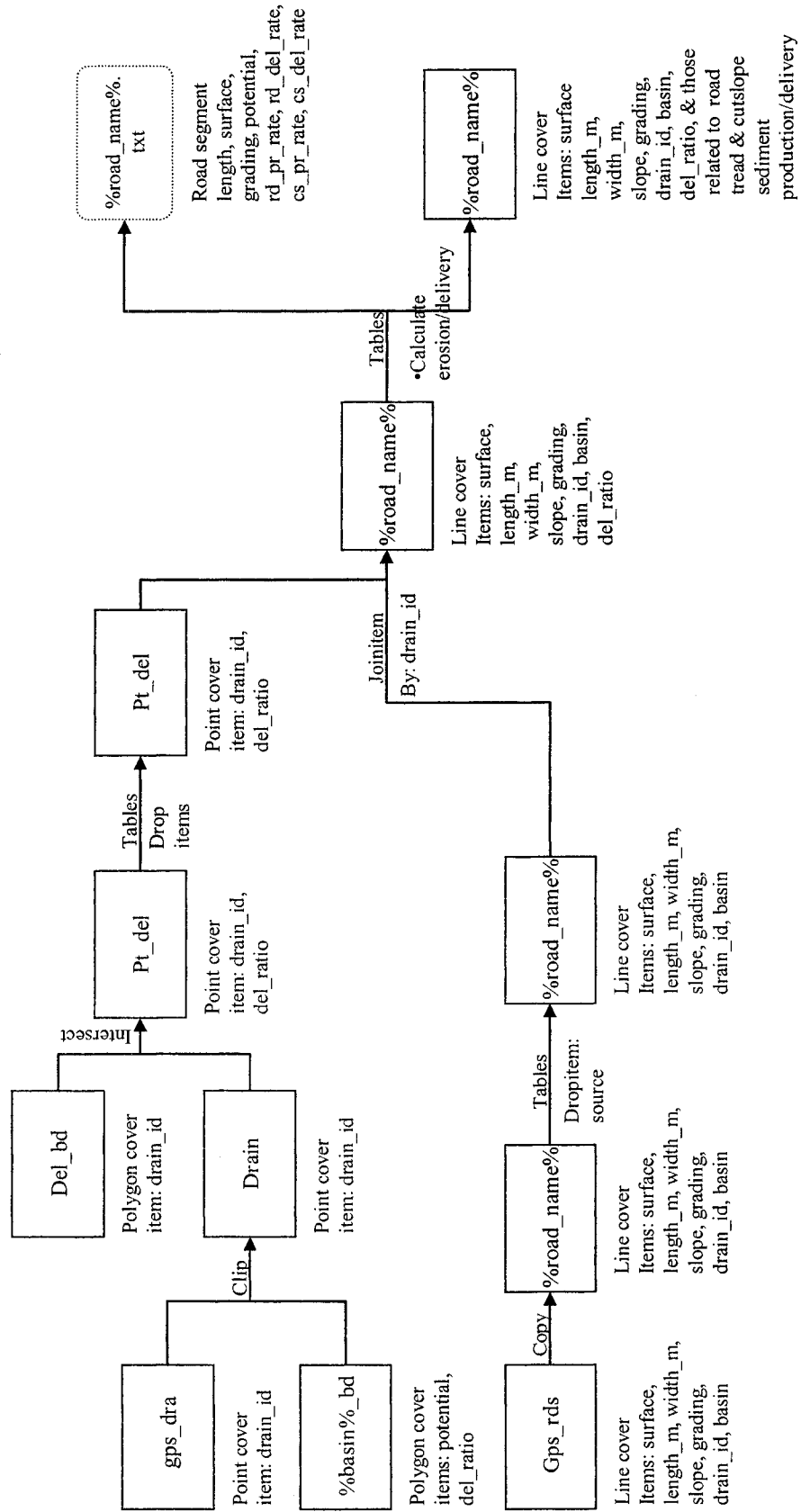
User-defined variables:

- Hi_pot: Defines the sediment delivery ratio for areas with high delivery potential.
- Mod_pot: Defines the sediment delivery ratio for wetland areas and those defined as having a moderate delivery potential.
- Basin: Defines the basin where the model is to be applied among the following three choices: Fish Bay (fb), Lameshur Bay (lb), and Cinnamon Bay (cb)
- Years: Defines the total time in years for which sediment production estimates are to be calculated.
- Rain_rate: Defines the total rainfall in cm yr^{-1} to be used for road erosion calculations.
- $\text{Rain} = \text{rain_rate} * \text{years}$
- Road_name: Defines the name of text file and cover containing the results of the road sediment production and delivery analysis.
- Nat_name: Defines the name of the text file and cover containing the results of the natural sediment production and delivery analysis.

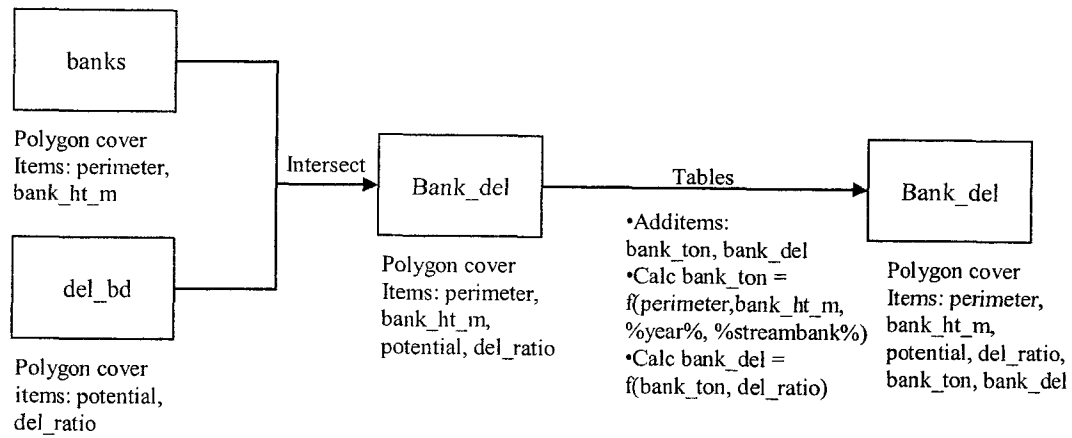
Routine: del_potential



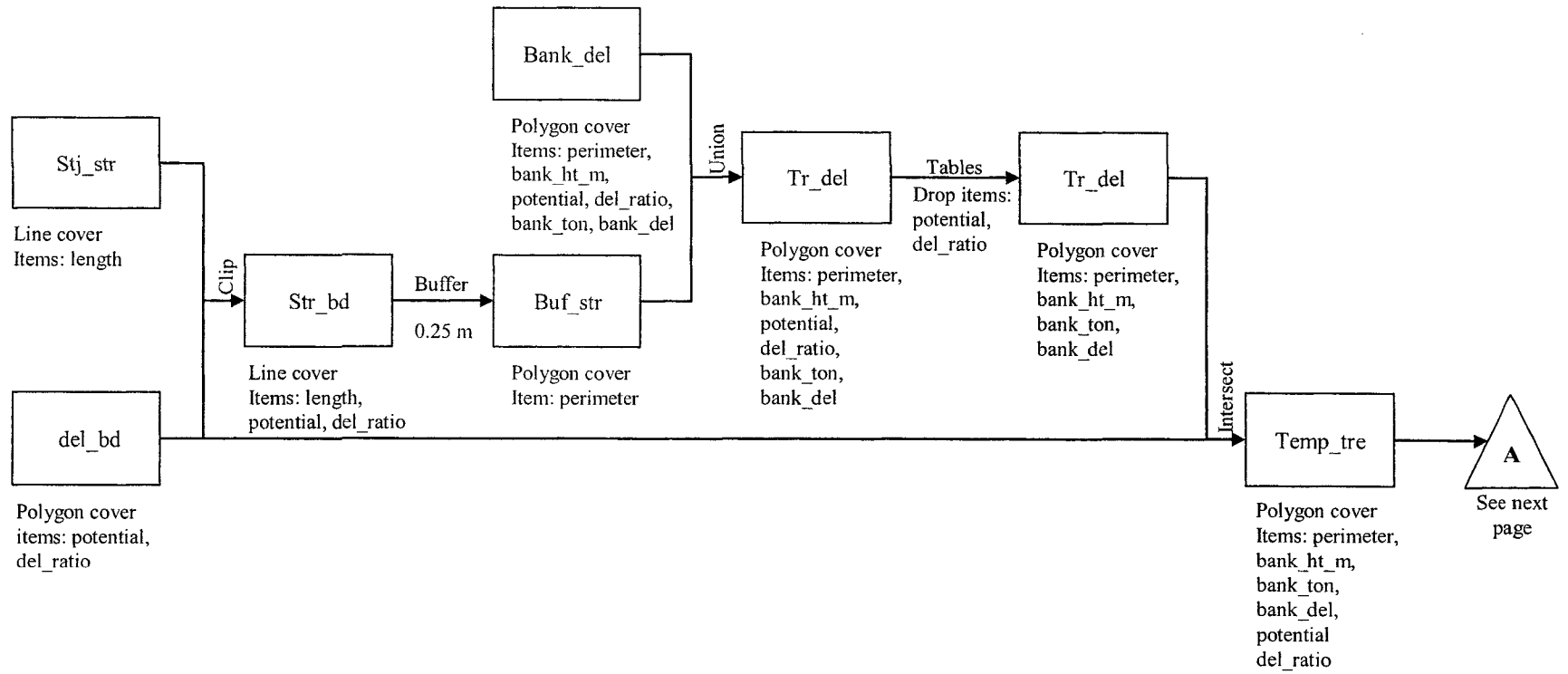
Routine: rd_erosion



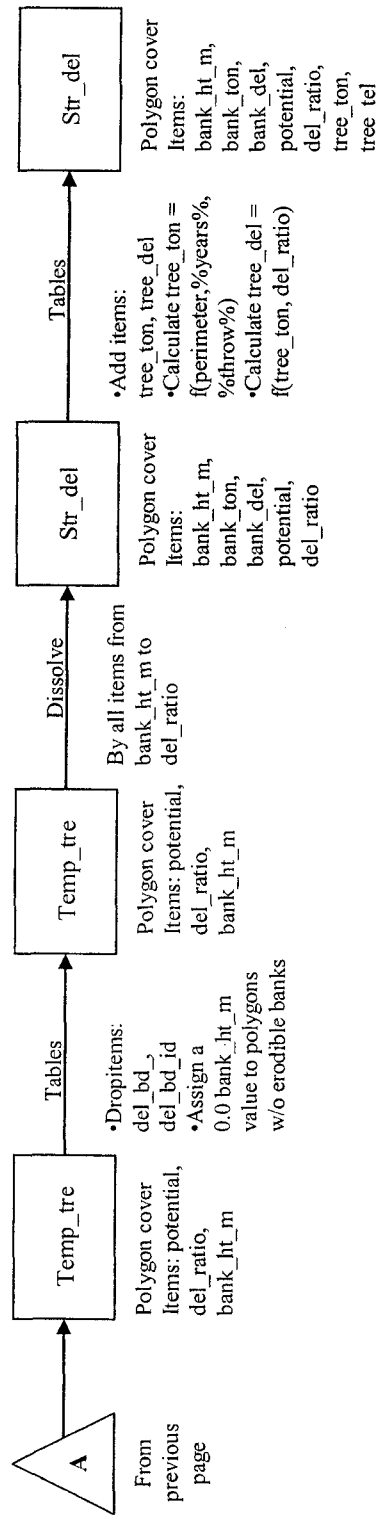
Routine: streambank



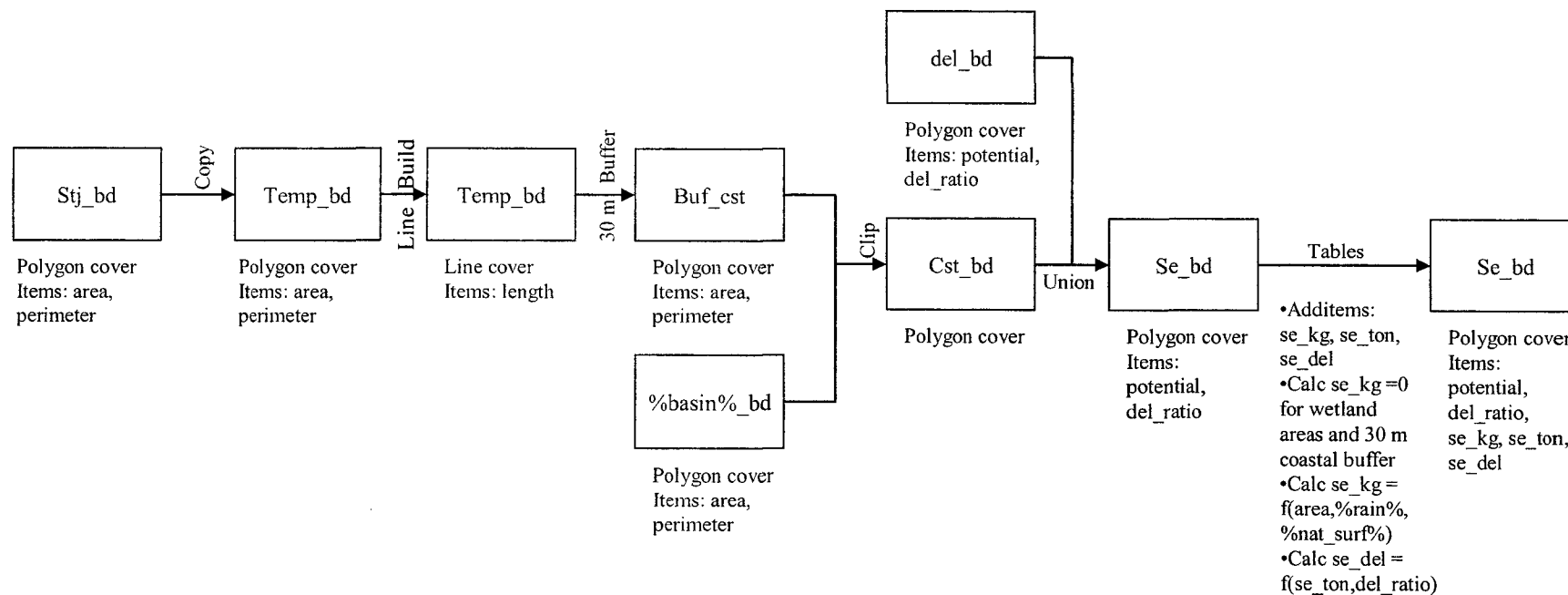
Routine: stream_total (Part I)



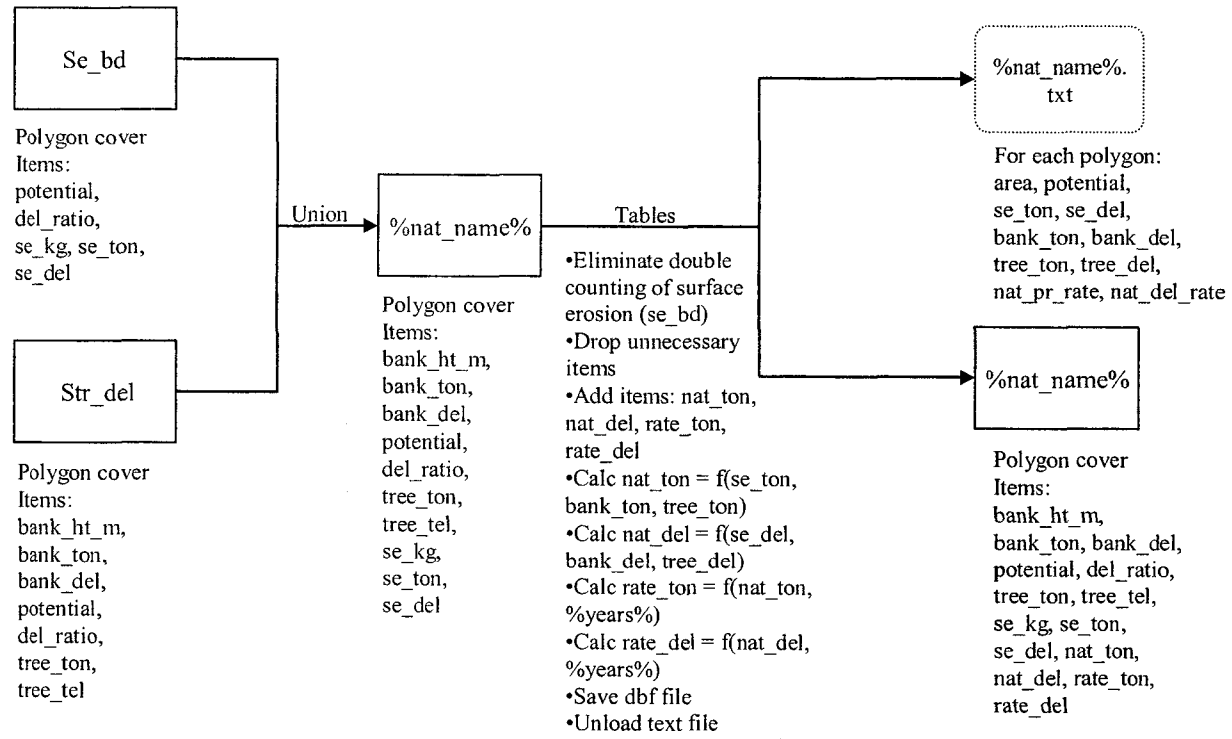
Routine: stream_total (Part II)



Routine: surf_erosion



Routine: nat_erosion



APPENDIX IV-D

STJ-EROS ARC MACRO LANGUAGE (AML) CODE

```

/*****
/* APPENDIX IV-D
/*
/* FILE NAME:   stj_eros.aml
/*
/* PROGRAMMER:  Carlos E. Ramos Scharron
/*              Colorado State University- Ft Collins CO
/*
/* DATE:        November 25, 2003
/*
/* PURPOSE:     This program, written in Arc Macro Language is intended to
/*              estimate rates of erosion and sediment delivery for unpaved
/*              roads and natural processes on the island of St. John,
/*              US Virgin Islands.
/*
/* RUN COMMAND: Once in the correct workspace type '&run stj_eros' at the ARC
/*              command line.
/*
/* DEPENDENCIES: This program is run in ArcInfo 8.2 and in its Tables module.
/*
/* TERMINATING  This program does not call any additional programs once it
/* CONVENTIONS: terminates.
/*
/* CALLING      The program requires the user to define the following
/* CONVENTIONS: variables:
/*              (1) %BASIN% as the name of the basin (watershed) for which
/*              analysis is to be conducted.
/*              (2) %YEARS% as the total number of years over which erosion
/*              and sediment delivery are to be calculated
/*              (3) %RAIN_RATE% as an annual rainfall rate.
/*              (4) %ROAD_NAME% as the name for the output file, data layer,
/*              and shapefile containing road erosion and sediment delivery
/*              results.
/*              (5) %NAT_NAME% as the name for output file, data layer, and
/*              and shapefile containing natural erosion and sediment
/*              delivery results.
/*
/* TERMINATING  This program does not call any additional programs when it
/* CONVENTIONS: terminates.
/*
/* ALGORITHMS:  After initializing variables that will be used to calculate
/*              sediment production rates, it performs some housekeeping
/*              commands to delete any pre-existing GIS data layers with
/*              the same names as those that will be created by the
/*              program. An interface then asks the user whether to
/*              continue with a brief on-screen introduction to the
/*              program or to move directly to begin entering model
/*              parameters. The MODEL routine is then invoked to control
/*              the general flow of the model. Once all of the routines are
/*              called the program asks the user whether to view a summary
/*              of the results by invoking the SUMMARY_RESULTS routine or
/*              to exit the program. Before exiting an on-screen message
/*              reminds the user of the names given to the GIS data layer
/*              and text files containing the model results.
/*
/*****

```

```
&terminal 9999
```

```

&sv treethrow = 0.17 /* tons per km of channel length per year
&sv bank_er = 10 /* kg per m^2 of bank surface per year
&sv undisturbed = 0.000064 /* kg per m^2 of undisturbed hillslope surface
/* per cm of precipitation occurring during events exceeding 6 cm of rain
&sv abandoned = 0.071 /* kg per m^2 of road surface, cm of precipitation
/* unit gradient
&sv graded = 4.73 /* kg per m^2 of road surface, cm of precipitation &
/* unit gradient to the 1.5th power
&sv ungraded = 1.88 /* kg per m^2 of road surface, cm of precipitation &
/*unit gradient to the 1.5th power
&sv cutslope = 9 /* % of sediment produced at the segment scale

```



```

&type ^      area potential se_ton se_ttl_del se_sus_del bank_ton
&type ^      bank_ttl_del bank_sus_del tree_ton tree_ttl_del tree_sus_del
&type ^      nat_pr_rate nat_t_del_rate nat_s_del_rate
&type ^
&type ^ The user may find the following covers useful for display purposes:
&type ^      %basin%_bd   del_bd   pt_del
&type ^
&type ^ ~~~~~
&return

```

```

&ROUTINE MODEL
/*****
/*
/* PURPOSE:      Controls the flow of the model by calling routines.
/*
/* REQUIRED      None
/* PRE-DEFINED
/* VARIABLES:
/*
/* IMPORTANT    None
/* CREATED
/* VARIABLES:
/*
/* SIDE         None
/* EFFECTS:
/*
/* ALGORITHM:   Routines are called in the following order:
/*
/*              (1) SET_SDR- Assigns the value of variables %HI_POT% and
/*              %MOD_POT% according to values chosen from a menu or entered
/*              by the user. These two variables are used as sediment delivery
/*              ratios (SDR's) to estimate sediment yields.
/*              (2) DEL_POTENTIAL- Assigns sediment delivery ratio values to the
/*              entire basin of interest according to its pre-determined
/*              sediment delivery potential.
/*              (3) SET_YEARS- Assigns the value of variable %YEARS% according
/*              to a value chosen from a menu or entered by the user. This
/*              variable defines the total number of years over which sediment
/*              yields are to be estimated.
/*              (4) SET_RAIN- Assigns the value of variable %RAIN_RATE%
/*              according to a value chosen from a menu or entered by the user.
/*              %RAIN_RATE% defines the annual rainfall rate in cm per year.
/*              (5) ROADS_NAME- Assigns the variable %ROAD_NAME% according to
/*              a value chosen from a menu or entered by the user. %ROAD_NAME%
/*              is the name that will be given to the GIS data layer and text
/*              file containing the sediment yield estimates for all road-
/*              related sediment sources.
/*              (6) NAT_NAME- Assigns the value of variable %NAT_NAME% according
/*              to a value chosen from a menu or entered by the user.
/*              %NAT_NAME% is the name of the GIS data layer and text file
/*              containing the sediment yield estimates for all natural sediment
/*              sources.
/*
/*              Once all parameters have been chosen by the user, the program
/*              provides an on-screen list of all of the parameters
/*              that were chosen. The user is ask whether to exit the program
/*              to re-enter the parameter values or to run the program with
/*              the values already chosen. Exiting quits the program, otherwise
/*              the program calls routine #7.
/*
/*              (7) RD_EROSION- Calculates sediment production and yield rates
/*              for all road-related sediment sources and stores them into a
/*              line GIS data layer and into a text file.
/*              (8) STREAMBANK- Calculates streambank sediment production and
/*              yield rates and stores them into a polygon GIS data layer.
/*              (9) STREAM_TOTAL- Calculates treethrow sediment production and
/*              yield rates and stores them into a polygon GIS data layer. The
/*              final layer also contains streambank sediment yield estimates.
/*              (10) SURF_EROSION- Calculates sediment production and yield
/*              rates from undisturbed surfaces and stores them into a polygon

```



```

&do
  &type /&ERROR!!! SDR for high potential areas must be greater than 0.5!
  &call set_sdr
&end
&else
&do
  &if %hi_pot% > 1 &then
    &do
      &type /&ERROR!!! SDR for high potential areas cannot be greater than 1.0!
      &call set_sdr
    &end
  &end
&if %mod_pot% < 0.0 &then
  &do
    &type /&ERROR!!! SDR for moderate potential areas cannot be negative!
    &call set_sdr
  &end
&else
  &do
    &if %mod_pot% > 0.5 &then
      &do
        &type /&ERROR!!! SDR for moderate potential areas cannot be greater than 0.5!
        &call set_sdr
      &end
    &end
  &end
&return

```

```

&ROUTINE DEL_POTENTIAL
/*****
/*
/* PURPOSE:   Assigns sediment delivery ratio values to the entire basin of
/*            interest according to its pre-determined sediment delivery
/*            potential.
/*
/* REQUIRED    HI_POT is the sediment delivery ratio (SDR) assigned to areas
/* PRE-DEFINED which have been identified as having a high potential for sediment
/* VARIABLES: delivery to the marine environment.
/*            MOD_POT is the SDR for areas with a moderate delivery potential.
/*
/* IMPORTANT  %BASIN% is the code name of the basin for which analysis is to be
/* CREATED    conducted. The user chooses the name from a menu listing the
/* VARIABLES: currently available choices.
/*            %WATSHED% is the full name of the basin chosen for analysis.
/*
/* SIDE       (1)A new polygon cover called del_bd is created.
/* EFFECTS    (2)TABLES is invoked.
/*
/* ALGORITHM: The user is prompted to choose a basin name from a menu list. The
/*            choice is assigned as the value of variable %BASIN%. The value of
/*            variable %WATSHED% is assigned according to the value of %BASIN%.
/*            In TABLES a new item called DEL_RATIO is added to the table.
/*            a new cover is created by clipping the sed_del layer with the
/*            %basin%_bd layer. Sediment delivery ratios chosen by the
/*            user in the SET_SDR routine are then assigned to this new
/*            layer. The numerical value of DEL_RATIO for each polygon is
/*            assigned according to its POTENTIAL and to the pre-established
/*            values of the variables %HI_POT% and %MOD_POT%.
/*
/*****

```

```

&type /&The user is now required to choose a basin for analysis. The model can be
&type applied to the following basins:
&type /& Cinnamon Bay (cb)
&type Fish Bay (fb)
&type Lameshur Bay (lb)/&
&if [query 'Press enter to continue.' .true.] &then &type Continuing...
&sv basin = [ getchoice cb fb lb -prompt 'Select a basin for analysis' ]
&select %basin%
  &when cb
    &sv watshed = Cinnamon Bay

```

```

&when fb
  &sv watshed = Fish Bay
&when lb
  &sv watshed = Lameshur Bay
&end
&type /&Creating sediment delivery cover for %watshed% .../&
clip sed_del %basin%_bd del_bd poly
tables
select del_bd.pat
additem del_bd.pat del_ratio 8 8 n 1
reselect potential = 'high'
calculate del_ratio = %hi_pot%
aselect
reselect potential = 'moderate'
calculate del_ratio = %mod_pot%
aselect
reselect potential = 'wetland'
calculate del_ratio = %mod_pot%
reselect potential = 'no'
calculate del_ratio = 0
quit
&type Done creating sediment delivery cover for %watshed%...
&return

&ROUTINE SET_YEARS
/*****/
/*
/* PURPOSE:    Assigns the value of variable %YEARS% according to a value    */
/*             chosen from a menu or entered by the user.                    */
/*
/* REQUIRED     None
/* PRE-DEFINED
/* VARIABLES:
/*
/* IMPORTANT   %YEARS% is the total number of years for which sediment production */
/* CREATED     and delivery are to be estimated.
/* VARIABLES:
/*
/* SIDE       None
/* EFFECTS:
/*
/* ALGORITHM: The user is prompted to choose the number of years over which
/*             sediment production and delivery are to be estimated from a number
/*             of options. The user is given the option to enter another value not
/*             offered in the menu. The value entered is then rounded and
/*             assigned to the %YEARS% variable. The years value is then tested
/*             to verify that it is greater than 0 and does not exceed 50. If this
/*             is not satisfied an error message prints on the screen and the user
/*             is asked to once again enter a value.
/*
/*
/*****/

&type /& Now the user will be requested to enter the total number of years
&type over which sediment production and sediment delivery will be calculated.
&type The number of years can be chosen by selecting a value from choices in
&type a menu or by entering a value once the "other" option has been selected.
&type Please note that any real values entered manually will be rounded and
&type that the model will only accept values between 1 and 50 years./&
&if [query 'Press enter to continue.' .true.] &then &type Continuing...
&sv time [getchoice 1 5 10 25 50 -prompt 'Choose total number of years' -other]
&sv years = [round %time%]
&if %years% <= 0 &then
  &do
    &type /&ERROR!!! Number of years must be greater than 0!
    &call set_years
  &end
&else
  &do
    &if %years% > 50 &then

```

```

        &do
            &type /&ERROR!!! Number of years must be less than or equal to 50.
            &call set_years
        &end
    &end
&return

&ROUTINE SET_RAIN
/*****
/*
/* PURPOSE:    Assigns the value of variable %RAIN_RATE% according to a value
/*             chosen from a menu or entered by the user.
/*
/* REQUIRED    %YEARS% is the total number of years chosen by the user in the
/* PRE-DEFINED SET_YEARS routine.
/* VARIABLES:
/*
/* IMPORTANT %RAIN_RATE% is the rainfall (in cm per year) for which sediment
/* CREATED   production and delivery are to be estimated.
/* VARIABLES: %RAIN% is the total rainfall (in cm) used to calculate sediment
/*             production from roads and undisturbed hillslopes.
/*
/* SIDE      None
/* EFFECTS:
/*
/* ALGORITHM: The user is prompted to choose an annual rainfall rate for which
/*             sediment production and delivery are to be estimated from a number
/*             of options. The user is given the option to enter another value not
/*             offered in the menu. The value entered is then rounded and assigned
/*             to the %RAIN_RATE% variable. The %RAIN_RATE% value is then tested to
/*             verify that it is greater than 70 and does not exceed 160. If this
/*             test is not satisfied an error message prints on the screen and the
/*             user is asked to enter another value. The %RAIN% value is then
/*             calculated as the product of %RAIN_RATE% times %YEARS%.
/*
*****/

&type /& Now the user will be requested to enter an annual rainfall rate in
&type cm per year. A rate can be chosen by selecting a value from choices in
&type a menu or by entering a value once the "other" option has been selected.
&type Please note that any real values entered manually will be rounded and
&type that the model will only accept values between 70 and 160 cm per year./&
&type Mean annual rainfall in St. John is spatially variable. While the
&type driest portions on East End and lower elevations of Fish Bay and
&type Lameshur Bay basins receive approximately 90 cm of rainfall per year,
&type the highest elevations around Bordeaux Mountain typically receive
&type about 130 cm per year. A 115 cm per year value is considered to be a
&type reasonable approximation to long-term mean rainfall rates for most
&type basins on the island. /&
&if [query 'Press enter to continue.' .true.] &then &type Continuing...
&sv annual_rain [getchoice 90 115 140 -prompt 'Choose an annual rainfall rate' -other]
&sv rain_rate = [round %annual_rain%]
&if %rain_rate% < 70 &then
    &do
        &type /&ERROR!!! Rainfall rate must be greater than 70 cm per year!
        &call set_rain
    &end
&else
    &do
        &if %rain_rate% > 160 &then
            &do
                &type /&ERROR!!! Rainfall rate must be less than or equal to 160 cm per year.
                &call set_rain
            &end
        &end
    &end
&sv rain = [calc %rain_rate% * %years%]
&return

```

```

&ROUTINE ROADS_NAME
/*****
*/
/* PURPOSE:   Assigns the value of variable %ROAD_NAME% according to a value */
/*           chosen from a menu or entered by the user. %ROAD_NAME% is the */
/*           name of the new output coverage and text file to be created by */
/*           this model. */
/*
/* REQUIRED   %BASIN% is the code name of the basin for which analysis is to be */
/* PRE-DEFINED conducted. */
/* VARIABLES:
/*
/* IMPORTANT %ROAD_NAME% is the user chosen name used for the layer and text */
/* CREATED   file containing the results of the sediment production and delivery*/
/* VARIABLES: estimates for roads. */
/*           %NAME_LENGTH% is the number of characters used by %ROAD_NAME%. */
/*
/* SIDE      None */
/* EFFECTS:
/*
/*
/* ALGORITHM: The user is prompted to choose a name from a number of options */
/*            in a menu. The user is given the option to enter another name not */
/*            offered in the menu. The number of characters in the chosen name */
/*            is assigned to variable %NAME_LENGTH% which is used to test whether */
/*            the chosen name has been given a name less than 8 characters in */
/*            length. If this test is not satisfied an error message prints on */
/*            the screen and the user is asked to enter another name. */
/*
*****/
&type /& Now the user will be requested to enter the names of the final coverages
&type and txt files containing the sediment production and delivery estimates
&type for roads and natural erosion processes. The names can be chosen by
&type selecting a value from choices in a menu or by entering a value once the
&type "other" option has been selected. Please note that the model will only take
&type names that are less than or equal to 8 characters in length./&
&if [query 'Press enter to continue.' .true.] &then &type Continuing...
&sv road_name [getchoice %basin%_rd r_%basin% -prompt-
'Choose a name for road erosion layer and results file' -other]
&sv name_length = [length %road_name%]
&if %name_length% = 0 &then
&do
&type /&ERROR!!! Please enter a name!
&call roads_name
&end
&if %name_length% > 8 &then
&do
&type /&ERROR!!! Please, enter a name with no more than 8 characters!
&call roads_name
&end
&if [exists %road_name% -cover] &then
&do
&type /&Cover %road_name% already exists!!
&if [query 'Delete current cover (yes or no)' .false.]-
&then kill %road_name% all
&else &call roads_name
&end
&return

&ROUTINE NAT_NAME
/*****
*/
/* PURPOSE:   Assigns the value of variable %NAT_NAME% according to a value */
/*           chosen from a menu or entered by the user. %NAT_NAME% is the */
/*           name of the new natural erosion coverage and text file to */
/*           be created by this model. */
/*
/* REQUIRED   %BASIN% is the code name of the basin for which analysis is to be */
/* PRE-DEFINED conducted. */
/* VARIABLES:

```

```

/*
/* IMPORTANT   %NAT_NAME% is the user chosen name used for the cover and text
/* CREATED    file containing the results of the sediment production and
/* VARIABLES:  delivery estimates for natural processes.
/*            %NAME_LENGTH% is the number of characters used by %NAT_NAME%.
/*
/* SIDE       None
/* EFFECTS:
/*
/* ALGORITHM: The user is prompted to choose a name from a number of options
/*            in a menu. The user is given the option to enter another name not
/*            offered in the menu. The number of characters in the chosen name
/*            is assigned to variable %NAME_LENGTH% which is used to test whether
/*            the chosen name has been given a name less than 8 characters in
/*            length. If this test is not satisfied an error message prints on
/*            the screen and the user is asked to enter another name.
/*
/*
/*****
&sv nat_name [getchoice %basin%_nat n_%basin% -prompt-
'Choose a name for natural erosion layer and results file' -other]
&sv name_length = [length %nat_name%]
&if %name_length% = 0 &then
&do
&type /&ERROR!!! Please enter a name!
&call nat_name
&end
&if %name_length% > 8 &then
&do
&type /&ERROR!!! Please, enter a name with no more than 8 characters!
&call nat_name
&end
&if %nat_name% = %road_name% &then
&do
&type /&ERROR!!! Please, enter a name other than %road_name%!
&call nat_name
&end
&if [exists %nat_name% -cover] &then
&do
&type Cover %nat_name% already exists!!!
&if [query 'Delete current cover (yes or no)' .false.]~
&then kill %nat_name% all
&else &call nat_name
&end
&return

&ROUTINE RD_EROSION
/*****
/*
/* PURPOSE:    Calculates sediment production and delivery rates for the basin
/*            chosen in the DEL_POTENTIAL routine using the attributes stored in
/*            GPS_RDS and GPS_DRA covers and the total rainfall and total time
/*            values chosen by the user during the SET_YEARS and SET_RAIN
/*            routines.
/*
/* REQUIRED     %BASIN% is the code name of the basin for which analysis is to be
/* PRE-DEFINED conducted.
/* VARIABLES:  %UNGRADED% is the regression coefficient used to calculate
/*            sediment production from ungraded roads.
/*            %GRADED% is the regression coefficient used to calculate
/*            sediment production from graded roads.
/*            %ABANDONED% is the rate of sediment production from abandoned
/*            roads.
/*            %RAIN% is the total rainfall (in cm) used to calculate road
/*            sediment production rates.
/*            %YEARS% is the total time in years over which sediment production
/*            and delivery rates are calculated.
/*            %ROAD_NAME% is the user-given name of the final cover and text
/*            file that contain the final results of the road erosion and
/*            sediment delivery analysis.
/*

```

```

/*          %SILT_LOSS% is the ratio of actual sediment production for the          */
/*          silt-size sediment fraction to that measured from sediment traps.      */
/*          %SILT_U_RD_FR%, %SILT_G_RD_FR%, %SILT_A_RD_FR%, %SILT_A_RD_FR% are    */
/*          the percent of sediment produced in the silt-size category for       */
/*          ungraded roads, graded roads, and abandoned roads, respectively.    */
/*          %UN_SUS_FR%, %GR_SUS_FR%, %AB_SUS_FR% are the percentages of         */
/*          sediment finer than 2 mm for ungraded roads, graded roads, and       */
/*          abandoned roads, respectively.                                        */
/*                                                                              */
/* IMPORTANT      None                                                         */
/* CREATED                                               */
/* VARIABLES:                                           */
/*                                                                              */
/* SIDE           (1)A new polygon cover called DRAIN is created and killed.     */
/* EFFECTS        (2)A new point cover called PT_DEL is created.                 */
/*                (3)A new line cover called %ROAD_NAME% is created.             */
/*                (4)TABLES is invoked.                                          */
/*                (5)A file called %ROAD_NAME%.txt is created.                  */
/*                                                                              */
/* ALGORITHM: The GPS_DRA point cover is clipped with the %BASIN%_BD cover to    */
/* eliminate all road drainage point outside of %BASIN%. The resulting          */
/* cover (DRAIN) is then intersected with the DEL_BD cover created               */
/* during the DEL_POTENTIAL routine to assign DEL_RATIO values to each          */
/* drainage structure according to its geographical location. The               */
/* %ROAD_NAME% line cover is copied from the GPS_RDS cover. TABLES is         */
/* invoked to dropitems from the PT_DEL.PAT and %ROAD_NAME%.AAT. A              */
/* jointem function is invoked from ARC using the DRAIN_ID item                 */
/* as the relate item to assign DEL_RATIO values to %ROAD_NAME%.AAT.           */
/* TABLES is invoked once again to add and calculate the value of              */
/* items that will contain the sediment production and delivery                 */
/* estimates for each road segment within %BASIN% according to their           */
/* values stored in the following items: LENGTH_M, WIDTH_M, SLOPE,              */
/* GRADING, and DEL_RATIO. The variables %YEARS% and %RAIN% are also           */
/* used to calculate these items. Sediment delivery rates are                  */
/* estimated for both total loads and the fraction expected to be               */
/* carried as suspended load. Finally, the results are unloaded                 */
/* into a file called %ROAD_NAME%.txt before exiting TABLES.                  */
/*                                                                              */
/*****

```

```

&type /&Beginning rd_erosion routine...
&type /&Selecting drainage points within %watershed%...
clip gps_dra %basin%_bd drain point /* Eliminates all drainage points outside
/* of %basin%
intersect drain del_bd pt_del point
kill drain all
copy gps_rds %road_name%
tables
dropitem pt_del.pat (! drain# drain-id type del_bd# del_bd-id !)
dropitem %road_name%.aat source
quit
jointem %road_name%.aat pt_del.pat %road_name%.aat drain_id
build %road_name% line
tables
additem %road_name%.aat temp_sed 12 12 n 1 /* Total road sed production
additem %road_name%.aat cslope_kg 10 10 n 1 /* Cutslope sediment production
/* equals 9% of total road sediment production
additem %road_name%.aat sed_kg 12 12 n 1 /* Road travelway sediment production
/* equals 91% of total road sediment production
additem %road_name%.aat rd_ton 8 8 n 2 /* Road travelway sed prod in tons
additem %road_name%.aat rd_del 8 8 n 2 /* Road travelway sed delivery in tons
additem %road_name%.aat cs_ton 8 8 n 1 /* Cutslope sed prod in tons
additem %road_name%.aat cs_del 8 8 n 2 /* Cutslope sed delivery in tons
additem %road_name%.aat rd_pr_rate 12 12 n 3 /* Travelway production rate
/* equals total production in tons divided by variable %YEARS%
additem %road_name%.aat rd_t_del_r 8 8 n 3 /* Travelway delivery rate
/* equals total delivery in tons divided by variable %YEARS%
additem %road_name%.aat cs_pr_rate 12 12 n 3 /* Cutslope production rate
/* equals cutslope production in tons divided by %YEARS%
additem %road_name%.aat cs_ttl_del_rate 15 15 n 3 /* Cutslope delivery rate
/* equals cutslope delivery in tons divided by %YEARS%

```

```

additem %road_name%.aat rd_sus_del_rate 15 15 n 3 /* Travelway suspended
/* sediment delivery rates
additem %road_name%.aat cs_sus_del_rate 15 15 n 3 /* Cutslope suspended
/* sediment delivery rates
additem %road_name%.aat un_ttl_del_rate 15 15 n 3 /* Travelway suspended
/* sediment delivery rates for ungraded roads
additem %road_name%.aat gr_ttl_del_rate 15 15 n 3 /* Travelway suspended
/* sediment delivery rates for graded roads
additem %road_name%.aat ab_ttl_del_rate 15 15 n 3 /* Travelway suspended
/* sediment delivery rates for abandoned roads
select %road_name%.aat
&type /&Beginning to calculate road erosion rates...
aselect
reselect basin cn [quote %basin%]
reselect grading = 'ungraded'
calculate temp_sed = length_m * width_m * ( -0.432 + ( %ungraded% * %rain% * ( slope
** 1.5 ) ) ) ~
* ( 1 + ( %silt_loss% * %silt_u_rd_fr% ) )
reselect temp_sed < 0
calculate temp_sed = 0
aselect
reselect basin cn [quote %basin%]
reselect grading = 'graded'
calculate temp_sed = length_m * width_m * ( -0.432 + ( %graded% * %rain% * ( slope **
1.5 ) ) ) ~
* ( 1 + ( %silt_loss% * %silt_g_rd_fr% ) )
reselect temp_sed < 0
calculate temp_sed = 0
aselect
reselect basin cn [quote %basin%]
reselect grading = 'abandoned'
calculate temp_sed = length_m * width_m * %rain% * %abandoned% * slope * ~
( 1 + ( %silt_loss% * %silt_a_rd_fr% ) )
aselect
reselect basin cn [quote %basin%]
calculate cslope_kg = temp_sed * %cutslope% / 100
calculate sed_kg = temp_sed - cslope_kg
reselect sed_kg < 0
calculate sed_kg = 0
aselect
calculate rd_ton = sed_kg / 1000
calculate cs_ton = cslope_kg / 1000
&type /&Beginning to calculate road sediment delivery rates for %watershed%...
calculate rd_del = rd_ton * del_ratio
calculate cs_del = cs_ton * del_ratio
calculate rd_pr_rate = rd_ton / %years%
calculate cs_pr_rate = cs_ton / %years%
calculate rd_t_del_r = rd_del / %years%
calculate cs_ttl_del_rate = cs_del / %years%
reselect basin cn [quote %basin%]
reselect grading = 'ungraded'
calculate rd_sus_del_rate = rd_t_del_r * %un_sus_fr%
calculate cs_sus_del_rate = cs_ttl_del_rate * %un_sus_fr%
calculate un_ttl_del_rate = rd_t_del_r
aselect
reselect basin cn [quote %basin%]
reselect grading = 'graded'
calculate rd_sus_del_rate = rd_t_del_r * %gr_sus_fr%
calculate cs_sus_del_rate = cs_ttl_del_rate * %gr_sus_fr%
calculate gr_ttl_del_rate = rd_t_del_r
aselect
reselect basin cn [quote %basin%]
reselect grading = 'abandoned'
calculate rd_sus_del_rate = rd_t_del_r * %ab_sus_fr%
calculate cs_sus_del_rate = cs_ttl_del_rate * %ab_sus_fr%
calculate ab_ttl_del_rate = rd_t_del_r
aselect
&type /&Done calculating road erosion & delivery rates!
dropitem %road_name%.aat (! gps_rds_gps_rds_id area perimeter temp_sed ~
sed_kg cslope_kg pt_del# pt_del-id del_ratio rd_ton rd_del cs_ton cs_del !)
select %road_name%.aat

```

```

aselect
&type /&Unloading %road_name%.txt ...
reselect basin cn [quote %basin%]
unload %road_name%.txt length_m surface grading potential ~
  rd_pr_rate rd_t_del_r rd_sus_del_rate cs_pr_rate cs_ttl_del_rate ~
  cs_sus_del_rate delimited init
  /* creates a file with all of the results, replaces any file with same
  /* name, comma-delimited file may be opened in Excel
quit
kill pt_del all
build %road_name% line
&type /&Exiting rd_erosion routine...
&return

&ROUTINE STREAMBANK
/*****
/*
/* PURPOSE:   Calculates streambank sediment production and delivery rates for
/*           the basin chosen in the DEL_POTENTIAL routine using the
/*           attributes stored in the BANKS cover and the total time values
/*           chosen by the user during the SET_YEARS routine.
/*
/* REQUIRED   %BANK_ER% is the rate of sediment production from erodible
/* PRE-DEFINED streambanks.
/* VARIABLES: %YEARS% are the years over which sediment production
/*            and delivery rates are calculated.
/*
/* IMPORTANT None
/* CREATED
/* VARIABLES:
/*
/* SIDE      (1)A new polygon cover called BANK_DEL is created.
/* EFFECTS    (2)TABLES is invoked.
/*
/* ALGORITHM: The BANKS polygon cover is intersected with the DEL_BD cover created*
/*            during the DEL_POTENTIAL routine to assign DEL_RATIO values to each *
/*            stream segment according to its geographical location within *
/*            %BASIN%. TABLES is invoked once again to add and calculate the *
/*            value of items that will contain the sediment production and *
/*            delivery estimates for each stream segment according to the *
/*            values stored in the following items: PERIMETER, BANK_HT_M, and *
/*            DEL_RATIO. The variables %BANK_ER% and %YEARS% are also used to *
/*            calculate these items. Sediment delivery rates are estimated for *
/*            both total loads and for the fraction of sediment finer than 2 mm, *
/*            which is expected to be transported in suspension. Command is *
/*            transferred back to the ARC prompt before the end of the routine. *
/*
/*
/* *****/
&type /&Beginning streambank erosion routine...
intersect banks del_bd bank_del poly /*Used to assign delivery potential to
  /* banks cover
tables
additem bank_del.pat bank_ton 8 8 n 3 /* Bank erosion in tons
additem bank_del.pat bank_ttl_del 12 12 n 3 /* Bank delivery total in tons
additem bank_del.pat bank_sus_del 12 12 n 3 /* Bank suspended sediment
/* delivery total in tons
select bank_del.pat
reselect inside = 100 /* Used to avoid calculating erosion for universal polygon.
calculate bank_ton = ( perimeter / 2 ) * 2 * bank_ht_m * %years% -
  * %bank_er% / 1000
calculate bank_ttl_del = bank_ton * del_ratio
calculate bank_sus_del = bank_ttl_del * %bank_sus_fr%
quit
&type /& Exiting streambank erosion routine...
&return

```

```

&ROUTINE STREAM_TOTAL
/*****
/*
/* PURPOSE:   Calculates treethrow sediment production and delivery rates for
/*           the basin chosen in the DEL_POTENTIAL routine using the
/*           STJ_STR line layer and the total time value chosen by the user
/*           during the SET_YEARS routine. The final polygon layer contains
/*           sediment production and delivery from both treethrow rates and
/*           streambank erosion.
/*
/*
/* REQUIRED   %TREETHROW% is the rate of sediment production by overthrown trees
/* PRE-DEFINED in the proximity of streams.
/* VARIABLES: %YEARS% is the total time in years over which sediment production
/*            and delivery rates are calculated.
/*
/* IMPORTANT None
/* CREATED
/* VARIABLES:
/*
/* SIDE      (1)A new polygon layer called STR_BD is created and killed.
/* EFFECTS   (2)A new polygon layer called BUF_STR is created and killed.
/*           (3)A new polygon layer called TR_DEL is created and killed.
/*           (4)A new polygon layer called TEMP_TRE is created and killed.
/*           (5)A new polygon layer called STR_DEL is created.
/*           (6)TABLES is invoked.
/*           (7)The polygon layer BANK_DEL is killed
/*
/* ALGORITHM: The STJ_STR line layer is clipped with DEL_BD-created
/*            during the DEL_POTENTIAL routine to eliminate stream segments
/*            located outside of %BASIN% in the new layer STR_BD.
/*            STR_BD is buffered to create the polygon layer BUF_STR. BUF_STR
/*            is then used in an UNION overlay with BANK_DEL-created
/*            during the STREAMBANK routine to assign bank erosion values to
/*            the stream polygons in BUF_STR. Some items in the new polygon layer
/*            (TR_DEL) are removed from its INFO table in TABLES in order to
/*            prepare it for the INTERSECT with DEL_BD which will
/*            assign delivery ratios to the polygons. Some items from this new
/*            polygon layer TEMP_TRE are dropped in TABLES to prepare it for the
/*            DISSOLVE command. DISSOLVE is performed using all remaining items
/*            so that polygons in original BANKS layer remain the same in
/*            order to avoid double counting of bank erosion. TABLES is invoked
/*            once again to add necessary items where the treethrow sediment
/*            production and delivery rate estimates are going to be stored.
/*            Treethrow production and delivery rates are a function of the
/*            PERIMETER and DEL_RATIO items and the %TREETHROW% and %YEARS%
/*            variables. Sediment delivery rates are estimated for both total
/*            loads and the fraction of sediment finer than 2mm, which is
/*            expected to be transported in suspension. The TABLES session is
/*            then terminated and the STR_BD, BUF_STR, TEMP_TRE, TR_DEL, and
/*            BANK_DEL layers are killed before the end of the routine.
/*
/*
/*****

&type /&Beginning with stream_total routine...
clip stj_str del_bd str_bd line
buffer str_bd buf_str # # 0.25 # line
union buf_str bank_del tr_del
tables
dropitem tr_del.pat (! potential del_ratio !) /* Done to avoid having empty
/* records in temp_tre after intersect command
quit
intersect tr_del del_bd temp_tre poly
tables
dropitem temp_tre.pat (! del_bd-id del_bd# tr_del# tr_del-id buf_str# buf_str-id ~
inside bank_del# bank_del-id banks# banks_banks_id !) /* Needed for dissolve
/* function to work as intended- to dissolve along all remaining items.
select temp_tre.pat
reselect bank_ht_m = 0 /* Selects polygons that were not in the BANKS cover.
/* These records actually have no value in the bank_ht_m item, but can be
/* selected with this command.
reselect temp_tre-id > 0 /* Eliminates the Universal polygon from the selection.

```

```

calculate bank_ht_m = 0 /* Assigns a 0 value to polygons not included in BANKS.
/* This step is also needed for the dissolve command to dissolve along polygons
/* in the BANKS original coverage and avoid double counting of bank erosion.
quit
dissolve temp_tre str_del #all
tables
additem str_del.pat tree_ton 8 8 n 3
additem str_del.pat tree_ttl_del 12 12 n 3
additem str_del.pat tree_sus_del 12 12 n 3
select str_del.pat
reselect potential = ''
nselect
calculate tree_ton = ( perimeter / ( 2 * 1000 ) ) * %years% * %treethrow%
calculate tree_ttl_del = tree_ton * del_ratio
calculate tree_sus_del = tree_ttl_del * %tree_sus_fr%
quit
kill (! str_bd buf_str temp_tre tr_del bank_del !) all
&type /&Exiting stream_total routine.../&
&return

&ROUTINE SURF_EROSION
/*****
/*
/* PURPOSE:   Calculates sediment production and delivery rates by surface
/*           erosion on undisturbed hillslopes for the basin chosen in the
/*           DEL_POTENTIAL routine.
/*
/*
/* REQUIRED   %UNDISTURBED% is the rate of sediment production by surface
/* PRE-DEFINED erosion on undisturbed hillslopes.
/* VARIABLES: %YEARS% is the total time in years over which sediment production
/*            and delivery rates are calculated.
/*            %RAIN_RATE% is the annual rainfall rate in cm per year.
/*            %RAIN% is the total rainfall in centimeters.
/*            %SILT_LOSS% is the ratio of actual sediment production for silt-
/*            sized material to that measured with sediment traps.
/*
/* IMPORTANT   None
/* CREATED
/* VARIABLES:
/*
/* SIDE       (1)A new line layer called TEMP_BD is created and killed.
/* EFFECTS    (2)A new polygon layer called BUF_CST is created and killed.
/*            (3)A new polygon layer called CST_BD is created and killed.
/*            (4)A new polygon layer called SE_BD is created.
/*            (5)TABLES is invoked.
/*
/* ALGORITHM: A copy of STJ_BD called TEMP_BD, which contains the entire St. John
/*            coastline is built as a line. A 30 m buffer is created around it
/*            and stored as the BUF_CST layer. This layer is then clipped by
/*            %BASIN%_BD to eliminate the entire buffered coastline with the
/*            excetion of the landward side of the coastline inside %BASIN%. The
/*            resulting layer (CST_BD)is then used in an UNION command with
/*            DEL_BD to assign the DEL_RATIO to the new layer SE_BD. TABLES is
/*            invoked to add items where production and delivery data will
/*            be stored. Manipulations using the reselect command avoid
/*            calculating sediment production and delivery for wetland areas
/*            and areas within 30 m of the coastline. Production and delivery
/*            are calculated as a function of the AREA and DEL_RATIO items and
/*            the %UNDISTURBED% and %RAIN% variables. Sediment delivery ratios
/*            are estimated for both total loads and the fraction finer than
/*            2 mm, which is expected to be transported in suspension. The
/*            TABLES session is then terminated and the TEMP_BD, BUF_CST, and
/*            CST_BD layers are killed before the end of the routine.
/*
*****/

&type /& Beginning with surface erosion routine.../&
copy stj_bd temp_bd
build temp_bd line
buffer temp_bd buf_cst # # 30 # line /* Creates a buffer around entire coastline.

```

```

/* No surface erosion is calculated for buffered coastline area.
clip buf_cst %basin%_bd cst_bd poly /* Conserves buffer for %basin% only
union cst_bd del_bd se_bd /* Combines buffered coastline with del_bd.
/* This then allows to calculate sed prod and delivery for each area and
/* to prevent calculating erosion for wetland and coastline areas.
tables
additem se_bd.pat se_kg 8 8 n 2
additem se_bd.pat se_ton 8 8 n 3
additem se_bd.pat se_ttl_del 12 12 n 3
additem se_bd.pat se_sus_del 12 12 n 3
select SE_BD.PAT
&type /& Calculating surface erosion on undisturbed surfaces.../&
reselect potential = '' /* Selects Universal polygon
nselect /* Eliminates universal polygon.
reselect inside = 1 /* Eliminates buffered coastline areas.
calculate se_kg = ( area * 0.14 * %rain% * %undisturbed% ) * -
( 1 + ( %silt_loss% * %silt_se_fr% ) ) /* This last portion of the equation is
/* meant to compensate for loss of silt over sediment traps that were
/* used to develop the empirical erosion rate function.
aselect
reselect potential = 'wetland'
calculate se_kg = 0 /* Surface erosion is not calculated for wetland areas.
aselect
calculate se_ton = se_kg / 1000
calculate se_ttl_del = se_ton * del_ratio
calculate se_sus_del = se_ttl_del * %se_sus_fr%
quit
kill (! temp_bd buf_cst cst_bd !) all
&type /&Exiting surface erosion routine.../&
&return

&ROUTINE NAT_EROSION
/*****
/*
/* PURPOSE: Places all sediment production and delivery estimates derived from*/
/* natural processes in a single polygon layer and text file. */
/*
/* REQUIRED %NAT_NAME% is the user-given name of the final layer and text */
/* PRE-DEFINED file containing the final results of the natural erosion and */
/* VARIABLES: sediment delivery analysis. */
/* %YEARS% is the total time in years over which sediment production */
/* will be calculated. */
/*
/* IMPORTANT None */
/* CREATED */
/* VARIABLES: */
/*
/* SIDE (1)A new polygon cover called %NAT_NAME% is created. */
/* EFFECTS (2)TABLES is invoked. */
/*
/* ALGORITHM: An UNION command is used to join STR_DEL and SE_BD into one single */
/* layer called %NAT_NAME% that contains sediment production and */
/* delivery estimates from treethrow, streambank erosion, and surface */
/* erosion of undisturbed hillslopes. TABLES is invoked and several */
/* manipulations are used to avoid double counting of surface erosion */
/* rates. Items that contain total sediment production and delivery */
/* estimates from natural processes are added and calculated. */
/* Production and delivery are calculated as a function of the */
/* SE_TON,BANK_TON, TREE_TON, SE_DEL, BANK_DEL, and TREE_DEL items */
/* and the %YEARS% variable. A file named %NAT_NAME%.txt containing */
/* all of the results is unloaded before the TABLES session is */
/* terminated. The SE_BD and STR_DEL layers are killed before exiting */
/* the routine. */
/*
/*****
&type /&Beginning nat_erosion routine...
union se_bd str_del %nat_name% /* Unions treethrow, streambank and surface erosion
/* estimates into one coverage.
tables
select %nat_name%.pat

```

```

reselect tree_ton > 0
calculate se_ton = 0 /* Avoids double counting of surface erosion estimates.
calculate se_ttl_del = 0 /* Avoids double counting of sediment delivery estimates.
calculate se_sus_del = 0
aselect
additem %nat_name%.pat nat_ton 8 8 n 2
additem %nat_name%.pat nat_ttl_del 12 12 n 2 /* Total sediment delivery
additem %nat_name%.pat nat_sus_del 12 12 n 2 /* Suspended sediment delivery
additem %nat_name%.pat nat_pr_rate 12 12 n 2 /* Total sediment production
additem %nat_name%.pat nat_t_del_rate 12 12 n 2 /* Total delivery rate
additem %nat_name%.pat nat_s_del_rate 12 12 n 2 /* Suspended delivery rate
select %nat_name%.PAT
calculate nat_ton = se_ton + bank_ton + tree_ton
calculate nat_pr_rate = nat_ton / %years%
calculate nat_ttl_del = bank_ttl_del + tree_ttl_del + se_ttl_del
calculate nat_sus_del = bank_sus_del + tree_sus_del + se_sus_del
calculate nat_t_del_rate = nat_ttl_del / %years%
calculate nat_s_del_rate = nat_sus_del / %years%
dropitem %nat_name%.pat (! se_bd# se_bd-id cst_bd# cst_bd-id inside del_bd# -
del_bd-id se_kg str_del# str_del-id !)
&type Unloading %nat_name%.txt ...
unload %nat_name%.txt area potential se_ton se_ttl_del se_sus_del bank_ton -
bank_ttl_del bank_sus_del tree_ton tree_ttl_del tree_sus_del nat_pr_rate ~
nat_t_del_rate nat_s_del_rate delimited init
/* creates a file with all of the results,
/* replaces any file with same name, comma-delimited file may be opened
/* from Microsoft Excel
quit
kill (! se_bd str_del !) all
build %nat_name% poly
&type /&Done with nat_erosion routine...
&return

&ROUTINE SUMMARY_RESULTS
/*****
/*
/* PURPOSE: Displays a summary of results for both road and natural erosion
/* and delivery rates on the screen.
/*
/*
/* REQUIRED %NAT_NAME% is the user-given name of the final cover and text
/* PRE-DEFINED file containing the final results of the natural erosion and
/* VARIABLES: sediment delivery analysis.
/* %ROAD_NAME% is the user-given name of the final cover and text
/* file containing the final results of the road erosion and
/* sediment delivery analysis.
/*
/* IMPORTANT A total of 22 new variables are created by this routine.
/* CREATED
/* VARIABLES:
/*
/* SIDE (1) ARCEDITs invoked.
/* EFFECTS (2) TABLES is invoked.
/*
/* ALGORITHM: The statistics command is used to sum the sediment delivery totals
/* of a number of items in %NAT_NAME%.PAT and %ROAD_NAME%.AAT.
/* ARCEDIT is invoked to set the values of several new variables.
/* After exiting ARCEDIT the TABLES module is invoked to drop
/* a number of items from the %ROAD_NAME% data layer. Finally, the
/* routine prints on the screen a table summarizing the overall
/* model results.
/*
/*
/*****
&if [exists %nat_name%.sta] &then kill %nat_name%.sta
&if [exists %road_name%.sta] &then kill %road_name%.sta
statistics %nat_name%.pat %nat_name%.sta
sum bank_ttl_del
sum bank_sus_del
sum tree_ttl_del
sum tree_sus_del
sum se_ttl_del
sum se_sus_del

```

```

sum nat_ttl_del
sum nat_sus_del
end
statistics %road_name%.aat %road_name%.sta
sum un_ttl_del_rate
sum gr_ttl_del_rate
sum ab_ttl_del_rate
sum cs_ttl_del_rate
sum cs_sus_del_rate
end
arcredit
edit %nat_name%.sta info
&sv bank_ttl_del_r = [show info 1 item sum-bank_ttl_del] / %years%
&sv bank_sus_del_r = [show info 1 item sum-bank_sus_del] / %years%
&sv tree_ttl_del_r = [show info 1 item sum-tree_ttl_del] / %years%
&sv tree_sus_del_r = [show info 1 item sum-tree_sus_del] / %years%
&sv se_ttl_del_r = [show info 1 item sum-se_ttl_del] / %years%
&sv se_sus_del_r = [show info 1 item sum-se_sus_del] / %years%
&sv nat_ttl_del_r = [show info 1 item sum-nat_ttl_del] / %years%
&sv nat_sus_del_r = [show info 1 item sum-nat_sus_del] / %years%
edit %road_name%.sta info
&sv un_ttl_del_r = [show info 1 item sum-un_ttl_del_rate]
&sv gr_ttl_del_r = [show info 1 item sum-gr_ttl_del_rate]
&sv ab_ttl_del_r = [show info 1 item sum-ab_ttl_del_rate]
&sv un_sus_del_r = %un_ttl_del_r% * %un_sus_fr%
&sv gr_sus_del_r = %gr_ttl_del_r% * %gr_sus_fr%
&sv ab_sus_del_r = %ab_ttl_del_r% * %ab_sus_fr%
&sv cs_ttl_del_r = [show info 1 item sum-cs_ttl_del_rate]
&sv cs_sus_del_r = [show info 1 item sum-cs_sus_del_rate]
&sv rd_ttl_del_r = ( %un_ttl_del_r% + %gr_ttl_del_r% + %ab_ttl_del_r% + %cs_ttl_del_r%
)
&sv rd_sus_del_r = ( %un_sus_del_r% + %gr_sus_del_r% + %ab_sus_del_r% + %cs_sus_del_r%
)
&sv min_cur_nat = ( ( %rd_sus_del_r% + %nat_ttl_del_r% ) / %nat_ttl_del_r% )
&sv max_cur_nat = ( ( %rd_ttl_del_r% + %nat_sus_del_r% ) / %nat_sus_del_r% )
&sv total_sus_del_r = ( %bank_sus_del_r% + %tree_sus_del_r% + %se_sus_del_r% + ~
%un_sus_del_r% + %gr_sus_del_r% + %ab_sus_del_r% + %cs_sus_del_r% )
&sv total_del_r = ( %bank_ttl_del_r% + %tree_ttl_del_r% + %se_ttl_del_r% + ~
%un_ttl_del_r% + %gr_ttl_del_r% + %ab_ttl_del_r% + %cs_ttl_del_r% )
quit
tables
dropitem %road_name%.aat (! un_ttl_del_rate gr_ttl_del_rate ab_ttl_del_rate ~
rd_sus_del_rate cs_sus_del_rate rd_pr_rate cs_pr_rate !)
quit
&type /&/&
&type _____/&
&type Source name      Susp. del. rate      Total del. rate
&type                (tons/year)         (tons/year)/&
&type _____/&
&type Streambank      [round %bank_sus_del_r% ] [round %bank_ttl_del_r% ]
&type Treethrow       [ %tree_sus_del_r% ] [ %tree_ttl_del_r% ]
&type Undisturbed     [ %se_sus_del_r% ] [ %se_ttl_del_r% ]
&type Ungraded rds    [round %un_sus_del_r% ] [round %un_ttl_del_r% ]
&type Graded rds      [round %gr_sus_del_r% ] [round %gr_ttl_del_r% ]
&type Abandoned rds  [ %ab_sus_del_r% ] [ %ab_ttl_del_r% ]
&type Cutslopes       [round %cs_sus_del_r% ] [round %cs_ttl_del_r% ]
&type _____/&
&type TOTAL          [ round %total_sus_del_r% ] [round %total_del_r% ]
&type _____/&/&
&type Natural sediment yield rates for the %watshed% basin range from
&type [round %nat_sus_del_r% ] to [round %nat_ttl_del_r% ] tons per year./&
&type Road sediment yield rates for the %watshed% basin range from
&type [round %rd_sus_del_r% ] to [round %rd_ttl_del_r% ] tons per year./&
&type Current sediment delivery rates into %watshed% range between
&type [round %min_cur_nat% ] and [round %max_cur_nat% ] times above undisturbed
conditions.
&type /&/&
&if [query 'Press enter to exit.' .true.] &then ~
&return

```

APPENDIX IV-E
LONG-TERM SUSPENDED SEDIMENT YIELD FROM THE
MAIN FISH BAY GUT WATERSHED

LONG-TERM SUSPENDED SEDIMENT YIELD FROM THE MAIN FISH BAY GUT WATERSHED

Purpose

The main objective of this component of the study was to quantify long-term sediment yield rates into Fish Bay from the Main Fish Bay Gut watershed. These yield rates were compared to estimated sediment yield rates resulting from the application of the GIS-based STJ-EROS sediment budget model to the same basin as a way to test the model results (Chapter 5).

Methods

Rainfall was measured at on the western area of Fish Bay Estate. Watershed-scale runoff response was monitored at the main Fish Bay Gut between October 1998 and October 2001. The gaging station consisted of a pressure transducer connected to a datalogger. The pressure transducer and datalogger were calibrated prior to installation in 1998. Instrument readings were checked against actual stage measurements at a frequency ranging from once a week to once every three months. The datalogger recorded instantaneous stream stage at 15-minute intervals. The drainage area at this location was determined with the digital elevation model for St. John, and it was 3.46 km².

A rating curve was developed to convert stage measurements into flow rates. The rating curve was developed based on a combination of field measurements and Manning's flow velocity equation (Dunne and Leopold, 1978). Field measurements were taken in November 1998 and they consisted in a detailed cross-section survey, a longitudinal profile of the stream reach, and three discharge measurements. Discharge measurements were taken with a current meter by wading the channel during discharge events (Buchanan and Somers, 1980). The maximum stream stage represented by these measurements was 1.13 m, which converts to a discharge rate

of $0.67 \text{ m}^3 \text{ s}^{-1}$ or 0.07 cm hr^{-1} . Measurements were not taken at higher flow rates due to the impossibility of wading the stream at higher flows.

Manning's equation (Dunne and Leopold, 1978) was used to estimate flow velocities for stream stages higher than 1.13 m. A longitudinal survey of the stream reach determined that the channel had a slope of 0.002 m m^{-1} . Manning's roughness coefficient for the stream reach was estimated as 0.06. The resulting rating curve is shown in Figure 1.

The runoff record from the main Fish Bay Gut lasted for a period of only 3.3 years. In order to estimate long-term runoff and sediment yield rates a longer record is preferred. A fifteen year record exists for the 0.95 km^2 Guinea Gut basin. This gaging station is run by the US Geological Survey and is approximately two kilometers west of the main Fish Bay Gut station.

The first step was to determine if the main Fish Bay Gut and Guinea Gut basins had similar runoff response in terms of peak discharges and total runoff. Peak discharge and overall runoff response measured at both stations was compared for the period extending from October 1998 to November 2001 by plotting individual storm hydrographs. Total runoff for both stations was also compared by constructing flow duration curves for the 15-minute discharge data. A flow duration curve indicates the percentage of time a given river discharge is exceeded (Julien, 1995). The following discrete flow rate intervals were used in developing the flow duration curves: 0.00, 0.01, 0.05, 0.10, 0.25, 0.50, and continuing on to 4.5 cm hr^{-1} at every 0.25 cm hr^{-1} increments (Table 1- Column A). The annual average flow rate for each discrete flow rate interval is calculated as the product of the total percent time of each flow category (Column C) times the average flow rate for the interval (Column D) and a conversion factor. The sum of the products for all flow rate intervals (Column E) equals the long-term runoff total. A close match of the flow duration curves for both stations permitted the estimation of long-term annual runoff and sediment yields for the Main Fish Bay Gut by use of the Guinea Gut flow duration curve.

Thirty-five suspended sediment samples were collected from the main Fish Bay Gut over ten different runoff events between October 1998 and February 2000 with a DH-48 sampler. The

samples were analyzed for suspended sediment concentration following standard methods (ASTM, 1977). A sediment-rating curve was determined by plotting suspended sediment concentration against discharge.

An annual average suspended sediment yield estimate for the main Fish Bay Gut was based on the 35 samples and the flow duration curve from Guinea Gut. Average annual suspended sediment yield for each flow rate interval in the Guinea Gut flow duration curve was calculated as the product of the total runoff for each flow rate class (Table 1-Column E) times the average suspended sediment concentration for the entire 35 sample data set. The sum of the total sediment yield for all flow rate categories (Column G) equals the long-term suspended sediment yield for the main Fish Bay Gut.

Results

Semi-annual hydrographs show runoff measured at the main Fish Bay Gut station between October 1998 and October 2001 (Figures 2a-2d). These figures show the ephemeral nature of streams that is typical of St. John. Long periods with no flow are occasionally interrupted by short-lived runoff events. These runoff events are generally associated with hurricanes or intense thunderstorms with high antecedent moisture levels.

The relationship between direct runoff in the main Fish Bay Gut and rainfall was examined for all 59 events between October 1998 and December 1999 that showed a runoff response on the stream (Table 2). These events produced a total rainfall of 90.8 cm, and had an average rainfall of 1.54 cm per event with values ranging from 0.08 to 12.9 cm. Runoff response for individual events had a mean of 0.22 cm. The total runoff was 12.9 cm for an overall runoff coefficient of 0.14 cm cm⁻¹. Direct runoff showed a non-linear relationship with total rainfall (Figure 3).

Main Fish Bay Gut hydrographs show that 4.3 cm hr⁻¹ was the highest runoff rate between 1998 and 2001 and this occurred during Hurricane Lenny on 17 November 1999

(Figures 2a-2d). The total runoff during this period was 51.2 cm. The total rainfall was 167 cm for an overall runoff coefficient of 0.31 cm cm⁻¹.

By combining field observations with the hydrographs shown in Figures 2a-2d it was possible to determine that discharge rates of less than 0.01 cm hr⁻¹ were not delivering runoff or sediment into the bay. Flow rates less than or equal to 0.01 cm hr⁻¹ were not sufficient to overtop and break a sandy-berm that separates a narrow wetland area from Fish Bay. This berm prevented runoff and sediment being carried by the gut to be delivered into the marine environment. By discarding all flows equal to or less than 0.01 cm hr⁻¹ it was estimated that only 4.4 cm, or 8% of the total 51.2 cm of runoff were delivered into Fish Bay.

Fourteen storm hydrographs from October 1998 to November 2001 show that runoff responses from Fish Bay Gut and Guinea Gut tend to be similar, particularly for events with peak flows exceeding 0.1 cm hr⁻¹ (Figures 4a-4n). A flow duration curve for the 15-year Guinea Gut flow record shows only slight discrepancies with the main Fish Bay gut curve (Figure 5). The flow duration curves for both basins show that flows of 0.01 cm hr⁻¹ are exceeded only 0.8 % of the time. Flows between 0.10 and 1.5 cm hr⁻¹ are slightly more common on Guinea Gut than on the main Fish Bay Gut, but flows exceeding 2.0 cm hr⁻¹ were more common on the main Fish Bay Gut than on Guinea Gut. Despite these differences it was concluded that the long-term Guinea Gut flow duration curve could be used to estimate runoff yields from the main Fish Bay Gut. Application of the flow duration curve from Guinea Gut estimated that on average only 3.3 cm of runoff are delivered into Fish Bay every year (Table 1).

Suspended sediment concentrations from flows ranging between 0.0004 and 0.61 cm hr⁻¹ (0.04 to 5.8 m³ s⁻¹) showed concentrations from 0.007 to 4.6 g L⁻¹ with a geometric average of 0.57 g L⁻¹ (Table 3). A plot of sediment concentration versus runoff rates showed no correlation (Figure 6), which precluded the use of a rating curve to estimate sediment yields. Use of the flow duration curve with the mean value of 0.57 g L⁻¹ resulted in an average suspended sediment yield of 65 tons yr⁻¹ or 19 tons per km² yr⁻¹ for the 3.46 km² main Fish Bay Gut watershed (Table 1).

References

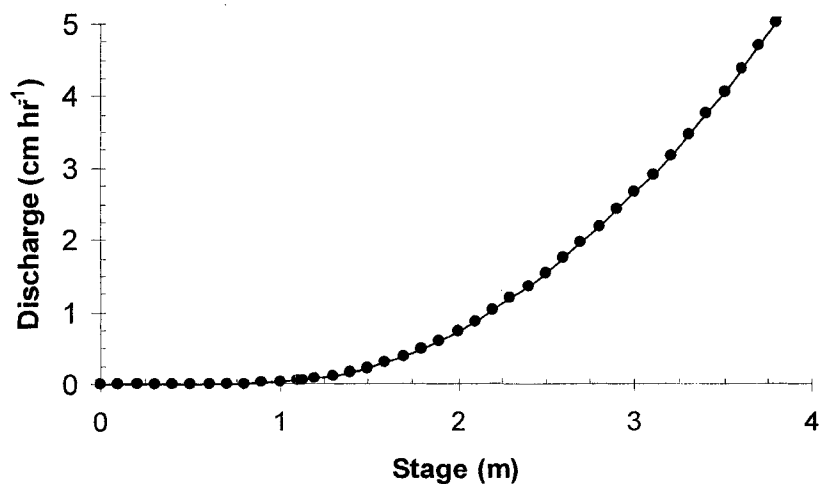
ASTM-D 3977-97. 1997. Standard test methods for determining sediment concentration in water samples. Annual Book of ASTM Standards. 11.01.

Buchanan TJ, Somers WP. 1980. Discharge measurements at gaging stations, Chapter A8, Book 3, Applications of hydraulics, US Geological Survey, 64 p.

Dunne T, Leopold LB. 1978 Water in environmental planning. WH Freeman and Company, New York, NY, 818 p.

Julien PY. 1995. Erosion and Sedimentation. Cambridge University Press, 280 p.

Figure 1. Stage-discharge rating curve for the Main Fish Bay Gut.



Figures 2a-2d. Runoff data collected at main Fish Bay Gut from 1998 to 2001.

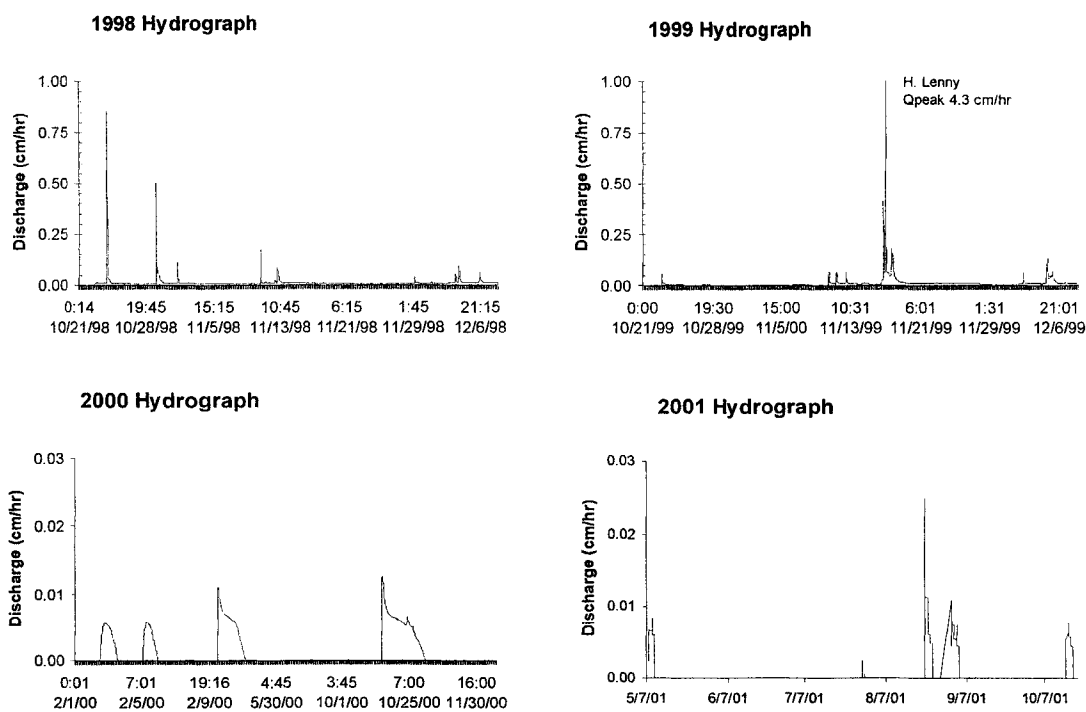
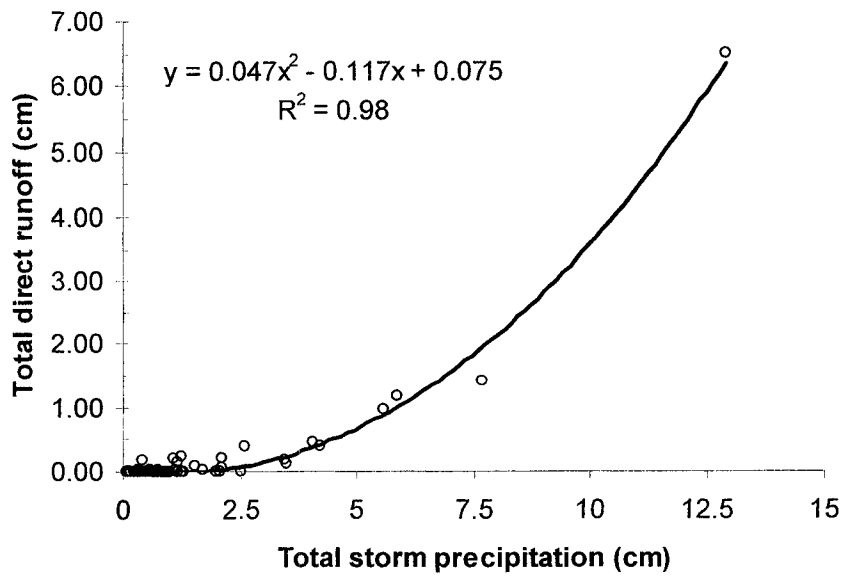
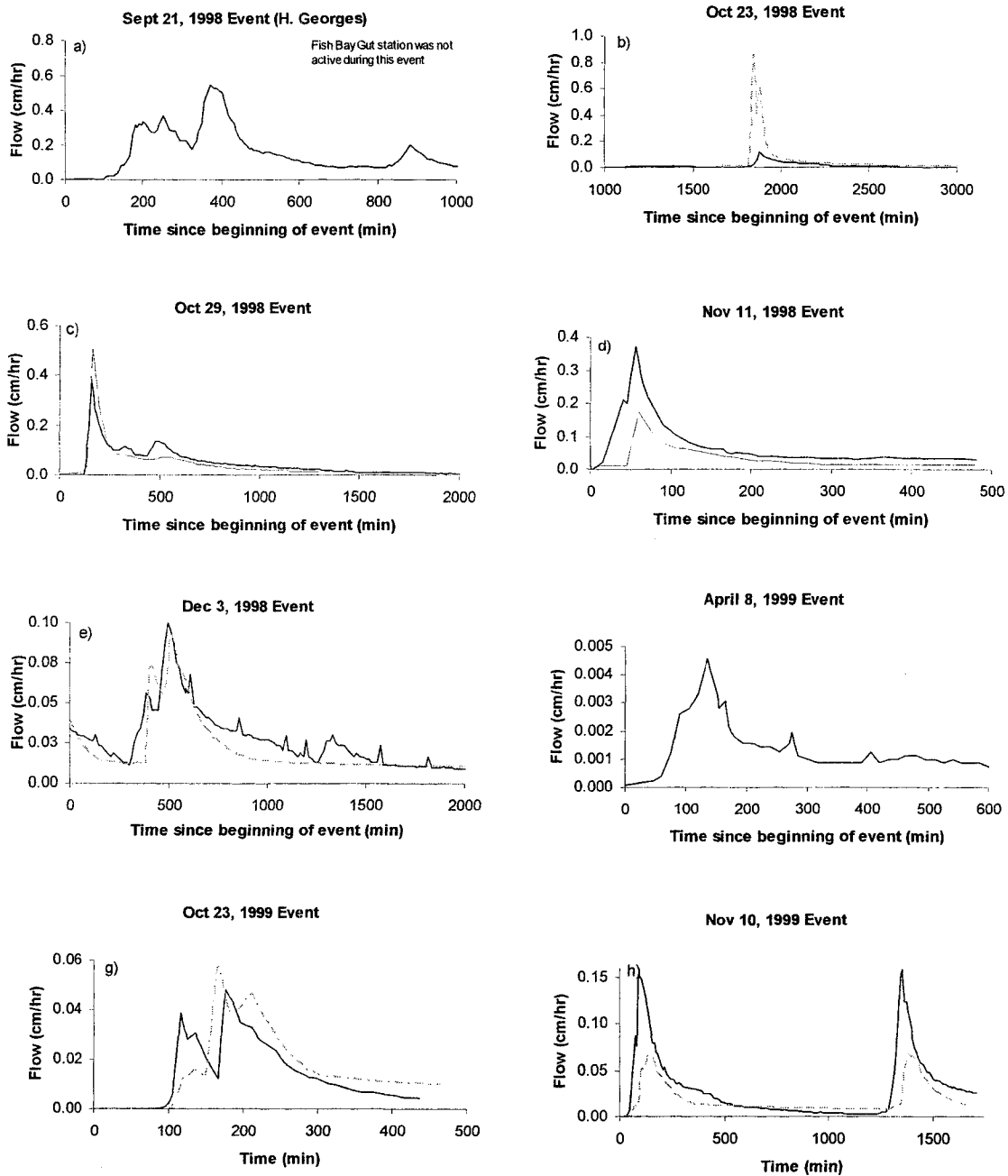


Figure 3. Relationship between storm precipitation and storm runoff at the main Fish Bay Gut.



Figures 4a-4n. Hydrographs for the fourteen events between October 1998 and November 2001 for Guinea Gut (solid black line) and the main Fish Bay Gut (dashed gray line).



Figures 4a-4n (cont.).

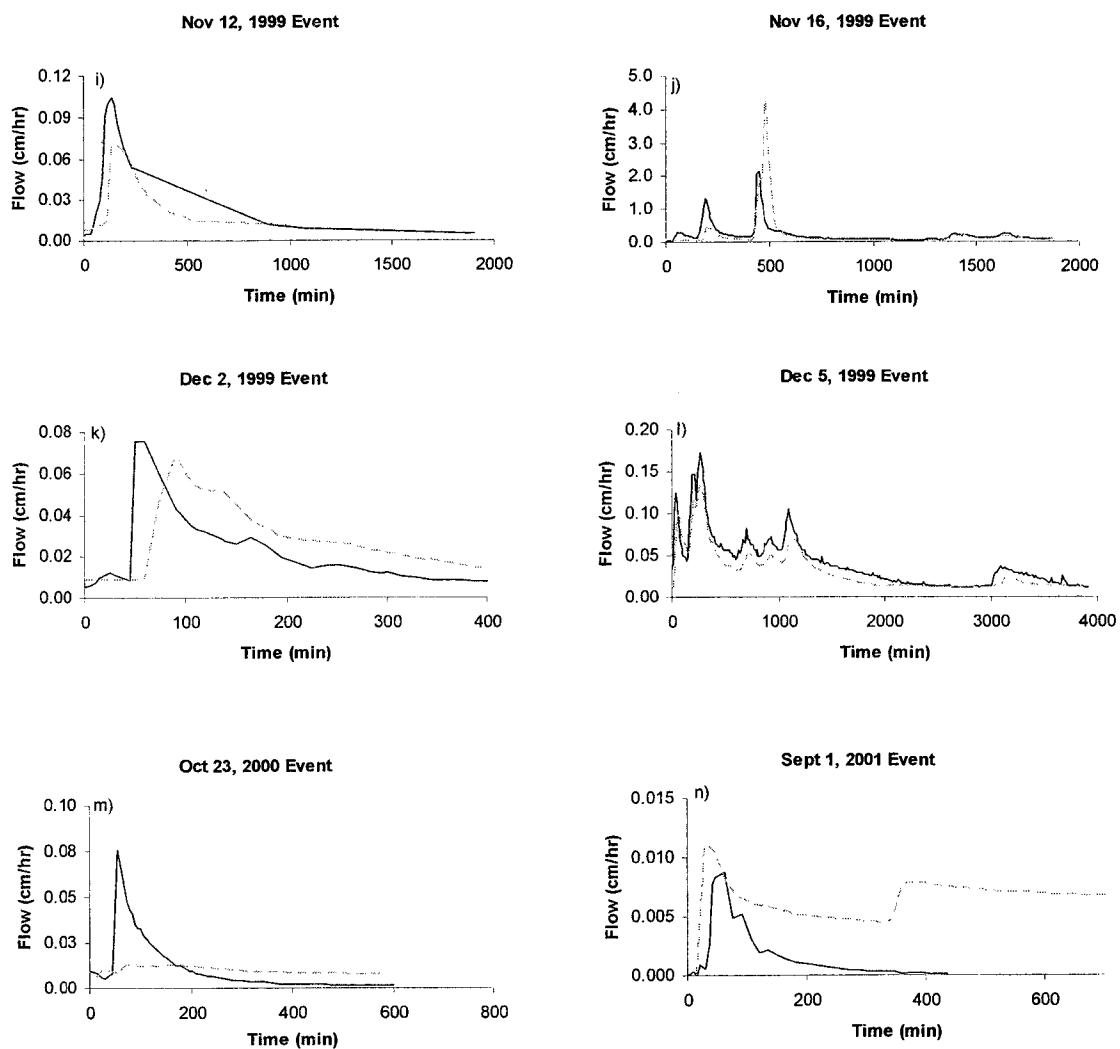


Figure 5. Flow duration curves for Guinea Gut and main Fish Bay Gut.

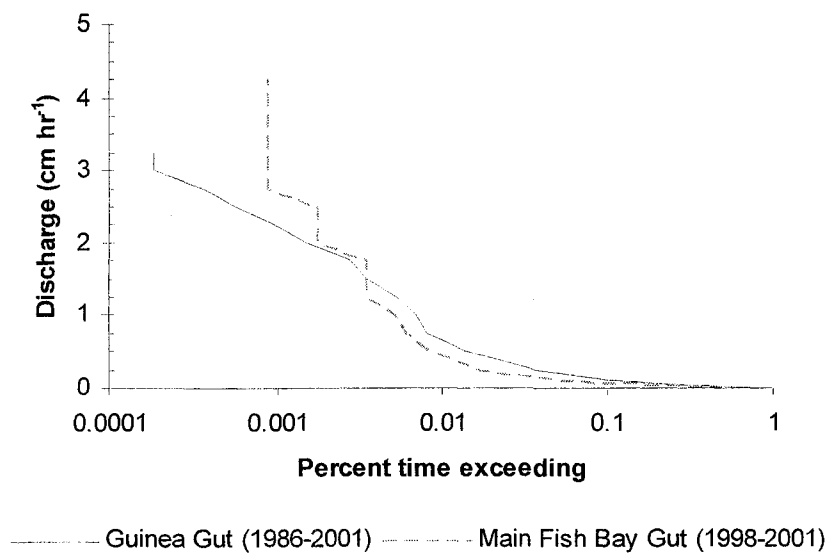


Figure 6. Sediment rating curve for 35 samples collected from the main Fish Bay Gut.

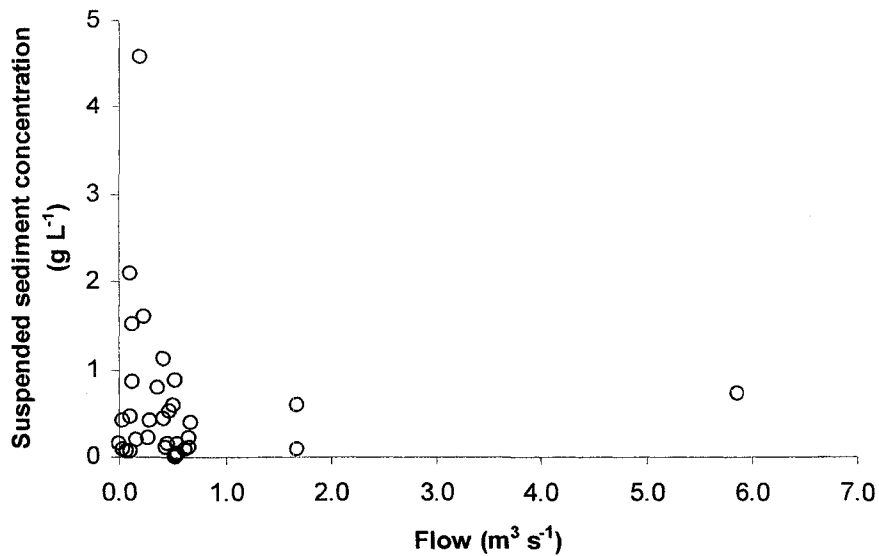


Table 1. Flow duration curve method for estimating long-term runoff and sediment yield rates from the main Fish Bay Gut.

(A) Flow rate (cm hr ⁻¹)	(B) Percent time exceeded	(C) Percent time for flow category	(D) Equivalent discharge for main Fish Bay Gut (m ³ s ⁻¹)	(E) Total runoff for flow rate class (cm yr ⁻¹)	(F) Sediment yield rate (kg min ⁻¹)	(G) Total sediment yield for flow rate category (tons)
0.0001	57		0.0010		0.033	
0.01	0.84	56	0.096		3.3	
0.05	0.23	0.62	0.48	1.4	16	27
0.1	0.099	0.13	0.96	0.84	33	17
0.25	0.038	0.061	2.4	0.67	82	13
0.5	0.014	0.024	4.8	0.27	164	5.3
0.75	0.0080	0.0058	7.2	0.063	247	1.2
1	0.0069	0.0011	9.6	0.012	329	0.24
1.25	0.0052	0.0017	12.0	0.018	411	0.36
1.5	0.0035	0.0017	14.4	0.018	493	0.36
1.75	0.0028	0.0007	16.8	0.008	575	0.16
2	0.0015	0.0013	19.2	0.014	657	0.28
2.25	0.00093	0.00056	21.6	0.0061	740	0.12
2.5	0.00056	0.00037	24.0	0.0041	822	0.081
2.75	0.00037	0.00019	26.4	0.0020	904	0.040
3	0.00019	0.00019	28.8	0.0020	986	0.040
3.25	0.00019	0.00000	31.2	0.0000	1068	0.000
3.5	0	0.00019	33.6	0.0020	1151	0.56
3.75	0	0				
4	0	0				
4.25	0	0				
4.5	0	0				
			Sum	3.3		65

Columns A, B, and C refer to Guinea Gut long-term data.

Table 2. Relationship between storm precipitation and storm runoff at the main Fish Bay Gut.

Date	Total storm precipitation (cm)	Direct runoff (cm)
21-Oct-98	1.98	0.00
23-Oct-98	3.45	0.17
23-Oct-98	0.97	0.010
24-Oct-98	5.59	0.97
26-Oct-98	1.68	0.018
30-Oct-98	5.89	1.2
1-Nov-98	0.43	0.18
9-Nov-98	0.89	0.003
11-Nov-98	1.07	0.22
12-Nov-98	2.59	0.40
27-Oct-98	0.48	0.00
18-Nov-98	0.58	0.003
22-Nov-98	0.15	0.00
28-Nov-98	0.43	0.00
29-Nov-98	2.08	0.07
3-Dec-98	1.09	0.04
4-Dec-98	4.06	0.45
7-Dec-98	1.24	0.23
10-Dec-98	0.64	0.00
13-Dec-98	0.23	0.003
15-Dec-98	0.76	0.008
21-Dec-98	0.66	0.00
22-Dec-98	0.61	0.015
24-Dec-98	0.74	0.017
27-Dec-98	0.48	0.003
1-Jan-99	0.08	0.00
5-Jan-99	0.13	0.00
6-Jan-99	0.25	0.00
10-Jan-99	0.23	0.00
11-Jan-99	0.23	0.00
14-Jan-99	0.25	0.00
15-Jan-99	0.84	0.00
15-Jan-99	0.89	0.013
19-Jan-99	0.36	0.00
23-Jan-99	0.53	0.00
24-Jan-99	0.76	0.00
26-Jan-99	0.53	0.00
3-Feb-99	0.48	0.003
6-Feb-99	1.29	0.00
8-Apr-99	3.5	0.11
12-Jun-99	1.52	0.095
1-Sep-99	0.94	0.00
12-Sep-99	0.76	0.00
13-Sep-99	2.06	0.00
19-Sep-99	0.33	0.00
27-Sep-99	1.24	0.00
28-Sep-99	2.51	0.00
14-Oct-99	1.17	0.00
10-Nov-99	2.11	0.20
11-Nov-99	4.24	0.38
15-Nov-99	0.56	0.03
17-Nov-99	12.9	6.5
20-Nov-99	0.23	0.003
23-Nov-99	0.33	0.023
3-Dec-99	1.17	0.15
4-Dec-99	7.7	1.4
20-Dec-99	0.48	0.008
25-Dec-99	0.53	0.005
27-Dec-99	0.86	0.005

Table 3. Suspended sediment data collected at the main Fish Bay Gut.

Date	Time	Stage (m)	Flow (cm hr ⁻¹)	Flow (m ³ s ⁻¹)	Co (g L ⁻¹)
24-Oct-98	734	1.91	0.61	5.9	0.73
11-Nov-98	1300	0.80	0.01	0.11	2.10
11-Nov-98	1330	0.79	0.01	0.11	0.47
29-Nov-98	545	1.02	0.04	0.41	0.43
29-Nov-98	615	0.96	0.03	0.29	0.43
29-Nov-98	715	0.91	0.02	0.21	4.59
29-Nov-98	745	0.88	0.02	0.16	0.20
29-Nov-98	815	0.85	0.01	0.13	0.86
10-Nov-99	2252	0.51	0.00	0.0037	0.16
10-Nov-99	2329	1.05	0.05	0.48	0.52
10-Nov-99	2340	1.07	0.05	0.53	0.89
11-Nov-99	7	1.12	0.07	0.65	0.23
11-Nov-99	27	1.08	0.06	0.55	0.02
11-Nov-99	101	1.02	0.04	0.41	1.13
11-Nov-99	1512	0.71	0.01	0.078	0.06
11-Nov-99	2020	1.04	0.05	0.46	0.16
11-Nov-99	2052	1.11	0.07	0.62	0.08
11-Nov-99	2115	1.08	0.06	0.55	0.05
11-Nov-99	2200	1.00	0.04	0.37	0.80
12-Nov-99	2059	0.86	0.01	0.14	1.53
12-Nov-99	2145	1.16	0.07	0.67	0.39
12-Nov-99	2215	1.13	0.06	0.61	0.09
12-Nov-99	2245	1.08	0.06	0.55	0.15
16-Nov-99	2111	0.93	0.03	0.24	1.62
17-Nov-99	840	1.42	0.17	1.7	0.59
17-Nov-99	840	1.42	0.17	1.7	0.09
17-Nov-99	1646	1.07	0.05	0.53	0.01
2-Dec-99	1710	1.12	0.07	0.65	0.12
2-Dec-99	1740	1.06	0.05	0.50	0.60
2-Dec-99	1910	0.95	0.03	0.27	0.22
5-Dec-99	1348	1.07	0.05	0.53	0.02
5-Dec-99	1825	1.03	0.05	0.43	0.10
23-Feb-00	1420	0.60	0.004	0.037	0.42
23-Feb-00	1448	0.62	0.00	0.044	0.08
23-Feb-00	1515	0.79	0.01	0.11	0.06
mean			0.06	0.59	0.57